Pacific Gas and Electric Company

EPIC Final Report: Attachment

Program	***Electric Program Investment Charge (EPIC)***
Project	***EPIC 2.03A: Test Smart Inverter Enhanced Capabilities – Photovoltaics (PV): Smart Inverter Modeling Report***
Reference Name	***EPIC 2.03A: Customer Cited Smart Inverters*** ***EPIC 2.03A: Smart Inverters***
Department	Grid Integration & Innovation
Executive Sponsor	Roy Kuga
Project Sponsor	Mark Esguerra
Business Lead (Modeling Subproject)	Fedor Petrenko
Technical Lead (Modeling Subproject)	Mike McCarty
Contact Info	EPIC_info@pge.com
Date	February 8, 2019
Version Type	Final

Pacific Gas and Electric Company®

EPIC 2.03A Project

December 2018

ELECTRIC POWER RESEARCH INSTITUTE
3420 Hillview Avenue, Palo Alto, California 94304-1338 ▪ PO Box 10412, Palo Alto, California 94303-0813 ▪ USA
800.313.3774 ▪ 650.855.2121 ▪ askepri@epri.com ▪ www.epri.com

DISCLAIMER OF WARRANTIES AND LIMITATION OF LIABILITIES

THIS DOCUMENT WAS PREPARED BY THE ORGANIZATION(S) NAMED BELOW AS AN ACCOUNT OF WORK SPONSORED OR COSPONSORED BY THE ELECTRIC POWER RESEARCH INSTITUTE, INC. (EPRI). NEITHER EPRI, ANY MEMBER OF EPRI, ANY COSPONSOR, THE ORGANIZATION(S) BELOW, NOR ANY PERSON ACTING ON BEHALF OF ANY OF THEM:

(A) MAKES ANY WARRANTY OR REPRESENTATION WHATSOEVER, EXPRESS OR IMPLIED, (I) WITH RESPECT TO THE USE OF ANY INFORMATION, APPARATUS, METHOD, PROCESS, OR SIMILAR ITEM DISCLOSED IN THIS DOCUMENT, INCLUDING MERCHANTABILITY AND FITNESS FOR A PARTICULAR PURPOSE, OR (II) THAT SUCH USE DOES NOT INFRINGE ON OR INTERFERE WITH PRIVATELY OWNED RIGHTS, INCLUDING ANY PARTY'S INTELLECTUAL PROPERTY, OR (III) THAT THIS DOCUMENT IS SUITABLE TO ANY PARTICULAR USER'S CIRCUMSTANCE; OR

(B) ASSUMES RESPONSIBILITY FOR ANY DAMAGES OR OTHER LIABILITY WHATSOEVER (INCLUDING ANY CONSEQUENTIAL DAMAGES, EVEN IF EPRI OR ANY EPRI REPRESENTATIVE HAS BEEN ADVISED OF THE POSSIBILITY OF SUCH DAMAGES) RESULTING FROM YOUR SELECTION OR USE OF THIS DOCUMENT OR ANY INFORMATION, APPARATUS, METHOD, PROCESS, OR SIMILAR ITEM DISCLOSED IN THIS DOCUMENT.

REFERENCE HEREIN TO ANY SPECIFIC COMMERCIAL PRODUCT, PROCESS, OR SERVICE BY ITS TRADE NAME, TRADEMARK, MANUFACTURER, OR OTHERWISE, DOES NOT NECESSARILY CONSTITUTE OR IMPLY ITS ENDORSEMENT, RECOMMENDATION, OR FAVORING BY EPRI.

THE FOLLOWING ORGANIZATION(S), UNDER CONTRACT TO EPRI, PREPARED THIS REPORT:

THE ELECTRIC POWER RESEARCH INSTITUTE (EPRI) PREPARED THIS REPORT.

This is an EPRI Technical Update report. A Technical Update report is intended as an informal report of continuing research, a meeting, or a topical study. It is not a final EPRI technical report.

NOTE

For further information about EPRI, call the EPRI Customer Assistance Center at 800.313.3774 or e-mail askepri@epri.com.

Electric Power Research Institute, EPRI, and TOGETHER…SHAPING THE FUTURE OF ELECTRICITY are registered service marks of the Electric Power Research Institute, Inc.

Copyright © 2018 Electric Power Research Institute, Inc. All rights reserved.

ACKNOWLEDGMENTS

The Electric Power Research Institute (EPRI) prepared this report for Pacific Gas and Electric Company (PG&E).

EPRI Principal Investigators:

Miguel Hernandez
Jouni Peppanen
Tanguy Hubert
Jeremiah Deboever

PG&E Principal Investigators: Mike McCarty, Fedor Petrenko, Olivia Trinko

The authors would also like to recognize the contributions of Matthew Deakin from the University of Oxford, who supported part of the modeling and analysis presented in this report during an internship with EPRI.

EXECUTIVE SUMMARY

This modeling effort explored the technical impacts and economic value of several of the smart inverter (SI) functions defined in California Electric Rule 21 ("CA Rule 21") and Hawaiian Electric Rule 14 ("HI Rule 14"). The modeling effort objectives were twofold: (1) inform PG&E on the successful utilization and configuration of residential SI to mitigate PV-driven impacts and expenditures; and (2) provide an understanding of the economic impact of SIs from various perspectives: PV customers activating SI functions, ratepayers, utility, and society.

As part of this modeling effort, six representative PG&E feeders were modeled and validated. In particular, while planning modeling methodologies usually focus exclusively on modeling the primary system (i.e., medium voltage), this modeling effort modeled low-voltage (LV) secondary circuits in great detail. Quasi-static time-series (QSTS) simulations explored 15,183 different scenarios parametrized by multiple technology penetration levels (PV and storage), load conditions, and PV generation profiles. Conclusions from this modeling effort assume a highly distributed PV penetration across each circuit since simulation models were focused on residential installations. While these six distribution feeders were carefully selected to inform on the possible benefits of activating SI functions, they only represent 0.2% of PG&E feeders.

For each of the six feeders, the PV-driven impacts and expenditures on the distribution grid operation were first analyzed, focusing on residential PV systems. Two strategies aiming to accommodate higher PV penetration levels were then evaluated and compared: one strategy relying on conventional distribution upgrades, the other on SI Volt-VAR and Volt-Watt functions. The scope of this modeling effort was limited to analyzing the effectiveness of Volt-VAR and Volt-Watt functions to specifically address PV-driven voltage violations. Traditional upgrades were triggered by decision rules reflecting potential thermal overloads and voltage rise issues, closely following PG&E's design and engineering practices. A critical evaluation of these practices suggested that, while thermal violations were always properly addressed, voltage issues could sometimes be left undetected as they can occur before the aggregate inverter nameplate exceeds the service transformer's kilovolt-ampere (kVA) nameplate.

The strategy leveraging SI Volt-VAR and Volt-Watt functions was shown to reduce, but not entirely suppress overvoltage conditions. Still, the reduction observed was generally comparable, and sometimes superior to the level of performance obtained with conventional upgrades. Active power curtailment, resulting from the activation of SI functions, appeared extremely limited: across all combinations of feeders, functions, inverter densities, and PV and load conditions considered, only 45 of the 8,414 PV installations modeled experienced active power curtailment greater than 1% across any of the analyzed 24-hour periods. The increase in inverter utilization appeared negligible.

The economic impact of activating SI functions was evaluated across four cost categories: (1) the increased electricity cost at feeder heads; (2) the bill increases to participants; (3) the avoided secondary voltage rise upgrades; and (4) the avoided secondary voltage rise studies, all resulting from activating SI functions. These cost categories were mapped to four standard cost tests, reflecting various stakeholder perspectives: PV customers activating SI functions, ratepayers, utility, and society. Time-differentiated annual energy usage profiles were constructed for each individual PV customer, and an algorithm emulating PG&E's billing system for three relevant retail electricity tariffs provided detailed estimates on potential bill increases. Several other key sensitivities influencing the results were explored.

The economic impacts were first evaluated for the six feeders selected. The approach was comparative in nature: differences impacting the cost categories according to which strategy was considered, conventional upgrades or SI functions, were analyzed; equipment upgrades required under both strategies were excluded from this comparative analysis, since they could not lead to any cost differences between the two strategies.

The activation of SI functions generally yielded a net positive economic impact across the six feeders considered when compared to the traditional upgrades. Yet, this benefit appeared to be relatively small: Total Resource Cost (TRC) values, assuming a linear PV penetration increase over time, ranged from a total Net Present Value (NPV) of -$4/customer (net cost) to $57/customer[1] (net benefit) <u>over 10 years</u> (in $2018). The benefits of activating SI functions generally increased at higher PV penetration levels, reflecting a larger number of transformer upgrades and secondary voltage rise studies avoided. The savings resulting from these avoided costs are expected to benefit electric ratepayers, interconnecting customers, and PV developers.

For each of the six feeders studied, an analysis of the "customer outliers" experiencing bill increases higher than the average PV customer was also conducted. Among 354,096 customer cases involving an annual bill increase higher than $3 (out of 474,633 customer cases), only 0.748% of the customer cases returned an annual bill increase higher than 3%. A possible two-step approach was identified to drastically limit the (already very small) number of customer outliers in practice: first, detect circuit locations prone to overvoltage conditions early; second, proactively implement distribution upgrades at these locations to ensure that nearby PV customers do not experience excessive active power curtailment, when compared to the average PV customer.

As a part of this modeling effort, an extensive literature review of relevant past studies was conducted. The novel contributions of this modeling effort, making it one of the most comprehensive publicly-available techno-economic assessments on this topic to date, include:

- Over 12,000 scenarios analyzed, including: 6 PG&E distribution feeders, 5 PV penetration levels, three Energy Storage (ES) penetration levels, three combinations of SI functions, five SI densities, five representative PV generation profiles, and three representative load profiles.
- For the six feeders studied, the modeling of secondary LV circuits at a level of detail that was significantly increased compared to standard modeling practices.
- An analysis of the manual adjustments of voltage regulation equipment settings to mitigate voltage impacts caused by PV at higher PV penetration levels. Manual adjustments were shown to be very effective at mitigating PV-driven voltage impacts, but complex to select.
- An analysis of the effectiveness of conventional distribution upgrades, as triggered by PG&E's current design and engineering practices. Among other things, results obtained for the six feeders

[1] The maximum NPV of $57 over 10 years was obtained on one modeled feeder with an atypical voltage class relative to other PG&E feeders. The next largest maximum NPV seen on a more typical feeder assuming a linear PV penetration increase was closer to $15 over 10 years.

suggested that PG&E's process for triggering preventive service transformer replacements potentially subject to thermal overloads was effective.

- An assessment of the effectiveness of SI functions at mitigating PV-driven voltage impacts. Simulation results suggested that SI functions were equally effective at addressing overvoltage conditions, when compared to conventional upgrades triggered by secondary voltage rise studies.
- A rigorous analysis of active power curtailment occurrences resulting from SI function activation across 474,633 individual PV customer cases, covering all possible combinations of sensitivity variables considered in this modeling effort.
- An evaluation of the economic impacts of SI functions combining highly detailed techno-economic modeling at the individual customer level, feeder level, and territory level. Specifically, a feeder clustering approach was used to extrapolate the economic findings to PG&E's entire service territory.
- An assessment of the "customer outliers," this small subset of PV customers experiencing bill increases higher than the average PV customer when activating SI functions, and the development of an approach to minimize the number of outliers in practice.

ABBREVIATIONS

AC	Alternating Current
AMI	Advanced Metering Infrastructure
ANSI	American National Standard Institute
CEC	California Energy Commission
CPF	Constant power factor
CPUC	California Public Utilities Commission
CSI	California Solar Initiative
CVR	Conservation voltage regulation
DC	Direct Current
DER	Distributed Energy Resource
ECC	Economic Carrying Cost
ES	Energy Storage
HECO	Hawaiian Electric Company
GHI	Global horizontal irradiance
GSF	Grid support functions
IEEE	Institute of Electrical and Electronics Engineers
InvControl	Invertor controller
IOU	Investor-owned utility
IVVC	Integrated Voltage-Var Control
kVA	Kilovolt ampere
kW	Kilowatt
kWh	Kilowatt-hour
LTC	Load Tap Changer
LV	Low Voltage
MV	Medium Voltage
MW	Megawatt
MWh	Megawatt-hour
NBC	Non-Bypassable Charge
NPV	Net Present Value
NREL	National Renewable Energy Laboratory
NSC	Net Surplus Compensation
PAC	Program Administrator Cost
PCT	Participant Cost Test
PG&E	Pacific Gas and Electric Company
PMPP	Power at maximum power point
PQS	Power quality score
PSCAD	Power System CAD software
PV	Photovoltaic
PVA	PV Profile A
RIM	Ratepayer Impact Measure
SCADA	Supervisory Control and Data Acquisition

SCE	Southern California Edison Company
SDG&E	San Diego Gas & Electric Company
SI	Smart inverter
SLF	Static load flow
TOU	Time of use
TRC	Total Resource Cost
V	Volt
VRS	Voltage rise study
VRU	Voltage rise upgrade
ZNE	Zero Net Energy

GLOSSARY

"Average" day: the day with the energy consumption closest to the average daily energy consumption over the whole 11-month period analyzed.

California Electric Rule 21: see *Rule 21.*

Cogen mode: mode in voltage regulating transformers to adjust for reverse power flow scenarios.

Combi-R21: combined Volt-VAR & Volt-Watt functions, as defined in CA Rule 21 at the time of writing.

Combi-R14: combined Volt-VAR & Volt-Watt functions, as defined in HI Rule 14 at the time of writing.

Conventional distribution upgrade: equipment upgrade on the distribution system traditionally considered to ensure normal operating conditions are maintained at higher PV penetration levels.

Cost-effectiveness indicator: a particular way of expressing a cost test. Examples of cost-effectiveness indicators include: net present value, net present value per customer, net present value per kW of PV installed, etc.

Cost test: economic metric defined to inform on the cost-effectiveness of a measure from the perspective of a particular stakeholder: participants implementing the measure, ratepayers, utility, society, etc. A cost test can be expressed using a variety of cost-effectiveness indicators.

Customer: energy user interconnected to the distribution grid through an electricity meter, and taking service on a specific retail electricity rate.

Customer case: the results obtained for a specific customer for a given combination of sensitivities (PV penetration level, smart inverter density, smart functions considered, etc.), in particular the changes potentially impacting the customer annual electricity bill. Each customer is associated to multiple cases, each case analyzing the impacts of different conditions on that unique customer.

CYME: power system modeling and analysis software.

DC/AC ratio: In this report, defined as the PV panel DC kW rating divided by the PV inverter AC kVA rating.

Energy storage (ES) penetration level: the proportion of PV customers (in %) that also have storage.

ES*x*: ES penetration levels in terms of the percentage of residential customers with PV systems that *also* have storage. (ES0-0% of PV customers, ES1-20%, ES3-75%, and ES2-40%).

Hawaiian Electric Rule 14: see *Rule 14.*

"Minimum" day: the day with the lowest energy consumption, as shown on the aggregated AMI profile.

Mitigation strategy: a set of actions taken to ensure that normal distribution operating conditions are maintained at higher PV penetration levels. This modeling effort compares two strategies: one relying on conventional distribution upgrades, the other leveraging smart inverter functions.

Participant cost test: cost test reflecting the perspective of participants implementing the measure (in this modeling effort, the activation of smart inverters).

"Peak" day: the day with the highest energy consumption, as shown on the aggregated AMI profile.

Program administrator cost: cost test reflecting the perspective of the utility when evaluating a measure.

PV customer: a customer operating a PV system.

PV penetration level: the proportion of customers (in %) that have PV. In this modeling effort, only residential customers have PV.

PV*x*: PV penetration levels in terms of residential customers with PV systems. (PV0-0%, PV1-25% of customers, PV2-50%, PV3-75%, and PV4-100%).

Ratepayer impact measure: Cost test reflecting the perspective of the ratepayers when evaluating a measure.

Rule 14: Document governing the interconnection, operating and metering requirements applicable to some generating facilities wishing to connect to the utility's distribution system in Hawaii.

Rule 21: Document governing the interconnection, operating and metering requirements applicable to some generating facilities wishing to connect to the utility's distribution system in California.

Quasi-static time series (QSTS): analysis approach to capture time-dependent aspects of power flow, including the interaction between the daily changes in load and PV output and control actions by feeder devices and advanced inverters.

Smart inverter: power inverter enabled with smart inverter functions.

Smart inverter density: the proportion of PV inverters (in %) that have smart functions capabilities.

Smart inverter function: autonomous control capability built into an inverter to help support grid operations.

SI*x*: smart inverter density levels in terms of the percentage of PV systems equipped with a smart inverter. (SI1-25% of PV systems, SI2-50%, SI3-75%, and SI4-100%).

Significant voltage violation: an overvoltage or undervoltage episode with a duration over one hour *or* a scope affecting more than 5% of the feeder buses.

Traditional distribution upgrade: see *conventional distribution upgrade*.

VV-R21: Volt-VAR function, as defined in CA Rule 21.

CONTENTS

LIST OF FIGURES

LIST OF TABLES

1
INTRODUCTION

1.1 Context of This Modeling Effort

The deployment of distributed solar PV in California has accelerated rapidly over the recent years, driven in part by customer preferences and a favorable legislative and regulatory environment.

California Electric Rule 21[2] ("CA Rule 21") is a key document governing the interconnection, operating and metering requirements to most generating facilities wishing to connect to the utility's distribution system, including PV. CA Rule 21 requirements were organized into three sets, or "phases," which are progressively becoming mandatory. Since September 8, 2017, all new PV interconnections are required to have SIs compliant with CA Rule 21 Phase I autonomous functions, including Volt-VAR control.[3] Furthermore, at the time of writing this report, CA Rule 21 requires all new PV systems interconnected after February 22, 2019 to comply with CA Rule 21 Phase II communications, and CA Rule 21 Phase III advanced functions including Volt-Watt mode.[4]

PG&E forecasts that by 2021, roughly half of all behind-the-meter (BTM) PV in California will be equipped with SIs and predicts nearly 100% SI penetration in California by 2028. Since most of the early PV inverter deployments did not have SI capabilities, the SI density (i.e., the proportion of PV systems with *SI*s), initially starting low, will progressively grow over time as old inverters are retired and new inverters are interconnected.[5] Figure 1 1 shows the past and projected BTM PV capacities and SI densities in California.

The rapidly growing fleet of smart PV inverters connected to PG&E's distribution grid has the potential to become a resource that can help maintain and/or enhance grid safety, reliability, and customer affordability. However, many challenges remain to be addressed for this potential to be fully realized. Some of these challenges are discussed in the SI white paper[6]recently published by the three California investor-owned utilities (IOU). This paper summarizes key learnings from past IOU-led SI demonstration projects, and highlights open questions related to the integration of Distribution Energy Resources (DER), including distributed PV enabled with SI capabilities.

---

2 Available: http://www.cpuc.ca.gov/Rule21/.

3 "Resolution E-4920. Approval, with Modifications, of Request for Modifications to Electric Rule 21 Tariff to Incorporate Smart Inverter Reactive Power Priority Setting." California Public Utilities Commission (CPUC), 26-Apr-2018. Available: http://docs.cpuc.ca.gov/PublishedDocs/Published/G000/M212/K527/212527968.PDF.

4 "Resolution E-4898. Approval, with Modifications, of Request for Modifications to Electric Rule 21 Tariff to Incorporate Smart Inverter Phase 3 Advanced Functions in Compliance with Decision 16-06-052." CPUC, 26-Apr-2018. Available: http://docs.cpuc.ca.gov/PublishedDocs/Published/G000/M200/K267/200267616.PDF.

5 It should be noted that currently, there is no requirement to replace legacy inverters with smart inverters.

6 "Enabling Smart Inverters for Distribution Grid Services," White paper by San Diego Gas & Electric Company (SDG&E), PG&E and Southern California Edison Company (SCE), Oct. 2018. Available: https://www.pge.com/pge_global/common/pdfs/about-pge/environment/what-we-are-doing/electric-program-investment-charge/Joint-IOU-SI-White-Paper.pdf.

Figure 1-1
Past and Projected Smart Inverter Penetration Levels in California[7]

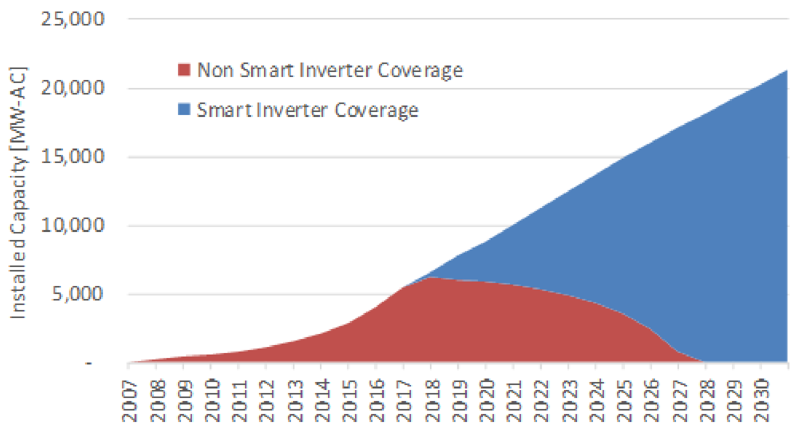

1.2 Overview of This Modeling Effort

The present modeling effort, performed for PG&E by the EPRI, analyzed the technical and economic impacts of growing densities of smart PV inverters connected to PG&E's distribution grid. The focus was placed on residential PV systems.

This modeling effort is a component of a larger PG&E EPIC 2.03A project titled "*Test Capabilities of Customer-Sited Behind-the-Meter Smart Inverters,*" which aims to demonstrate the functionalities and grid impacts of BTM smart PV inverters.[8] The overall project has three key activities: field testing of SIs at two different locations; lab testing of SIs; and a SI modeling effort (this report). The key learnings gained from this larger PG&E EPIC 2.03A project at the time of writing this report are summarized in.[8]

This report documents the findings of the SI modeling effort that evaluated the technical impacts of residential PV and residential PV + storage deployments,[9],[10] without and with SIs. In addition, an analysis of the economic impacts on the six feeders was conducted, comparing traditional network re-enforcement strategies involving distribution upgrades, to scenarios leveraging grid support provided by SIs.

7 See footnote 3, *supra*.

8 "EPIC 2.03A: Smart Inverters – Interim Report," PG&E, Jul. 2018. Available: https://www.pge.com/pge_global/common/pdfs/about-pge/environment/what-we-are-doing/electric-program-investment-charge/PGE-EPIC-Project-2.03a.pdf?WT.mc_id=Vanity_epicinterimreport-SmartInverters.

9 In the PV + storage deployments, the storage was assumed to be AC-coupled (i.e., to have a separate inverter). No smart inverter functions were assumed to be activated for the ES inverter as the focus was on smart PV inverter impacts and benefits. In practice, CA Rule 21 also requires storage inverters to be compliant with the Volt-VAR and Volt-Watt functions analyzed in this report. This modeling effort further assumed that the storage operation is not influenced by the PV smart inverter functions.

10 This modeling effort focused on residential systems both due to timing constraints within this project's schedule and since the field deployment of the EPIC 2.03A project focused on commercial PV systems.

The key objectives of this modeling effort were twofold:

- Inform PG&E of the opportunities for successful utilization and configuration of SI functions on PG&E distribution circuits through computer modeling and analysis.
- Provide an understanding of the economic impacts of SI functions by comparing the merits of accommodation strategies relying on grid upgrades, to new approaches leveraging SI support capabilities.

EPRI has previously documented the common functions for SIs.[11] This reference documents the body of work and recommendations on SI functions from a decade-long collaborative of over 600 utilities and technology stakeholders. These recommendations were incorporated into virtually all recent SI standards and specifications, as well as many grid codes in the U.S. and internationally, including CA Rule 21 and Institute of Electrical and Electronics Engineers (IEEE) Standard 1547.

The present modeling effort focused on two SI voltage support functions: *Volt-VAR* and *Volt-Watt*, as defined in CA Rule 21, HI Rule 14 (a set of requirements similar to CA Rule 21 for the state of Hawaii), and in the *Common Functions of Smart Inverters* report (see footnote 10). Specifically, the present modeling effort analyzed three combinations of autonomous Volt-VAR and Volt-Watt functions and settings:

1. Volt-VAR function, assuming the default CA Rule 21 settings at the time of writing this report (referred to as “VV-R21”);
2. Combined Volt-VAR and Volt-Watt functions, assuming the default CA Rule 21 settings at the time of writing this report (referred to as “Combi-R21”); and
3. Combined Volt-VAR and Volt-Watt functions, assuming the default HI Rule 14 settings at the time writing this report (referred to as “Combi-R14”).

This modeling effort performed detailed techno-economic analysis of these SI functions, and compared their implementation and impacts to conventional strategies relying on distribution upgrades to mitigate PV-driven impacts and expenditures. Chapter 5 discusses the function settings evaluated in further detail.

[11] “Common Functions for Smart Inverters: 4th Edition,” EPRI, Palo Alto, CA, EPRI Technical Update 3002008217, Dec. 2016. Available: https://www.epri.com/#/pages/product/3002008217/.

The two SI functions considered, Volt-VAR and Volt-Watt, were assumed to operate only when PV systems were generating. In other words, the SIs were assumed to *not* consume or produce reactive power at night ("no VARs at night"). This assumption was based on the CA Rule 21 and IEEE 1547-2018 requirements: at the time of writing this report, CA Rule 21 requires DER inverters to be capable of consuming or producing reactive power when the inverters are at or above 20% of their rated active power; moreover, IEEE 1547-2018[12] requires DER inverters to be capable of consuming or producing reactive power when inverters are at or above 5% of their rated active power.[13] Assuming "no VARs at night" also allowed the modeling effort to focus on the SI value related to PV integration. Although SIs were assumed to not consume/produce any reactive power outside of PV generation times, this modeling effort recognizes that SIs may also support voltage regulation beyond reducing overvoltages caused by PV. During PV generation times, this modeling effort did not distinguish between (1) the value provided by SIs mitigating voltage rise events *resulting from PV*; and (2) the value provided when regulating high/low voltages caused by factors *not directly related to PV.*[14] However, by comparing cases with conventional upgrades to cases with SI functions, this modeling effort did analyze the impact SI functions had on deferring PV interconnection costs.

This modeling effort analyzed Volt-VAR function with VAR priority (as opposed to watt priority).[15] This focus results from California Public Utilities Commission Resolution E-4920, which made VAR priority a requirement as part of CA Rule 21 after July 28, 2018.[16] Compared to Volt-VAR with watt priority, Volt-VAR with VAR priority has the potential to be more effective in reducing high voltages due to PV in situations where PV output is high, resulting in a high voltages, and the smart PV inverter has limited to no headroom for the Volt-VAR function to provide reactive power and help to reduce the voltage. On the other hand, Volt-VAR with VAR priority has the potential to result in curtailed PV generation at times of high PV output, when the inverter prioritizes reactive power over active power. This modeling effort evaluated the effectiveness of Volt-VAR with VAR priority to mitigate high voltages caused by PV. This modeling effort also evaluated the amount of PV production that could potentially get curtailed when Volt-VAR with VAR priority is activated. It is important to note that secondary voltage rise addressed by SI Volt-VAR activation depends on the inverter absorbing VARs from the utility distribution system.

The following section introduces the key activities conducted as part of this modeling effort, and how each activity maps to the chapters constituting this report.

---

12 IEEE 1547-2018 – IEEE Standard for Interconnection and Interoperability of DER with Associated Electric Power Systems Interfaces.

13 In fact, IEEE 1547-2018 requires smart inverters to be capable of consuming or producing reactive power when the inverter output is greater than 5% of the inverter rated active power, or the inverter steady-state active power capability, whichever is greater. This means that IEEE 1547-2018 accounts for inverters with a minimum steady-state active power capability higher than 5% of the rated active power output. In this modeling effort, the minimum active power output of PV systems was assumed to be 0 kilowatts (kW). In other words, the PV systems were assumed to start producing active power and be available to consume or produce reactive power immediately after the PV generation profile would become nonzero.

14 As introduced in Chapter 3, the baseline feeder models analyzed (i.e., without PV) had no overvoltages or undervoltages. Thus, this report only assesses the potential value of smart inverters in mitigating voltage excursions occurring when PV penetration levels increase. While manual changes to voltage regulation equipment settings were considered in this modeling effort to address overvoltages caused by PV (see Chapter 4), these manual changes did not address all overvoltages, and in some cases introduced some undervoltages.

15 Both defined in footnote 10, *supra*.

16 See footnote 3, *supra*.

1.3 Modeling Effort Activities and Report Structure

This modeling effort had five key activities. Each activity is described in one of the chapters constituting this report, as illustrated in Figure 1-2:

- **Detailed Feeder Modeling (Chapter 3)**: Six (6) PG&E feeders were modeled in high detail in OpenDSS with PV, PV SIs, and ES. The distribution feeders were modeled down to the residential customers, including detailed secondary LV circuit models, as well as detailed representation of residential customer load and PV generation based on Advanced Metering Infrastructure (AMI) and residential solar PV measurements.
- **Baseline PV Assessment (Chapter 4)**: The baseline distribution impacts were analyzed for five PV penetration levels (0%, 25%, 50%, 75%, and 100% of eligible residential customers), each with three ES penetration levels (0%, 20%, and 40% of residential PV customers). The baseline analysis was performed without considering either conventional distribution upgrades, or SI functions. In this section of the modeling effort, PV impacts were recorded, but violations were not addressed.
- **Conventional Upgrade Analysis (Chapter 5)**: Conventional distribution upgrades were identified to integrate PV and ES at the technology penetration levels analyzed, addressing any violations. Smart inverter functions were not considered in this phase of the modeling effort.
- **Smart Inverter Analysis (Chapter 6)**: The effectiveness of using SIs to address voltage impacts due to PV was considered. While this modeling effort assessed SI impacts on both primary and secondary voltages, the residential smart PV inverters analyzed were mainly effective at addressing secondary voltage impacts caused by PV. Similar to the conventional upgrade analysis, *thermal* overloads were addressed with conventional upgrades, since the SI functions analyzed in this modeling effort are not designed to effectively address thermal impacts. Indeed, as learned in the field testing component of this PG&E EPIC 2.03A project[8] (and several other past studies presented in Chapter 2), SIs are more effective at regulating voltages at higher SI densities. In this modeling effort, SI density levels of 0%, 25%, 50%, 75%, and 100% (percentage of residential PV systems) were analyzed to assess the merits of SI voltage support during the transitional period during which legacy PV inverters without smart functions will progressively be retired (see Figure 1-1). This chapter also presents an important sensitivity analysis on the impacts that the smart PV inverter facility wiring (i.e., the wiring between the customer panel and the PV inverter) can have on the SI operation, and the resulting distribution impacts. Despite the impacts that the facility wiring can have, to the best of EPRI's knowledge, this sensitivity has not been as thoroughly analyzed in prior modeling and simulation studies. However, National Renewable Energy Laboratory (NREL) and Hawaiian Electric Company (HECO) analyzed the impact of the facility wiring in the modeling effort reviewed in Chapter 2.
- **Economic Analysis (Chapter 8)**: The economic implications of growing SI densities were considered. The economic impacts of activating SI functions were estimated across four cost categories, through the lens of four cost tests. In addition, a more detailed analysis for a subset of customers particularly impacted by the activation of SI functions was conducted.

This report also includes the following chapters:

- **Chapter 1** (this chapter) provides an overview of the modeling effort and its context, and explains the structure of this report.
- **Chapter 2** summarizes the relevant literature, and compares the contributions of this modeling effort to relevant past studies.
- **Chapter 7** compares the *technical* impacts and merits of the conventional mitigation strategy relying on distribution upgrades analyzed in Chapter 5 to the strategy leveraging SI functions analyzed in Chapter 6.

Figure 1-2
Key Activities of This Modeling Effort and Structure of This Report

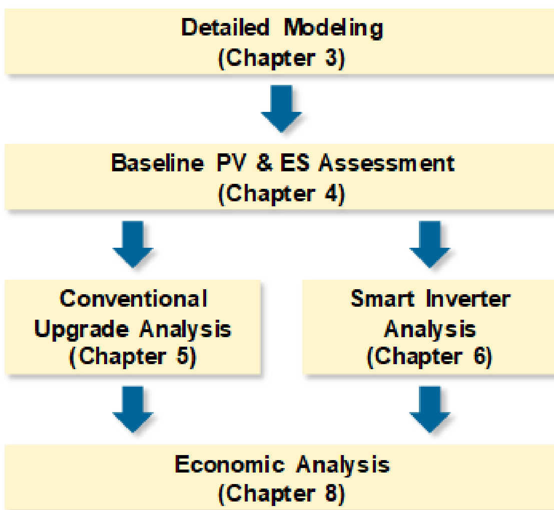

2
COMPARATIVE REVIEW OF RECENT STUDIES EVALUATING SMART INVERTER IMPACTS

2.1 Introduction

This chapter provides a critical review and comparative analysis of 13 recent studies that included one or several of the following components:

- Modeling and simulation of the impacts of PV and smart PV inverters on the distribution system;
- Analysis of the economic value of smart PV inverters; and
- Comparison of the technical and/or economic merits of strategies using conventional distribution upgrades to mitigate adverse PV impacts, to mitigation strategies leveraging SI functions.

The review presented in this chapter is intended to provide an overview of selected state of the art past studies. However, it was not feasible to review all relevant past studies here. As follows, an overview of the 13 past studies reviewed is presented first. Table 2-1 provides a comparative description of each modeling effort. Gaps and limitations identified in past studies and directly addressed by this modeling effort are highlighted. The second part of this chapter provides a summary of each of the 13 studies reviewed.

2.2 Summary of Comparative Review

2.2.1 Similarities and Differences

The 13 studies reviewed all applied distribution system modeling and simulation, including PV and SIs, to address a set of research objectives that varied from modeling effort to modeling effort.

All studies performed different combinations of static load flow (SLF), quasi-static time-series (QSTS) and/or hosting capacity analyses. Additionally, one modeling effort performed dynamic analysis on simplified distribution feeder models. For the set of studies that performed QSTS with load and PV profiles, all but one modeling effort utilized the EPRI OpenDSS simulation tool. Five studies represented secondary circuits. Only two (EPRI-APS and NREL-HECO) of these five studies represented secondary circuits at a level of detail comparable to this modeling effort.

The range of PV systems, PV penetration levels, PV deployment types, SI functions, and SI densities considered varied from modeling effort to modeling effort. Five studies evaluated distributed PV, but none of the five studies modeled PV on a number of feeders and at a level of detail comparable to this modeling effort. One modeling effort (NREL-HECO) analyzed the combined use of Volt-VAR and Volt-Watt. Two studies (NREL-HECO and NREL-PG&E-HECO-SolarCity) evaluated SI densities other than 0% and 100%. Two studies assessed the impact of residential ES systems, but none of the reviewed studies analyzed more than one ES penetration level, contrary to this modeling effort.

Among the nine studies that performed some type of time-series simulation, only three studies evaluated PV curtailment due to SI functions, and none of these three considered manual changes to voltage regulation equipment settings at higher PV penetration levels, an element that was included in this modeling effort (NREL-HECO modeling effort considered manual changes to all Load Tap Changers

(LTC) to “no control” mode, sometimes referred to as “reverse idle,” where during reverse power flow the LTCs stayed on the tap they were prior to identifying the reverse power flow. Manual setting changes to or addition of new voltage regulators were not considered as HECO does not use voltage regulators.).

Three studies evaluated conventional distribution upgrades, two of which performed economic comparison between strategies leveraging SI functions, and strategies relying on conventional distribution measures. One modeling effort considered manual adjustments to voltage regulation equipment settings at increased PV penetration levels. Two studies assessed the value of Integrated Voltage-Var Control (IVVC) that automatically adjusts voltage regulation equipment states.

Three of the studies reviewed included both technical *and* economic analysis of SI impacts. Four studies analyzed more than six PG&E (or California) feeders, but only two of these four studies included economic analysis, and none of these four studies modeled secondary circuits, or adjusted existing feeder voltage regulation settings at increased PV penetration levels, two elements that were considered in this modeling effort.

In conclusion, several of the studies reviewed analyzed more feeders than this modeling effort, but at a limited level of detail. Other studies were conducted at a level of detail similar to this modeling effort, but analyzed a smaller number of feeders.

2.2.2 Unique Contributions of This Modeling Effort

This EPIC 2.03A modeling effort appears to be one of the most comprehensive techno-economic assessments to date comparing conventional strategies using distribution upgrades to mitigate adversarial PV impacts, to strategies leveraging SI functions.

The novel contributions of this modeling effort include:

- Detailed analysis of manual adjustments to feeder voltage regulation equipment settings at increased PV penetration levels. This contribution is discussed in Chapter 4.
- Over 12,000 sensitivities analyzed, including: 6 feeders, 5 PV penetration levels, 3 ES penetration levels, 3 combinations of SI functions, 5 SI densities, 5 representative PV generation profiles, and 3 representative load profiles. These sensitivities are introduced in Chapters 4 and 6.
- The modeling of secondary LV circuits at a high level of detail. The approach for modeling secondary circuits is presented in Chapter 3.
- A method addressing the complexity of re-adjusting the settings of feeder voltage regulation equipment at higher PV penetration levels. This contribution is presented in Chapter 4.
- The modeling of conventional distribution upgrades that includes all relevant decision rules triggering these upgrades, as per PG&E’s design and engineering practices. This is discussed in detail in Chapter 5.
- A rigorous analysis of active power curtailment occurrences resulting from smart function activation across 474,633 individual PV customer cases, covering all possible combinations of sensitivity variables considered in this modeling effort. These results are presented in Chapters 6 and 8.
- An evaluation of the economic impacts of SI functions combining highly detailed techno-economic modeling at the individual customer level, together with a feeder clustering approach to extrapolate the findings for PG&E’s entire service territory. These results are presented in Chapter 8.

- An assessment of the “customer outliers,” this small subset of PV customers experiencing bill increases higher than the average PV customer when activating SI functions, and the development of an approach to minimize the number of outliers in practice. This contribution is presented in Chapter 8.

Table 2-1
Comparative review of selected past studies

Review Index	Entities Involved	Modeling effort Completion Year	Distribution Integration Measures	Voltage Regulation Equipment Settings Adjusted	Distribution Modeling Tools (Analysis Types)	# Feeders / # CA Feeders / # PG&E Feeders	PV Types	PV Penetration Levels / PV Deployments	SI Functions	SI Densities	Energy Storage Analysis	Secondary Circuits Modeled	QSTS Specifics	Analysis of PV Curtailment Due to SI Functions	Economic Analysis
This modeling effort	EPRI for PG&E	2018	Yes	Yes	OpenDSS (SLF, QSTS)	6 / 6 / 6	Residential	0%, 25%, 50%, 75%, 100%	Volt-VAR (1 curve) and combined Volt-VAR Volt-Watt (2 different curves), all with var priority	0%, 25%, 50%, 75%, 100%	0%, 20%, 40% of residential PV customers with storage	Detailed secondary modeling leveraging 121 construction types, AMI and PV measurement data	A large number of sensitivities analyzed each with daily QSTS simulations at 15-min time-interval for 3 characteristic load days and 5 characteristics PV days	Yes	Yes
1	DNV GL for CPUC	2017	Yes	No	Synergi (SLF, QSTS)	75 / 75 / 20	>100 kW systems	0%-160% of peak load / Feeder end & a random distributed deployment (each 100kW)	Volt-VAR watt priority (+sensitivity on var priority)	0%, 100%	Considered as a mitigation measure (assumed 4h duration)	No	PV outputs from 0% to 100% and back to 0%, voltage regulation equipment fixed, fixed load	No	Cost estimation of the cheapest PV integration measure
2	Quanta for PG&E	2012	No	No	CYME (SLF), PSCAD (dynamic/transient)	20 / 20 / 20	distributed PV (customer class specific kW rating)	0%, 5%, 10%, 20%, 50%, 100% of peak load / a random deployment	None	N/A	None	No	No QSTS but dynamic / transient analysis using simplified feeder models & 188 distinct SLFs	No	None
3	Navigant for PG&E	2015	Yes	Capacitor bank controls only	CYME (SLF)	20 / 20 / 20	distributed PV & wholesale PV	From 0% to 100% of feeder capacity	None (apart from CPF)	None	None	No	None	No	Analysis of T&D costs & benefits of PV
4	NREL for HECO	2018 & 2017	No	LTC controls only	OpenDSS (QSTS)	3 / 0 / 0	residential PV with larger (~500kW) FIT PVs	Current, near-term, long-term (150% to 620% of feeder day-time minimum load)	CPF 0.95, Volt-VAR, combined Volt-VAR & Volt-Watt	From 0% to 62% of PV penetration (0% and 100% of new residential PVs)	Sensitivity analysis of 30% of PV customers with storage	Yes: Mix of actual constructions and typical construction types, only 1 feeder with AMI data, all PVs followed the same profile	15-min resolution over a week, sensitivity analysis with annual QSTS	Yes	None
5	SDG&E, SolarCity	2016-2018	No	No	OpenDSS (QSTS)	1 / 1 / 0	residential PV aggregated to the primary circuit	1 PV penetration level (2.2 MW of PV)	CPF	1 density (1.2 MW out of total 2.2 MW of PV)	None	No	3-day QSTS simulations for 2 load profiles both with 3 PV profiles	Yes	None
6	EPRI	2015	No	No	OpenDSS (SLF, QSTS)	7 / 0 / 0	Utility-scale PV	1 penetration/deployment	CPF, Volt-VAR, Volt-VAR + dynamic reactive current	100%	None	No	4 days analyzed: peak/off-peak load, clear/variable solar profile	No	None
7	EPRI, NREL, SNL, PG&E, SCE, SDG&E	2016	No	No	OpenDSS (SLF, hosting capacity)	7 / 7 / 3	Utility-scale PV	Numerous penetrations & deployments up to feeder hosting capacity	CPF, Volt-VAR, Volt-Watt	100%	None	No	N/A	No	None

Table 2-1 (Continued)
Comparative Review of Selected Past Studies

Review Index	Entities Involved	Modeling effort Completion Year	Distribution Integration Measures	Voltage Regulation Equipment Settings Adjusted	Distribution Modeling Tools (Analysis Types)	# Feeders / # CA Feeders / # PG&E Feeders	PV Types	PV Penetration Levels / PV Deployments	SI Functions	SI Densities	Energy Storage Analysis	Secondary Circuits Modeled	QSTS Specifics	Analysis of PV Curtailment Due to SI Functions	Economic Analysis
This modeling effort	EPRI for PG&E	2018	Yes	Yes	OpenDSS (SLF, QSTS)	6 / 6 / 6	Residential	0%, 25%, 50%, 75%, 100%	Volt-VAR (1 curve) and combined Volt-VAR Volt-Watt (2 different curves), all with var priority	0%, 25%, 50%, 75%, 100%	0%, 20%, 40% of residential PV customers with storage	Detailed secondary modeling leveraging 121 construction types, AMI and PV measurement data	A large number of sensitivities analyzed each with daily QSTS simulations at 15-min time-interval for 3 characteristic load days and 5 characteristics PV days	Yes	Yes
8	EPRI, NREL, SNL, PG&E, SCE, SDG&E	2015	No	No	OpenDSS (hosting capacity)	16 / 16 / 6	Utility-scale PV	Numerous penetrations & deployments up to feeder hosting capacity	None	N/A	None	Yes: Generic secondary models with service transformer & a separate service line for each customer	N/A	No	None
9	EPRI for APS	2017	Yes	No	OpenDSS (SLF, QSTS, hosting capacity)	2 / 0 / 0	Residential PV	As deployed in the field during the project	Volt-VAR	100%	Yes: Two 2MW/2MWh storage systems	Yes: all secondary circuits were modeled using GIS & AMI data	Daily QSTS @ 1-min resolution, etc.	Yes	None
10	EPRI	2013	No	No	OpenDSS (hosting capacity)	4 / 0 / 0	Utility-scale PV	Numerous penetrations & deployments up to feeder hosting capacity	CPF 0.95 & 0.98, Volt-VAR, Volt-Watt	0%, 100%	None	No	Sensitivity analysis on SI function time-varying impacts	No	None
11	EPRI	2015	No	No	OpenDSS (hosting capacity)	4 / 0 / 0	Utility-scale and residential PV	Numerous penetrations & deployments up to feeder hosting capacity	CPF 0.95 & 0.98, Volt-VAR, Volt-Watt	0%, 100%	None	No	N/A	No	None
12	NREL, Duke Energy	2016	No	Yes (IVVC-based control, no manual adjustments considered)	Alstom Grid's e-terra distribution	1 / 0 / 0	Utility-scale PV	1 real PV system	CPF 0.95, Volt-VAR	0%, 100%	None	No	40 days at 1-min resolution	No	Yes (value of autonomous SI functions & IVVC)
13	NREL, PG&E, HECO, SolarCity	2016	No	Yes (voltage optimization scheme for CVR)	OpenDSS	2 / 1 / 1	Small (residential & commercial)	50, 75, 100, 125, 150% (of feeder peak load), 1 random deployment	Volt-VAR (with custom profile)	0%, 25%, 50%, 75%, 100%	None	Yes: Generic secondary models with service transformer & a separate service line for each customer	Annual simulation at 1-hour resolution	Yes	None
14	DOE, EPRI, multiple utilities	2013	No	No	OpenDSS	1 / 0 / 0	Utility-scale and residential PV	Numerous penetrations & deployments up to feeder hosting capacity	CPF 0.95, 0.98, Volt-VAR, Volt-Watt	0%, 100%	None	Yes: Generic secondary models with service transformer & a separate service line for each customer	330days at 5s resolution using measurements from 256 field sites	No	None

1. Residential Zero Net Energy Building Integration Cost Analysis[17]

This report presents a modeling effort performed by Det Norske Veritas Germanischer Lloyd (DNV GL) for the CPUC analyzing the grid integration costs of customer-sited PV between 2016 and 2026. The report compares a base scenario with projected PV growth in California to an alternative scenario with projected PV growth resulting in from the requirement for all new residential construction in California to be Zero Net Energy (ZNE) by 2020. The modeling effort analyzed 75 feeders from the three CA IOUs (20 from PG&E). The modeling effort used PG&E feeders identified by Navigant in an earlier modeling effort.[18]

The modeling effort analyzed PV impacts on static voltage (Rule 2 +/-5%), transient voltage (CA Rule 21 +/-3%), thermal loading (100% of rated), and reverse power flow (over voltage regulation equipment). Further PV impacts related to protection and beyond were not analyzed. For each feeder, PV penetration levels exceeding the technical criteria were analyzed, and mitigation measures and their associated costs were identified. Based on the results, an integration cost function was derived for each of analyzed 75 feeders. The integration cost functions of the analyzed feeders were then extrapolated to the rest of the feeders in the utility service territory leveraging PV penetration forecast.

For each feeder, two PV deployments (all at the furthest bus and distributed equally at increments of up to 100 kW) were analyzed. Different penetration levels from 0% to 160% were analyzed. For each deployment, SLF and quasi-static time-series analysis (QSTS) were performed to identify potential violations. SLF was performed with rated DG output for minimum (MIN) and peak load. PV generation profile(s) were not used for the QSTS analysis. Instead, PV impacts were studied when PV output was varied from peak to zero and then back to peak without allowing voltage regulation equipment to operate. The report does not clearly specify which load modeling approach was followed.

For each case with violations, the cheapest mitigation measure was identified. The mitigation measures considered include control upgrades on voltage regulators (cogen mode for voltage regulators or LTC), additional voltage regulation equipment, reconductoring, and ES. Due to the lack of data, the modeling effort did not consider circuit reconfiguration/load transfer as an alternative integration measure. The report does not clearly state how the upgrade measures were identified. In particular, the report does not specify if setting adjustments were considered for the feeder voltage regulation equipment.

The modeling effort only analyzed PV installations with a capacity of 100 kW and beyond. Secondary circuits were not modeled and residential customer load and PV were not represented in detail.

The modeling effort considered SI functions as one of the mitigation measures. Most of the analysis assumed *watt priority* for Volt-VAR function. In this configuration, the PV inverters did not consume any reactive power during peak PV output, and the modeling effort concluded that SI functions were not an effective PV integration measure. A sensitivity analysis of Volt-VAR with *var priority* was also performed in the modeling effort. The results of this sensitivity analysis indicated that Volt-VAR with *var priority* could considerably reduce/limit overvoltages caused by PV and thus, significantly reduce PV integration costs. As a result, the modeling effort recommended the volt-ampere reactive (VAR) priority mode.

---

17 "Residential Zero Net Energy Building Integration Cost Analysis - Customer Distributed Energy Resources Grid Integration Study," Prepared by DNV GL for CPUC, 10007451-HOU-R-02-D, Oct. 2017. Available: http://www.cpuc.ca.gov/WorkArea/DownloadAsset.aspx?id=6442455013.

18 "Impact of Solar Photovoltaic (PV) Systems on the Pacific Gas and Electric Distribution Grid (Volume 1, Rev. 1)," Prepared by Quanta Technology for PG&E, Dec. 2012.

2. Impact of Solar Photovoltaic (PV) Systems on the Pacific Gas and Electric Distribution Grid[19]

This report presents the findings from a modeling effort performed by Quanta for PG&E. The modeling effort evaluated the steady-state and dynamic distribution system impacts of distributed PV on PG&E's service territory. The steady-state analysis was performed in CYME and the dynamic impacts in Power System CAD software (PSCAD). The modeling effort also analyzed mitigation measures to address adverse PV impacts.

The modeling effort analyzed only small residential PV; larger commercial or industrial PV systems were not analyzed. Secondary circuits were not modeled due to the lack of data (secondary circuits were not modeled in CYME). As a result, the modeling effort did not represent PV secondary circuit impacts.

The modeling effort did not analyze SI functions. All PV systems were assumed to operate at unity power factor.

A clustering method was applied to select 20 PG&E feeders for analysis. The modeling effort analyzed 5%, 10%, 20%, 50%, and 100% PV penetration levels (total rated PV output of the feeder peak load). A random PV deployment was analyzed for each feeder and PV penetration level. All customers within a given customer class were assumed to have the same PV size. No diversity in PV installation sizes was considered.

Generic voltage regulation settings and states were utilized for the feeders analyzed. No changes to the settings or states were considered at higher PV penetration levels. The modeling effort also simplified open-delta voltage regulator banks to be closed-delta voltage regulator banks. All capacitors were assumed to be either fixed (ON during summer and OFF during winter), or controlled based on time or temperature (ON during day-time, OFF during night-time). Voltage override was considered for time and temperature-controlled capacitors. No changes to capacitor control settings were considered as PV penetration levels were being increased in simulations.

The modeling effort analyzed PV impacts on steady-state voltages, feeder element loadings (reverse power flow), dynamic voltage fluctuations (impact of PV output variability), transient overvoltages (islanding and other switching events), and operational issues (voltage regulation equipment states, general protection concerns).

The steady-state impacts were analyzed by performing a SLF for annual noon-time feeder MAX and MIN load levels. For both load levels, separate load flows were performed for all day-time hours with PV generation (6AM-7PM). As a result, 188 SLF simulations were performed for each feeder. All PV systems on all feeders were assumed to follow the same generic PV profile.

Instead of QSTS, dynamic studies were performed with PSCAD on reduced feeder models that involved a number of simplifications: the PSCAD models only included the feeder main 3-phase trunks; a number of PVs were lumped together as a large PV system; the dynamic analysis was performed over a 60-min time-period; all PVs we assumed to follow the same profile. Additionally, although not clearly stated in the report, the PSCAD models were apparently 3-phase, thus ignoring the influence of voltage and current unbalance, and ignoring the complex behavior of single-phase controlled voltage regulation banks, including open-delta voltage regulator banks on three-wire feeders.

[19] See footnote 18, *supra*.

The modeling effort concluded that the 4 kV feeders analyzed and some of the 12 kV feeders analyzed were sensitive to PV impacts whereas the 21 kV feeders and other 12 kV feeders were not sensitive to PV impacts. The modeling effort recommended SI Volt-VAR function to reduce voltage issues, voltage regulation equipment tap operations, and other impacts due to PV. The modeling effort also recommended using intelligent voltage regulators and capacitor bank controllers as opposed to fixed capacitor banks and unidirectional voltage regulators.

3. Distributed Generation Solar Photovoltaic Transmission & Distribution Impact Analysis[20]

This report presents a modeling effort performed by Navigant for PG&E. The objective of this modeling effort was to develop a range of transmission and distribution costs and benefits associated with interconnecting high levels of PV on PG&E's service territory. The modeling effort analyzed the impacts, costs and benefits of interconnecting low, medium and high PV penetration levels.

Two types of PV systems were analyzed: highly distributed "retail" PV and larger "wholesale" PV. The wholesale PV systems were modeled individually whereas the retail PV systems were lumped on feeder segments. The modeling effort analyzed PV penetration levels from 10% to 100% of the feeder capacity.

The modeling effort analyzed 20 PG&E feeders that were selected in an earlier modeling effort by Quanta.[21] This modeling effort involved both distribution SLF performed in CYME and transmission analysis performed in Positive Sequence Load Flow. The modeling effort quantified PV impacts in the following criteria: line thermal loading, steady-state voltages, voltage flicker, protection system impacts, and voltage regulation equipment operations.

No secondary circuits were modeled. As a result, secondary-level system impacts, secondary upgrades, or any of the associated costs were not considered. However, the modeling effort limited the voltage variations allowed on the primary circuit to slightly less than +/-5%.

This modeling effort considered several conventional distribution upgrades to mitigate PV impacts, including: PV off-nominal power factor, reconductoring lines, upgrading substations, and new feeder voltage regulation equipment. PV off-nominal power factor was observed to be very effective in mitigating PV voltage-related issues. No SI functions were analyzed apart from the off-nominal power factor. PV curtailment due to potentially limited inverter capacity was not analyzed.

The distribution system benefits evaluated resulting from PV deployments included: substation/feeder capacity deferral, reduced distribution losses, improved voltage regulation, and enhanced reliability/security. The primary benefit was observed to be capacity deferral. However, the merit of PV deployments in deferring capacity was also observed to be limited due to the non-coincidence of peak load and PV generation. The modeling effort found that interconnecting PV resulted in positive net costs for all considered scenarios although the benefits were higher and the costs lower for some favorable scenarios than for other less favorable scenarios. The modeling effort found wholesale PV interconnection costs to be higher (per interconnected megawatt (MW)) compared to retail PV due to the higher impacts that concentrated retail PV was observed to cause.

---

20 "Distributed Generation Solar Photovoltaic Transmission & Distribution Impact Analysis," Prepared by Navigant for PG&E, Aug. 2015.

21 See footnote 18, *supra*.

4. Simulation of Hawaiian Electric Companies Feeder Operations With Advanced Inverters and Analysis of Annual Photovoltaic Energy Curtailment and Advanced Inverter Voltage Controls: Simulation and Field Pilot Findings[22,23]

These two reports present a collaborative research project between NREL and HECO. The project analyzed the trade-offs of the grid benefits and curtailment impacts from the activation of selected SI grid support functions (GSF). The project had two parts. The first part referred to as the "VROS modeling effort"[24] was carried out in 2017. The second part of the project[25] continued the work in 2018. In addition to distribution modeling and simulation, the 2018 work also included a field validation. This following is a review of the distribution modeling and simulation aspects addressed in both reports, with a focus on the 2018 findings.

The project assessed three PV penetration levels (current, pending projects/near future, and high-penetration). For each penetration level, QSTS simulations were performed at 15-min resolution over the "highest voltage week" on three Hawaii (O'ahu island) feeders (on two substations) with existing high penetration of rooftop PV systems. The modeling effort also performed QSTS for a subset of the cases.

Detailed OpenDSS feeder models were implemented including detailed substation and secondary system models. The secondary circuits in the suburban area of Feeder 34 were modeled specific to each secondary circuit as the model information was obtained from the specific developers of the suburban areas. The other secondary circuits were modeled based on typical HECO secondary construction types as the actual secondary circuit models were not available. The secondary construction types were chosen based on customer type, overhead vs. underground, transformer nameplate rating, and the transformer customer count. The secondary circuits created were not validated due to the lack of voltage measurement data. The 2018 modeling effort found that customers experiencing the highest curtailment were on generic extreme secondary circuit models (implemented by NREL) that did not reflect real HECO secondary circuits (either in terms of secondary line lengths, or total nameplate PV capacity per transformer). This emphasizes the importance of accurate and realistic secondary circuit modeling.

On one of the three feeders, loads were represented with AMI data. On the two other feeders, loads were modeled with feeder head load allocation that does not capture secondary level load variability. No diversity in PV operating profiles was considered as all PV systems were assumed to follow the same normalized operating profile.

According to the report, HECO primarily applies substation LTCs as opposed to voltage regulators and/or capacitor banks. As a result, the modeling effort only considered adjustments to the LTC settings and did not consider adding new voltage regulation equipment as PV penetration levels were being increased in the simulations. The LTCs were set to "no control," sometimes referred to as "reverse idle,"

---

22 J. Giraldez, A. Nagarajan, P. Gotseff, V. Krishnan, and A. Hoke, "Simulation of Hawaiian Electric Companies Feeder Operations with Advanced Inverters and Analysis of Annual Photovoltaic Energy Curtailment," Golden, Colorado, Technical Report NREL/TP-5D00-68681, Sep. 2017. Available: https://www.nrel.gov/docs/fy17osti/68681.pdf.

23 J. Giraldez et al., "Advanced Inverter Voltage Controls: Simulation and Field Pilot Findings," NREL, Golden, Colorado, NREL Technical Report NREL/TP-5D00-72298, Oct. 2018.

24 See footnote 22, *supra*.

25 See footnote 23, *supra*.

where during reverse power flow the LTCs stayed on the tap they were prior to identifying the reverse power flow. Instead, the modeling effort analyzed four SI GSF: (1) constant power factor (CPF) 0.95 (inductive); (2) Volt-VAR with VAR priority; (3) Constant Power Factor (CPF) 0.95 (inductive) combined with Volt-Watt; and (4) Volt-VAR with VAR priority combined with Volt-Watt. The modeling effort used HI Rule 14 Volt-VAR and Volt-Watt settings. All PV systems were assumed to have Direct Current/ Alternating Current (DC/AC) -ratio of 1.2.

The modeling effort applied a combination of OpenDSS built-in SI model and custom Python-based SI models. Custom models were implemented to obtain certain capabilities not available from OpenDSS at the time of the modeling effort, and address convergence issues with the OpenDSS SI models that the modeling effort team encountered. These OpenDSS convergence issues have been likely addressed since then, since this EPIC 2.03A modeling effort did not experience any convergence issues when using OpenDSS SI models for the Volt-VAR and combined Volt-VAR and Volt-Watt functions, both assuming VAR priority. More details on the SI modeling performed in this EPIC 2.03A modeling effort can be found in Chapter 6. The custom Python-based SI model implemented by NREL in the 2017 modeling effort converged one PV system at a time (as opposed to reaching convergence for all PV systems simultaneously). This resulted in overestimating the active power curtailment experienced by PV systems that were among the first to converge. The NREL team addressed this issue in the 2018 work by modifying the custom-made Volt-Watt control.

The modeling effort found Volt-VAR to be more effective than CPF 0.95 at addressing PV overvoltages. This finding was naturally expected since the minimum power factor of HI R14 Volt-VAR is 0.90, which results in notably higher reactive power consumption than the CPF 0.95 analyzed. The modeling effort also found Volt-VAR to result in lower PV curtailment and feeder head reactive power consumption when compared to CPF 0.95.

The activation of reactive power priority was recommended as a measure to avoid momentary overvoltages. The combination of Volt-VAR with Volt-Watt was also recommended to mitigate rarely occurring high overvoltages. The HI Rule 14 Volt-VAR function was found to be very effective in mitigating/avoiding overvoltages due to PV. Moreover, Volt-Watt was found to be effective in mitigating the rarely occurring very high overvoltages. Volt-Watt was also found to be activated very infrequently.

The 2018 modeling effort (with refined SI Python modeling) found the maximum curtailment due to combined Volt-VAR and Volt-Watt to be low. The average customer curtailment was 0.23% and the highest individual customer curtailment was 1.7%. Combining Volt-VAR with Volt-Watt resulted in a very small increase in curtailment. The curtailment was observed to depend on PV penetration, SI density, and SI function.

The 2018 modeling effort analyzed the impact that very high overvoltages could have on PV curtailment. The results suggest that the Volt-Watt function could unexpectedly reduce PV curtailment by allowing more PV systems to continue generating during very high overvoltage episodes, defined as going beyond the IEEE 1547 overvoltage disconnect limit of 1.1 per unit (p.u.). However, it is important to note that in practice, the utility is responsible for addressing such extremely high voltage situations with appropriate distribution upgrades, which may limit the number of very high overvoltage instances where the Volt-Watt functions could provide value.

The 2018 modeling effort included cases that considered distribution upgrades on secondary circuits. All secondary circuits with a total PV nameplate over 200% of the transformer kVA nameplate were upgraded. In such cases, when the circuit supplied less than 10 customers, the transformer was upgraded. For secondary circuits with more than 10 customers, the secondary circuit was divided into two secondary circuits (a second transformer was added). The secondary upgrades considered reduced the occurrence of extreme voltages and the active power curtailment resulting SI function activations.

The modeling effort did not model the PV facility wiring, i.e., the wiring between the customer panel and the PV inverter. However, the 2018 field pilot analyzed field data from PV inverters and found that, due to PV wiring, the SI voltages could be notably higher than the customer panel voltages, which could lead to higher-than-expected PV curtailment. This EPIC 2.03A modeling effort analyzed the impact of PV facility wiring in detail.

The 2018 modeling effort assessed HECO PV interconnection screens and concluded that the screens were conservative, but effective in identifying customers with potential overvoltages due to PV. Some refinements to the screens were proposed. The 2018 modeling effort emphasized the value of having sufficient visibility to customer voltages before interconnecting new PV systems, to detect potential high voltage problems early.

The modeling effort analyzed the distribution impacts from residential ES systems. ES were randomly assigned to 30% of the customers with rooftop PV. ES was modeled with OpenDSS ES model. ES control was implemented in Python. ES was sized to prevent export at all times. The ES case resulted in lower curtailment values due to less PV exports. The modeling effort also analyzed utility-scale ES. ES located at the substation was observed to slightly reduce LTC tap operations, but, as expected, did not improve customer voltages. Similarly, a utility-scale ES located close to the PV customers did not notably reduce customer curtailment, due to the medium-voltages (MV) staying quite low. This EPIC 2.03A modeling effort analyzed the impact from different penetrations of residential PV and ES without and with SIs.

5. San Diego Gas & Electric's Demonstration Project C – With Existing Distributed Energy Resources (DER) on Circuit 701[26,27,28]

These references discuss a SDG&E's demonstration titled "project C – with existing Distributed Energy Resources (DER) on Circuit 701." The purpose of this project was to demonstrate DER locational benefits by validating the ability of DER to achieve net benefits consistent with locational net benefits analysis. In particular, this project aimed to demonstrate the ability of DER to provide voltage and power quality services through SI voltage and VAR support functions, potentially deferring capital investments in voltage regulation equipment. The project evaluated CPF and Volt-VAR functions through two project phases: a modeling phase, and a field demonstration phase.

In the modeling phase of the project, SDG&E partnered with NREL and SolarCity to assess SI voltage and reactive power support via distribution modeling and simulation. The modeling effort analyzed PV with and without SIs on one SDG&E distribution feeder. The analysis was restricted to one PV penetration level, one PV deployment, and one SI density. CPF was analyzed for 0.95, 0.90, and 0.85 (both inductive and capacitive). Three different Volt-VAR curves were analyzed. The SI functions were assessed by

---

26 "Demonstration Projects C and E Final Reports of San Diego Gas & Electric Company (U 902 E)." CPUC, 14-Sep-2018.

27 F. Ding et al., "Voltage support study of smart PV inverters on a high-photovoltaic penetration utility distribution feeder," in 2016 IEEE 43rd Photovoltaic Specialists Conference, Portland, OR, USA, 2016.

28 F. Bell, A. Nguyen, M. McCarty, K. Atef, and T. Bialek, "Secondary voltage and reactive power support via smart inverters on a high-penetration distributed photovoltaic circuit," in 2016 IEEE Power & Energy Society Innovative Smart Grid Technologies Conference, Minneapolis, MN, USA, 2016.

performing 3-day QSTS simulations for two load profiles (max and min), both for three PV profiles. The modeling effort assumed a DC/AC ratio <1.0, i.e., the PV inverters were assumed to be oversized with respect to the PV panels. The modeling effort also assumed the Volt-VAR curve to be based on available VARs (as opposed to the inverter rated VARs). Moreover, the modeling effort assumed watt priority (as opposed to VAR priority). As a result, the PV active power output was never curtailed in the modeling effort, but the inverter reactive power output depended notably on the available VARs. Finally, the modeling effort assumed that the Volt-VAR function was able to provide VARs outside of PV generation times ("VARs at night"). The modeling effort found Volt-VAR to maintain the feeder voltages in a narrower band compared to CPF. Volt-VAR curves without deadband or smaller deadband resulted in tighter voltage bands. The modeling effort emphasized that Volt-VAR benefits could have been greater had reactive power priority been applied.

In the field demonstration phase of the project, SDG&E worked with SolarCity to install of a total of 400 kW PV systems equipped with SIs.[29] The field demonstration location was identified based on sites where SolarCity was actively installing large numbers of PV systems, and where SolarCity was willing to partner with SDG&E to install new SIs. The primary circuit voltages for the demonstration feeder selected appeared to never exceed the American National Standards Institute (ANSI) limits. Therefore, no primary circuit voltage regulation benefits achieved by SIs could be demonstrated, or even necessary. The fact that the SI penetration achieved was relatively small compared to the total feeder loading is another factor explaining that only limited grid impacts were observed after deploying the SIs. As part of the field demonstration, CPFs of 0.95 inductive and capacitive and Volt-VAR with three different curves were evaluated. Compared to CPF, Volt-VAR was observed to result in a flatter and less variable voltage profile. More aggressive Volt-VAR curves and Volt-VAR curves without a dead band were observed to be more effective. SIs were also observed to be theoretically capable of maintaining the power factor of the analyzed service transformer at unity.

6. Analysis to Inform CA Grid Integration: Methods and Default Settings to Effectively Use Advanced Inverter Functions in the Distribution System[30]

This EPRI report presents default PV CPF and Volt-VAR settings that can be leveraged without additional analyses regardless of where SIs are located. The report also presents three methods to determine appropriate SI CPF settings to reduce the voltage impact due to PVs. While these three methods vary in complexity, data requirements, and effectiveness, all were found to help reduce voltage rise due to PV.

The modeling effort found that CPF can be effective in mitigating voltage rise issues. The modeling effort also found that identifying good CPF settings for a single DER system can be straightforward. On the other hand, CPF also always draws reactive power from the grid (even when not needed) and this reactive power, which can be large for feeders with high DER penetration, must be sourced from somewhere. It is also less straightforward to identify effective CPF settings for feeders with high DER penetrations (due to multiple DERs). The report proposes three methods to identify CPF settings that vary in complexity and effectiveness. The report shows results for the three methods being applied to seven feeders with high DER penetration.

---

[29] The original project plan involved installing 700 kW of PV with smart inverters, but the number was reduced as SolarCity withdrew from the project due to communication issues and increasing costs.

[30] Analysis to Inform CA Grid Integration: Methods and Default Settings to Effectively Use Advanced Inverter Functions in the Distribution System. EPRI, Palo Alto, CA: 2015. 3002007139. Available: https://www.epri.com/#/pages/product/000000003002007139/.

DER location was found to play a key role in the effectiveness of DER VAR control. The location impact is illustrated in Figure 2-1. VAR control is most effective in the middle of the feeder where both short-circuit impedance and X/R ratio are high. On the other hand, VAR control may be less effective at the end of the feeder where X/R ratio is low, or at the feeder head where the short-circuit impedance is small. This report focused on large DER installations connected to the primary (medium voltage) circuit. In LV secondary circuits, short-circuit impedances are higher and X/R ratios depend notably on the service transformer and the secondary circuit impedances.

Figure 2-1
Distribution Feeder Regions Where DER VAR Control Is Most or Less Effective

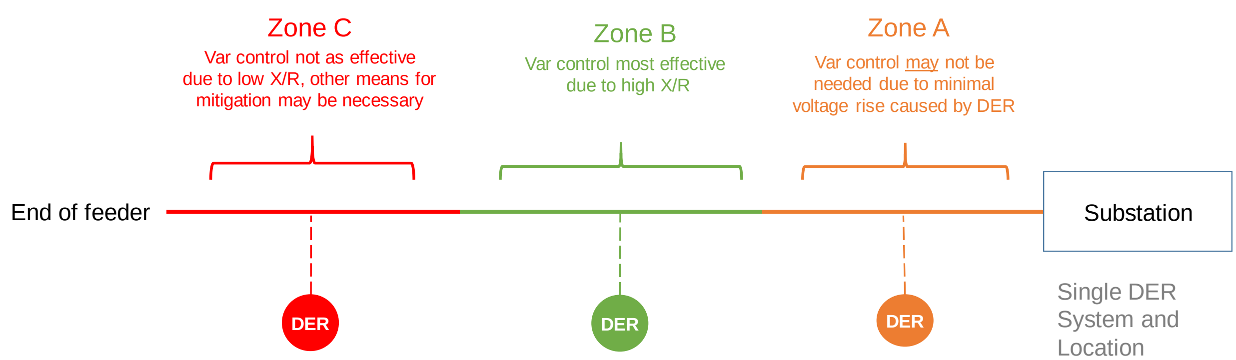

In addition to CPF, this EPRI modeling effort analyzed default Volt-VAR function settings proposed in the draft version of the IEEE 1547. QSTS was performed in OpenDSS for seven distribution feeders to assess the effectiveness of the default Volt-VAR settings. The QSTS was performed over four characteristic days (two load and two PV days). The default Volt-VAR settings were found to reduce but not fully mitigate the overvoltages and voltage variations due to PV. This was in part explained by the Volt-VAR curve that only resulted in 20% of reactive power at ANSI C84.1 limits of 0.95 and 1.05p.u. Note that at the ANSI limits, CA Rule 21 (resp. HI Rule 14) Volt-VAR curve results in 10% (resp. 30%) of reactive power.

This EPRI report also analyzed combined Volt-VAR and dynamic reactive current (also known as adaptive Volt-VAR control), which is intended to reduce voltage variability due to PV. Compared to Volt-VAR alone, combined Volt-VAR and dynamic reactive current resulted in reduced voltage variations.

7. Analysis to Inform CA Grid Integration Rules for PV: Final Report on Inverter Settings for Transmission and Distribution System Performance[31]

This report presents the research performed by EPRI, NREL, Sandia National Laboratories (SNL) with data provided from PG&E, SCE, and SDG&E. The research was supported by the fourth solicitation of the California Solar Initiative (CSI). This research determined optimal default settings for DER SI functions. The SI functions considered included CPF, Volt-VAR, and Volt-Watt. Additionally, SI functions aimed to improve transmission system response were analyzed in the report, but are not discussed in the following.

The report suggested SI function settings and methods to determine settings that can be used to improve the accommodation of PV. The methods proposed for identifying the SI settings are listed in Table 2-2. The proposed methods for identifying CPF settings are identical to the methods documented in footnote 23. Methods with three levels of complexity and expected level of effectiveness are proposed for identifying Volt-VAR function settings: the Level 1 method uses default curve proposed, e.g., by IEEE 1547; the Level 2 method is based on the feeder voltage profile; the Level 3 method is similar to Level 2, but considers PV interconnection transformer impedance.

Table 2-2
Overview of The Methods Developed to Determine Smart Inverter Settings[32]

Level	Complexity	Power Factor	Volt-VAR	Volt-Watt
0	None	Unity Power Factor	Disabled, Unity Power Factor Applied	Disabled, Unity Power Factor Applied
1	Low	Based on Feeder X/R Ratio	Generic Setting	Generic Setting
2	Medium	Based on Feeder Model and PV Location	Based on Feeder Model and PV Location	Not Analyzed
3	High	Based on Feeder Model and PV Location	Based on Feeder Model, PV Location, and Service Transformer Impedance	Not Analyzed

31 "Analysis to Inform CA Grid Integration Rules for PV: Final Report on Inverter Settings for Transmission and Distribution System Performance," Electric Power Research Institute, Palo Alto, CA, EPRI Technical Report 3002008300, 2016. Available: http://www.calsolarresearch.ca.gov/images/stories/documents/Sol4_funded_proj_docs/EPRI4_Smith/CSIRD_D_Sol4_EPRI_Analysis-to-Inform-CA-Grid-Integ-Rules-for-PV_FinalRpt_2016-09.pdf.

32 See footnote 30, *supra*.

Seven feeder models (including three from PG&E), which were previously selected and modeled in the CSI3 project,[33] were analyzed in this report. The research focused on the voltage impacts (steady-state primary and secondary overvoltage, primary and secondary voltage deviation, voltage unbalance) that are the main beneficiary from SI GSFs. The distribution system impacts of utility-scale PV were analyzed through detailed hosting capacity analysis. Hosting capacity analysis was based on analyzing PV impacts over a large number of stochastic PV deployments, each consisting of a number of 500 kW utility-scale PV systems placed at five randomly chosen feeder 3-phase buses. PV impacts were analyzed for each deployment for min and max loading scenarios. The hosting capacity analysis did not include QSTS analysis. Possible interactions between SI functions and feeder voltage regulation equipment were not addressed in the modeling effort. PV output curtailment potentially resulting in from SI functions was not assessed.

SI functions were observed to increase overvoltage hosting capacity on all feeders analyzed. The improvement depended on the feeder characteristics, just as hosting capacity does. A good balance between hosting capacity increase and feeder reactive power consumption was achieved by the default IEEE 1547 settings. Smart inverter functions with higher reactive power consumption were observed to increase the feeder losses and reactive power demand.

8. Alternatives to the 15% Rule: Final Project Summary[34]

This report presents research performed by EPRI, NREL, SNL with collaboration from PG&E, SCE, and SDG&E. This research was supported by the third solicitation of the CSI. This research aimed to improve utility application review and approval process for interconnecting DERs to the distribution system. The key activities in the project included: data collection from the utility partners, clustering analysis of all the feeders from the utility partners to select representative feeders, detailed modeling of the representative feeders, and PV impact assessment on the feeders, and the development and validation of refinements to the utility interconnection screening processes.

Clustering analysis was performed to identify a set of representative feeders.[35] The clustering analysis was based on groups of feeder characteristics including: nominal voltage level, feeder length, main conductor type, voltage regulation schemes (LTC, voltage regulators, switched capacitor banks), and load mix (residential, commercial, industrial). The clustering analysis selected 16 representative feeders. A subset of seven out of the 16 feeders selected by the clustering analysis performed in this research was further analyzed.[36] This EPIC 2.03A modeling effort analyzed six PG&E feeders out of the 16 feeders. Of these six feeders, three were analyzed also.[37]

Detailed hosting capacity analysis was performed for the 16 representative feeders leveraging OpenDSS. The considered hosting capacity constraints were: primary and secondary overvoltage, primary and secondary voltage deviation, regulator voltage deviation, sympathetic breaker tripping, breaker

33 "Alternatives to the 15% Rule: Final Project Summary," Electric Power Research Institute, Palo Alto, CA, EPRI Technical Report 3002006594, Dec. 2015. Available: https://www.epri.com/#/pages/product/000000003002006594/.

34 See footnote 33, *supra*.

35 Clustering Methods and Feeder Selection for PV System Impact Analysis. EPRI, Palo Alto, CA: 2014. 3002002562. Available: https://www.epri.com/#/pages/product/000000003002002562/.

36 See footnote 31, *supra*.

37 See footnote 31, *supra*.

reduction of reach, breaker/fuse coordination, and element fault current levels. Hosting capacity was analyzed for both utility-scale and distributed residential/commercial PV.

One key finding was that every feeder had a unique response to PV due to the endless combinations of feeder characteristics and customer load dynamics on the feeder. Specific feeder characteristics impact the feeder's response to PV. A characteristic can help to identify whether PV has an impact, but a characteristic cannot be used to identify the magnitude of the impact. PV impact was observed to considerably depend on feeder voltage class, resistance, voltage regulators, and PV system connection. The characteristics were observed to interact in complex ways ultimately dictating the feeders PV hosting capacity. As a result, the detailed hosting capacity analysis results could not be directly mapped to other feeders. While all the feeders within a cluster are not expected to have the same response to PV, feeders from different clusters are more likely to have different responses to PV.

As a result of the uniqueness of each feeder's response to PV, the report recommends analyzing each feeder instead of attempting to estimate a feeder's response from another feeder's response. However, since it is not practical to apply to every single utility feeder the detailed hosting capacity analysis performed in the modeling effort, approaches were developed to streamline the PV impact analysis. The detailed hosting capacity analysis performed in the modeling effort led to the development of the original EPRI streamlined hosting capacity methodology that has since then evolved into the EPRI DRIVE tool.[38]

9. Arizona Public Service Solar Partner Program: Advanced Inverter Demonstration Results[39]

This report documents the research findings through early 2017 of the Solar Partner Program, where Arizona Public Service (APS) and EPRI have sought to evaluate PV SIs and improve PV integration into APS system. In addition to SI, this project also assessed ES and IVVC as measures to maintain power quality and reliability. In the first phase of the research (2015-01/2017), 1,600 utility-owned and operated residential PV systems (>10 MW capacity) were deployed and their effects on the grid were studied.

Six distribution feeders were monitored and controlled as part of this research. Two of the six feeders were selected for modeling and simulation work. The selected feeders were modeled in detail in OpenDSS. Secondary circuits and individual customers were modeled in detail leveraging data from Geographic Information System (GIS) and AMI.

Detailed hosting capacity analysis was performed on the two feeders modeled. Compared to PVs with nominal power factor, CPF 0.98 was shown to notably increase the voltage-related hosting capacity on the two feeders. Detailed modeling and analysis of SI Volt-VAR and Volt-Watt functions and settings was also performed. For each function and setting, a QSTS analysis was performed at 1-min granularity over two representative load days (peak and min) and three solar profiles (clear, variable, overcast). Several performance metrics were tracked to compare the SI settings. However, the SI setting analysis was based on the relatively low SI penetration on the analyzed feeders.

---

38 J. Smith, L. Rogers, and M. Rylander, "Defining a Roadmap for Successful Implementation of a Hosting Capacity Method for New York State," Palo Alto, CA. EPRI Report ID: 3002008848., 2016. Available: https://www.epri.com/#/pages/product/000000003002008848/.

39 "Arizona Public Service Solar Partner Program: Advanced Inverter Demonstration Results," Electric Power Research Institute, Palo Alto, CA, EPRI Technical Report 3002011316, May 2017.

In addition to modeling and simulation, this project included extensive field testing of SIs. In the testing, the SI functions were turned on for a day, and then turned off for a day. The field testing analyzed fixed power factor, Volt-VAR, active power limiting, and fixed reactive power functions. Several settings were analyzed for each function.

The project operated Volt-VAR functions with VAR priority. The resulting curtailment was minor due to the relatively modest DC/AC-ratio of 1.1 and PV output reduction caused by thermal degradation.

The project found Volt-VAR to be the most effective SI function for the APS feeders selected with dynamic load changes (due to temperature changes). More aggressive Volt-VAR curves were observed to be more beneficial in reducing adverse voltage impacts. At low SI densities, even aggressive SI settings were not observed to interfere with voltage regulation equipment operations. Due to the low SI penetration levels, the primary feeder voltages were not noticeably influenced by SI. Retrofitting legacy PV inverters with SI capabilities could potentially improve the overall value of SIs.

10. Grid Impacts of Distributed Generation With Advanced Inverter Functions: Hosting Capacity of Large-Scale Solar Photovoltaic Using Smart Inverters[40]

This EPRI report analyzes the impact of SI GSF on distribution feeders through hosting capacity analysis. Hosting capacity of utility-scale PV was analyzed on four feeders leveraging OpenDSS.

The hosting capacity analysis was performed using the following principle. PV penetration is increased up to 10MW by adding a 500kW PV system to a randomly chosen feeder location (from a list of pre-identified probable locations for PV interconnection). For each PV penetration level and random PV deployment, PV impacts are analyzed. This process is repeated for a large number of random PV deployments resulting in a range of hosting capacity for each PV penetration level. The same hosting capacity analysis was performed without and with SI functions. OpenDSS built-in SI model was used. The modeling effort analyzed CPF (0.95 and 0.98), two Volt-VAR curves, and two Volt-Watt curves.

Almost all SI functions increased hosting capacity. In some cases, hosting capacity was radically increased by a SI function. Power factor control was effective at increasing minimum hosting capacity, and Volt-VAR control in increasing maximum hosting capacity. In most cases, CPF 0.95 resulted in higher hosting capacity than CPF 0.98. Poor Volt-VAR setting was observed not to increase hosting capacity.

To assess the time-varying impacts of the SI functions and settings analyzed, a sensitivity analysis was performed using QSTS in OpenDSS. The SI functions had very different time-varying impacts highlighting the importance of assessing SI functions with QSTS.

11. Smart Grid Inverters to Support Photovoltaic in New York Distribution Systems[41]

This EPRI report studies the impacts of SI GSFs on New York distribution feeders through hosting capacity analysis. Hosting capacity analysis (methodology similar to footnote 40) without and with SI GSFs is performed to assess the additional amount of PV that can be accommodated if SI functions were used. The modeling effort analyzed CPF (0.95 and 0.98), Volt-VAR (with two separate curves), and

---

40 "Grid Impacts of Distributed Generation with Advanced Inverter Functions: Hosting Capacity of Large-Scale Solar Photovoltaic Using Smart Inverters," Electric Power Research Institute, Palo Alto, CA, EPRI Technical Report 3002001246, Dec. 2013.

41 "Smart Grid Inverters to Support Photovoltaic in New York Distribution Systems," Electric Power Research Institute, Palo Alto, CA, EPRI Technical Report 3002006278, Apr. 2015.

Volt-Watt (with two separate curves). Both small-scale and large-scale (≥500kW) PV was analyzed. The hosting capacity analysis was performed leveraging OpenDSS.

Almost all SI functions were found to be effective in increasing the hosting capacity for both small-scale and large-scale PV. However, the increase depended on the feeder and the SI function and its settings. CPF 0.95 increased the hosting capacity the most. Volt-VAR effectiveness depended on the settings. Small-scale PV with Volt-VAR function was observed to cause adverse voltage impacts if not properly coordinated with feeder voltage regulation equipment.

12. Feeder Voltage Regulation With High-Penetration PV Using Advanced Inverters and a Distribution Management System – A Duke Energy Case Study[42]

This report presents a collaborative research project between Duke Energy, Alstom Grid (now GE Grid Solutions), and NREL on SI and distribution management system (DMS) control alternatives for large (1-5 MW) PV systems and their distribution impacts. The project compared three methods to manage voltage variations due to PV: (1) PV nominal power factor (baseline case); (2) autonomous CPF (0.95) and Volt-VAR functions; and (3) IVVC coordinated with DMS with the objective of regulating voltage and reducing feeder demand through CVR scheme. The review presented in the following focuses on the distribution modeling and simulation, and the economic analysis aspects of the project.

The project analyzed one feeder from Duke's North Carolina service territory with an existing 5 MW PV system. The distribution modeling and analysis in this project included annual[43] QSTS at 1-minute time resolution using Alstom Grid's e-terra distribution operator training simulator DMS system as a simulation engine. The system was expanded with Python scripting.

The existing feeder voltage regulation scheme (PV with nominal power factor) was effective in regulating the feeder voltages with the PV. The feeder experienced infrequent short-duration voltage excursions outside ANSI C84.1 Range A.[44] The value of operating the feeder head voltage regulators in cogen mode was emphasized.

The autonomous SI functions provided limited value in reducing the feeder short-duration voltage excursions, and had no impact on the voltage regulation equipment operation count. The PV system was located close to the substation and thus, was not able to limit the voltage excursions that happened at loads downstream on the feeder when PV output was either low or zero.

The IVVC scheme notably reduced the voltage excursions and reduced the operations of the voltage regulation equipment. The IVVC tended to leverage reactive power from the capacitors and/or from the inverters to regulate the feeder voltages. This resulted in somewhat higher (lower) feeder reactive power demand during high (low) solar output. The IVVC operation was also observed to somewhat increase the feeder losses.

---

42 B. Palmintier et al., "Feeder Voltage Regulation with High-Penetration PV Using Advanced Inverters and a Distribution Management System – A Duke Energy Case Study," NREL, Golden, Colorado, NREL/TP-5D00-65551, Nov. 2016. Available: https://www.nrel.gov/docs/fy17osti/65551.pdf.

43 The report does not clearly express whether the QSTS was performed over a year or over a 40-day period.

44 The report does not clearly express if the simulated voltage excursions had both magnitude and duration outside ANSI C84.1 service voltage range A. In other words, it is not clear if the excursions would be considered to exceed ANSI C84.1 requirements.

This project also included a cost-benefit assessment of the scenarios analyzed considering the value/cost of PV energy production, losses, loads, and switching equipment wear/tear (accelerated replacements).

13. Photovoltaic Impact Assessment of Smart Inverter Volt-VAR Control on Distribution System Conservation Voltage Reduction and Power Quality[45]

This report analyzes the impact of distributed PV with Volt-VAR control on voltage reduction energy savings and distribution power quality. The report proposes a voltage reduction methodology and a composite power quality metric "power quality score" (PQS) that is calculated from steady-state voltages, voltage deviation, voltage unbalance, reactive power demand, and energy losses. The report uses the PQS metric to compare power quality between cases.

The proposed voltage reduction methodology and the PQS are analyzed on two distribution feeders, one from HECO and one from PG&E. Generic secondary circuit models were implemented for the feeders. The service transformers were modeled based on the typical utility impedance values. For the PG&E feeder, every customer was connected on a 50-ft secondary line with type chosen based on transformer and load information. For the HECO feeder, residential (commercial) customers were connected to the service transformer with a 60-ft 1/0 Al (100-ft 4/0 Al) service line. No further diversity was considered in the secondary circuit topologies. The loads were represented with feeder head load allocation. All PVs were assumed to follow the same normalized PV profile. This load and PV modeling approach does not represent secondary circuit level load, PV, and voltage variability.

For each PV penetration and SI density, PV system and SI locations were randomly chosen (a higher penetration always built on the lower one). Every customer was assigned a PV system that was sized to displace 80% of the customer load. The PV systems were assumed to have a DC/AC-ratio of 1.25. Volt-VAR control was assumed to use VAR priority and the PV inverters were assumed to produce VARs at night. The Volt-VAR curve parameters were tweaked to optimize the performance. The Volt-VAR curve was assumed to supply VARs with up to 60% of the inverter nameplate, which is notably higher than the values of CA Rule 21 and HI Rule 14 Volt-VAR curves.

Annual QSTS simulations were performed at 1-hour time-resolution in OpenDSS for PV penetration levels 50%, 75%, 100%, 125% and 150% (of feeder peak load) and SI densities 0%, 25%, 50%, 75% and 100%. The impact of SI Volt-VAR on voltage reduction energy savings and feeder power quality was analyzed.

The modeling effort assessed PV energy curtailment due to SI functions. For the PG&E feeder, the percentage of the PV curtailment (of total PV generated energy on the feeder) was in all cases <0.7%. For the HECO feeder, the percentage of the PV curtailment (of total PV generated energy on the feeder) was in all cases <1.3%. The curtailment was smaller than the energy savings obtained by the proposed voltage reduction methodology. The modeling effort concluded that voltage optimization, which is able to flatten and lower the feeder voltage profile, has the potential to reduce feeder overall energy curtailment. Volt-VAR was observed to improve the proposed power quality metric on the analyzed feeders.

14. DOE/VT/EPRI Hi-Pen PV Project, Phase III – Smart Inverter Modeling Results, Variability Analysis, and Hosting Capacity Beyond Thresholds[46]

---

[45] F. Ding et al., "Photovoltaic Impact Assessment of Smart Inverter Volt-VAR Control on Distribution System Conservation Voltage Reduction and Power Quality," Technical Report NREL/TP-5D00- 67296, December 2016.

This reference discusses the results from a multi-year high PV penetration project by EPRI that was supported by Department of Energy (DOE) and EPRI member utilities. In this project, EPRI collected multi-year, high-resolution solar data across geographically diverse distribution feeders. EPRI then processed and managed that data, integrated distinct feeder characteristics, and conducted analyses to assess the PV generation variability and its potential impact on utility operations and planning. The project involved deploying hundreds of remote monitoring units and analyzing dozens of distribution feeders across the U.S. This reference discusses the phase 3 of the project that was related to SI modeling, variability analysis, and hosting capacity analysis.

The reference discusses the analysis of a utility feeder that was modeled in OpenDSS in an earlier phase of the project. The impact of SI functions on the feeder PV hosting capacity was evaluated. The hosting capacity method was based running thousands of potential small-scale and large-scale PV deployments. PV impact on the feeder voltage magnitudes and voltage deviation was evaluated without and with SI functions. The reference assessed CPF (1.00, 0.98 and 0.95), two Volt-VAR functions, two Volt-Watt functions, and dynamic reactive current function. The highest hosting capacity improvement was obtained by one of the analyzed Volt-VAR curves and CPF 0.95. Volt-VAR benefits depended on the Volt-VAR settings.

The reference also discusses the PV monitoring and variability assessment performed in the project. In particular, the smoothing that occurs from a single panel to a feeder-level, and from second-level to hour-level are discussed. PV variability can look different at different aggregation levels and at different time-intervals. Therefore, it is important to carefully consider the time and locational granularity necessary to address the objectives of a given modeling effort.

The reference also shows the results for a detailed QSTS analysis performed over 330 days at 5-second resolution using 256 solar inputs. PV impacts on overvoltages and changes to voltage regulation equipment operations are discussed in detail. The results showed hosting capacity to predict relatively accurately the duration of overvoltages. The results also showed voltage regulation equipment operations to decrease with distributed PV and somewhat increase with concentrated PV.

---

[46] M. Rylander, W. Sunderman, J. Smith, C. Trueblood, S. Coley, and T. Key, "DOE/VT/EPRI Hi-Pen PV Project, Phase III Smart Inverter Modeling Results, Variability Analysis, and Hosting Capacity Beyond Thresholds," Blacksburg, Virginia, 08-May-2013. Available: http://dpv.epri.com/media/epri_phase_iii_results.pdf.

15. Common Functions for Smart Inverters: 4th Edition[47]

This reference is the fourth edition of "Common Functions for Smart Inverters." This report documents the body of work that has been completed by a collaborative of over 600 utility and technology stakeholders over a decade with the objective to define a foundation for the integration of DER. This report contains the collaborative recommendations for the industry. The findings from this report can be found in all SI standards and specifications, as well as many grid codes in the U.S. and internationally, including IEEE 1547 and CA Rule 21. This report includes Volt-VAR and Volt-Watt functions that are analyzed in this PG&E EPIC 2.03A modeling effort. This report also introduces VAR and watt precedencies of the Volt-VAR function, as well as the combination of Volt-VAR and Volt-Watt functions. No technical or economic analysis of SI functions is included in this report.

---

[47] "Common Functions for Smart Inverters: 4th Edition," Electric Power Research Institute, Palo Alto, CA, EPRI Technical Update 3002008217, Dec. 2016. Available: https://www.epri.com/#/pages/product/3002008217/.

3
DETAILED FEEDER MODELING

This modeling effort modeled and simulated six (6) PG&E distribution feeders. This chapter discusses the detailed modeling of these feeders *before* PV ES, and PV SIs were added. The feeder models are introduced, the detailed modeling of the secondary circuits is presented, and the baseline feeders without PV are validated. The modeling of PV and ES is discussed in Chapter 4, and the modeling of SIs is discussed in Chapter 6.

3.1 Feeder Model Overview

Six PG&E distribution feeders were analyzed in this modeling effort. Models for these feeders were developed by EPRI in a prior modeling effort[48] (referred to as "CSI3" or "the CSI3 project" in the following) funded as part of the third solicitation of the CSI.

In this prior CSI3 project, a detailed clustering analysis[49] was performed on all CA IOU feeders to identify a set of representative feeders suitable for hosting capacity analysis. The clustering was performed based on a number of feeder characteristics including: climate, fraction of residential load, voltage class, length/impedance, # of voltage regulators/capacitors, etc. The clustering analysis performed in the CSI3 project informed the selection of 16 representative CA feeders (including five from PG&E), on which detailed PV hosting capacity analysis was performed.[50]

Subsequently, seven of the 16 CSI3 feeders (including three from PG&E) were further analyzed in a research project funded as part of the fourth solicitation of the CSI 4 (CSI4).[51] The CSI4 project identified optimal default settings for SI functions and analyzed the setting performance on the feeders. Moreover, five of the 16 CSI3 feeders (including two from PG&E) are currently being analyzed in an on-going EPRI-led research project funded by California Energy Commission (CEC) solicitation 16-079.[52] This CEC project performs QSTS-based hosting capacity analysis of utility-scale PV on the feeders.

Six of the PG&E feeders modeled in CSI3 were selected for further analysis as part of this EPIC 2.03A modeling effort. Using these CSI3 feeder models allowed the project team to leverage past clustering work, as well as feeder models that had already been developed and validated in OpenDSS.

The characteristics of the six PG&E feeder models analyzed in this project are summarized in Table 3-1. The feeders were chosen from six distinct CSI3 feeder clusters to represent a wide diversity of feeder response to PV. Although this limited selection was not necessarily comprehensive, the feeders represent a range of primary circuit connections, circuit lengths, voltage classes, residential customer counts, climate zones, voltage regulation equipment counts and types, etc. The feeders also represent a range of feeder topologies as illustrated in Figure 3-1.

---

48 See footnote 33, *supra*.

49 See footnote 35, *supra*.

50 Additionally, CSI3 project selected 6 CA IOU feeders (2 from PG&E) for validation.

51 See footnote 31, *supra*.

52 "Impact Assessment & Secure Implementation of CA Rule 21 Phase 3 Smart Inverter Functions to Support High PV Penetration – EPC-16-079 Grant Request Form," CEC, 14-Jun-2017. Available: https://www.energy.ca.gov/business_meetings/2017_packets/2017-06-14/Item_14f_EPC-16-079.pdf.

Table 3-1
Feeders Characteristics

Feeder Name	Feeder B	Feeder L	Feeder M	Feeder N	Feeder S	Feeder W
Primary circuit connection	4-wire (Wye)	3-wire (Delta)	3-wire (Delta)	4-wire (Wye)	3-wire (Delta)	3-wire (Delta)
Tot. 3ph length (miles)	6	6	71	27	50	129
Primary Voltage (kV)	4.16	12	12	20.78	12	12
No. Res. Customers	1137	1476	2012	2925	1037	664
Climate Zone	3 (Coastal)	4 (Coastal)	2 (Interior)	3 (Coastal)	13 (Interior)	12 (Interior)
Voltage Regulators	0	0	4	0	2	4
Voltage Boosters	0	0	1	0	0	1
Capacitor banks	0	2	6	6	6	6
Analyzed in CSI3	Yes	Yes	Yes[53]	Yes	Yes	Yes
Analyzed in CSI4	Yes	No	No	Yes	Yes	No
Analyzed in CEC 16-079	Yes	No	No	No	Yes	No

53 In the CSI3 project, Feeder M was used for validation due to the large amount of unmonitored PV on the feeder.

Figure 3-1
Layout of the Six PG&E Feeders Analyzed in This Modeling Effort

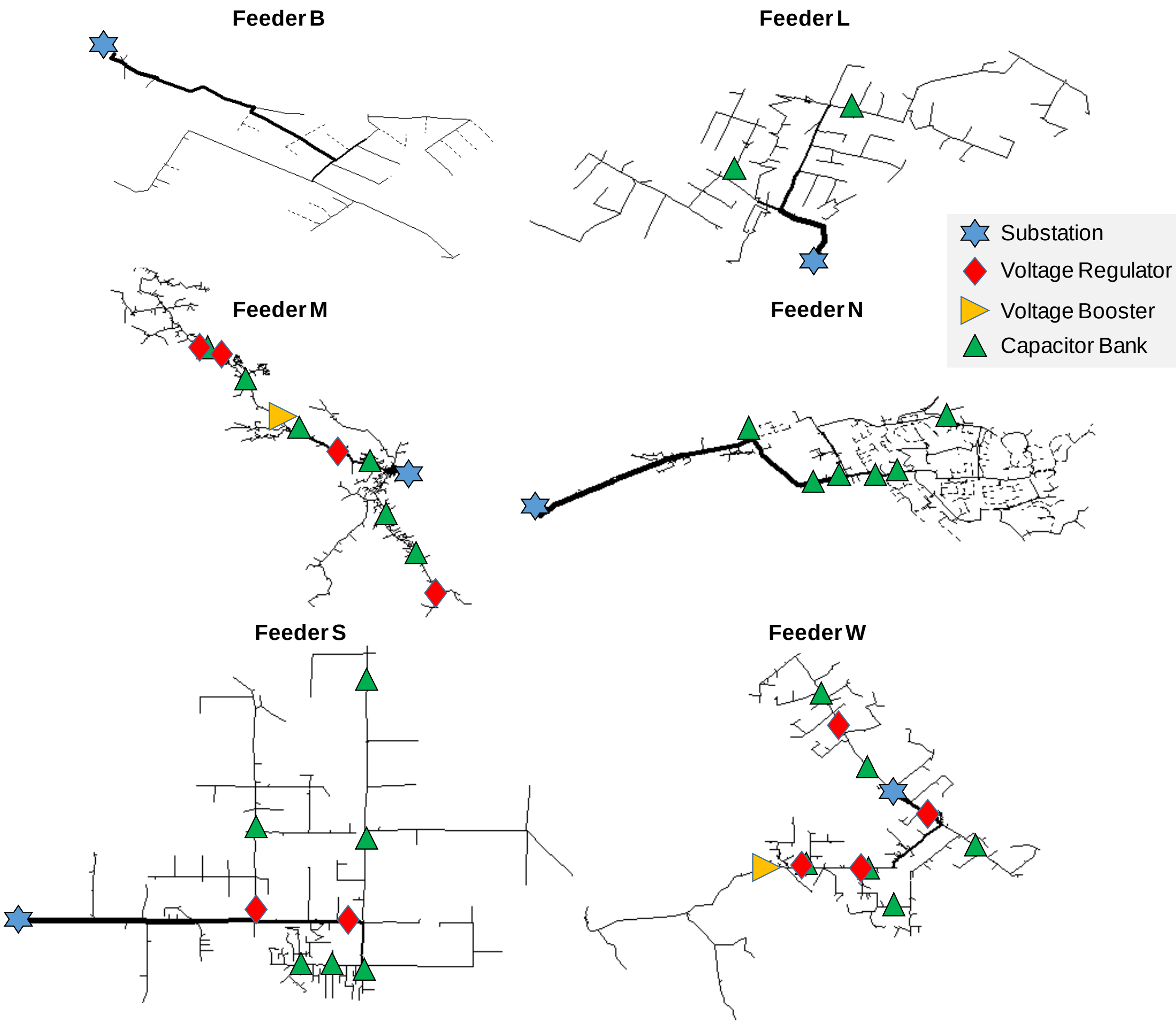

3.2 Review of Feeder Models

The CYME models for the feeders analyzed were provided by PG&E and converted into OpenDSS as part of the CSI3 project. The CSI3 project also validated the converted models and refined the original CYME models by adding substation models, etc. As a result, the CSI3 feeder models included a detailed substation representation (LTC/feeder head regulators where applicable and parallel feeders), 3-phase representation of the feeder medium voltage circuit sections, detailed representation of the feeder voltage regulators and capacitor banks and their controls, etc.

In this EPIC 2.03A modeling effort, EPRI and PG&E first jointly reviewed the CSI3 feeder models to identify whether any updates were necessary to account for changes that may have impacted the feeders since the CSI3 models were developed. The review process validated the feeder topologies, peak and MIN load profiles, load allocations, capacitors, changes in loads, etc.

Several changes were identified and applied to the feeder models as a result of this review process. The changes included removing/disconnecting some capacitor banks. Some topology changes impacting Feeders N and S were also identified. In particular, since development of the CSI3 models, Feeder S was split into two separate feeders. These topology changes on Feeder N and S were not considered in this modeling effort, since the objective of this modeling effort was not to represent the current configuration of the analyzed six feeders in detail, but rather to evaluate different types of PG&E feeders and their response to PV and SIs.

After the CSI3 OpenDSS feeder models were reviewed and validated, their level of detail was significantly improved by implementing highly granular secondary circuit models. This process is discussed in the following section.

3.3 Secondary Circuit Modeling

3.3.1 Need for Detailed Secondary Models

This modeling effort analyzed the impacts of the *Volt-VAR* and *Volt-Watt* functions of *residential* PV systems equipped with SIs. The operation of the Volt-VAR and Volt-Watt functions primarily depends on the voltage at the SI terminals. Therefore, to properly assess the operation of the functions, the SI terminal voltage must be simulated with sufficient accuracy.

Residential customers are supplied over LV secondary circuits that consist of a MV to LV service transformer, and service lines that connect the customers to the transformer LV terminal. The voltage drop (due to load) or voltage rise (due to PV) over a secondary circuit can be up to 3 to 5 volts on a 120-volt basis (0.025 p.u. to 0.417 p.u.), depending on the secondary circuit construction and the secondary circuit load and DER characteristics. Accurate secondary circuit models are critical to properly assess the techno-economic impacts of residential PV systems with SI functions.

The CSI3 modeling effort incorporated generic secondary circuit models into the OpenDSS feeder models. In that particular effort, the generic secondary circuit models had the following characteristics:

- Each secondary circuit was modeled either as single-phase or three-phase, and was supplied by either a single-phase or a three-phase service transformer.
- Each customer was assumed to be connected to the service transformer by a dedicated single-phase or three-phase service line. In other words, a so-called "star" secondary circuit topology was assumed. All service lines were assumed to have a length of 125 ft. A single generic single-phase or three-phase conductor type was assumed for each service line.
- Each customer (as shown in the PG&E CYME models) was represented with a single-phase or three-phase load. The load demands were assigned with feeder head allocation based on the customer peak day kilowatt-hour (kWh). All loads with a given (primary circuit) phase connection were assumed to follow the same active power profile.[54] The load (constant) power factors were assigned based on the customer classes.

The secondary circuit models implemented in the CSI3 modeling effort were a notable improvement over the common utility practice of *not* modeling the secondary circuits at all. However, such generic secondary circuit models do not accurately capture the diversity of real secondary circuit topologies, service line types and lengths, and customer load dynamics. Consequently, this EPIC 2.03A modeling

---

[54] Since the PG&E CYME feeder models did not include phasing information, CSI3 modeling effort estimated the feeder phasing. It is common for utilities to have incomplete records of the feeder phasing in GIS.

effort invested considerable effort into increasing the level of detail of the *residential*[55] secondary circuit models for the six feeders analyzed.

3.3.2 Detailed Secondary Modeling

All the residential secondary circuits were assumed to be split-phase and were modeled with single-phase equivalent circuits.[56]

The availability of data was a challenge for increasing the secondary circuit model detail. PG&E, similar to many other utilities, does not include secondary circuits in the distribution feeder models. PG&E also did not have any easy way to gather the information necessary to model the secondary circuits in detail, within the accelerated timeline defined for this modeling effort. To balance the need for modeling secondaries with an increased level of detail, with the level of effort required to gather the necessary data, PG&E gathered information for approximately 10% of all the secondary circuits with residential customers in each of the six feeders studied, representing a wide variety of secondary topologies, service line conductor types, and customer counts.[57]

PG&E also provided EPRI with the following information:

- Typical service transformer impedances per transformer nameplate and primary voltage class. Split-phase service transformers with secondary voltage class 120/240 V was the only type considered in this modeling effort.
- Distribution transformer thermal ratings (i.e., the allowed transformer rating as a percentage of the transformer kVA nameplate).[58] PG&E distribution transformer thermal ratings are defined with respect to the transformer kVA nameplate, transformer location (coastal vs. interior), and the time of the year (season). Since the load days analyzed in this modeling effort (discussed later in this chapter) all occurred during the summer,[59] the distribution transformers on the analyzed feeders were assigned the summer ratings based on the feeder location and the transformer nameplate.
- Typical impedances and ampacities per service line conductor type.
- Customer count and peak day energy use of each service transformer. This information was included in the OpenDSS models as part of the CSI3 modeling effort.

55 Since this modeling effort focused on residential PV, only residential secondary circuits were refined. CSI3 modeling effort had identified customer types based on the customer classification in the CYME feeder models.

56 Split-phase secondary circuits can be perfectly represented with single-phase equivalent circuits when the 120-volt leg currents are equal. Otherwise, the single-phase model is a simplification that ignores the impact of the 120-volt leg voltage and current unbalance. Even under 120-volt leg unbalance, the 240-volt voltages are accurately represented. For details, see: J. Peppanen, C. Rocha, J. A. Taylor, and R. Dugan, "Secondary Low-Voltage Circuit Models – How Good is Good Enough?" IEEE Transactions on Industry Applications, vol. 54, no. 1, pp. 150–159, Jan. 2018.

57 PG&E provided the following number of secondary configurations per feeder: 9 for Feeder B, 15 for Feeder L, 39 for Feeder M, 19 for Feeder N, 22 for Feeder S, and 17 for Feeder W.

58 PG&E Distribution Transformer Capability. Electric Design Manual, PG&E. 2015.

59 Summer as defined in footnote 58, *supra*.

Based on this information, all single-phase secondary circuits serving only residential customers were refined as follows:

- A secondary circuit configuration was chosen based on the service transformer nameplate rating, overhead vs. underground, and customer count.
- A single-phase transformer with updated PG&E default impedance parameters was added. The LV winding voltage base was set to 240 V. Climate-zone specific PG&E thermal ratings were applied.
- Single-phase equivalent models of the triplex conductors and single-phase (240-volt phase-neutral connected) loads were added based on the chosen secondary configuration until the transformer customer count was met. If the transformer had more customers than the secondary circuit configuration, the configuration was repeated as many times as necessary.

Single-phase load spots serving both residential and non-residential customers in the original CYME models were split into two distinct secondary circuits in OpenDSS, one serving all the residential customers and another serving all the non-residential customers in the original secondary circuit. This approach was agreed jointly by EPRI and PG&E since the actual service transformer configuration was not certain in the original feeder models. The actual configuration could have consisted of a single transformer, or multiple transformers. For both circuit, a separate service transformer was assigned with type (including the nameplate rating) identical to the original service transformer. Then, residential secondary circuit was refined with the approach described above. The non-residential secondary circuit was not adjusted.

Nearly all of the secondary configurations provided by PG&E were single phase. After careful consideration of alternatives, EPRI and PG&E agreed to model all three-phase residential secondary circuits with three separate single-phase residential secondary circuits.[60] This was accomplished by replacing the three-phase service transformer with three single-phase transformers with a total nameplate as close as possible to the original three-phase transformer. For example, a 15 kVA three-phase transformer was replaced with three 5 kVA transformers. The three-phase transformer customer count was equally distributed to the three single-phase transformers. Then, each of the three single-phase secondary circuits was modeled with the steps listed above.

[60] In practice, the three-phase secondary circuits may consist of a combination of 208 V three-phase larger customers (e.g., apartment complexes) and split-phase residential customers. Modeling these secondary circuits in full detail would have required significant additional data, including the number of 3-phase and split-phase-served customers, the topologies for both service types, etc. Modeling and analysis of PV and smart inverter impacts in such “mixed” secondary circuits would be an interesting area of future work.

Figure 3-2
Principle of Modeling a Three-Phase Residential Secondary Circuit With Three Single-Phase Secondary Circuits

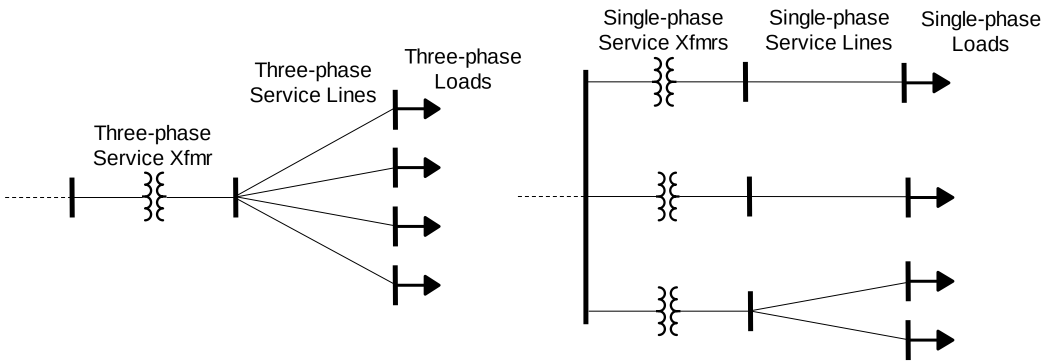

Three-phase secondary circuits serving both residential and non-residential customers were first split into residential and non-residential three-phase secondary circuits as described above for single-phase service transformers serving residential and non-residential customers. Then, the residential three-phase secondary circuit was modeled with three single-phase residential secondary circuits as described above. An example of this approach is shown in Figure 3-2.

The above secondary modeling principles were applied for all the analyzed feeders. The resulting secondary circuit models represent a wide range of real PG&E secondary circuits including the variety of service transformers, secondary topologies, service line types and lengths, and customer counts per transformer. The refined models added a significant level of detail to the OpenDSS feeder models compared to the original CSI3 feeder models with generic secondary circuits. Figure 3-3 illustrates the difference between the old generic secondary models and the refined detailed secondary models.

Figure 3-3
Old Generic Secondary Circuit Models vs. Refined Detailed Secondary Circuit Models

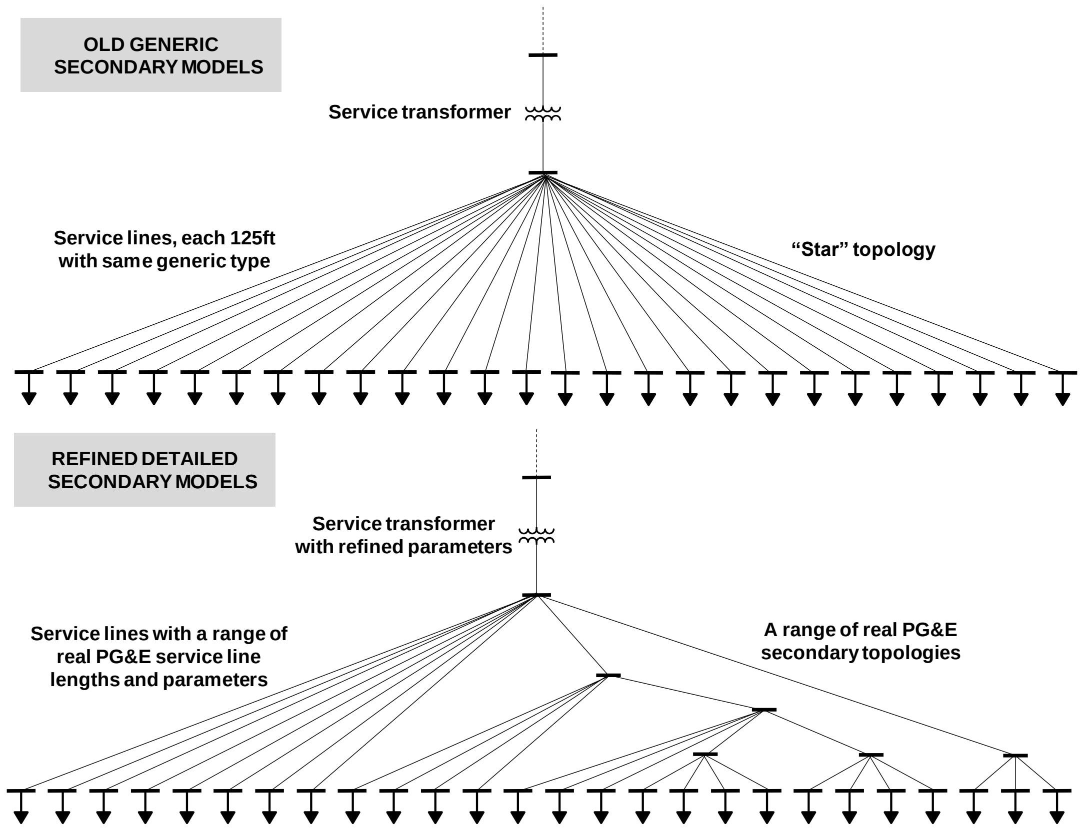

Figure 3-4 illustrates the distribution of secondary circuit configurations on the six feeders. The modeling resulted in a wide distribution of secondary circuit configurations. Some configurations were more frequently deployed than others. Moreover, three out of nine Feeder B and one of the 15 Feeder L secondary configurations were not utilized at all, as the applied selection process identified no matching secondary circuits on the feeders. PG&E provided a set of unique secondary configurations for each feeder. In other words, e.g., configuration #1 for Feeder B may be very different from configuration #1 for Feeder S.

At this point, the residential loads were still represented with feeder head load allocation, which does not consider the variability and diversity of residential loads. The next step entailed modeling the residential loads in detail using PG&E AMI data.

Figure 3-4
The Distribution of the Applied Secondary Configurations on the Analyzed Feeders

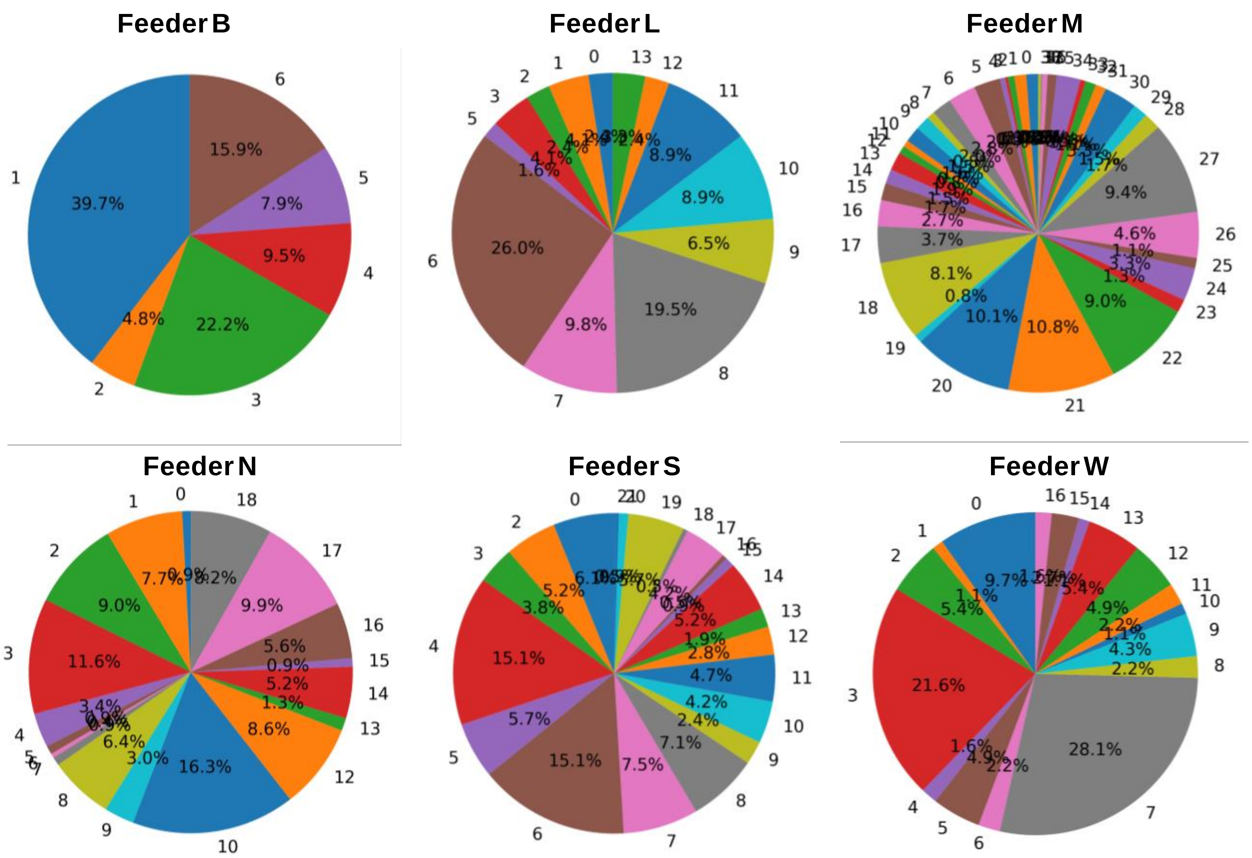

Having implemented the detailed secondary circuit models, the next step was to model the residential loads in detail. In this modeling effort, over 12,000 daily QSTS simulations were performed to analyze various sensitivities. This large number of simulations and the accelerated timeline for this modeling effort made it impractical to perform each of the 12,000+ daily QSTS simulations over a long time period, such as a year. Instead, this modeling effort analyzed three characteristic load days and five characteristic PV days to reflect the diversity of different feeder load and PV generation conditions. The selection of PV days and the PV modeling is discussed in further detail in Chapter 4. The next section discusses the modeling of the residential and non-residential loads over the three characteristic days considered.

3.4 Residential Customer Load Modeling

The load profile of individual residential customers tends to be much more variable than the aggregated load at the feeder head, as illustrated in Figure 3-5. Individual residential customer load profiles are typically characterized by "needle peaks" (short periods of high demand surrounded by low demand) caused by the duty cycles of large appliances, etc. The variability of residential loads results in variability in residential secondary circuit voltages that can influence the operation of residential smart PV inverters. A detailed representation of the residential loads is therefore necessary to accurately assess the operation of residential SIs.

Figure 3-5
Example Feeder Head Load Profile (Left) vs. AMI Load Profiles (Right) Over a Day

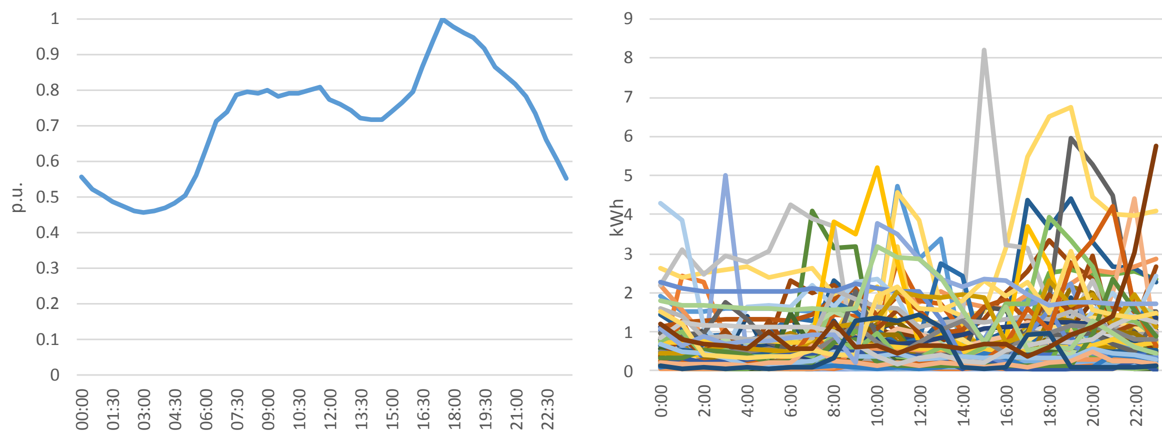

PG&E provided EPRI with 100 anonymized residential AMI profiles that were randomly selected for each of the six feeders analyzed. The profiles consisted of kWh recordings over a time period of approximately 11 months. Reactive power or voltage recordings were not provided. An example AMI profile is shown in Figure 3-6.

Figure 3-6
Example AMI Profile Over the 11-Month Time-Period

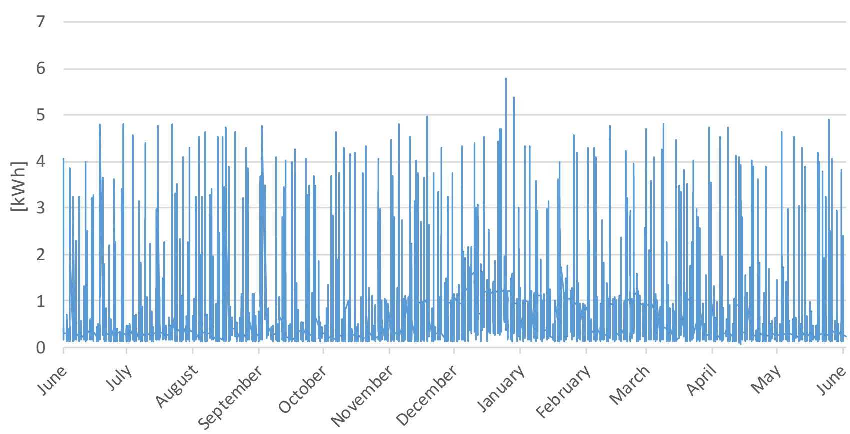

The data set was cleansed by removing profiles that were characterized by:

- More Than 30 Consecutive Days Without Consumption: Such profiles could represent customers that were traveling etc., but could also represent vacant premises. It was considered not desirable to include these particular cases as part of this modeling effort.
- Time-Resolution Other Than One Hour: These profiles were ignored for simplicity.
- Existing PV Installations: Due to the lack of geographically and time-wise coincident PV generation profiles, it was not possible to disaggregate PV generation from load in such AMI profiles. Instead, residential PV was represented separately from load in this modeling effort to allow for a precise assessment of the operation of residential PV system with SIs.

After removing the profiles following the criteria detailed above, between 64 and 86 profiles were left for each feeder, as listed in Table 3-2. This profile count was considered adequate to represent the diversity of residential customer loads for this modeling effort.

Table 3-2
Number of AMI Profiles Per Feeder Remaining After Data Cleansing

Feeder	Number of AMI Profiles
Feeder B	86
Feeder L	86
Feeder M	84
Feeder N	70
Feeder S	64
Feeder W	86
Total	476

Next, three characteristic load days (*peak*, *average*, and *minimum*) were selected for each of the six feeders analyzed. First, an aggregated AMI profile was calculated for each feeder by adding all the (remaining) AMI profiles on the feeder. Then, the three characteristic days were chosen as follows:

- "Peak" Day: The day with the highest energy consumption, as shown on the aggregated AMI profile;
- "Minimum" Day: The day with the lowest energy consumption, as shown on the aggregated AMI profile; and
- "Average" Day: The day with the energy consumption closest to the average daily energy consumption over the whole 11-month period analyzed.

To summarize, three characteristic load days were selected for each of the six feeders (18 days total). This brings the total number of unique daily AMI profiles to 476×18=8568. The AMI profiles for the three characteristic load profiles for Feeder B are visualized In Figure 3-7. These 8568 daily AMI load profiles were used throughout this modeling effort to represent the diversity of residential customers' load behavior in the sensitivities described in Sections 4.1 and 6.1.

Figure 3-7
AMI Profiles for the Three Characteristic Load Days for Feeder B

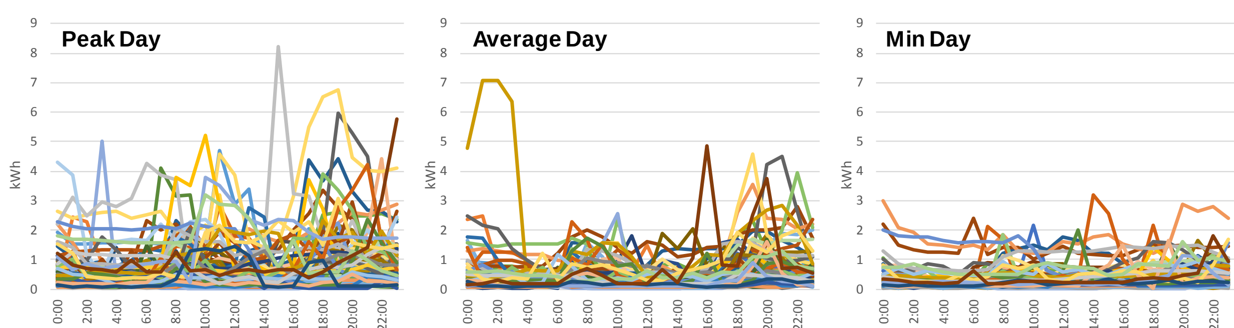

Then, the residential customers of each feeder were assigned one of the (remaining) AMI profiles listed in Table 3-2. This was done as follows:

- The transformer kWh parameters (from CYME) were scaled so that the sum of the transformer kWh properties on each feeder was equal to the feeder peak load day energy consumption from Supervisory Control and Data Acquisition (SCADA). This step accounted for changes in the peak load that had taken place since the CSI3 modeling effort.
- As shown in Figure 3-8, each customer on a transformer was randomly assigned one of the AMI profiles from the feeder. The profiles were assigned so that the transformer total peak day energy consumption from AMI (the sum of the peak day energy consumptions of the AMI profiles assigned to the transformer) was as close as possible to the scaled transformer (peak day target) kWh property. This step ensured that the AMI profiles were assigned in a reasonable way and, e.g., no AMI profile with very high energy demand was assigned to a transformer with a very low energy demand. The peak day energy demands of the AMI profiles are shown in Figure 3-9. The profiles represented a good diversity in the peak day energy consumption. This indicates that the profiles represent a relatively diverse group of residential customers.

Figure 3-8
Simplified Flow Diagram for AMI Profile Assignation

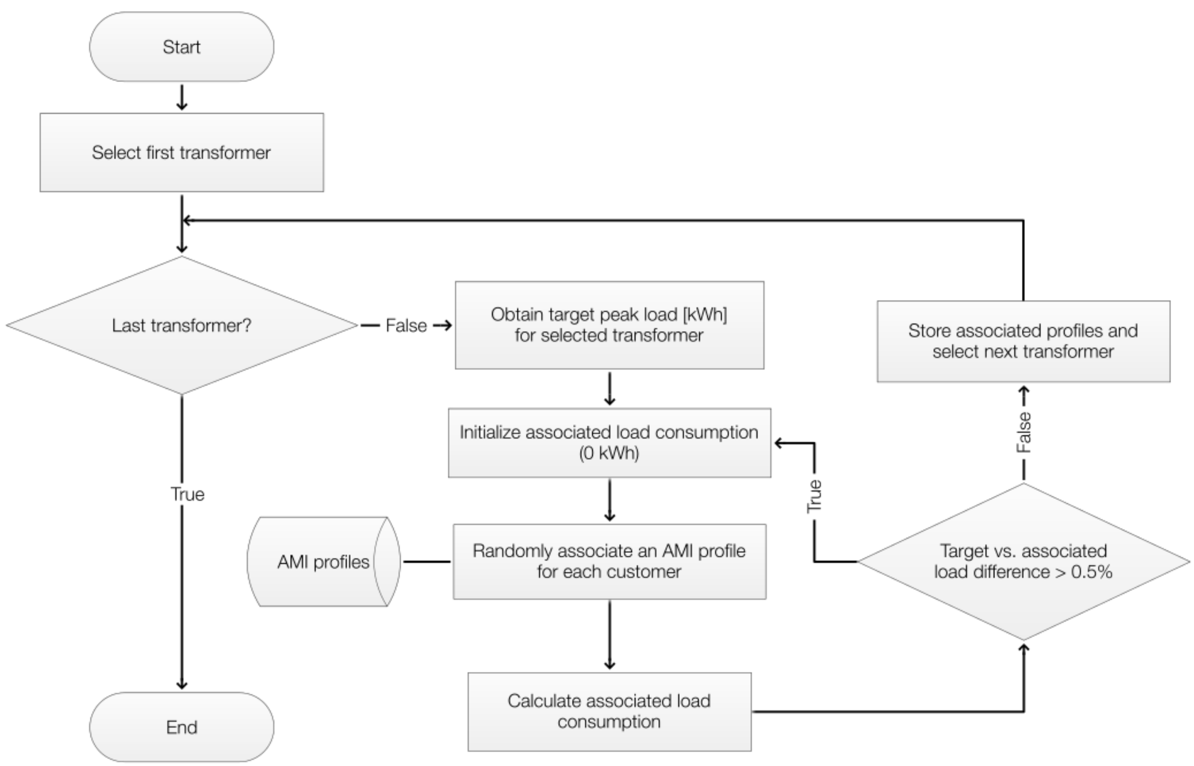

Figure 3-9
The Peak Day Energy Consumptions of the Ami Profiles Sorted in Ascending Order

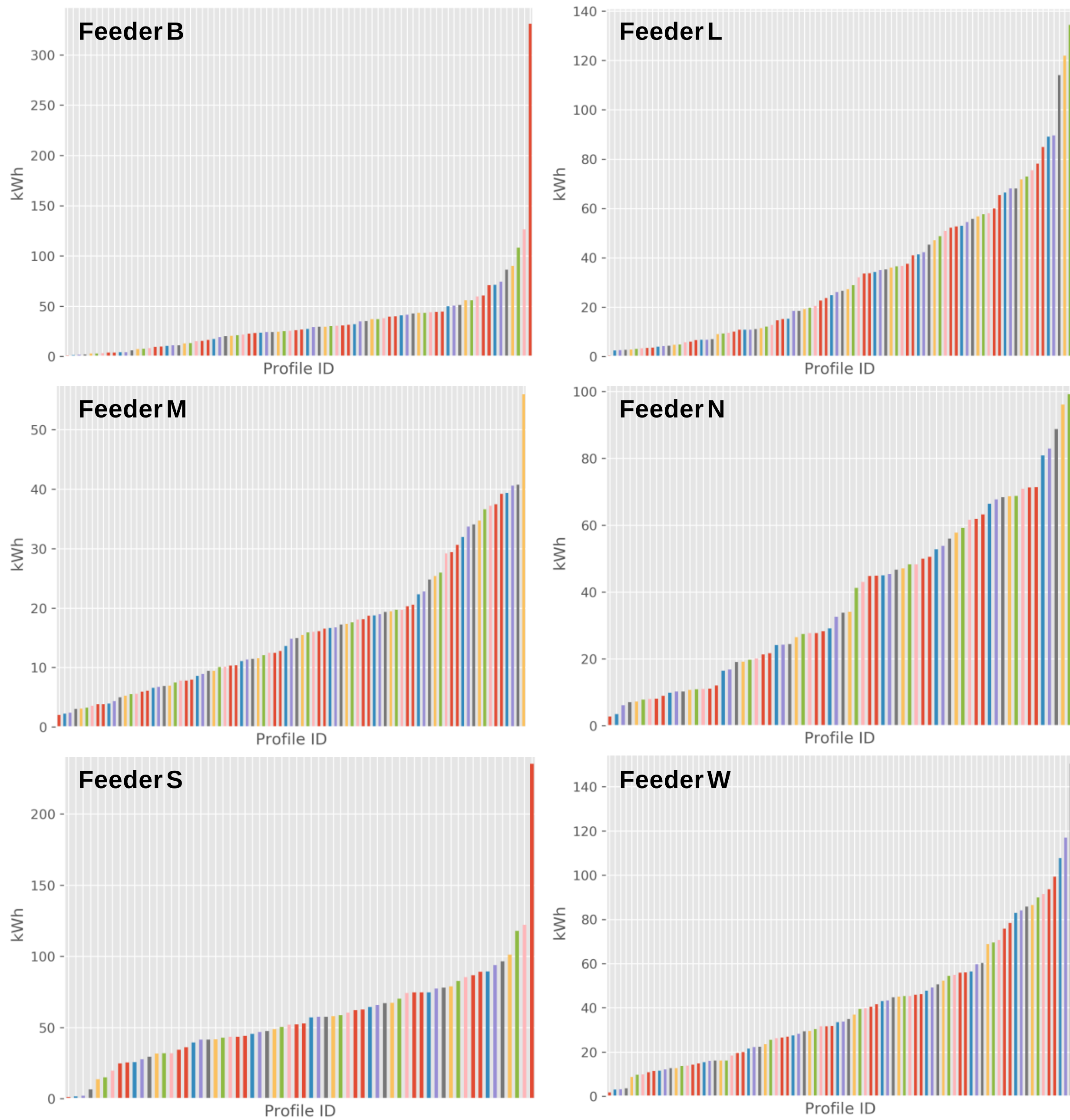

It was also important to track that the AMI profiles were assigned roughly equally and the assignation algorithm did not significantly prefer some profiles over others. Using all the AMI profiles leads toward a more diverse representation of the customer behavior. Figure 3-10 shows the number of customers each AMI profile was assigned to on a given feeder. The AMI profile IDs are sorted in ascending order of peak day energy consumption. The figure shows that all profiles are more or less equally used. More importantly, the assignation was not skewed towards profiles with smaller or larger energy consumption.

Figure 3-10
Number of Customers Assigned to each AMI Profile, for Each Feeder Analyzed. The AMI Profile IDs Are Sorted in Ascending Order of Peak Day Energy Consumption, as Shown in Figure 3-9.

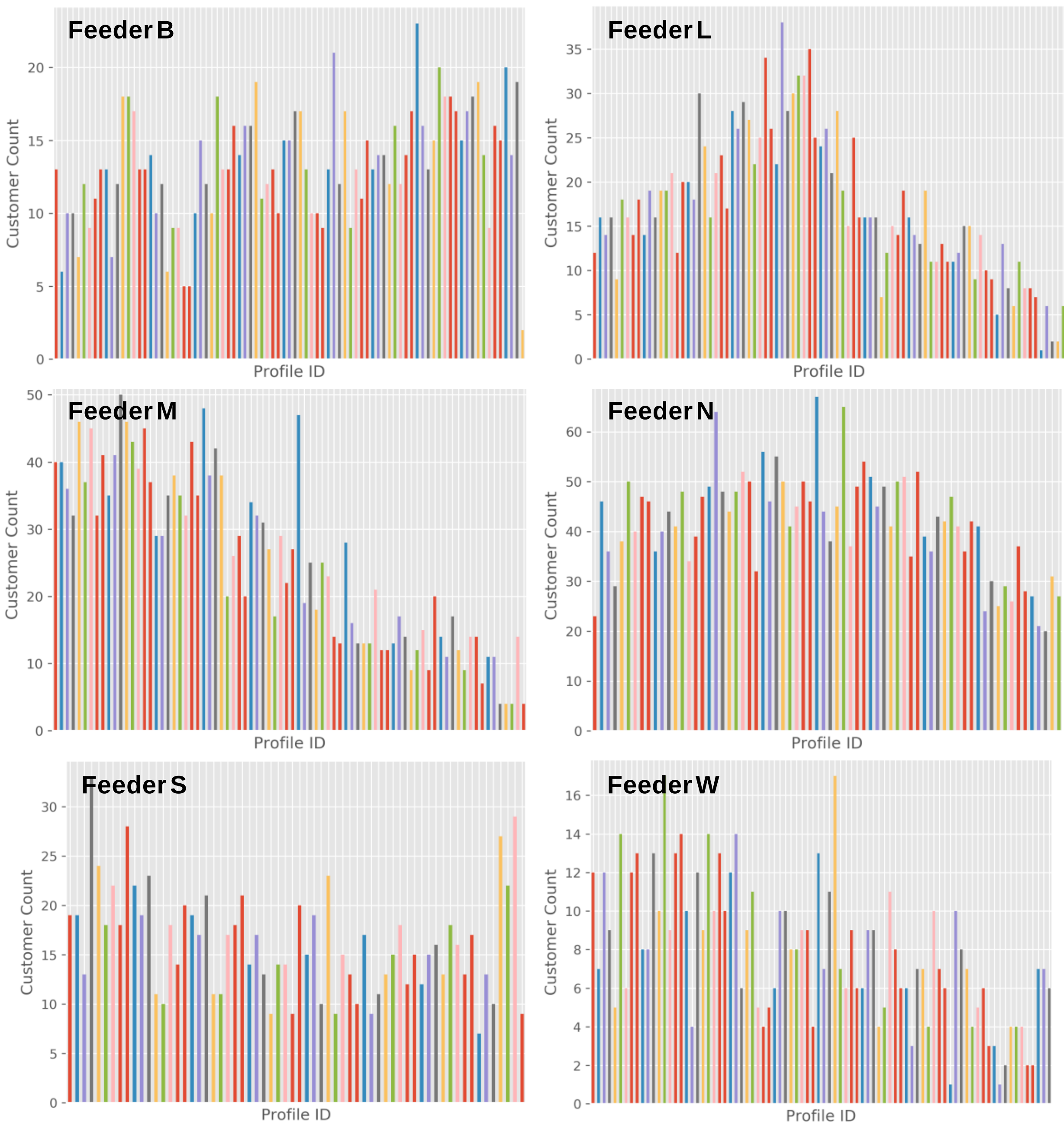

Ideally, the transformer total peak day kWh of the assigned AMI profiles would be equal to the scaled CYME model peak day kWh properties. As shown in Figure 3-11, the two kWh values match very closely for most transformers. Only 41 transformers (out of the total 1569 transformers on all the feeders) have an absolute difference >10 kWh. All but 6 of these transformers supply 1 or 2 customers and the AMI profile assignation algorithm was unable to find profile(s) that exactly matched with the transformer CYME kWh. The remaining 6 transformers either had many customers and a small kWh, or few customers and a large kWh. In both cases, there were no suitable AMI profiles to match the transformer CYME kWh exactly. In other words, for >97.8% of all the transformers on the six feeders, the AMI profile allocation represented the transformer kWh very accurately. For the remaining 2.2% of the transformers, a more accurate selection of AMI profiles was not available. Thus, it was concluded that each customer was successfully assigned an AMI profile, based on the information available.

Figure 3-11
Service Transformer Peak Day Total kWh Values of the Assigned AMI Profiles vs. Scaled CYME Model Peak Day kWh Properties. Transformers From All the Feeders Are Shown in Descending Order of Scaled CYME kWh Values.

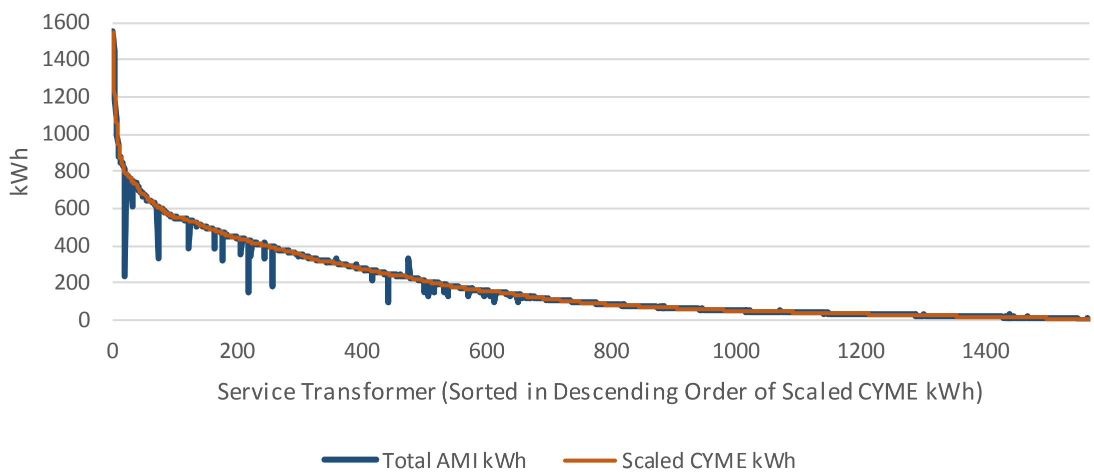

3.5 Non-Residential Customer Load Modeling

This section discusses the *non*-residential customer load modeling using feeder head SCADA measurements, aggregated residential AMI load, and PV data.

PG&E provided EPRI with 15-min feeder head SCADA measurements for 'minimum', 'peak' and 'average' load days. PG&E identified the load days as follows:

- The 'minimum' load day was chosen as the day with the MIN daytime load (kW) over a year;
- The 'peak' load day was chosen as the day with the highest load (kW) over a year; and
- The 'average' load day was found by calculating the average hourly load across the entire year (e.g., the average load day load at noon was equal to the average load at noon over the year).

The feeder head data included total active and reactive power measurements for three feeders (Feeders M, N and W), and feeder head (phase-average) current measurements for three feeders (Feeders B, L and S). For the latter three feeders, the feeder head powers were derived from the currents assuming a nominal voltage and a (constant) unity power factor. Figure 3-12 illustrates the peak, MIN, and noon-time active power load of the analyzed feeders over the three characteristic load days.

Figure 3-12
Peak, Minimum, and Noon-Time Load of the Analyzed Feeders Over the Three Characteristic Load Days

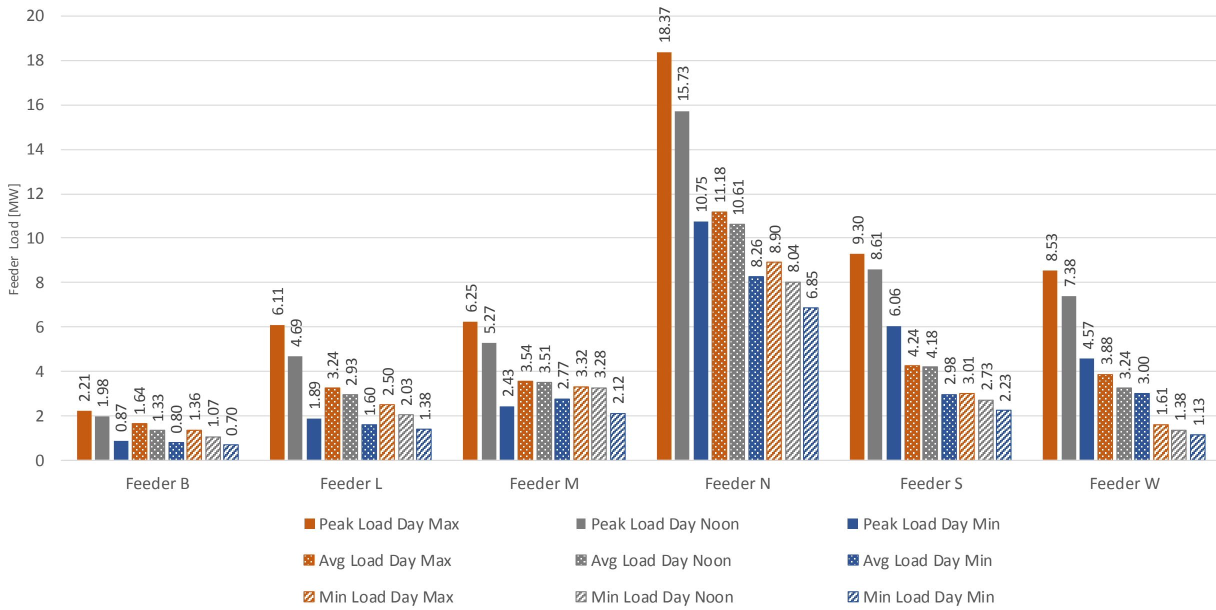

The non-residential load modeling required two steps. First, the feeder head native load (the load without PV) was estimated. Second, the aggregated feeder non-residential load was calculated as the difference of the feeder native load and the feeder aggregated AMI load. These steps are discussed next.

3.5.1 Estimating the Feeder Native Load

All the six analyzed feeders had some existing PV. In this modeling effort, it was important to remove the impacts of the existing PV since the objective was to analyze the feeders for a range of PV, ES, and SI penetration levels, starting from a base condition without any PV on the feeders. Therefore, no existing PV was included in the feeder models. Additionally, it was necessary to remove the impacts of the existing PV from the feeder head power profiles that were used to represent the nonresidential feeder loads.

Although the nameplate capacity of the existing PV was known for all the feeders, no geographically and time-wise coincident PV generation profiles were available. As a result, it was not straightforward to estimate the 'native load' (i.e., the load without the PV) for the characteristic load days. This lack of visibility to DER operation is a widely-recognized challenge for utilities.

The PV generation on the feeders was roughly estimated by scaling normalized clear sky global horizontal irradiance (GHI) profiles by a heuristically selected scaling factor. The clear sky GHI profiles were obtained with pvlib-python Python package.[61] The GHI profiles were obtained separately for each feeder location and the 15th day of the month of the characteristic load day. The scaling factors were selected separately for each feeder between 0 kW and the total PV nameplate capacity on the feeder.[62]

---

61 Available: https://pvlib-python.readthedocs.io/en/latest/clearsky.html#ineichen-and-perez.

62 The nameplate PV capacity was not directly used for scaling since it resulted in high PV generation and thus, unreasonably high noontime load on some of the feeders.

The scaling factor was identified by trial-and-error adjusting the factor until the feeder native load profile met the expectations of the PG&E engineers.

After the PV generation had been estimated for three characteristic load days on all the feeders, the feeder native load was estimated by adding the feeder head kW measurements and the estimated PV kW profiles. The resulting native load profiles were compared to the SCADA feeder head measurement profiles in Figure 3-13. For Feeders B and L, the native load and measured load profiles were identical since the reasonable PV nameplate was set to 0 kW. This was done since a higher value would have resulted in a second noon-time peak in the native load profiles that was not expected for the two feeders. For the remaining four feeders, a non-zero reasonable PV nameplate was applied resulting in differences between the native and measured load profiles.

Figure 3-13
Measured Load vs. Estimated Native Load of the Analyzed Feeders

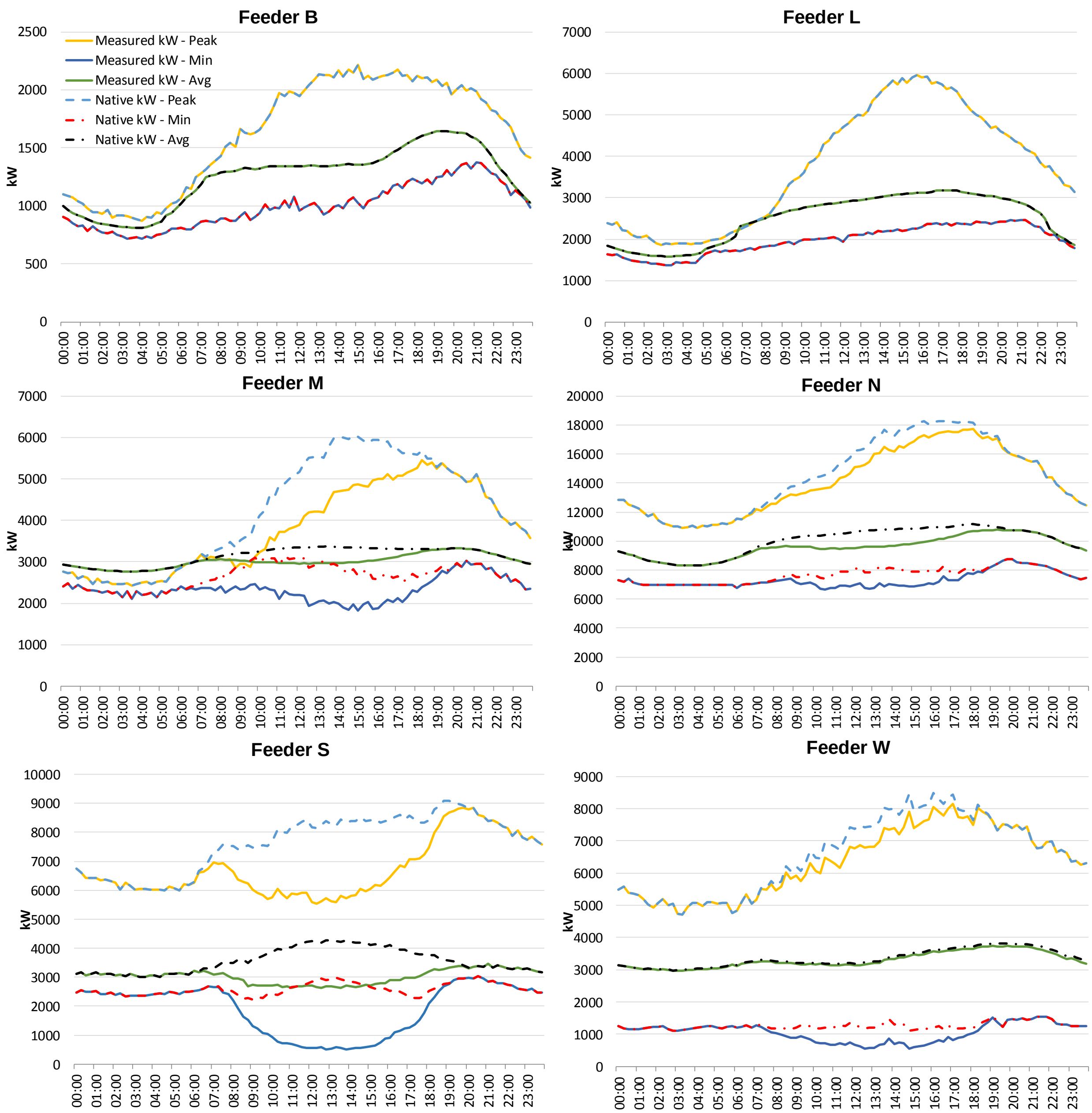

3.5.2 Estimating the Non-Residential Load for Each Feeder

After the native load of the feeders had been estimated, the next step was to use the native load and the aggregated AMI load to estimate the non-residential load of the feeders. The aggregated AMI loads were obtained by performing a QSTS after removing all the non-residential loads from the feeder models and setting the residential loads to follow their assigned AMI profiles. The aggregated AMI loads (+some losses) were obtained from the simulated feeder head demand. Then, the non-residential load profiles were obtained as the difference of the feeder head native load and the simulated aggregated

AMI load. The resulting non-residential load profiles are compared to the aggregated AMI profiles in Figure 3-14. The figure validates that the obtained load profiles for the non-residential customers look reasonable.

Figure 3-14
The Share of Residential and Non-Residential Load of the Total Feeder Load

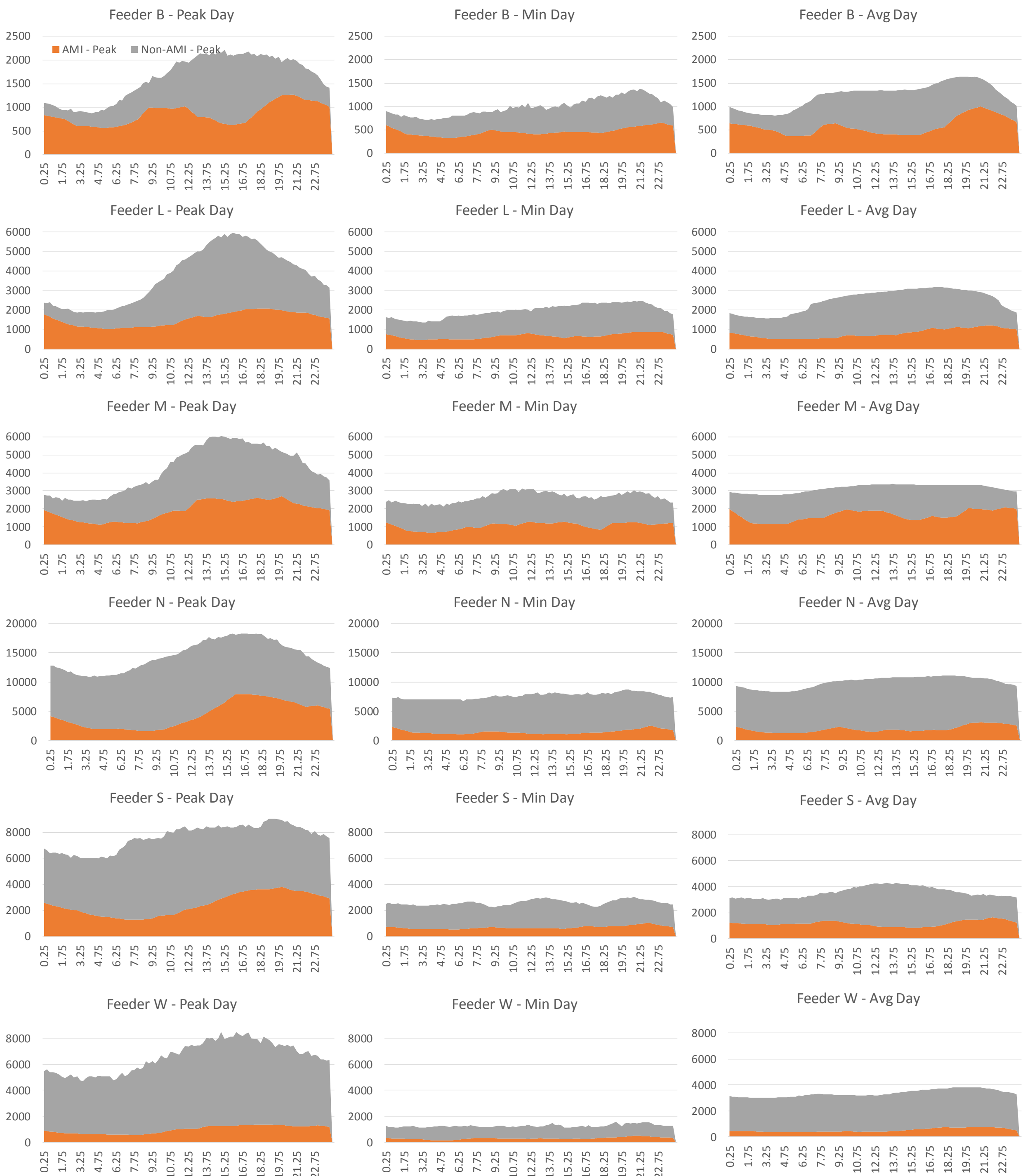

3.5.3 Final Load Allocation of Non-Residential Customers

As the final phase in modeling the non-residential customers' loads, the loads were allocated as follows:

- Simulate the feeder head currents and powers with QSTS including the non-residential customer loads only. Residential customer loads were disconnected.
- Scale the original load allocation currents with the ratio of the peak powers of the calculated nonresidential customers' load and the simulated feeder head power.
- Allocate the non-residential customers using the scaled feeder head currents (equal phase currents) and the non-residential transformer kWh values from the original CYME models.
- Normalize the non-residential customer load profile.

The resulting non-residential load profiles were validated by comparing the simulated and the calculated peak powers and the total energies of the aggregated non-residential loads. These steps conclude the modeling of the non-residential customers' loads. This also concludes the detailed feeder modeling work. The next section discusses the validation of the refined feeder models.

3.6 Validation of the Detailed Feeder Models

After all the applied model refinements, it was necessary to validate that the resulting feeder models represented reasonable and expected operational characteristics. Moreover, to allow more straightforward analysis of the SI function impacts, it was preferred to have baseline feeder models without any thermal overloads or voltage issues.[63] Having such "clean" baseline feeder models (without PV) ensured that any adverse impacts identified in the analysis of PV, ES and SI were due to PV, ES and SI and not some other pre-existing condition.

This section discusses the validation of the detailed baseline feeder models. The validation was based on analyzing the QSTS simulation results from each of the three characteristic load days.

3.6.1 Validation of Thermal Overloads

As expected, none of the feeders had any primary circuit thermal overloads. However, since the residential customer loads were represented from AMI data that was not from each particular customer, a small number of service transformers and service lines were overloaded. The overloaded transformers were replaced with a transformer with the next available nameplate kVA rating. Similarly, the overloaded service lines were replaced with a line with the next available ampacity.

3.6.2 Validation of Feeder Voltages

Based on an AMI voltage assessment, PG&E was not aware of any voltage issues on the analyzed feeders. Therefore, it was assumed that any voltage violations experienced in the simulation were caused by slight differences between the feeder models and the actual feeders. As such, LTC, voltage regulator and capacitor bank settings were modified to ensure that the feeder voltages remained within reasonable bounds for the three characteristic load days.

After the voltage equipment settings were modified (and after the overloaded service transformers and lines were upgraded), the feeders had no further overvoltages or undervoltages. Figure 3-15 shows the MV and LV level maximum and minimum voltages of the analyzed feeders over the three characteristics days after the voltage regulation equipment settings had been adjusted and the overloaded service

[63] Moreover, the analyzed feeder models had no known thermal overload or voltage issues.

transformers and lines were replaced. As can be seen for Feeder L at peak load, there are some rare occurrences in which the minimum voltage at MV level showed lower values than the minimum voltage at LV level. This behavior corresponds to the minimum voltage experienced by the un-regulated tertiary bus at the substation transformer instead of secondary voltage rise in the model.

Figure 3-15
Medium-Voltage (MV) and Low-Voltage (LV) Level Maximum and Minimum Voltages of the Analyzed Feeders Over the Three Characteristics Days After Validation

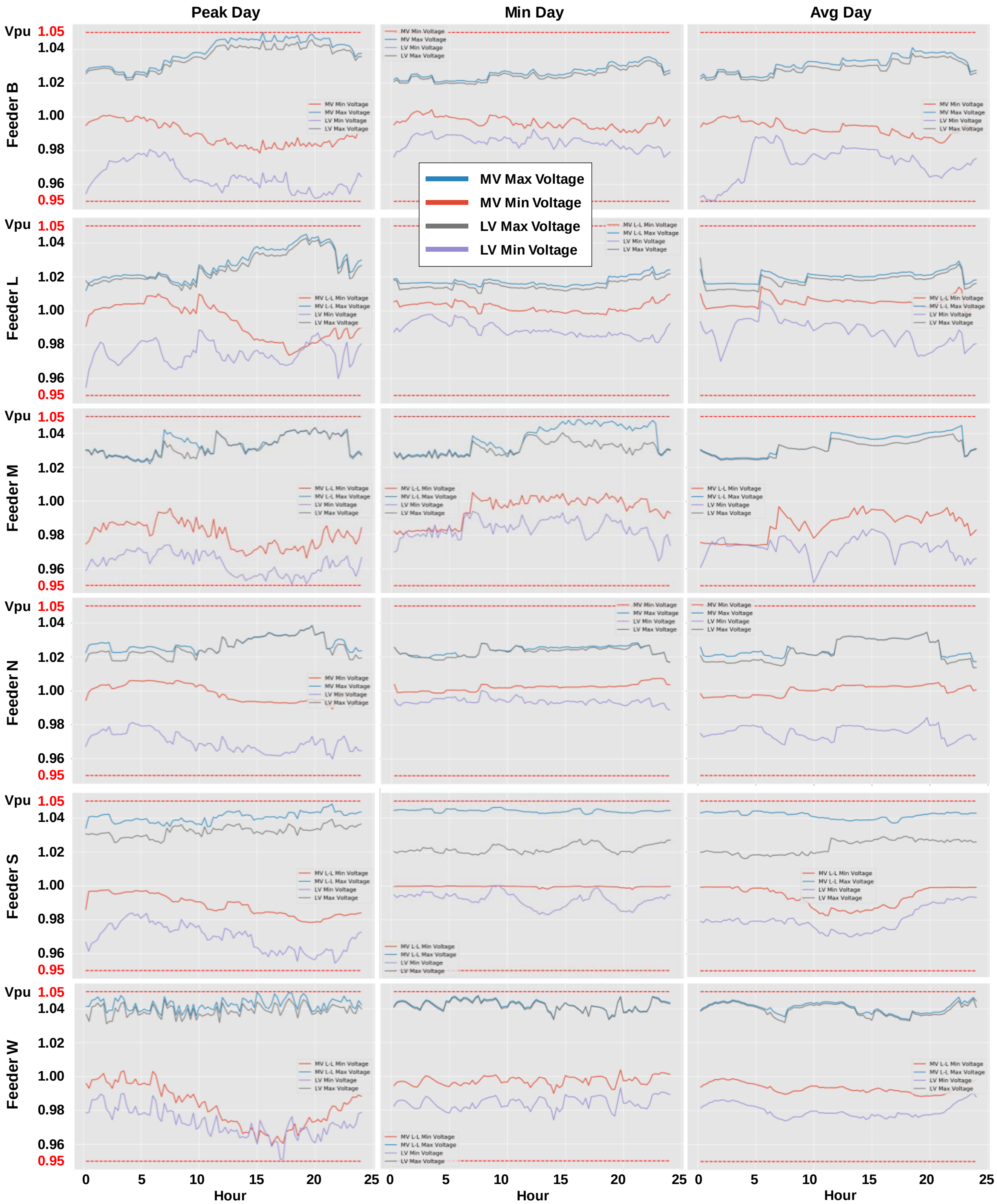

3.6.3 Validation of Feeder Secondary Voltage Drops

In addition to the voltage validation discussed above, it was also validated that the feeders have no secondary circuits with maximum voltage outside of PG&E's design guidelines. As a result of this criteria, a total of three secondary lines and one service transformer located at Feeder B were upgraded to the next available size.

3.7 Conclusions

This modeling effort analyzes residential PV, ES, and SI functions on six PG&E feeders. The feeders were modeled in OpenDSS in an earlier research project.[64] In this modeling effort, a significant modeling effort was made to increase the granularity of the feeder models for an accurate representation the distribution impacts of PV and ES, as well as for an accurate assessment of SI functions operation. The model refinements include:

- Detailed LV secondary feeder models from service transformers to the customer panels;
- Representation of residential load diversity and variability through real PG&E residential AMI data; and
- Improved representation of non-residential loads leveraging PG&E feeder head SCADA data and estimated aggregated residential load profiles.

In these steps:

- 2,246 secondary circuits modeled in detail leveraging 120 typical PG&E secondary circuit configuration;
- 2,246 service transformers were modeled in detail;
- 11,512 service lines were added to the feeders; and
- 9,251 residential customers were associated with real PG&E AMI profiles.

Following these refinements, the feeder models were validated in detail, to ensure a reliable foundation from which subsequent analysis will depend. This validation resulted in feeder models that represent realistic operation of PG&E distribution feeders.

[64] See footnote 33, *supra*.

4

BASELINE ASSESSMENT OF PV ON THE FEEDERS

This chapter presents the baseline assessment of PV conducted for each of the six feeders studied. This baseline corresponds to the amount of residential PV generation that can be accommodated before any violations occur, with or without ES. To this end, representative PV profiles associated with each feeder were first determined. Then, PV systems were associated with the customers and the rating of each PV system was identified. Each PV penetration level considered in this modeling effort was defined as a percentage of *residential* customers with PV; *non-residential* customers were not associated to any PV installations. Next, ES systems were associated with the PV customers for each ES penetration level and the size and operation of each ES system was determined.

After the modeling steps above, baseline assessment of PV was conducted assuming that that SI functions were not activated. As part of the baseline PV assessment, for each of the six feeders, the settings for all *existing* voltage regulating equipment were adjusted when appropriate, for each of the PV penetration level considered. In particular, the LTC and voltage regulator control was switched to co-generation mode ("cogen mode"). All setting updates presented in this chapter reflect field operations that distribution engineers would perform to optimize use of existing regulation equipment when higher PV penetration levels are reached. Finally, the thermal and voltage impacts of the growing PV generation levels were analyzed.

4.1 Cases Studied

The technical assessment conducted as part of this modeling effort was performed considering a set of characteristic conditions that describe a range of loading, PV and ES scenarios:

- Three types of daily load profiles: peak, MIN and average, as described in Chapter 3.
- Five types of characteristic daily PV profiles, representative of a diversity of PV generation conditions through the year.
- Four PV penetration levels, each defined as a percentage of residential customers that operate a PV installation: 25%, 50%, 75%, and 100%. For example, a PV penetration level of 25% means that 25% of the residential customers connected to a given feeder have PV. Non-residential customers were not associated any PV installations in this modeling effort.
- Three ES penetration levels, defined as a percentage of residential customers with PV, that *also* have storage: 0%, 20%, and 40%. For example, a ES penetration level of 20% means that 20% of the residential customers operating PV also operate a storage system.

The tree of scenarios presented in Figure 4-1 illustrates the various PV penetration levels, ES levels, load type days, and PV generation profiles considered; a complete scenario enumeration is provided for one of the feeders considered.

The various combinations of characteristic conditions for the six feeders modeled represent a total of 1,080 scenarios that were individually simulated with OpenDSS. Each scenario was simulated with 15-minute resolution QSTS over 24 hours of the system operation.

Figure 4-1
Characteristic Conditions Defining All Scenarios Considered

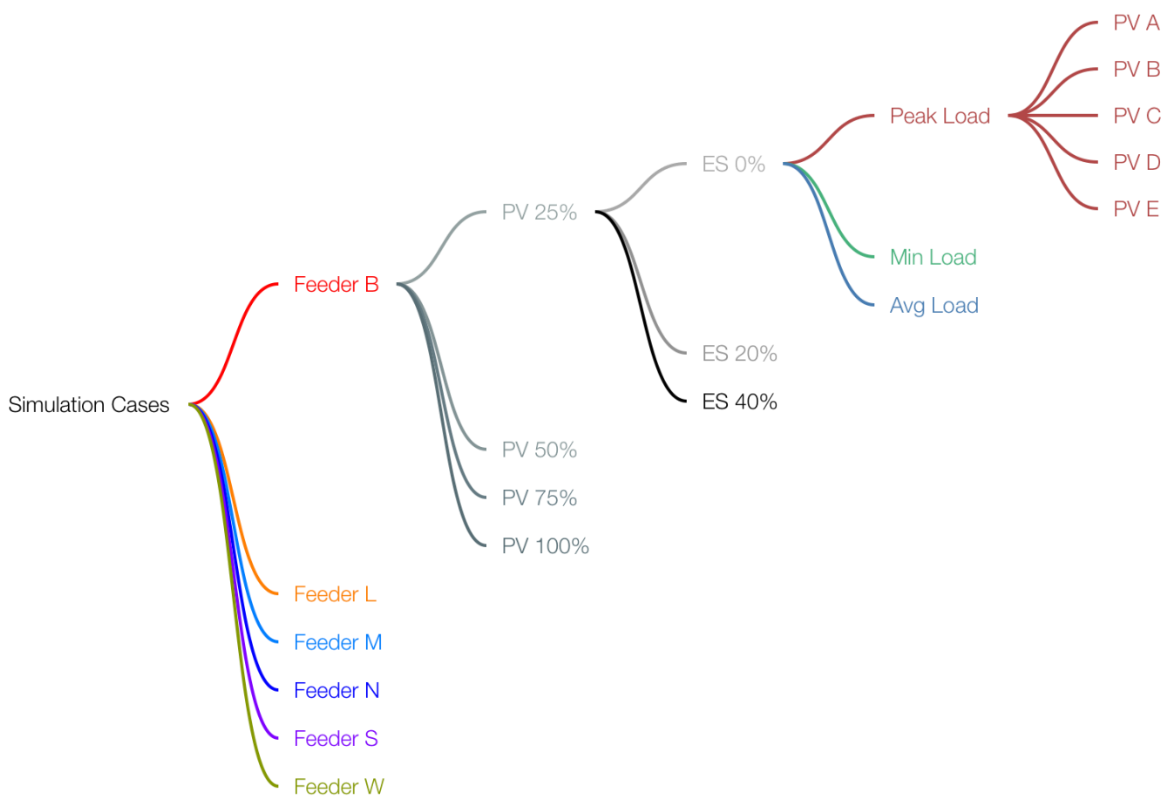

4.2 PV Modeling

The operation of PV installations was modeled leveraging the "PVSystem" object in OpenDSS. The modeling approach was designed to investigate the effects of PV systems, with the objective of accurately representing the diversity of actual residential PV installations and their condition, as observed in the field. Specifically, the diversity of meteorological conditions was captured by considering several representative daily PV profiles; efficiency factors derived from measured PV generation profiles were also considered, reflecting shading, tilting, temperature, and electrical losses. This diverse set of PV installations and conditions allowed for simulation and analysis of SI operations for realistic scenarios, for each of the six feeders modeled.

The implementation of this modeling approach was achieved with the following settings:

- Each PV residential installation was modeled with an independent "PVSystem" object;
- PV systems were modeled with single-phase connections at 240 V;
- PV profiles were included with 15-minute resolution as normalized scaling factors obtained from a sample of measured residential AC power generation powers in California;
- Irradiance property from "PVSystem" objects was set to unity in order to represent per-unit multipliers from PV profiles;

- Power factor was set to unity to avoid reactive power generation when SI functions are not activated;
- Percentage of DC power required for inverter operation (%cutin and %cutout) was set to 0.01% to follow the power generation characteristics from the measured AC power generation profiles;
- The rated max power of the PV array (Pmpp) was set to individually selected capacities according to the PV sizing approach described in Section 4.2.2;
- The kVA rating of inverter was set to reflect a DC/AC ratio equal to 1.2;[65] and
- PV systems were modeled as directly connected to the point of interconnection of each residential customer; however, PV wiring sensitivity analysis was performed for a selected scenario as described in Chapter 6.

The following sections describe the process and modeling assumptions related to the PV generation profiles and implementation in the simulation models.

4.2.1 PV Profile Selection

It was impractical to perform the large number of QSTS simulations over a whole year. Instead, a number of representative PV days were chosen to represent the diversity of PV generation through the year. To select these representative days, two factors were considered:

- The climate-based geographical diversity, capturing the differences in weather between different climate zones; and
- The local device diversity, capturing a realistic range of shading, tilt angle, orientation and other efficiency related aspects.

The representative PV generation profiles were selected following a two-stage process. First, clustering techniques were applied to typical meteorological data to characterize the climate zone associated with the six feeders considered. The first stage of the process provided the characteristics of five representative PV days used in this modeling effort. The first stage of the process also resulted in the annual distribution of the five representative days for each climate zone (and thus, feeder). In the second stage of the process, daily PV generation field measurement profiles were selected for each of the five representative PV day types. The following sections provide additional information for each stage of this process.

4.2.1.1 Typical Meteorological Data: Clustering Analysis and Day Selection

To capture climate-based geographical diversity, typical meteorological year data was obtained from the 2016 Building Energy Efficiency Standards.[66] Note that the six feeders analyzed are located in five distinct climate zones (Feeder B and Feeder N are in the same climate zone).[67] Clustering analysis was performed on the meteorological data obtained for the five climate zones to select representative PV days and the annual distribution of the representative PV days in the five climate zones. In this

---

65 In this report, DC/AC ratio is defined as the PV panel DC kW rating/PV inverter AC kVA rating. In practice the DC/AC ratios vary and are mainly driven by economic considerations. A more detailed discussion can be found, e.g., from: https://www.eia.gov/todayinenergy/detail.php?id=35372. PG&E performed an internal analysis confirming that DC/AC ratio of 1.20 was representative of existing residential PV installations.

66 2016 Building Energy Efficiency Standards for Residential and Nonresidential Buildings," CEC, June 2015. Available: https://www.energy.ca.gov/title24/2016standards/.

67 Feeders were located on the following climate zone numbers: Feeder B (3), Feeder L (4), Feeder M (2), Feeder N (3), Feeder S (13), and Feeder W (12).

modeling effort, different types of PV days were characterized based on "Clearness Index," α, and "Variability Index," β[68] that represent the normalized area and the line integral of a PV profile with respect to a selected base PV profile. The indices are defined as

$$\alpha = \frac{\sum_{i=1}^{n}\sqrt{(x[i]-x[i-1])^2-\Delta t^2}}{c_\alpha},$$

$$\beta = \frac{\Delta t \sum_{i=1}^{n} x[i]}{c_\beta},$$

where $x[i]$ is the PV profile GHI at time i, Δt is the length of the GHI measurement time interval, and c_α, c_β, are constants evaluated with respect to the representative PV profile $x_0[i]$, as

$$c_\alpha = \sum_{i=1}^{n}\sqrt{(x_0[i]-x_0[i-1])^2-\Delta t^2},$$

$$c_\beta = \Delta t \sum_{i=1}^{n} x_0[i] .$$

The clearness and variability indices are designed to capture the energy and variability of PV irradiance (and hence PV generation). Figure 4-2 illustrates three PV day types: sunny, cloudy, and overcast. Sunny PV profiles (Figure 4-2 (a)) tend to have low variability α and high clearness β, cloudy PV profiles tend to have high clearness α and high variability β (Figure 4-2 (b)), and overcast PV profiles tend to have low clearness α and low variability β (Figure 4-2 (c)).

Figure 4-2
Examples of Normalized Daily Profiles for (a) Sunny PV Day With High Clearness and Low Variability, (b) Cloudy PV Day With High Clearness and High Variability, and (c) Overcast PV Day With Low Clearness and Low Variability

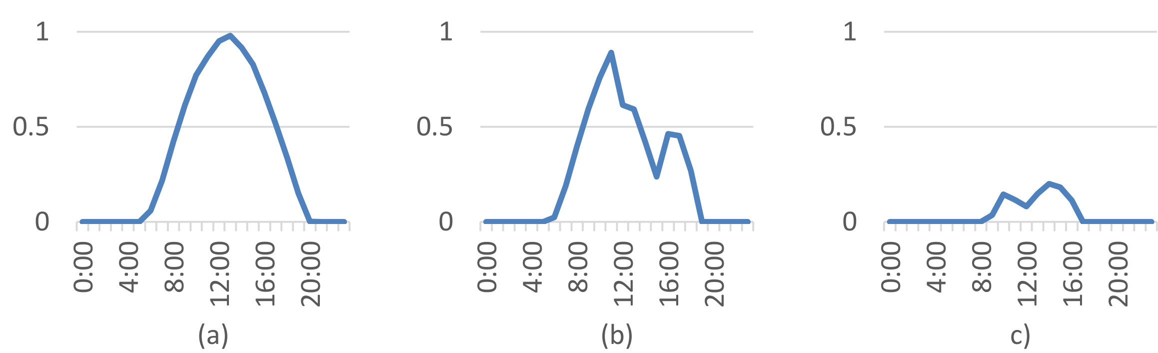

While the representative PV profile x_0 is arbitrary, it is typically chosen so that the maximum clearness index and variability indices area not much greater than unity. It should be noted that the possible magnitude of variability increases with the time resolution. For example, the maximum variability of one-minute data is much greater than the maximum variability of one-hour data.

---

68 Stein, J.S., Hansen, C.W. and Reno, M.J., 2012, April. The variability index: A new and novel metric for quantifying irradiance and PV output variability. In World Renewable Energy Forum (pp. 13-17). Denver, CO.

Here, the constant scaling factors c_α and c_β were first identified based on sunny day chosen from the annual meteorological GHI profile. These identified scaling factors were then used to calculate the clearness and variability indices for each of the feeders. Figure 4-3 shows a scatter plots of the clearness index values vs. the variability index values for the 365 days of the GHI profiles from the five climate zones.

Figure 4-3
Scatter Plot of the Clearness Index Values vs. the Variability Index Values for the 365 Days of the GHI Profiles From the Five Climate Zones

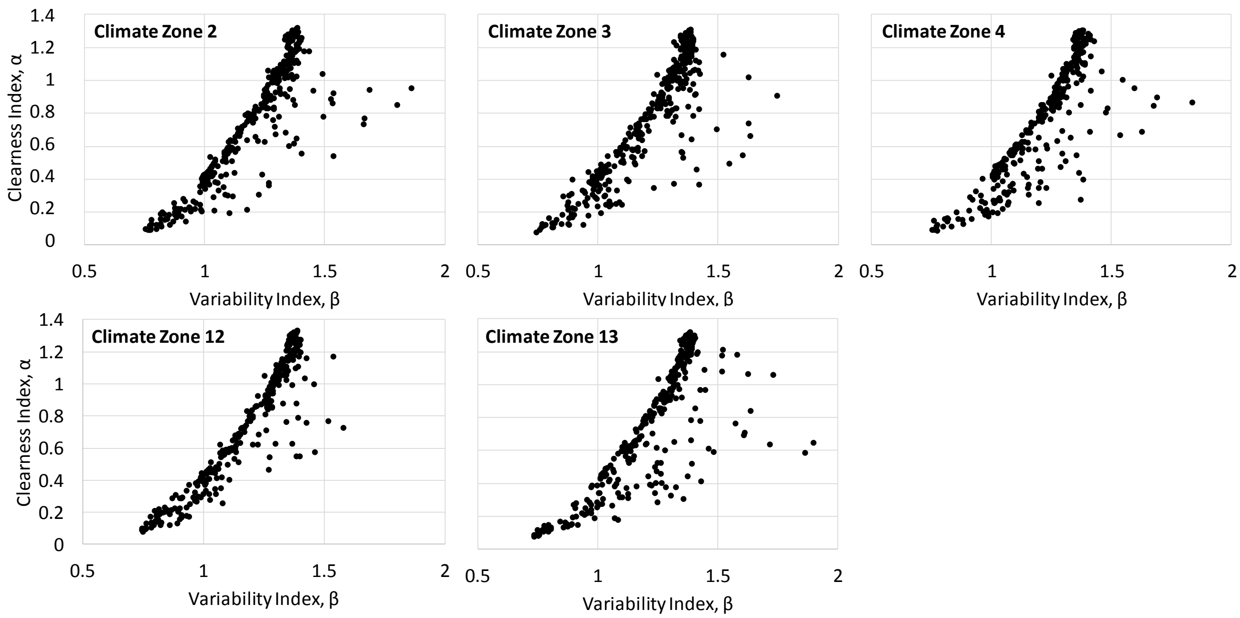

Next, a nearest-neighbor based heuristic clustering approach was used to choose representative PV days. Each daily GHI profile k, with associated clearness and variability (α_k, β_k) , was clustered based on

$$\text{Cluster}(k) = \arg\min_j \, (\alpha_j^{\text{Cl}} - \alpha_k)^2 + (\beta_j^{\text{Cl}} - \beta_k)^2$$

for $j = 1,2, \ldots, n$ clusters associated with n 'discriminant points' $(\alpha_j^{\text{Cl}}, \beta_j^{\text{Cl}})$. The discriminant points, which were an input for the clustering analysis, were chosen based on a trial-and-error method to yield a reasonable looking set of clusters. Based on the chosen discriminant points, the clustering algorithm divided the data into different clusters. Then, the cluster centroids were calculated as the weighted average of the data points in the cluster. The five cluster centroids were chosen as the five representative days for the climate zone. The number of clusters is a key variable to choose for clustering analysis. Here, different cluster counts were analyzed and ultimately, five clusters (i.e. $n = 5$) were found to sufficiently well represent different PV day types for the purposes of this modeling effort. Figure 4-4 illustrates the chosen discriminant points and the resulting clusters and cluster centers for the 365 days in the annual GHI profile from climate zone 2.

Figure 4-4
Clustering of PV Profiles Into a Number of Days That Represent Diverse PV Generation Conditions

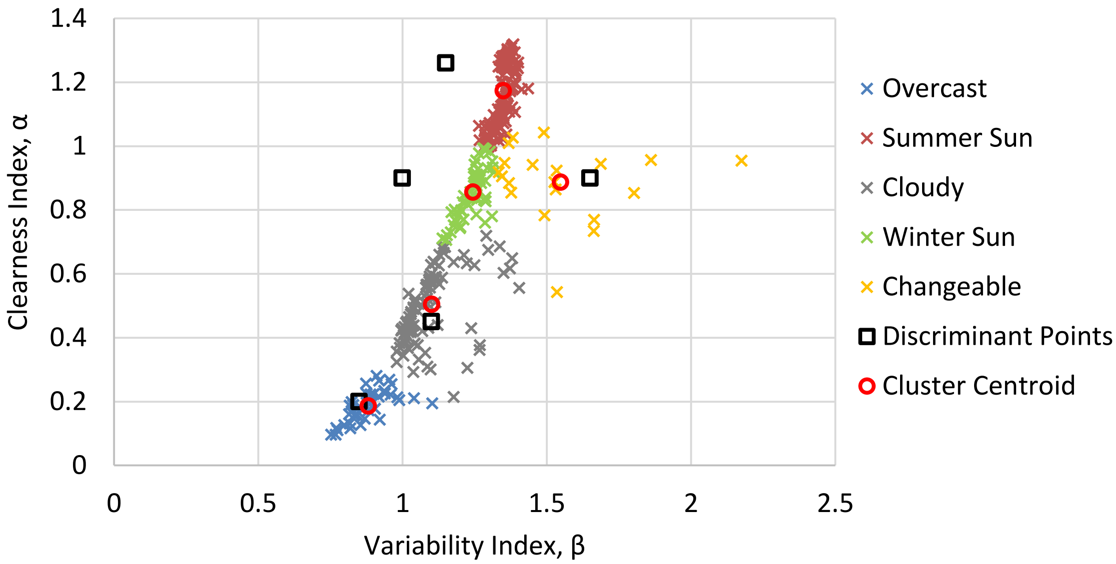

The clustering analysis discussed above was performed separately for each of the five climate zones.[69] The clustering analysis resulted in five cluster centers (i.e., five representative PV days) for each of the five climate zones. The obtained cluster centers were very similar for all the climate zones and as a result, the same representative PV days were chosen for all the climate zones. The representative PV days were selected as the averages the five climate zones' cluster centers. The geographic diversity between feeder climate zones was represented through the distribution of the five representative PV days. Figure 4-5 shows the share of the days per each cluster for the five climate zones. These shares are also the shares of the representative PV days for each climate zone. Note that the shares differ between the climate zones. These differences are utilized in this modeling effort to characterize the geographical diversity of meteorological conditions for PV generation purposes.

69 The same discriminant points were used for all the five climate zones as this resulted in reasonable clusters for each climate zone.

Figure 4-5
Distribution of Representative PV Days Over a Typical Year for the Five Climate Zones of the Six Analyzed Feeders

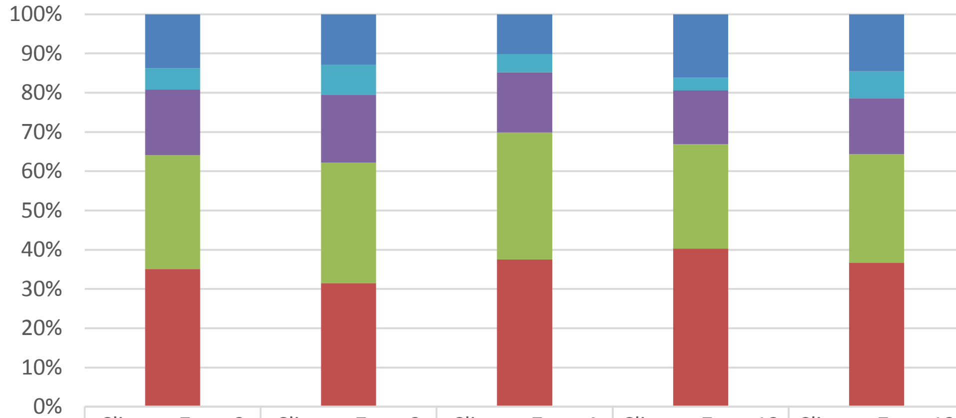

	Climate Zone 2 (Feeder M)	Climate Zone 3 (Feeders B & N)	Climate Zone 4 (Feeder L)	Climate Zone 12 (Feeder W)	Climate Zone 13 (Feeder S)
PV Profile E (Overcast)	13.7%	12.9%	10.1%	16.2%	14.5%
PV Profile D (Changeable)	5.5%	7.7%	4.7%	3.3%	6.8%
PV Profile C (Cloudy)	16.7%	17.3%	15.3%	13.7%	14.2%
PV Profile B (Winter Sun)	29.0%	30.7%	32.3%	26.6%	27.7%
PV Profile A (Summer Sun)	35.1%	31.5%	37.5%	40.3%	36.7%

4.2.1.2 PV Time Series Day Selection

The meteorological data, which was used for the clustering analysis above, could not be used to represent the local diversity in PV generation resulting in from diverse installation types and generating conditions. Instead, this modeling effort utilized PV generation measurement data from the Grid Integration of ZNE Communities[70] to represent the local diversity in PV generation. The utilized data set consist of 15-minute PV AC generation output for 15 residential customers, each located on the same feeder. The measured generation profiles show diversity through the effects of shading, tilting, differences in generation efficiency, etc.

As mentioned previously, the clearness and variability indices are dependent on the time scale chosen. Therefore, the PV generation data was down-sampled from 15-minute to 1-hour granularity so that the centroids would scale appropriately with the 1-hour meteorological data used for the clustering analysis above. Then, an average PV generation profile was calculated as an average over the 15 PV generation measurement profiles and the clearness and variability indices were calculated for the average PV generation profile. Figure 4-6 shows the clearness and variability indices for the average PV generation profile and the cluster centers obtained from the clustering analysis discussed above. Next, five representative PV days were chosen as the days closest to each of the cluster centers. This resulted in 15 profiles for each of the 5 representative PV days. The resulting PV profiles, shown in Figure 4-7, represent a wide range of meteorological conditions:

---

70 "Grid Integration of Zero Net Energy Communities," EPRI. Jan. 2017. Available: http://www.calsolarresearch.ca.gov/images/stories/documents/Sol4_funded_proj_docs/EPRI_Ram/CSIRDD_Sol4_EPRI_Grid-Integration-of-ZNE-Communities_FinalRpt_2017-01-27.pdf.

- Profile A ('summer sun') is taken from the summer, and represents peak solar irradiance;
- Profile B ('winter sun') is taken from the autumn, and represents low solar irradiance;
- Profile C ('cloudy') represents a cloudy day, with clouds particularly early in the morning;
- Profile D ('changeable') represents extreme variability in cloud cover, resulting in large swings in time; and
- Profile E ('overcast') shows an overcast day.

Figure 4-6
The Clearness and Variability Indices OF THE Down-Sampled Average PV Profile

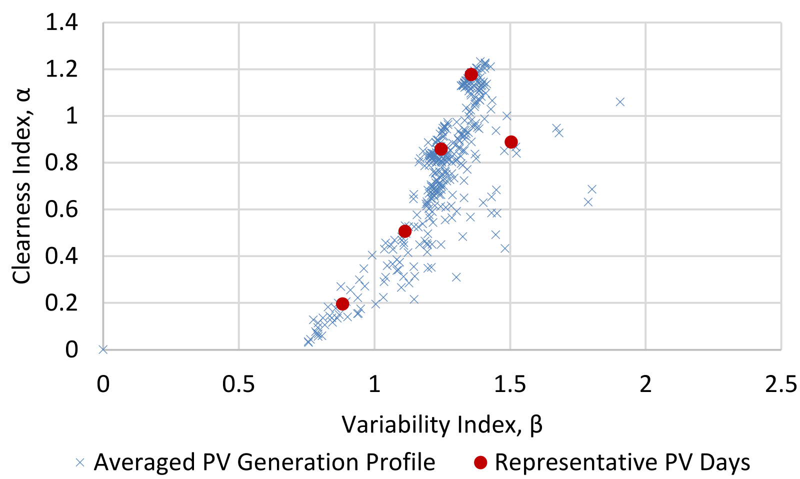

Figure 4-7
The Selected 15 PV Generation Profiles for the Five Representative PV Days

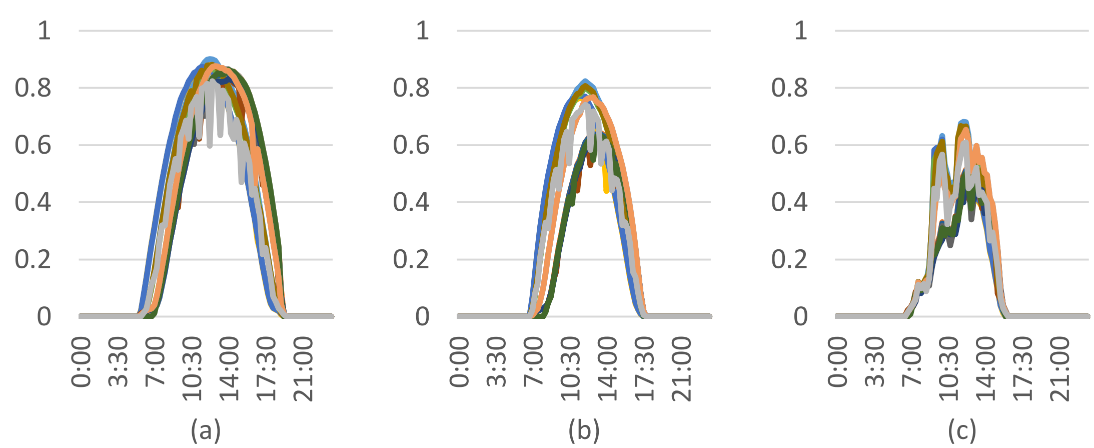

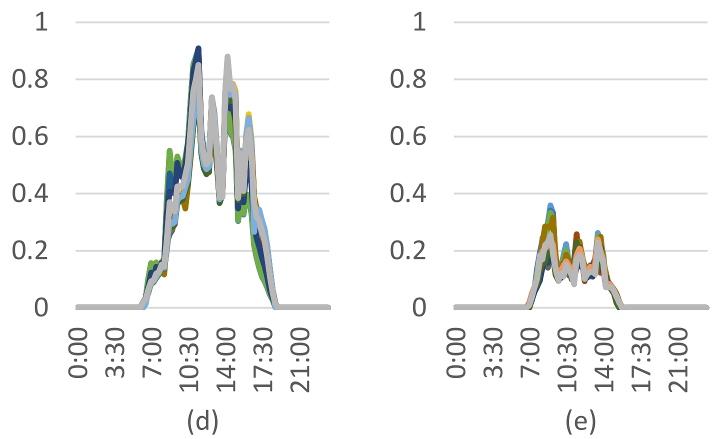

4.2.2 *PV Sizing and Deployment*

At the time of this modeling effort, residential customers in PG&E territory taking service on a Net Energy Metering (NEM) 2.0 tariff can size their PV system to have an annual energy production up to 100% of their total load consumption.[71] In this modeling effort, it was conservatively assumed that all customers interconnecting PV would size their PV installation as large as possible. As a result, the PV system sizes were chosen so that the PV generating capacity was 100% of the customer annual load demand (as calculated with the AMI measurement data). PG&E performed an internal analysis to confirm that the dominant PV system size was based on 100% of the customer annual load demand.

To determine the PV system sizes for all customers, the average daily energy consumption was calculated for all AMI profiles used to represent the residential customers as described in Chapter 3. Figure 4-8 shows the average daily energy consumption for all the AMI profiles on Feeder B and Feeder M.

Next, the average daily energy generated by a PV system on the locations of each of the six feeders was estimated using NREL's PVWatts® calculator.[72] The difference in the energy generated between the six feeder locations (calculated as kWh/day per kW installed PV) appeared to vary by less than 5% as illustrated in Figure 4-9. Therefore, for each feeder, the mean PV generation capability was assumed to be 4.40 kWh/day for each kW (DC) of PV installed.

---

71 "Electric Schedule NEM – Net Energy Metering Service," PG&E. Nov. 2016. Available: https://www.pge.com/tariffs/tm2/pdf/ELEC_SCHEDS_NEM.pdf.

72 "PVWatts® Calculator," Alliance for Sustainable Energy, LLC in Golden, CO, 80401. Available: https://pvwatts.nrel.gov/.

Figure 4-8
The Average Daily Energy Consumption of the AMI Profiles on Feeder B and M

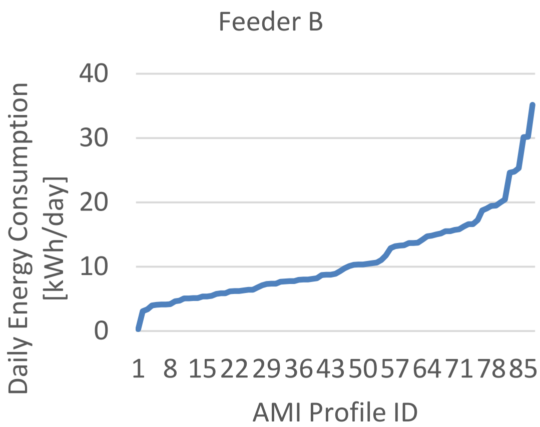

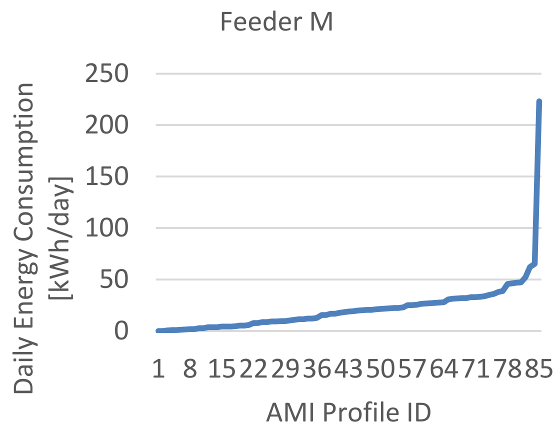

Figure 4-9
Average Daily Energy Generated by a 1-kW PV (DC) Installation

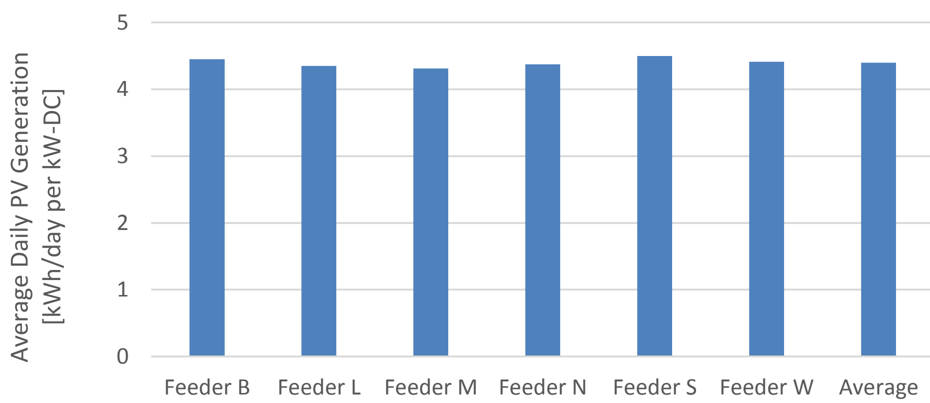

In this modeling effort, residential customers with very low average daily energy consumption were assumed to be unlikely to install PV at any PV penetration level. This classification was performed by comparing the residential customer average daily energy consumption (see Figure 4-8 for examples for two feeders) to the estimated PV generation obtained by a 1-kW (DC) PV installation (see Figure 4-9): customers with an average daily energy consumption below 4.4 kWh/day were not associated with a PV system, regardless of the PV penetration level considered.

All other residential customers were associated with a PV system with a size that was calculated by dividing the customer average daily energy consumption (calculated based on the annual AMI profile) by 4.4 kWh/day. Only discrete PV sizes at 0.25 kW increments were considered. The resulting PV panel nameplate capacities (kW-DC) are shown in Figure 4-10 for all the customers on Feeder B and Feeder M. All PV systems were assumed to have a DC/AC ratio of 1.20. In other words, for each PV installation, the total PV panel array nameplate was assumed to be 20% oversized compared to the PV inverter nameplate AC capacity. The PV inverter capacities were calculated by dividing the PV panel (DC) capacity by 1.2.

Figure 4-10
Assigned PV System Nameplate Capacities (kW-DC) for All Customers on Feeder B and Feeder M

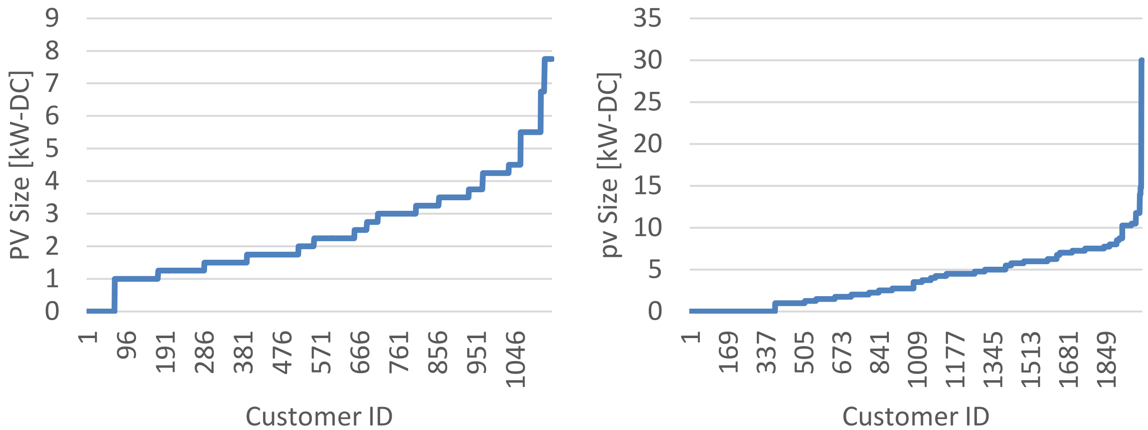

The deployment of the independently sized PV installations was randomly assigned in decreasing order for each of the PV penetration levels considered. For the 100% penetration level, each residential customer (load) that was eligible for PV was assigned one. At lower penetration levels, PV was systematically and randomly removed. As a result, all PV that is connected at 25% will also exist at 50% (and also in 75% and 100%). Figure 4-11 shows the total installation count for each PV penetration level and each feeder.

Figure 4-11
Number of PV Installations Per Feeder and PV Penetration Level

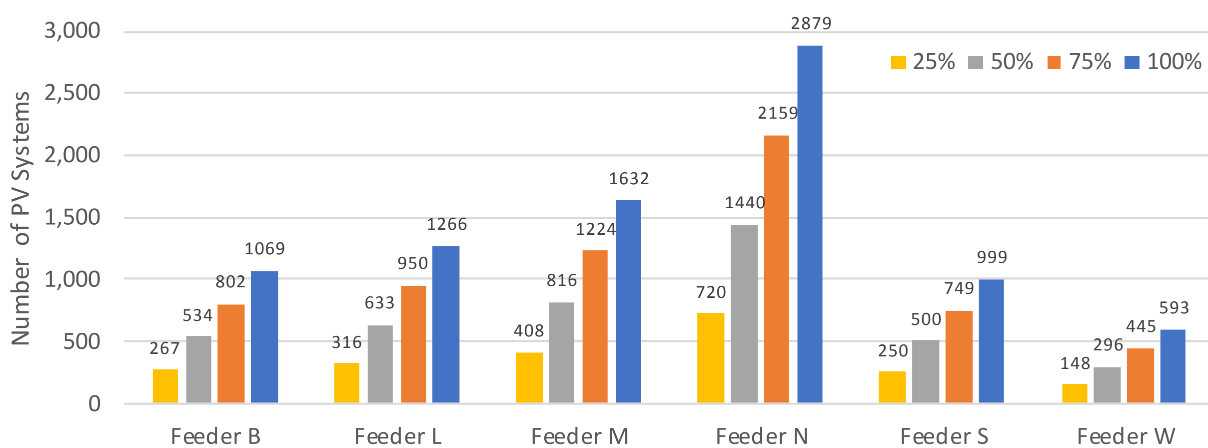

Figure 4-12 shows the resulting aggregated PV capacities per PV penetration level and feeder. The aggregated capacities vary from 0.60 MW on Feeder W at 25% PV penetration level to 9.76 MW on Feeder N at 100% PV penetration level.

Figure 4-12
Installed Aggregated PV (DC) Rating Per Feeder and PV Penetration Level

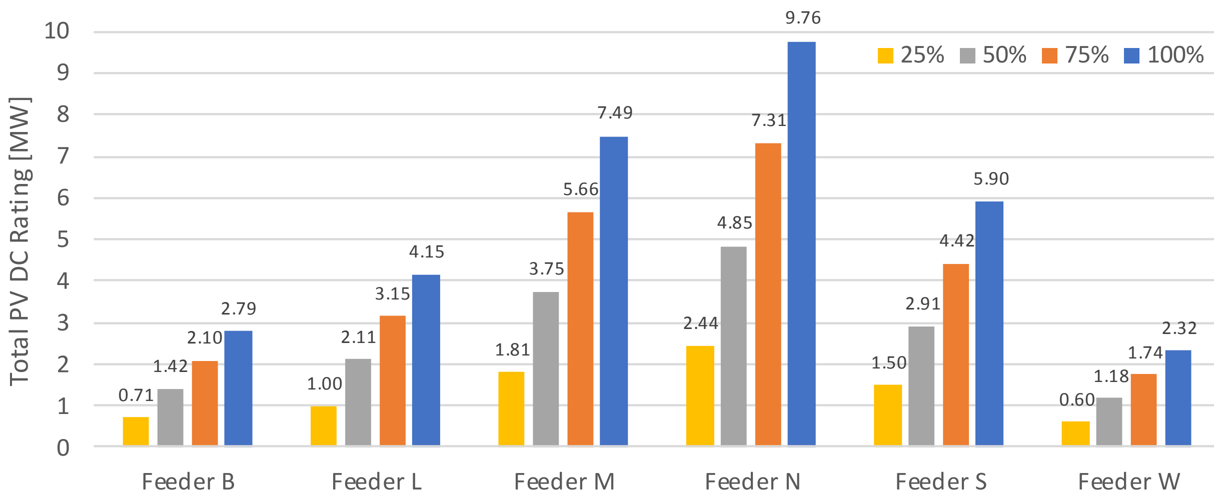

There are various ways to define PV penetration level. Since the focus of this modeling effort was on residential PV, this modeling effort defined penetration level was defined as percentage of the residential customers with PV. To enable comparing the analyzed PV penetration levels to other studies, Figure 4-13 shows the aggregated PV capacity compared to the MAX, MIN and noon-time loading conditions on each feeder. Compared to the feeder MIN load, the aggregated PV ranges from 396.7% on feeder B to 142.5% on feeder N. Compared to the feeder peak load, the aggregated PV ranges from 126.2% on feeder B to 27.2% on feeder W. Finally, compared to feeder noon-time load, the aggregated PV ranges from 262% on feeder B to 121.4% on feeder N. The large range in values is explained by the share of residential customers and residential customer load on each feeder, as well as by the range of feeder load over the analyzed characteristic load days. Table 4-1 summarizes the aggregated installed generation capacity in comparison with the loading conditions of interest for each feeder of interest.

Figure 4-13
Analyzed PV Penetration Levels vs. Feeder Peak, Min and Min Noon-Time Load

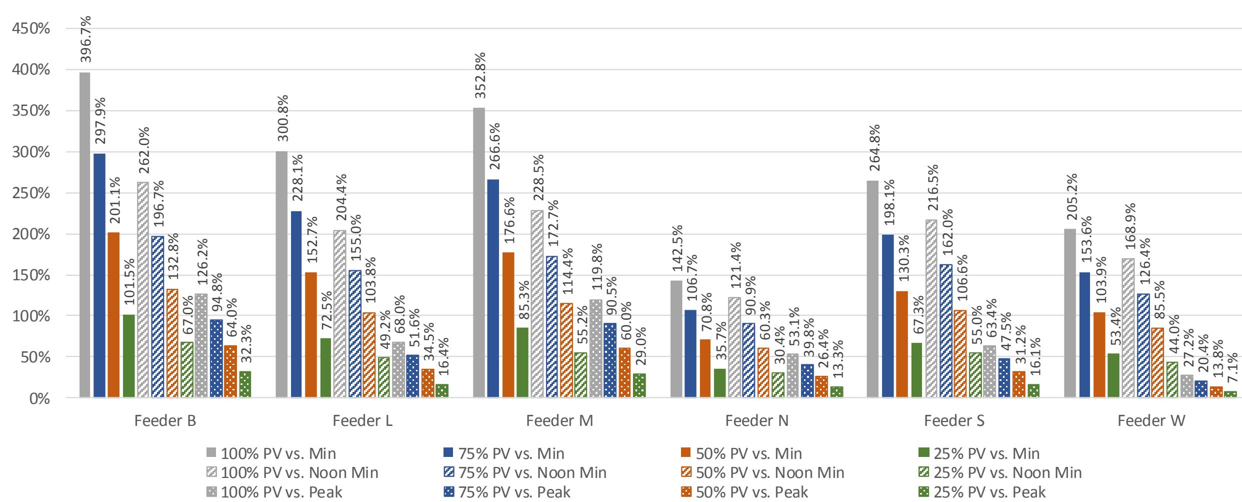

Table 4-1
The Peak, Minimum and Noon-Time Load of Each Feeder and Each Characteristic Load Day Compared to the Analyzed PV Penetration Levels

Circuit		Feeder B	Feeder L	Feeder M	Feeder N	Feeder S	Feeder W
Peak Load Day	Peak Load (kW)	2212	6107	6248	18375	9305	8534
	Min Load (kW)	872	1888	2435	10747	6059	4574
	Load at Noon (kW)	1985	4691	5268	15732	8611	7380
Min Load Day	Peak Load (kW)	1364	2498	3322	8903	3011	1612
	Min Load (kW)	704	1381	2122	6850	2229	1132
	Load at Noon (kW)	1066	2031	3276	8039	2727	1376
Avg. Load Day	Peak Load (kW)	1639	3236	3544	11184	4245	3881
	Min Load (kW)	803	1600	2774	8256	2979	3003
	Load at Noon (kW)	1327	2930	3511	10611	4184	3239
PV 25%	PV count	267	316	408	720	250	148
	Total kW	715	1000	1810	2444	1500	605
	PV kW vs. Peak Load (%)	32.3%	16.4%	29.0%	13.3%	16.1%	7.1%
	PV kW vs. Min Load (%)	101.5%	72.5%	85.3%	35.7%	67.3%	53.4%
	PV kW vs. Noon Min Load (%)	67.0%	49.2%	55.2%	30.4%	55.0%	44.0%
PV 50%	PV count	534	633	816	1440	500	296
	Total kW	1415	2108	3748	4852	2906	1176
	PV kW vs. Peak Load (%)	64.0%	34.5%	60.0%	26.4%	31.2%	13.8%
	PV kW vs. Min Load (%)	201.1%	152.7%	176.6%	70.8%	130.3%	103.9%
	PV kW vs. Noon Min Load (%)	132.8%	103.8%	114.4%	60.3%	106.6%	85.5%
PV 75%	PV count	802	950	1224	2159	749	445
	Total kW	2096	3149	5657	7309	4416	1739
	PV kW vs. Peak Load (%)	94.8%	51.6%	90.5%	39.8%	47.5%	20.4%
	PV kW vs. Min Load (%)	297.9%	228.1%	266.6%	106.7%	198.1%	153.6%
	PV kW vs. Noon Min Load (%)	196.7%	155.0%	172.7%	90.9%	162.0%	126.4%
PV 100%	PV count	1069	1266	1632	2879	999	593
	Total kW	2792	4153	7487	9763	5903	2324
	PV kW vs. Peak Load (%)	126.2%	68.0%	119.8%	53.1%	63.4%	27.2%
	PV kW vs. Min Load (%)	396.7%	300.8%	352.8%	142.5%	264.8%	205.2%
	PV kW vs. Noon Min Load (%)	262.0%	204.4%	228.5%	121.4%	216.5%	168.9%

4.3 Energy Storage Modeling

Three penetration levels of residential ES systems were analyzed in this modeling effort: 0%, 20%, and 40% of the residential customers with a PV system. Non-residential customers, or residential customers without PV were not associated with an ES system. The residential customers were assumed to solely leverage the ES systems to reduce their time-of-use (TOU) tariff, i.e., to shift their energy consumption from the peak energy price period to the off-peak energy price period. Moreover, the ES systems were restricted to charge only from PV generation and the energy exports from the battery banks were not allowed.[73] Therefore, the ES dispatch was modeled to discharge the entire stored energy during the peak energy price period as quickly as possible without exceeding the customer load consumption in the same period.

The ES modeling performed in this modeling effort had two parts. First, the ES system power and energy capacities were determined for each customer with a storage system. This was achieved by considering both the average load (in kWh/day) and the PV nameplate capacity (in kW) of each customer. For this purpose, a 5-kW battery unit with 12 kWh capacity and 90% of round-trip efficiency was considered as a 'basic module' in this modeling effort. This modeling effort assumed that ES system adoption will continue to be primarily driven by use cases such as backup power and for increased self-

[73] For the purpose of this modeling effort, the ES was assumed to be AC coupled without smart inverter functions. In practice, CA Rule 21 would require the storage inverter to also be compliant with the analyzed Volt-VAR and Volt-Watt functions.

consumption of PV. Therefore, a lookup table, derived from public sizing tools such as,[74] was used to estimate the number of the basic modules that a given customer would have. The lookup table is illustrated in Figure 4-14. For most customers, the average daily energy consumption was below 100 kWh (as illustrated in Figure 4-8) and the PV capacity was less than 10 kW (as shown in Figure 4-10). As a result, most ES installations assigned consisted of one or two 'basic modules', i.e., up to 10 kW – 24 kWh.

Figure 4-14
Number of Energy Storage Modules Required With Respect to Average Daily Energy Consumption and PV Nameplate Rating

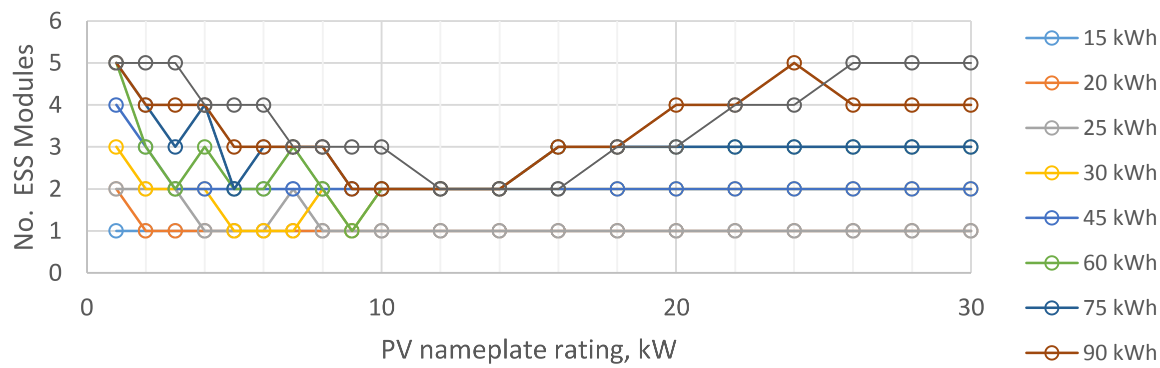

4.3.1 *Energy Storage Dispatch*

In this modeling effort, ES was assumed to be primarily used to reduce the customer TOU tariff by moving customer peak price period consumption to off-peak price period. The on-peak price period was assumed to be between 4-9 p.m., and all other times to be off-peak.

Since separate daily QSTS simulations were performed in this modeling effort, it was important to ensure that the ES net energy consumption during the day was zero.[75] To account for this, two cases of distinct ES operation were considered, dependent on the PV profile and the customer installed ES capacity:

1. If the customer's PV generation during the day prior the on-peak period was sufficiently large to cover the customer's total on-peak load (4 p.m. – 9 p.m.), and if the storage had sufficiently large capacity, then exactly enough energy was charged to the storage during the day prior to the peak load period to cover the customer's load during the on-peak period.

2. If the customer's PV generation prior to the on-peak period was not sufficiently large to cover the customer's on-peak load, or if the storage capacity was not sufficiently large, the storage was set to charge as much energy as possible prior to 4 p.m. Then, during the on-peak period, the storage was set to discharge as much energy as it had stored.

---

74 "Powerwall: The Tesla Home Battery," Tesla Inc., 2018. Available: [https: //www.tesla.com/powerwall.](https://www.tesla.com/powerwall) Accessed: August 2018.

75 Otherwise, the ES systems could have distorted the results and the conclusions of this modeling effort by generating or consuming energy during a given QSTS simulation that in reality would have to be compensated by charging or discharging during the following day.

In Case 1, if the load was slightly higher (or lower) than predicted, so long as the battery was not completely empty, the storage would be able to increase the export slightly, and charge more the next day; on the other hand, if it charged slightly less, then it needed to charge slightly less the next day. In Case 2 on the other hand, the best the storage could do was to fully charge and then, fully discharge. As a result, Case 1 and Case 2 represent storage operations that maximize the benefit to the customer.

In this modeling effort, the ES devices were modeled by adjusting the customer load profile using the "Loadshape" object of OpenDSS. Particularly, the customer power consumption, PV generation and ES capacities were considered and combined to create a custom load profile in which the customer load profile was adapted to consider the operation of the ES device. This approach resulted in 50,640 distinct customer load profiles that were calculated off-line prior to the QSTS simulations to represent the ES deployments analyzed in this modeling effort. Figure 4-15 shows an example load shape for a residential customer with sufficiently high PV generation to store the energy required to supply the customer's energy consumption during on-peak time. After considering the available PV generation and the customer demand from 4-9 p.m., the storage profile was calculated to reflect the charge and discharge shapes. Finally, the new load shape was derived from the ES profile and the original load consumption profile. This net consumption was then applied as the "Loadshape" property for this customer for this particular characteristic load day and representative PV day. The net load of this customer shows no power consumption during on-peak period, and the full exported power provided by the PV installation is visible during a fraction of the PV generation period. For comparison, Figure 4-16 shows an example of insufficient PV generation that resulted in a discharge time shorter than the on-peak period.

Figure 4-15
Example of Sufficient Solar Energy Storage Operation: Left: Original Load and Generation Profiles; Center: ES Profile and New Loadshape (Considering ES But Not PV); and Right: Net Household Load (With Load, ES, and PV Generation)

Figure 4-16
Example of Insufficient Solar Energy Storage Operation. Left: Original Load and Generation Profiles; Center: ES Profile and New Loadshape (Considering ES But Not PV); and Right: Net Household Load (With Load, ES, and Generation)

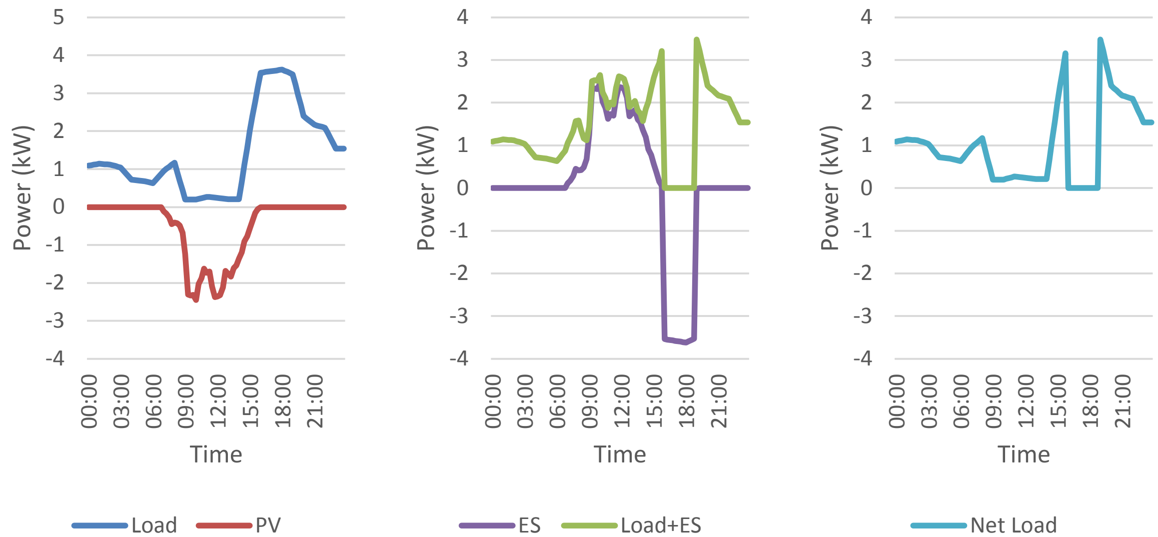

4.4 Baseline Assessment of PV and Energy Storage Impacts

This section will discuss the baseline assessment of PV and ES impacts. This baseline assessment quantified the impacts from PV and ES without considering PV SIs or conventional distribution measures to mitigate the impacts.

4.4.1 Metrics for Feeder Analysis Impacts

In this modeling effort, a large number of daily 15-minute QSTS simulations were performed to analyze smart PV inverters and ES. A large set of time-series results (96 values per result metric and QSTS simulation) was recorded for each QSTS simulation. The recorded *QSTS time-series result metrics* include, but are not limited to:

- Highest and lowest feeder voltages at the MV and LV level
- Service transformer voltages and secondary voltage rises to each PV customer
- All element overloads
- Feeder head powers and voltages
- Distribution losses
- States (tap, or on/off) and voltages for each capacitor bank, voltage regulator, and load-tap changer (LTC)
- PV system active power, reactive power, and voltage for each PV customer
- Load active power, reactive power, and voltage for each PV customer.

Given the large number of QSTS simulations conducted on each feeder (183 simulations per feeder without SI functions, and many more with SI functions), it was not practical to analyze the time-series result metrics for each QSTS simulation separately. It would also not have been straightforward to compare different QSTS simulations using the time-series result metrics. Thus, a set of *QSTS simulation* *summary metrics* was defined to establish a numeric value (as opposed to 96 values) summarizing each key time-series result of interest from a given QSTS simulation. The metrics are summarized in Table 4-2.

A key focus of this modeling effort was to analyze the impact of smart PV inverters on feeder steady-state voltages. Thus, a number of steady-state voltage metrics were defined to capture the highest and lowest voltage magnitudes, and the duration (hours) and the scope (feeder area) of the overvoltages and undervoltages experienced. In this modeling effort, voltages above 1.05 p.u. and below 0.95 p.u. were considered overvoltages and undervoltages, respectively. These voltage limits were chosen to reflect the service voltage limits defined in PG&E Electric Rule 2[76] and the service voltage Range A limits defined in ANSI C84.1-2016.[77] Both PG&E Rule 2 and ANSI C84.1 do not expressly prohibit infrequent and limited periods of voltages outside these limits. In this modeling effort, the concept of *significant voltage violation* was defined to represent infrequent and limited periods of voltages outside the permissible ranges. Significant overvoltages were defined as overvoltages with either a duration over one hour *or* a scope affecting more than 5% of the feeder buses. Significant undervoltages were defined analogously. In this modeling effort, the concept of significant voltage violations was applied as a threshold for the effectiveness of PV SI functions, and for the need of distribution upgrade measures.

A secondary voltage rise metric was defined to capture the secondary system impact on high voltages. Three element loading metrics were defined to capture any overloads experienced.

Seven feeder loading metrics were identified to represent the max forward and reverse power flows, the total active and reactive energy at the feeder head (including PV and ES), and the total kWh consumption of loads on the feeder. Distribution losses and voltage regulation equipment operation counts were also captured. Finally, a metric was chosen to record the total PV generation on the feeder.

The metrics defined in Table 4-2 will be used extensively in the remaining of this report. Some of these metrics are used later in this chapter to present the results of the baseline PV impact assessment. The metrics are further utilized when presenting the QSTS results obtained after performing distribution upgrades (Chapter 5), and with PV SI functions (Chapter 6). The metrics are also extensively utilized in Chapter7 when comparing the results from the baseline PV impact assessment, presented in this chapter, to the results obtained with distribution upgrades (Chapter 5), and SI functions (Chapter 6). Chapters 5, 6, and 7 all leverage also various “composite metrics” that further aggregate the metrics listed in Table 4-2 for *groups* of QSTS simulations to, for example, compare the results obtained across multiple PV penetration levels.

---

[76] “PG&E Electric Rule 2.” PG&E, 31-Jul-1990. Available: https://www.pge.com/tariffs/tm2/pdf/ELEC_RULES_2.pdf.

[77] “ANSI C84.1-2016 American National Standard for Electric Power Systems and Equipment – Voltage Ratings (60 Hertz).” ANSI, 2016.

Table 4-2
QSTS Simulation Summary Metrics

Category	Metric Label	Unit	Description
Steady-state voltage	Max MV Voltage	p.u.	Max. feeder voltage at medium voltage (MV) buses
	Max LV Voltage	p.u.	Max. feeder voltage at low voltage (LV) buses
	Min MV Voltage	p.u.	Min. feeder voltage at MV buses
	Min LV Voltage	p.u.	Min. feeder voltage at LV buses
	Time Above Max MV Voltage	hours	Total time with at least one MV bus above 1.05pu
	Time Below Min MV Voltage	hours	Total time with at least one MV bus below 0.95pu
	Time Above Max LV Voltage	hours	Total time with at least one LV bus above 1.05pu
	Time Below Min LV Voltage	hours	Total time with at least one LV bus below 0.95pu
	Max pct Buses with Overvoltage	%	Max percentage of buses with overvoltages
	Overvoltage at Max pct Buses	p.u.	Max voltage at the time instance with the max percentage of feeder buses with overvoltage condition
	Max pct Buses with Undervoltage	%	Max percentage of feeder buses with undervoltages
	Undervoltage at Max pct Buses	p.u.	Min voltage at the time instance with the min percentage of feeder buses with overvoltage condition
	Trfs with overvoltage	N/A	Number of service transformers with overvoltages at any downstream bus
Secondary Voltage Rise	Max V rise	p.u.	Max secondary voltage rise (voltage rise between PV customer panel and service transformer primary @240V base).
Element Loading	Overloaded Elements Count	N/A	Number of feeder elements with at least one-time step of overload
	Time with Overloads	Hours	Total time with at least one element overloaded
	Highest Overload	%	The highest loading (% of limit) of all overloaded elements (0% if no overloads experienced)
Feeder Load	Max kW Feeder Head - Forward	kW	Max feeder head active power consumption
	Max kVAR Feeder Head - Forward	kVAR	Max feeder head reactive power consumption
	Max kW Feeder Head - Reverse	kW	Max feeder head active power generation
	Max kVAR Feeder Head - Reverse	kVAR	Max feeder head reactive power generation
	kWh Feeder Head	kWh	Total feeder head active energy
	kvarh Feeder Head	kvarh	Total feeder head reactive energy
	Feeder kWh Consumption	kWh	Total active energy consumed by loads
Distribution Losses	Feeder kWh Losses	kWh	Total active losses in energy
Voltage Regulation Equipment Operation	LTC Operations	N/A	Number of LTC operations
	Reg Operations	N/A	Number of regulator operations
	Cap Operations	N/A	Number of cap operations
PV Generation	PV kWh generation	kWh	Total active energy generated by all PV systems
	PV Inverter Utilization	%	PV inverter average percentage utilization (% of inverter kVA rating)
	PV kvarh generation	%	PV inverter total kvarh generation (% of inverter kVA rating)

4.4.2 Approach to Adjust Voltage Regulator and Capacitor Settings

This modeling effort compared the merits of two strategies to mitigate adverse PV impacts at various PV penetration levels: one strategy relying on conventional distribution upgrades, the other leveraging SI functions. To this end, it was necessary to realistically represent the distribution measures that PG&E would apply as the PV penetration levels grow. This includes the possible adjustment of various control settings for *existing* distribution equipment.

This modeling effort assumed that all PG&E LTCs and line voltage regulators will have bi-directional capabilities as PV penetrations grow.[78] In particular, all LTCs and voltage regulators were assumed to include a cogeneration mode (or 'cogen mode'), which ensures proper operation of the equipment when the regulating equipment sees reverse power flow caused by downstream DERs, but when the source side of the regulating equipment has not changed as discussed, e.g., in.[79] Although some PG&E LTCs and line voltage regulators do not currently have bi-directional capabilities, this assumption is realistic since bi-directional capability is typically required for LTCs and voltage regulators that may experience reverse power flow caused by PV. Note that bi-directional capabilities are required independently of whether SIs are used or not. As a result, the costs associated with enabling the bi-directional capabilities were not considered in the economic analysis that was performed in this modeling effort. Additionally, the economic analysis excluded equipment upgrades that were required in both scenarios with conventional measures and SI functions.

A first line of measures applied by PG&E to address overvoltages caused by PV is to modify the settings of the existing voltage regulation equipment deployed on each feeder. Such manual setting changes, relatively cost-effective to perform since they leverage *existing* feeder voltage regulation equipment, can be very effective at addressing adverse voltage impacts caused by PV. As a result, this modeling effort assumed that manual setting changes to existing voltage regulation equipment are always performed, whether SI functions are used, or not. Thus, the manual setting changes were considered as a part of the baseline PV impact assessment, and before any other conventional distribution measures or SIs were considered. The costs associated with the manual setting changes were not considered in the economic analysis performed in this modeling effort. Thanks to these setting changes, the PV voltage impacts observed as part of the baselines assessment were less severe than what would have been observed without implementing these manual setting changes. However, the consideration of these manual setting changes represented PG&E existing engineering practices more realistically, and thus resulted in a more realistic assessment of the baseline PV impacts.

In this modeling effort, manual changes were considered to the following voltage regulation equipment settings:

- Capacitor time control settings, including entirely turning OFF the capacitors, if needed.
- Enabling the cogen mode on all LTCs and voltage regulators.
- LTC/voltage regulator cogen mode reverse voltage regulation set points.

---

78 In practice, PG&E adds bidirectional capability to regulators when an interconnection modeling effort indicates reverse power flow or when the regulator is replaced for some other reason.

79 "CL-7 Voltage Regulator Control; Installation, Operation, and Maintenance Instructions," Eaton Corporation. April 2018 Available: http://www.eaton.com/content/dam/eaton/products/medium-voltage-power-distribution-control-systems/voltage-regulators/cl-7-regulator-control-instructions-mn225003en.pdf.

- LTC/voltage regulator cogen mode forward voltage regulation set points were adjusted in some instances, but were largely left unchanged since the forward set points had already been adjusted in Chapter 3.
- LTC/voltage regulator cogen mode forward and reverse R and X settings were also largely left unchanged since it was assumed that the forward R and X settings had already been properly identified by to reflect the "load center" of each feeder to be regulated. It was also assumed that the cogen mode reverse R and X settings should be similar to the forward mode since the PV was distributed based on the load resulting in a "generation center" similar to the "load center."

Voltage regulation equipment settings could be adjusted by performing SLF analysis for feeder boundary conditions that include:

- Peak load without PV
- Minimum (daytime) load with maximum PV generation
- Minimum load without PV
- Minimum (daytime) load with maximum PV output

In this modeling effort, SLF analysis was not applied as the feeder loads and PV had been represented with detailed time-series models (as detailed in Chapter 3). Indeed, because of the time-series applied for the load and PV models, it was not immediately clear which load or PV power levels should have been assumed to perform a SLF analysis. For example, representing the loads with load allocation would not have represented the worst-case conditions experienced by the secondary circuits. Furthermore, representing the PV generation with rated PV output would have resulted in overly conservative extreme scenarios. In this modeling effort, the manual changes to the voltage regulation equipment settings were identified by performing daily QSTS simulations with the following steps (the QSTS simulation in the first step 1. was performed for peak PV profile with MIN load profile):

1. Perform daily QSTS simulation and obtain the feeder time-series voltage profile.
2. Based on the feeder time-series voltage profile, identify the time-instance with the extreme voltage conditions. If no overvoltages or undervoltages are experienced, go to step 4. Otherwise, plot a "static" voltage profile for the time instance.
3. Based on the "static" voltage profile, identify manual changes to voltage regulation equipment settings to address the extreme voltage conditions and go back to step 1.
4. Run daily QSTS for all the 15 load and PV profile combinations (3 load profiles and 5 PV profiles). If no overvoltages or undervoltages are experienced, stop. Otherwise, identify the day with the most extreme voltage violations and go to step 1.

The process above was performed separately for each feeder starting with the highest PV penetration level (100%). In the second step, it was found that the QSTS simulations with MAX reverse power (PV profile A) at the feeder head with MIN load conditions was effective to address overvoltage conditions at noon time, while the MAX reverse power (PV profile A) with MAX load was effective to adjust the regulating equipment to avoid undervoltage conditions. Once the setting change process had been finished for the 100% PV penetration level, the identified settings were applied for all the lower PV penetration levels that experienced overvoltages and/or undervoltages. Then, QSTS simulations for all the load profiles and PV profiles were performed and the resulting feeder time-series voltage profiles were analyzed. If any overvoltages or undervoltages were experienced, the process above was repeated separately for each PV penetration levels that had overvoltages or undervoltages.

This process to adjust the manual voltage regulation equipment settings was rigorous but turned out to be extremely tedious. While it was relatively straightforward to identify settings that avoided all overvoltages and undervoltages for a given daily QSTS simulation, the adjusted settings frequently resulted in overvoltages or undervoltages in another daily QSTS simulation. The settings would have to be re-adjusted, but then result in violations in yet another daily QSTS simulation.

Voltage violations frequently occurred in QSTS simulations where no violations would have been expected based on the PV and load profile (e.g., cloudy PV profile with average load profile). Voltage violations were also frequently experienced at unexpected times of the day, e.g., at solar ramping up or down times, when a given voltage regulation equipment changed from forward powerflow to reverse powerflow, or vice versa.

To summarize, violations were often caused by a highly complex interplay between feeder voltage regulation equipment, and sometimes occurred only with a particular load and PV profile combination. The QSTS simulation results obtained after completing all setting adjustments are presented in the following section.

4.4.3 Results From Baseline PV Impact Assessment

After all the manual changes to the voltage regulation equipment settings had been determined, a total of 45 QSTS simulations (3 load profiles, 5 PV day profiles, and 3 ES penetration levels) were performed for each PV penetration level on each feeder (1,080 QSTS simulations in total). In each simulation, the metrics described in Section 3.4.1 were recorded. If any of the 45 QSTS simulations reported a voltage or thermal violation, the circuits were considered unable to accommodate that penetration of PV. Figure 4-16 summarizes these QSTS simulation results per feeder, PV penetration level, and ES penetration level. Note that each row, which represents 15 daily QSTS simulations (3 load profiles and 5 PV profiles), is marked as 'FALSE' if at least one QSTS simulation displayed one violation, and is marked 'TRUE' otherwise.

The manual changes to the voltage regulation equipment settings were quite effective in mitigating voltage violations as shown in Figure 4-16 and discussed with QSTS simulation results in Chapter 7. Nevertheless, some of the voltage violations caused by high PV penetration levels were deemed impossible to resolve with manual changes to voltage regulation equipment settings. In such cases, due to the complexities described in the previous section, it was impossible to guarantee that there were indeed no settings that could have fixed some of the remaining voltage violations. However, even if such settings existed despite the comprehensive approach followed, the extreme complexity of their identification would likely make this mitigation approach impractical in practice.

Based on the results shown in Figure 4-16, Feeder L and N could accommodate up to a PV penetration level of 75% (i.e., 75% of residential customers with PV). Feeders M and S were constrained by significant voltage issues even at low PV penetration levels, while Feeders B and W were limited by thermal violations. Moreover, none of the six feeders was able to accommodate a PV penetration level of 100% without some type of mitigation – involving either some conventional distribution upgrades, as analyzed in Chapter 5, or the use of SI functions, as analyzed in Chapter 6. The QSTS simulation results presented in Figure 4-16 are analyzed in further detail in Chapter 5, where they are used as a reference to which the two types of mitigation strategies evaluated in this modeling effort are compared. It is important to highlight that the summary in Figure 4-16 is associated with QSTS simulation results, while the conventional distributions system upgrades were applied based on PG&E's design criteria. Chapter 5 presents the differences between these frameworks, and Chapter 7 includes more detail about the severity of each feeder impact.

Figure 4-17
Summary of Baseline PV Assessment Results for Significant Voltage Violations and Thermal Overloads

	PV Level	ES Level	Significant Voltage Violation	Overload
Feeder B	PV1	ES0	FALSE	TRUE
		ES1	FALSE	TRUE
		ES2	FALSE	TRUE
	PV2	ES0	FALSE	TRUE
		ES1	FALSE	TRUE
		ES2	FALSE	TRUE
	PV3	ES0	TRUE	TRUE
		ES1	FALSE	TRUE
		ES2	TRUE	TRUE
	PV4	ES0	TRUE	TRUE
		ES1	TRUE	TRUE
		ES2	TRUE	TRUE
Feeder L	PV1	ES0	FALSE	FALSE
		ES1	FALSE	FALSE
		ES2	FALSE	FALSE
	PV2	ES0	FALSE	FALSE
		ES1	FALSE	FALSE
		ES2	FALSE	FALSE
	PV3	ES0	FALSE	FALSE
		ES1	FALSE	FALSE
		ES2	FALSE	FALSE
	PV4	ES0	TRUE	TRUE
		ES1	TRUE	TRUE
		ES2	TRUE	TRUE
Feeder M	PV1	ES0	FALSE	TRUE
		ES1	TRUE	TRUE
		ES2	TRUE	TRUE
	PV2	ES0	TRUE	TRUE
		ES1	TRUE	TRUE
		ES2	TRUE	TRUE
	PV3	ES0	TRUE	TRUE
		ES1	TRUE	TRUE
		ES2	TRUE	TRUE
	PV4	ES0	TRUE	TRUE
		ES1	TRUE	TRUE
		ES2	TRUE	TRUE
Feeder N	PV1	ES0	FALSE	FALSE
		ES1	FALSE	FALSE
		ES2	FALSE	FALSE
	PV2	ES0	FALSE	FALSE
		ES1	FALSE	FALSE
		ES2	FALSE	FALSE
	PV3	ES0	FALSE	FALSE
		ES1	FALSE	FALSE
		ES2	FALSE	FALSE
	PV4	ES0	FALSE	TRUE
		ES1	FALSE	TRUE
		ES2	FALSE	TRUE
Feeder S	PV1	ES0	TRUE	FALSE
		ES1	TRUE	FALSE
		ES2	TRUE	FALSE
	PV2	ES0	TRUE	FALSE
		ES1	TRUE	FALSE
		ES2	TRUE	FALSE
	PV3	ES0	TRUE	TRUE
		ES1	TRUE	TRUE
		ES2	TRUE	TRUE
	PV4	ES0	TRUE	TRUE
		ES1	TRUE	TRUE
		ES2	TRUE	TRUE
Feeder W	PV1	ES0	FALSE	TRUE
		ES1	FALSE	TRUE
		ES2	FALSE	TRUE
	PV2	ES0	FALSE	TRUE
		ES1	TRUE	FALSE
		ES2	TRUE	TRUE
	PV3	ES0	TRUE	TRUE
		ES1	TRUE	TRUE
		ES2	TRUE	TRUE
	PV4	ES0	TRUE	TRUE
		ES1	TRUE	TRUE
		ES2	TRUE	TRUE

4.5 Conclusions

This chapter presented the technical considerations for the baseline assessment of the PV generation impacts for each of the six feeders analyzed. Following the modeling approach presented, a total of 8,438 PV installations were deployed and analyzed across all six feeders, assuming five different representative PV generation profiles. The five representative PV profiles were selected leveraging clustering techniques applied to actual meteorological datasets to capture a range of representative weather conditions: *summer clear sky* (high irradiance, no variation), *autumn clear sky* (low irradiance, no variation), *cloudy* (morning variation), *extremely variable clouds* (large irradiance swings), and *overcast* (low irradiance). Additionally, diverse local generation conditions were also considered in the modeling of PV systems. These efficiency-related factors were applied through the inclusion of a subset of normalized power generation measurements that were associated to the 8,438 individually-sized PV installations modeled.

In addition to PV, residential ES was also modeled with two penetration levels considered, 20% and 40% of PV customers, to evaluate the potential impact of this technology across the modeling effort. Solar ES installations were modeled through over 50,000 load shapes that have been generated to represent a dispatch strategy based on the reduction of consumption at peak energy price periods.

Based on the inclusion of PV and ES models, a detailed impact modeling effort was conducted, where a set of metrics were defined and calculated from the QSTS simulation results. As a part of this baseline

PV impact assessment, manual changes to feeder existing voltage regulation equipment settings were analyzed as the first measure to mitigate voltage violations caused by PV. The manual changes to the feeder regulation equipment settings turned out to be very effective in mitigating voltage impacts caused by PV. However, determining effective setting changes required a rigorous and very tedious process. After the setting changes, the PV impacts were analyzed to establish a baseline to determine the level of PV penetration at which each of the six feeders would start experiencing operational issues.

5

ACCOMMODATING INCREASED PV PENETRATION LEVELS WITH CONVENTIONAL MEASURES

This chapter analyzes the conventional distribution upgrades that would be required to accommodate the PV penetration levels and deployment scenarios introduced in Chapter 3 on each of the analyzed six feeders introduced in Chapter 2. Chapter 6 and Chapter 7 will analyze the extent to which the use of autonomous smart PV inverter functions could help to defer these upgrades.

First, a detailed technical analysis, consistent with PG&E's design and engineering practices, was used to identify the conventional distribution upgrades required to accommodate each of the PV penetration levels on each feeder. The upgrades were identified separately for the MV primary circuits and the LV secondary circuits. Since this modeling effort analyzed the impacts and benefits of *residential* smart PV inverters, almost all upgrades necessary were associated with the LV secondary circuit equipment.

After the conventional upgrade measures were identified and applied to each feeder at each PV penetration level, a QSTS-based PV impact assessment (identical to Chapter 3) was performed to determine the effectiveness of these measures at addressing adverse PV impacts.

5.1 Upgrades to the Medium-Voltage Primary Circuits

This section discusses the distribution upgrades that were necessary at the MV primary circuit level. In this modeling effort, *no primary circuit thermal overloads were experienced at any of the PV penetration level considered on any of the six feeders analyzed*. However, some MV primary circuit voltage violations were experienced with some PV penetration levels on some feeders. As follows, the primary circuit upgrades necessary to address these violations are discussed.

As discussed in Chapter 4, manual changes to *existing* voltage regulation equipment settings were considered as the first measure that PG&E would apply as PV penetrations grow. As also discussed in Chapter 4, the manual setting changes were very effective in mitigating voltage violations caused by PV. Finally, as discussed in Chapter 4, a comprehensive and tedious process was required to identify effective changes to the voltage regulation equipment settings. It turned out very challenging to effectively coordinate multiple voltage regulating equipment (LTCs, line voltage regulators and switching capacitors) to avoid voltage violations at all analyzed feeder load and PV conditions. In particular, it was observed to be challenging to effectively coordinate multiple cascaded voltage regulators that saw forward to reverse (or vice versa) power flow changes at different times due to the distributed PV. More details on the manual changes to the voltage regulation equipment settings can be found in Chapter 4. These findings indicate that centrally controlled automated voltage regulation schemes enabled by Advanced Distribution Management Systems and the added visibility to distribution operations provided by AMI voltage measurements can be very valuable if not necessary to effectively regulate feeder voltages with high penetrations of distributed PV.

The manual changes to the existing voltage regulation equipment settings addressed the primary circuit voltage violations caused by PV for all feeders at all PV penetration levels, except for Feeder M from PV penetration levels PV2 (50%) through PV4 (100%). On this feeder at these PV penetration levels, it was not possible to identify manual setting changes that could have addressed all the primary circuit voltage violations caused by PV. The reasoning for this is illustrated in Figure 5-1, which shows the feeder QSTS max/min primary MV circuit and secondary LV circuit voltages over the over the MIN load day – sunny PV day – 100% PV penetration – 0% ES penetration. Clearly, around the noon, when PV generation is high, the feeder has both LV circuit overvoltages and undervoltages. The overvoltages and undervoltages are illustrated in the line-neutral voltage profile.[80] In particular, it was not possible to adjust the settings of the first voltage regulator (at ~6 kilometers (km) from the substation) so that all the overvoltages before the second voltage regulator (at ~16km from the substation) could be avoided. Moreover, attempting to do this, immediately resulted in increased undervoltages in higher loading and/or lower PV generation conditions.

Feeder M had a voltage booster (at ~10km from the substation) in the location illustrated in yellow in Figure 5-2. The voltage booster, due to the lack of controllability, was unable to adjust for different feeder conditions (e.g., reverse power flow) boosting the voltage on its secondary regardless of the feeder condition. Since manual setting changes could not provide adequate regulation, the required system upgrade identified for Feeder M at a PV penetration levels from 50% to 100% was to replace the problematic voltage booster with a controllable voltage regulator. Then, the settings of the feeder voltage regulation equipment were adjusted using the process described in Chapter 4 until acceptable feeder voltage regulation was achieved. Under MIN load conditions, while this voltage regulator upgrade successfully resolved all undervoltage conditions, some minor overvoltage and undervoltage conditions persisted under some loading and PV generation conditions. However, these remaining voltage violations were deemed not to warrant adding further voltage regulation equipment on the feeder.

---

80 Note that since feeder M is a 3-wire (delta) feeder, the primary circuit voltages (continuous lines) should be ignored in the L-N voltage profile. Instead, the L-N voltage profile is intended to voltages at the secondary circuits (dashed lines), which were modeled as single-phase line-neutral connected as explained in Chapter 3.

Figure 5-1
Illustration of Why Feeder M Required an Additional Voltage Regulator. The Maximum and Minimum Primary Medium-Voltage Circuit and Secondary Low-Voltage Circuit Voltages Over the Minimum Load Day – Sunny PV Day – 100% PV Penetration – 0% Energy Storage Penetration (Top), Line-Line Voltage Profile for Hour 12.5 (Bottom Left), and Line-Neutral Voltage Profile for Hour 12.5 (Bottom Right).

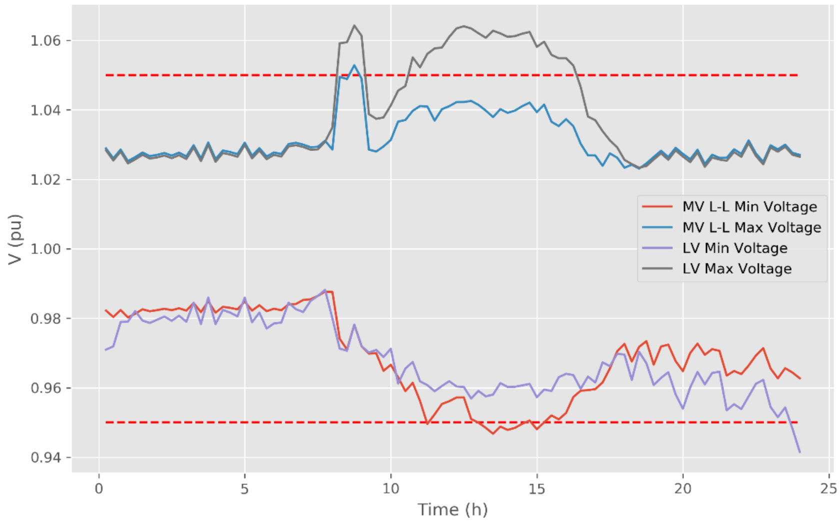

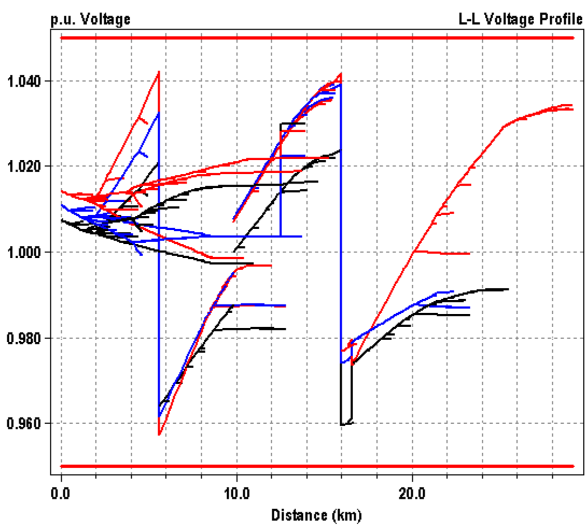

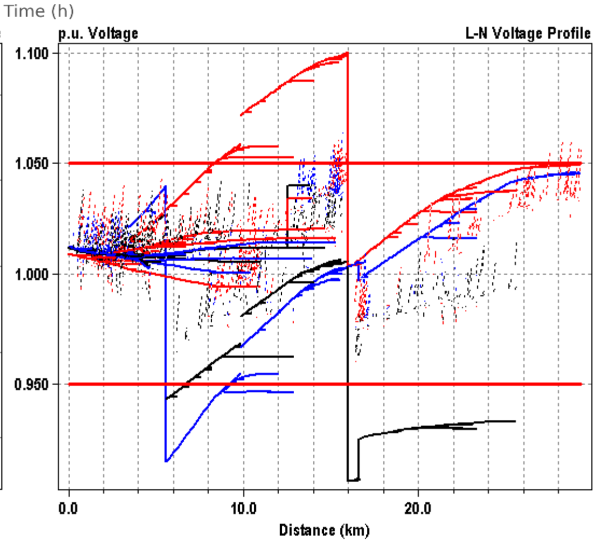

Figure 5-2
The Existing Voltage Regulation Equipment on Feeder M

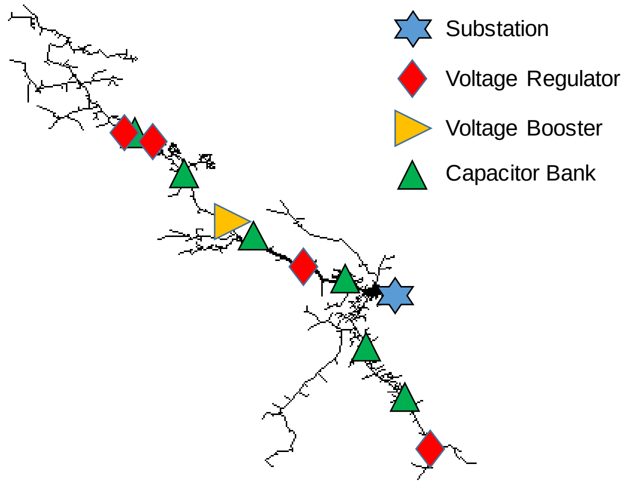

5.2 Upgrades to the Low-Voltage Secondary Circuits

As part of the PV interconnection process, PG&E determines whether the existing secondary circuit serving the customer, who has applied for the PV interconnection, can accommodate the proposed PV system without adverse impacts. This section defines the step-by-step process followed to determine which equipment upgrades are required and when, closely following PG&E's interconnection analysis practices.

This modeling effort emulated PG&E's decision-rules triggering distribution upgrades with a high fidelity to provide a realistic point of comparison when evaluating the cost of all conventional measures required by these rules, and their effectiveness compared to SIs. In particular, in several instances, the need for upgrades beyond PG&E's existing practices was identified, but the upgrades were not implemented to ensure that the results of this modeling effort closely reflected current PG&E practices. As a part of this analysis, the effectiveness of PG&E's decision-rules triggering distribution upgrades to avoid adverse PV impacts were evaluated across all PV penetration levels and feeders considered in this modeling effort.

PG&E's current practice to identify the distribution secondary circuit equipment upgrades that are required to accommodate a new PV interconnection includes comparing the *aggregated* PV inverter nameplate rating downstream of a service transformer, to the *nameplate* rating of the service transformer. If the aggregated PV inverter nameplate rating does not exceed the service transformer nameplate rating, the new PV system can be interconnected without any secondary circuit equipment replacements. On the other hand, if the aggregated inverter rating is higher than the transformer nameplate, a secondary voltage rise study (VRS) is triggered to assess whether any customers downstream of the transformer are likely to experience high voltages.

The aggregated inverter rating is also compared to the service transformer *thermal* rating (for details, see Chapter 2) to determine whether the new interconnection could cause service transformer thermal overloads under extreme reverse power flow conditions. This process is based on a conservative assumption that the PV system would be generating at their inverter nameplate value while there would be no downstream loads to counteract the generation.

When the aggregated inverter nameplate downstream of a service transformer exceeds the transformer nameplate, a secondary VRS is performed to investigate if any customers would experience a voltage rise above PG&E guidelines under the maximum PV output power and no-load conditions. As part of the modeling effort, secondary circuit upgrades are identified to reduce the likelihood that any customer would experience overvoltages.

This complete decision process is illustrated in the logic flow diagram in Figure 5-3.

Figure 5-3
Logical Flow Diagram to Determine Whether a Service Transformer Needs to be Upgraded. PV_{peak} Refers to the Aggregated PV Inverter Nameplate, $XFMR_{kvaRating}$ to the Service Transformer Nameplate Rating, and $XFMR_{thermal}$ to the Service Transformer Thermal Rating.

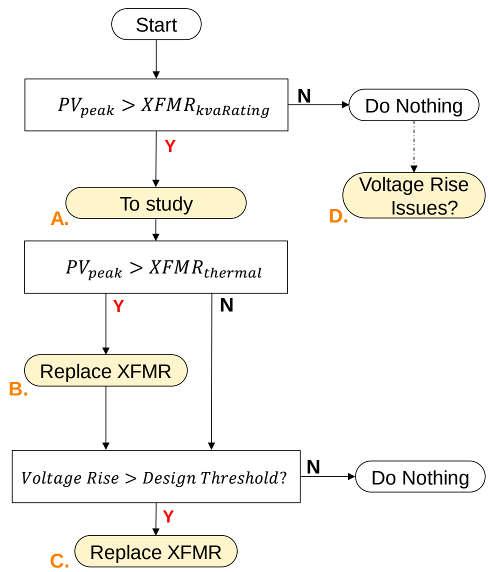

Four metrics were recorded when the replacement assessment discussed above was conducted:

1. The *number of secondary voltage rise studies* (see point A on Figure 5-3) provided an estimate of the number of secondary voltage rise studies that would be performed by the time a specific PV penetration level would be achieved on each of the six feeders (see Section 5.4 for further details).
2. The *number of transformer replacements due to potential thermal violations* (point B) was recorded to provide insight on service transformer replacements necessary due to thermal reasons. Since SI functions are not effective in avoiding thermal violations, this metric was not used as an input to the economic analysis presented in Chapter 8.
3. The *number of transformer replacements due to potential voltage rise violations* (point C) was recorded to capture the replacement costs associated with voltage quality. Since SI functions are effective in reducing voltage rise caused by PV, this metric was used as an input to the economic analysis presented in Chapter 8.
4. The *number of voltage rise violations* captures the number of secondary circuits, where the PG&E voltage rise threshold was exceeded, but where the aggregated inverter rating did not exceed the transformer nameplate rating and thus, did not trigger a secondary VRS. This metric

tracks the number of instances where PG&E's current design criteria would have missed high voltage rises.

5.2.1 *Replacements Due to Thermal Overloads*

As part of PG&E's design criteria approach, highlighted in Figure 5-3, service transformers were upgraded once the aggregated downstream inverter nameplate rating exceeded the thermal rating of the service transformer. For instance, in the baseline feeder model in Chapter 3, a single-phase service transformer on Feeder B had a 15-kVA nameplate rating ($XFMR_{kvaRating}$) and a thermal rating of 22.5 kVA ($XFMR_{thermal}$). However, distributed PV systems were installed downstream of this transformer with a total inverter nameplate rating of 26.25 kVA at 100% PV penetration. Thus, the PV installations triggered both secondary voltage rise studies, and a transformer replacement due to thermal overload. Table 5-1 shows the thermal loading and the maximum voltage rise[81] on the secondary circuit, both for the original transformer size, and for the larger transformer size identified as a required replacement.

Table 5-1
Example of a Service Transformer Replacement Due to Potential Thermal Overload

Iteration	XFMR rating	Thermal loading ($PV_{rating}/XFMR_{thermal}$)	Max voltage rise [$120V_{base}$]
Original Transformer Size	15 kVA	116.7%	6.18 V
Upgraded Transformer Size	25 kVA	40.4%	3.18 V

This process was repeated for all transformers on each feeder for each of the for PV penetration levels (PV1-25%, PV2-50%, PV3-75%, and PV4-100%). The number of service transformers requiring an upgrade was recorded and is shown in Figure 5-4. As expected, the number of transformer replacements increases as the PV penetration level increases. As shown in Figure 5-4, the PV penetration level of 25% (PV1) does not trigger any transformer upgrades as a result of thermal violations on any of the six feeders analyzed.

81 The voltage rise from the service transformer primary to the PV customer at 120-volt base.

Figure 5-4
Number of Service Transformer Replacements Due to Thermal Violation Sorted by Feeder and PV Penetration Level

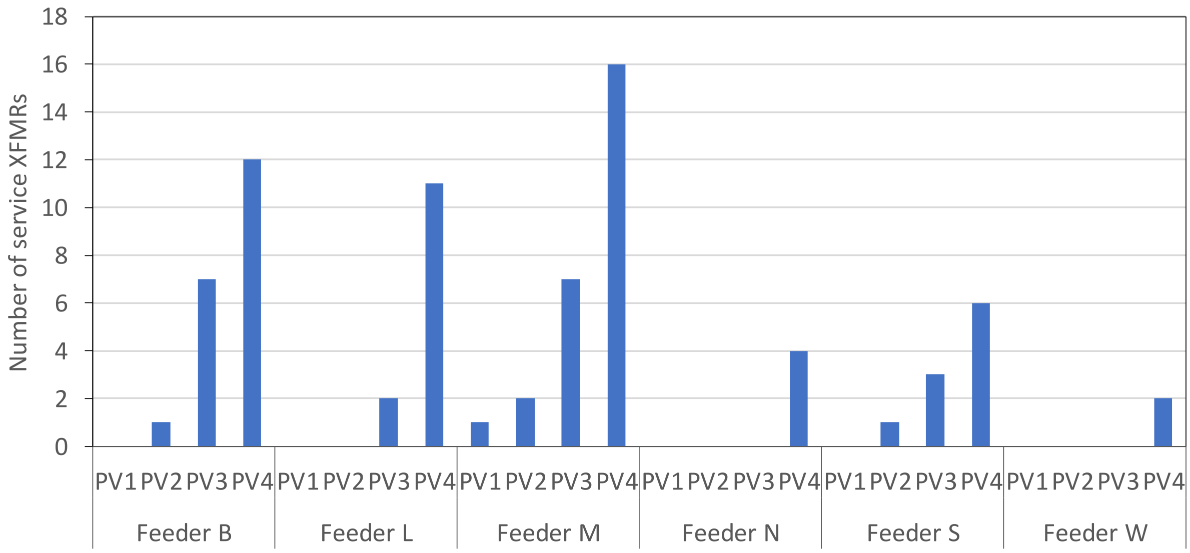

A key observation from these results is that Feeder B, Feeder L, and Feeder M all have a similar number of replacements. However, due to the differences in feeder sizes, the percentage of residential transformer replacements is quite different between these three feeders as shown in Figure 5-5. Note that the total number of replacements is normalized with the number of 'residential' transformers since this is where all PV systems are considered.

Figure 5-5
Percentage of Service Transformers Upgraded Due to Thermal Violation Sorted by Feeder and PV Penetration Level

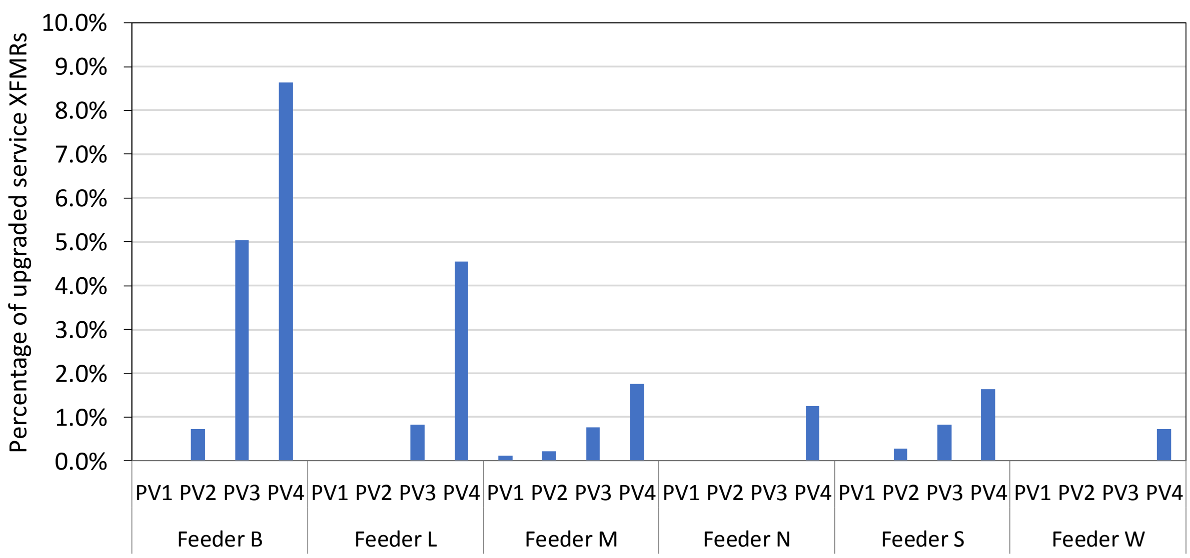

A follow-up question associated with the transformer replacements was whether a certain transformer size (i.e., nameplate capacity) was more prone to require upgrades. Figure 5-6 summarizes the number of service transformers upgraded due to thermal overloads by original transformer size. Although no specific pattern can be observed in these results, all thermal upgrades in this analysis were on transformers rated at 50 kVA or below. However, the smaller number of large transformers could explain this result.

Figure 5-6
Number of Service Transformers Upgraded Due to Thermal Overloads Sorted by Original Size (kVA) and by Feeder

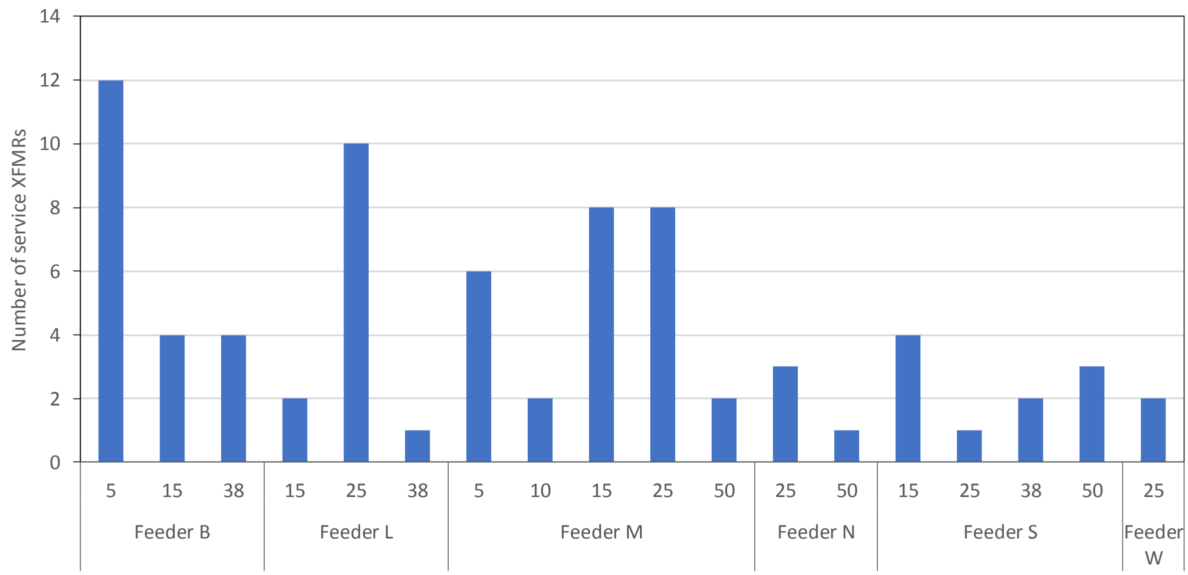

5.2.2 *Replacements Due to Voltage Rise Issues*

Similar to replacements due to thermal overloads, transformer upgrades were sometimes required to avoid high secondary circuit voltage rise caused by PV. For example, consider a single-phase transformer on Feeder W that had the original nameplate capacity of 15 kVA and the thermal rating of 19.5 kVA. At 100% PV penetration, 16.04 kVA of PV (rated inverter power) were added downstream of that transformer. Since the total PV inverter nameplate did not exceed the transformer thermal rating, an upgrade due to thermal violation overload was not required. However, since the total PV inverter nameplate exceeded the nameplate rating of the transformer a secondary VRS was triggered, concluding that an upgrade was necessary to avoid a significant voltage rise (above PG&E guidelines). Table 5-2 provides the values used as part of the decision process for this example.

Table 5-2
Example of a Service Transformer Replacement Due to Voltage Rise Issues (Above PG&E Guidelines)

Iteration	XFMR rating	Thermal loading ($PV_{rating}/XFMR_{thermal}$)	Max voltage rise [$120V_{base}$]
Original Transformer Size	15 kVA	82.3%	4.18 V
Upgraded Transformer Size	25 kVA	53.5%	3.10 V

Note that a transformer replacement was implemented only if it addressed the voltage rise issue. Transformers were upgraded at most two available nameplate ratings higher than the original nameplate value. If replacing the transformer (with two sizes larger transformer) was not sufficient to resolve the voltage rise issues, service lines upgrades were investigated. In this modeling effort, this was rarely necessary and was conducted on a case by case basis. Additional details can be found in the Appendix.

The replacements triggered by voltage rise issues were determined for each of the six analyzed feeders and for each of the four PV penetration levels considered. Figure 5-7 shows the service transformers upgraded due to secondary voltage rise studies per feeder and PV penetration level. Note that the numbers reported in Figure 5-7 correspond to point C in Figure 5 3, where the primary reason triggering a replacement is voltage rise, and not thermal violations.

Figure 5-7
Number of Service Transformers Upgraded Due to Voltage Rise Violations Sorted by Feeder and PV Penetration Level

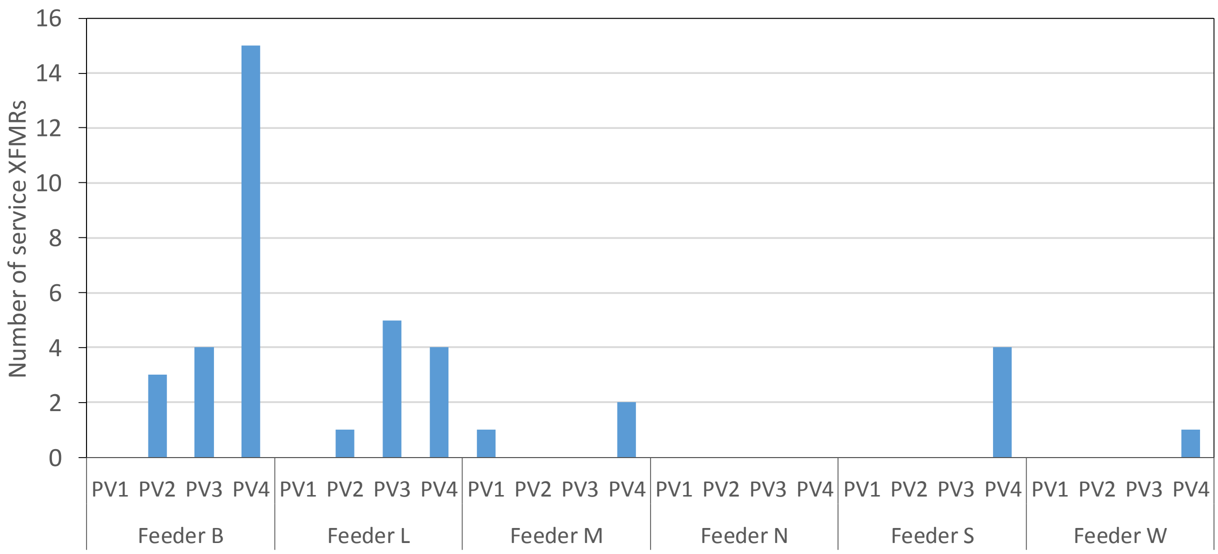

Curiously Feeder M has a transformer replacement at a PV1 (25%) penetration level but not PV2 (50%) or PV3 (75%) penetration levels. This is because this transformer replacement is triggered by *voltage rise* issues at low PV penetration levels, and as the PV penetration level increases, this specific transformer becomes *thermally* overloaded. Therefore, the transformer is still being replaced as the penetration level increases (and their remain voltage rise issues at those higher PV penetration levels) but the replacement is now flagged as a *thermal* replacement, and therefore does not appear on Figure 5-7, which only counts the transformer replacements triggered by the voltage rise criteria.

Figure 5-8 shows the share of the residential transformers replaced due to voltage rise criteria per feeder and PV penetration level. Feeder B, which is a 2.4 kV system, experiences a larger percentage of voltage rise issues compared to the 12 kV or 21 kV systems analyzed in this modeling effort. In addition to the feeder voltage class, this behavior could be explained by the feeder secondary construction types, including the service transformer types utilized, etc. Figure 5-9 shows the replacements per the original transformer size (kVA). Similar to transformers replaced due to thermal violations, smaller transformers tend to be frequently replaced due to voltage rise issues. However, this could be at least partly explained by the larger share of small transformers.

Figure 5-8
Percentage of Service Transformers Upgraded Due to Voltage Rise Violation (Without Thermal Violations) Sorted by Feeder and PV Penetration Level

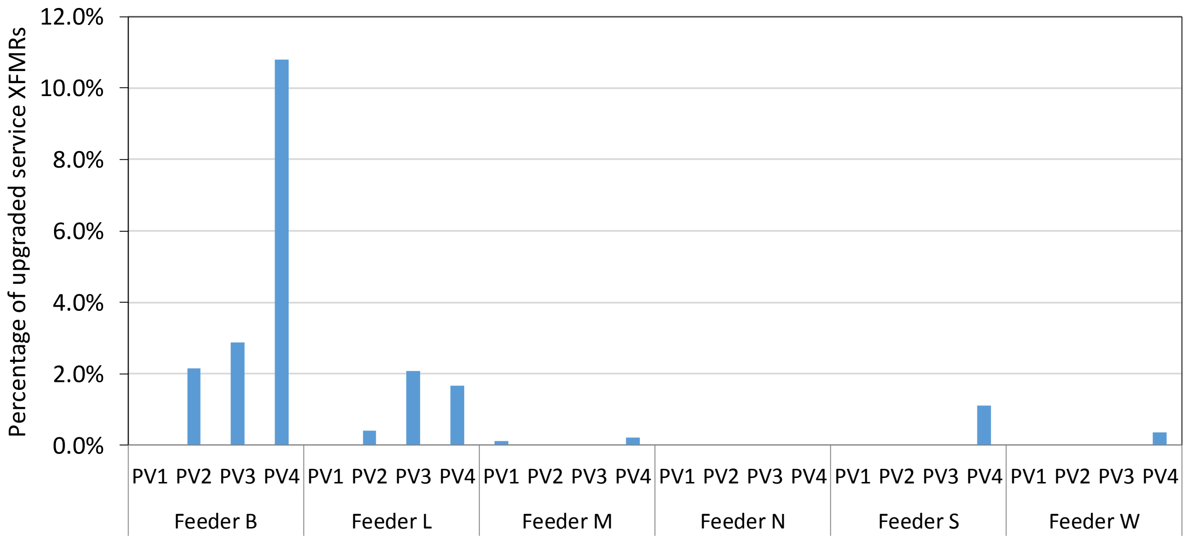

Figure 5-9
Number of Service Transformers Upgraded Due to Voltage Rise Issues Sorted by Original Size (kVA) and by Feeder

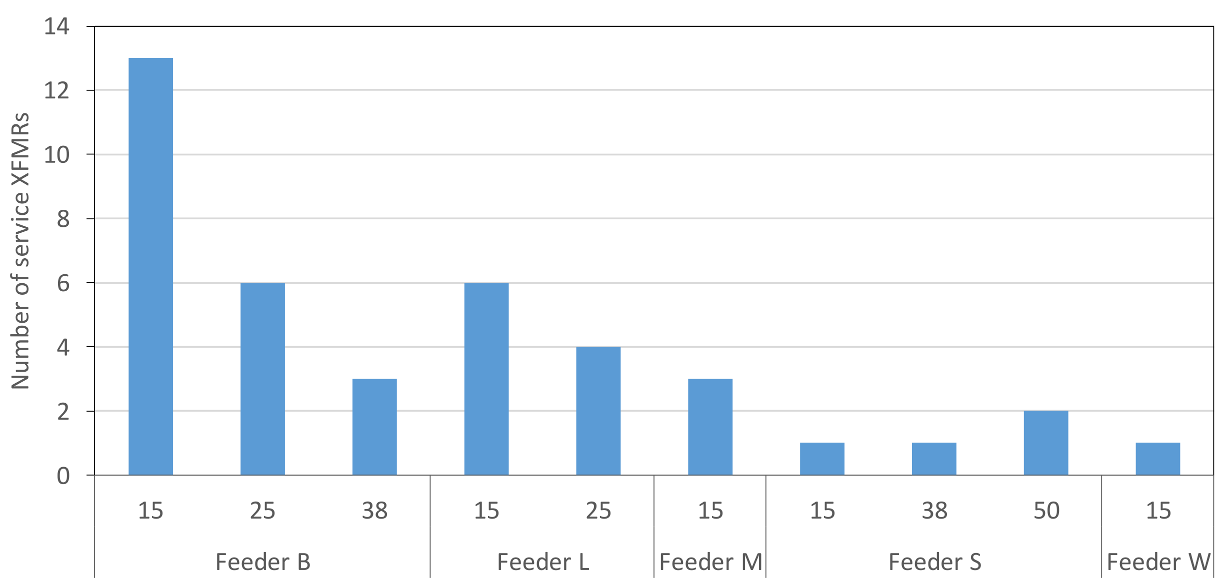

Again, all replacements triggered by a voltage rise violation occurred on transformers rated at 50 kVA or below.

5.3 Missed Potential Voltage Rise Issues

After adding all thermal and voltage rise replacements to the feeder models, a secondary VRS was conducted on *all* service transformers connected to each of the six feeders to capture the number of voltage rise violations that were missed when triggering replacements based on PG&E's design criteria process. Specifically, the key assumption behind the criteria triggering voltage rise replacements is that voltage rise issues (above PG&E guidelines) are *unlikely* to occur when the aggregated inverter rating of all PV systems connected downstream of a given service transformer *is less than* the nameplate rating of that transformer. The validity of this assumption was tested by determining the number of residential transformers with voltage rise issues that remain after applying all replacements flagged following PG&E's design criteria. Figure 5-10 shows the number of remaining service transformers with voltage rise issues per feeder and PV penetration level. The transformers reported in Figure 5-10 were not flagged for a secondary VRS during the service transformer upgrade process since the total PV inverter nameplate did not exceed the transformer nameplate. Had a secondary VRS been triggered for these transformers, they would have experienced maximum voltage rise above PG&E guidelines.

Figure 5-10
Number Of Remaining Service Transformers With Voltage Rise Issues

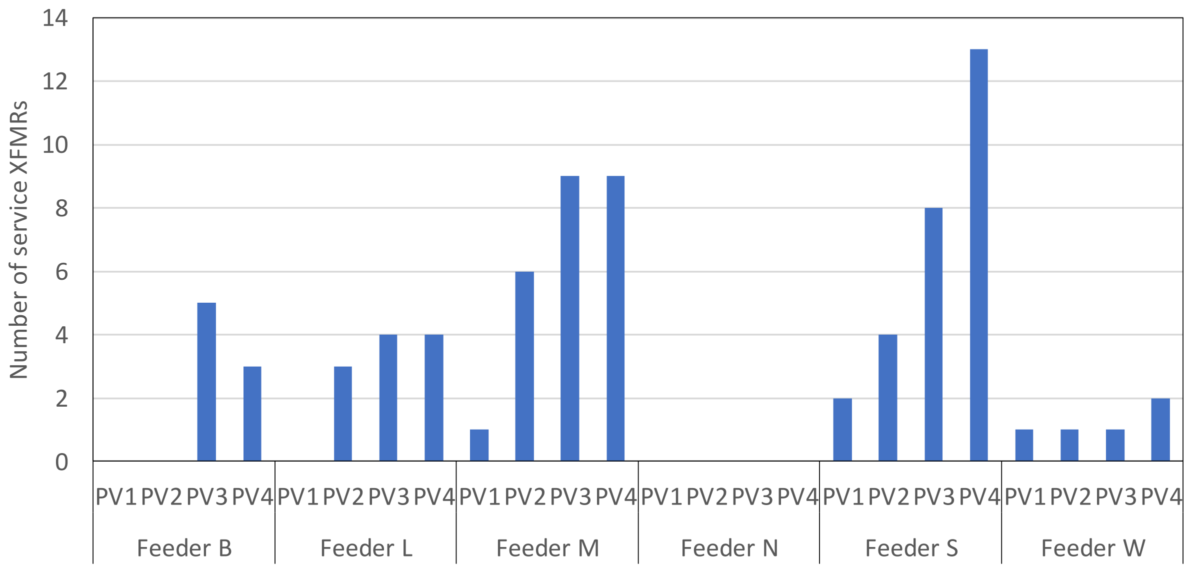

Considering the number of service transformers for each feeder, the number of missed voltage rise issues detected is small. However, when considering the number of upgraded transformers identified for each case (i.e., for each of the six feeders, at each of the four PV penetration levels considered), these missed violations could potentially double the number of replacements required on a feeder, as illustrated in Figure 5-11.

For example, Feeder S at a PV penetration level PV4 (100% had a total of 10 upgrades, with four of these upgrades resulting from voltage rise issues. However, simulation results show that the criteria used to flag voltage rise replacements missed 13 other service transformers where voltage rise issues were observed in the QSTS simulations. In other words, for this specific example, the existing decision process used to flag transformer upgrades (Figure 5 3) only captured four of the 17 replacements (23.5%) and missed 13 of the 17 replacements (76.5%).

The results presented suggest that, in some cases, the nameplate comparison approach used as a technical criterion to trigger transformer replacements (Figure 5-3) may miss voltage rise issues (as observed most noticeably for Feeders M and S). These results do not necessarily mean that a service transformer upgrade (had one been triggered by a secondary VRS) would have resolved the voltage rise issue. These results also do not necessarily mean that customers served by the transformer with voltage rise issues would necessarily experience overvoltages caused by PV. However, these results indicate that, in some cases, voltage rise issues caused by PV may exist even when the service transformer had sufficiently high capacity to properly accommodate the PV. In such cases, voltage rise issues may be largely result from high service line impedances (long service lines and/or low conductor gauge).

Figure 5-11 Number of Service Transformers With Voltage Rise Issues Categorized by Upgrades and Missed Voltage Rise Violations

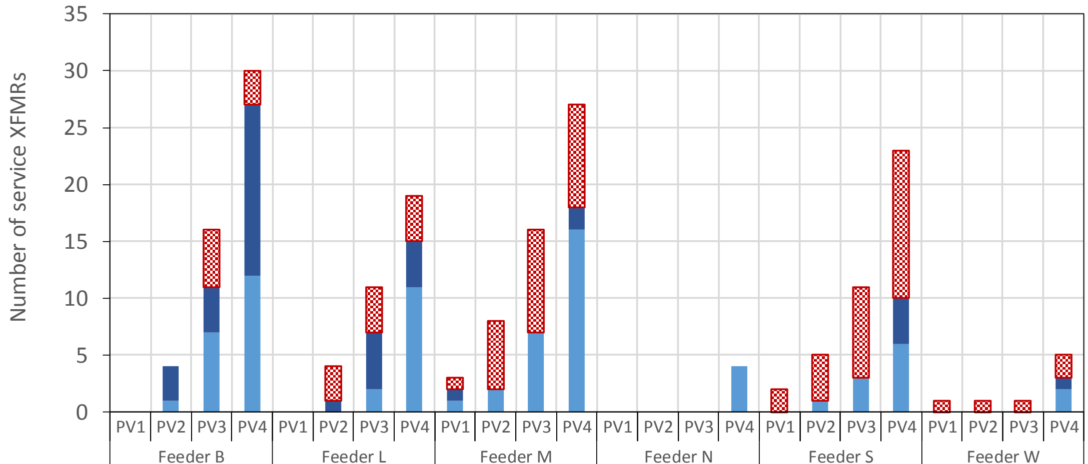

	Feeder B PV1	PV2	PV3	PV4	Feeder L PV1	PV2	PV3	PV4	Feeder M PV1	PV2	PV3	PV4	Feeder N PV1	PV2	PV3	PV4	Feeder S PV1	PV2	PV3	PV4	Feeder W PV1	PV2	PV3	PV4
Missed Voltage Rise	0	0	5	3	0	3	4	4	1	6	9	9	0	0	0	0	2	4	8	13	1	1	1	2
Upgd: Voltage Rise	0	3	4	15	0	1	5	4	1	0	0	2	0	0	0	0	0	0	0	4	0	0	0	1
Upgd: Thermal	0	1	7	12	0	0	2	11	1	2	7	16	0	0	0	4	0	1	3	6	0	0	0	2

5.4 Secondary Voltage Rise Studies

Another metric analyzed in this chapter is the number of secondary voltage rise studies triggered for each of the PV penetration levels considered. This metric is important since secondary voltage rise studies come at a cost that is passed directly to the PV interconnection applicants.

Unlike system upgrades, the number of secondary voltage rise studies conducted until a decision to replace a transformer is reached directly depends on the order at which the PV interconnection requests were received by PG&E. For example, for a given set of PV systems connected behind the same service transformer and representing a range of kW sizes, a sequence of requests seeing all smaller PV systems apply first may take a larger number of studies to reach the threshold triggering a transformer replacement due to voltage rise issues, when compared to an another sequence of requests seeing all larger PV systems submitting a request first.

While the actual number of secondary voltage rise studies will always depend on the order at which interconnection requests are received, which is unique to each transformer and cannot be predicted in advance, this section presents a method to *estimate* the total number of secondary voltage rise studies.

From the method described in Figure 5-3, under PG&E's current design and engineering practices, a secondary VRS is triggered any time the aggregated capacity of all inverters connected downstream of a given transformer exceeds the nameplate rating of that transformer. Example 1 in Figure 5-12 shows a transformer to which a total of four PV systems are connected. Although the aggregated inverter capacity does not exceed its thermal rating, which would trigger requiring a "thermal" replacement, the aggregated inverter capacity is still above the kVA rating of the transformer, which must have triggered at least one secondary VRS. However, as represented on Figure 5-12, in the case of Example 1, a first

VRS was triggered by the interconnection request submitted by PV Project #3, and a second one was triggered by PV Project #4. Therefore, in this illustrative example, a total of two secondary voltage rise studies were triggered before reaching the final PV penetration level. Example 2 in Figure 5-12 shows another hypothetical scenario requiring a transformer replacement where four secondary voltage rise studies would have been triggered.

These examples illustrate that the number of secondary voltage rise studies depends directly on the order in which the interconnection requests are received, and whether one or several transformer replacements took place during that process.

To address this challenge, for each of the PV penetration levels considered, this modeling effort randomly generated the order in which interconnection requests were received for each service transformer modeled, and computed the total number of studies assuming that any transformer replacements would be executed if deemed necessary *only after receiving the last PV interconnection request for that transformer*. The latter assumption, while introducing a negligible variation in the number of studies, provides an upper estimate of the number of secondary voltage rise studies for a given PV penetration level, for each of the service transformers modeled.

Figure 5-12
Example Illustrating the Estimation of the Number of Secondary Voltage Rise Studies

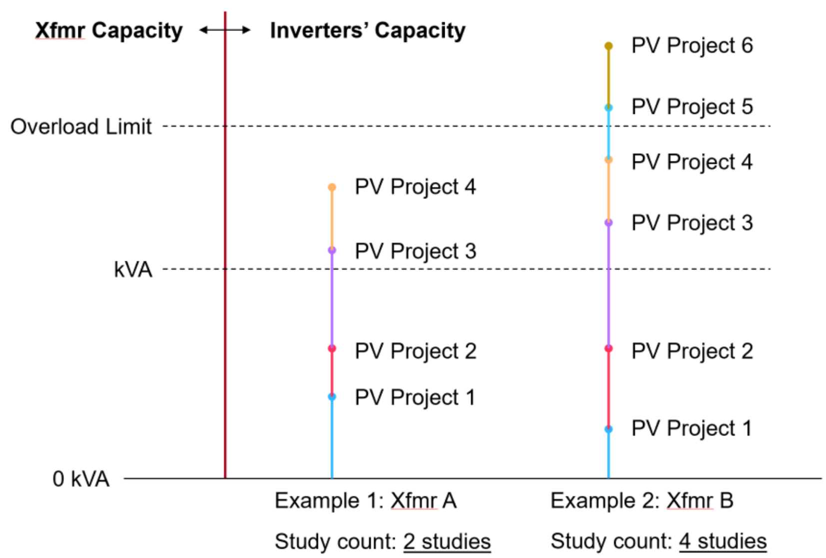

This approach to estimate the total number of secondary voltage rise studies for each PV penetration level was applied to each of the six feeders modeled. Results are presented in Figure 5-13.

Figure 5-13. Estimated Count (Upper Bound) of the Number of Secondary Voltage Rise Studies Conducted Per Feeder and Per PV Penetration Level

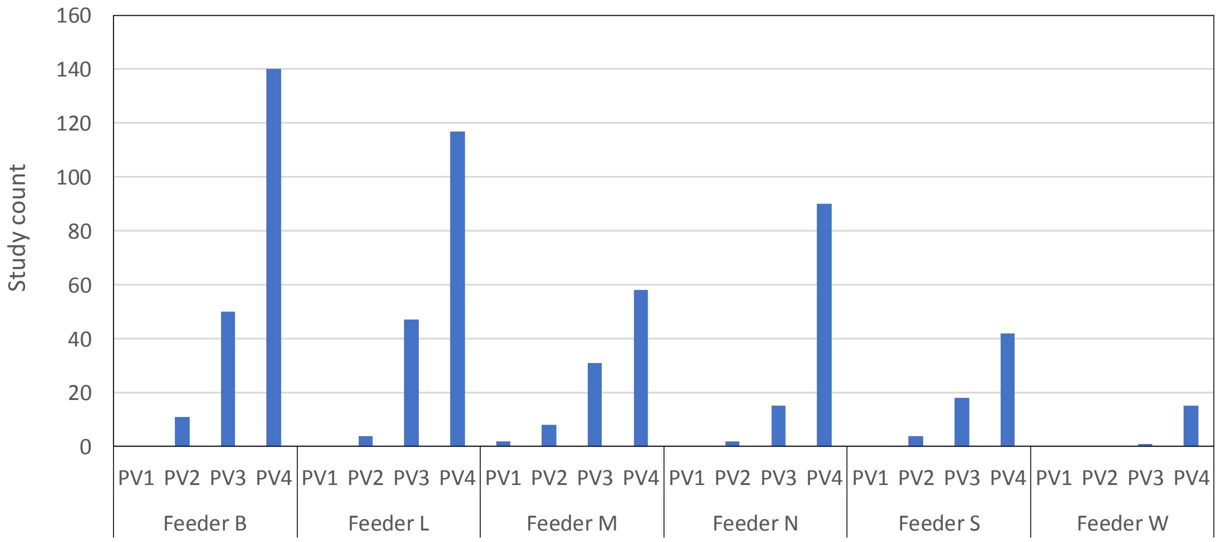

While lower penetration levels show a lower number of secondary voltage rise studies, this is due to the random nature in which PV systems are interconnected. In reality, customer PV adoption may be less organic and highly concentrated on some transformers, requiring a larger number of secondary voltage rise studies. Figure 5-14 shows the estimated upper bound of the number of secondary voltage rise studies as a share of the total number of interconnection projects for each level of PV penetration. Again, Feeder B showed a larger percentage of PV interconnection projects requiring secondary voltage rise studies, which is consistent with the higher number of required equipment replacements observed in Figure 5-7.

Figure 5-14
Percentage of Interconnection Projects Requiring a Secondary Voltage Rise Study Per PV Penetration Levels for Each Feeder

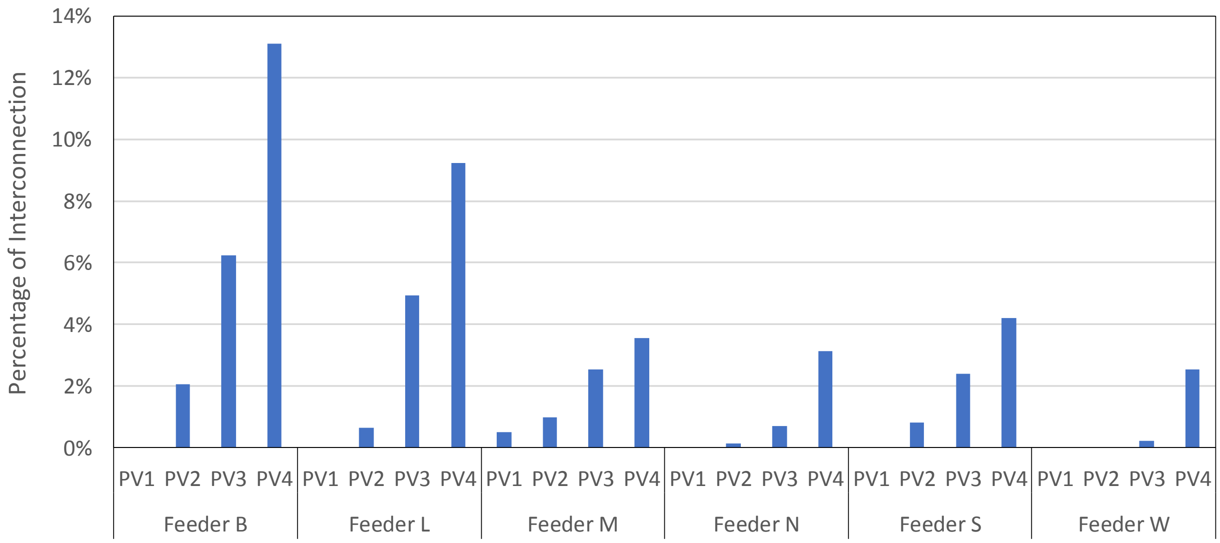

5.5 QSTS Simulation Results and Discussion

In the previous sections of this chapter, the identification and deployment of conventional upgrades to support higher PV penetration levels was presented, consistent with PG&E's current engineering practices. In this section, all equipment replacements flagged as part of this process were applied to the feeder models presented in Chapter 3. The objective was to evaluate the effectiveness of these upgrades at alleviating adversarial PV impacts at higher PV penetration levels.

As described in the previous chapters, multiple daily 15-minute QSTS simulations were performed to represent the breadth of conditions a feeder experiences in real field conditions. This includes three different representative daily load profiles (see Section 3.4), five representative daily PV profiles (see Section 4.2.1), four PV penetration levels (see Section 4.2.2), and three ES penetration levels (see Section 4.3). The analysis of each of the possible combinations for these parameters required 45 QSTS simulations per PV level per feeder, leading to 180 QSTS simulations per feeder, and a total of 1,080 QSTS simulations across all six feeders. The results of these QSTS simulations, presented in the remainder of this chapter, provide insights into the effectiveness of the conventional upgrades triggered by the nameplate comparison approach (Figure 5-3)[82] to address adversarial PV impacts.

5.5.1 Thermal Overloads

The nameplate comparison approach presented in Figure 5-3 focuses on the No-load/Max-PV case to flag any transformer replacements that might be necessary to avoid any thermal violations. The probability of this No-load/Max-PV scenario is obviously low, given that all PV systems considered in this modeling effort are located downstream of a residential transformer where some residual load consumption is always present. But the No-load/Max-PV reflects sizing requirements for the highest theoretical reverse power flow.

82 And the additional voltage regulator on Feeder M.

When analyzing the QSTS simulation results obtained for the baseline models presented in Chapter 3 (without any system upgrades implemented), the highest number of service transformers experiencing thermal violations always occurs at the highest PV penetration level considered (100%) for all six feeders modeled, confirming that PV systems, especially at high penetration levels, can create thermal overloads, see Figure 5-15. However, when comparing these results to the number of replacements presented in Figure 5-4, it can be observed that the number of transformer replacements recommended always *exceeds* the number of transformers recorded as overloaded when no upgrades are applied. This finding suggests that the nameplate comparison approach triggering thermal replacements based on the No-load/ Max-PV assumption is rather conservative.

Figure 5-15
Maximum Number of Service Transformers With a Thermal Violation From All Cases on a Specific Feeder and a Specific PV Penetration Level for the Baseline Models

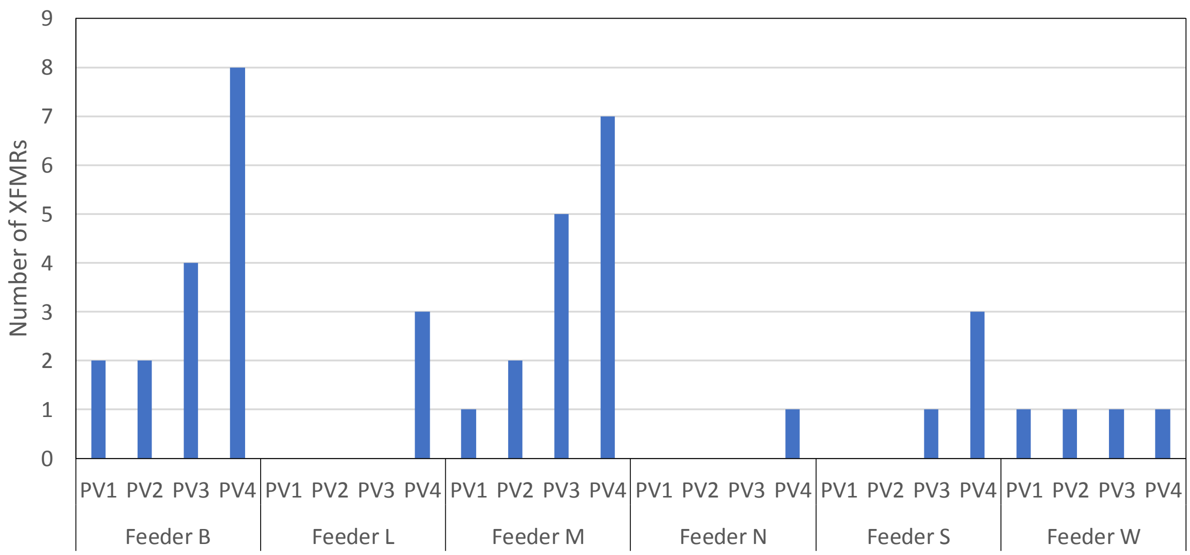

Figure 5-16 shows that the design criteria triggering thermal replacements is very effective in reducing the number of violations at higher PV penetration levels, when comparing the number of violations flagged in the baseline assessment to the number of violations flagged after the thermal replacements flagged are added to the feeder models. The few remaining thermal violations at lower PV penetration levels are reflecting highly isolated occurrences where an ES system happens to charge while high load demand is observed on one customer, temporarily pushing a transformer beyond its limit (<3% overload). These occurrences are therefore not related to any PV impacts. More details on these results can be found in Chapter 6.

Figure 5-16
Maximum Number of Service Transformers With a Thermal Violation From All Cases on a Specific Feeder and a Specific PV Penetration Level After Applying System Upgrades

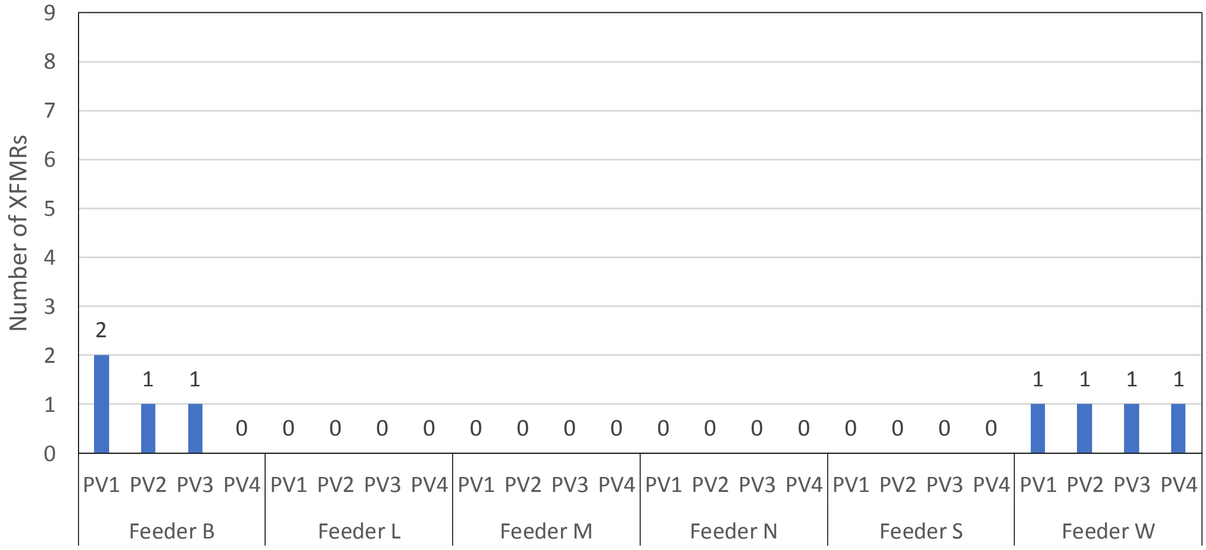

Although one or two thermal violations are still recorded for some of the scenarios simulated, most of the QSTS results reflect scenarios free of any thermal violations after all thermal upgrades flagged are applied.

Recall that 45 QSTS simulations were run per PV level, per feeder, reflecting a range of parameters (load profiles, PV profiles, ES penetration levels). Figure 5-17 represents the number of thermal violations for each of the 45 QSTS simulations (shown in y-axis) per PV penetration levels, per feeder, *before* the thermal upgrades are applied. Figure 5-18 shows the same results, but *after* the thermal upgrades are added to the feeder models.

For example, for Feeder B, at PV penetration level PV4 (100%), *before* the thermal upgrades were applied (Figure 5-17), 12 QSTS simulations were free of any thermal violations, six QSTS simulations recorded one violation, six QSTS simulations recorded three violations, three QSTS simulations recorded four violations, three QSTS simulations recorded five violations, 14 QSTS simulations recorded seven violations, and one QSTS simulation recoded eight violations. *After* the upgrades were applied (Figure 5-18), all 45 QSTS simulations were free of any violations.

Figure 5-17
Number of QSTS Simulations (Y-Axis) Reported With Their Respective Number of Transformers (Data Labels) Having Thermal Violations for the Baseline Models

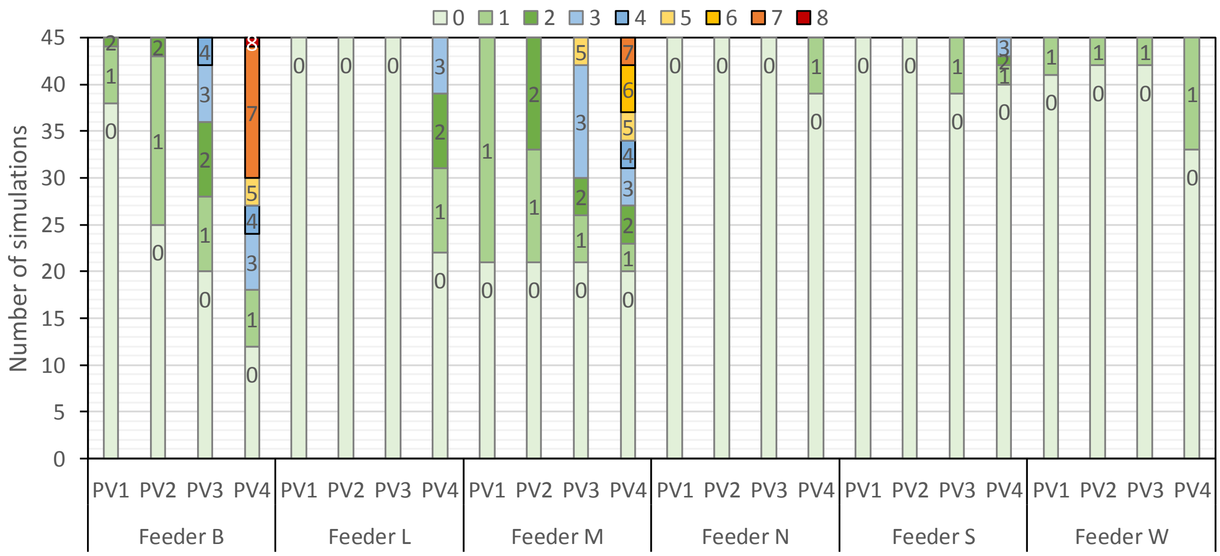

Figure 5-18
Number of QSTS Simulations (Y-Axis) Reported With Their Respective Number of Transformers (Data Labels) Having Thermal Violations After Applying System Upgrades

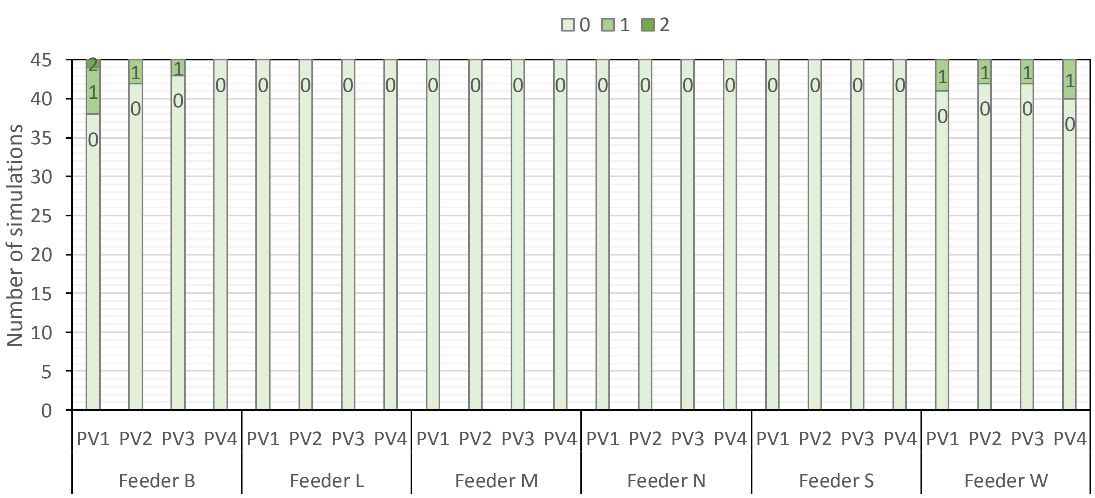

5.5.2 Voltage Rise Outside Design Guidelines

As previously discussed, the approach described in Figure 5-3 to flag voltage rise replacements was found to miss a number of *potential* voltage rise issues (Section 5.3). Still, the QSTS simulations provide a more realistic approximation of whether or not voltage rise outside design guidelines (considered a violation in this section) would have actually been experienced based on different load/PV day types. Thus, the MAX number of voltage violations (in terms of number of transformers) is reported in Figure 5-19 for any load/PV day type and ES penetration level combination. At all PV penetration levels for each feeder, the number of transformers with voltage rise issues is lower than the numbers reported in Figure 5 10. The reason for this is that the secondary voltage rise studies (Figure 5-10) are based on no-load/peak-PV condition, which is unlikely to occur in the QSTS simulations (Figure 5-19).

Figure 5-19
Maximum Number of Service Transformers With a Voltage Rise Outside Design Guidelines From All Considered QSTS Scenarios

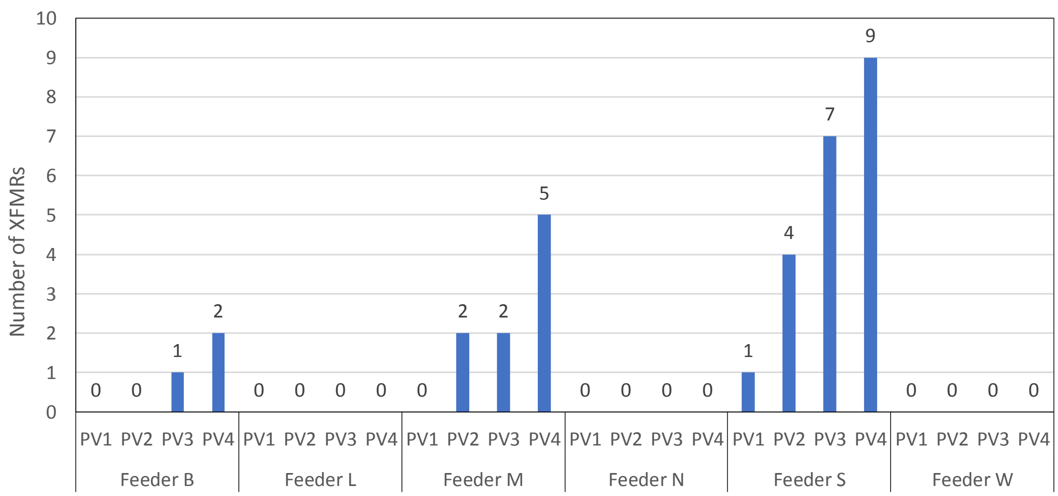

Figure 5-19 represents, for each feeder and each PV penetration level, the worst scenario across all representative daily load and PV profiles considered in this modeling effort. However, Figure 5-19 does not represent whether the violation(s) recorded occur only in one QSTS, representing a specific combination of load and PV profiles, or consistently across all QSTS (i.e., all the various scenarios considered for that feeder and PV penetration level).

To this end, Figure 5-20 represents the number of voltage violations for each of the 45 QSTS simulations (shown in y-axis) per PV penetration level, per feeder, *before* the secondary voltage rise upgrades are applied. Figure 5-21 shows the same results, but *after* the secondary voltage rise upgrades are added to the feeder models.

Figure 5-20
Number of QSTS Simulations (Y-Axis) Reported With Their Respective Number of Transformers (Data Labels) Having Voltage Rise Outside Design Guidelines for the Baseline Models

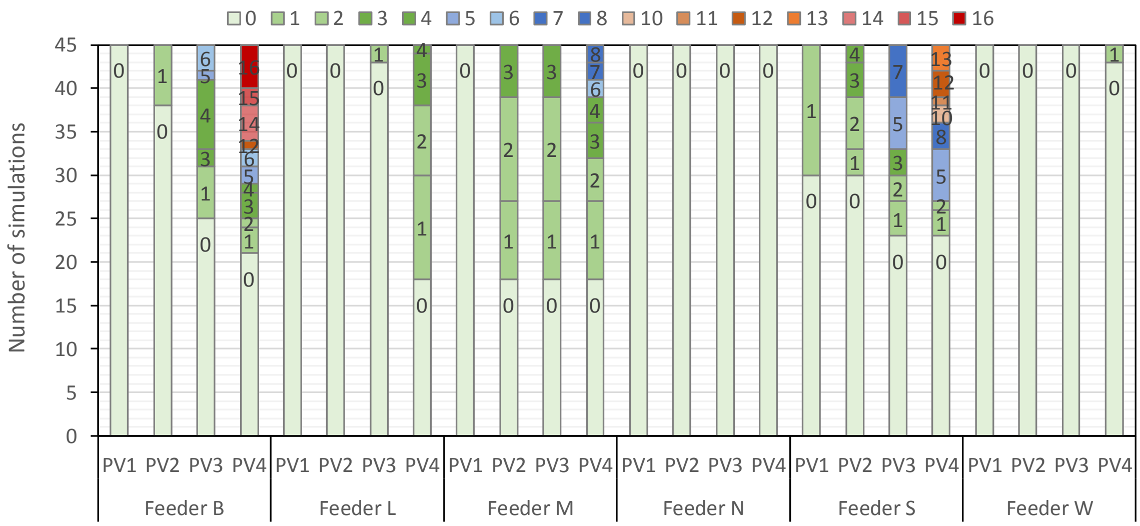

Figure 5-21
Number of QSTS Simulations (Y-Axis) Reported With Their Respective Number of Transformers (Data Labels) Having Voltage Rise Outside Design Guidelines After Applying System Upgrades

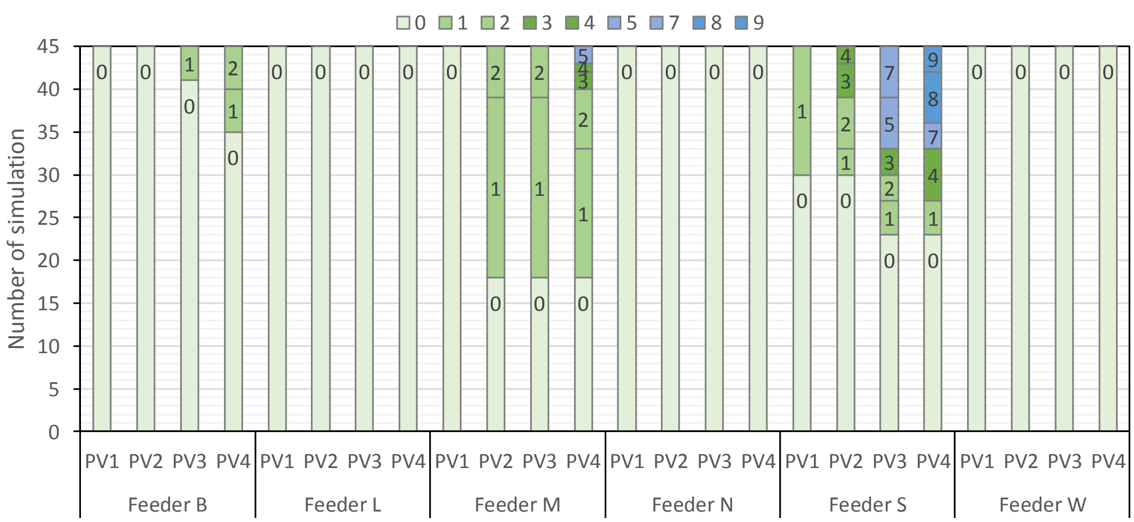

The results presented in Figure 5-21 suggest that the current decision criteria triggering voltage rise replacements does not fully suppress voltage rise issues. Yet, these results reflect significant improvements when the conventional upgrades flagged are properly implemented, as seen in the drastic reduction of the number of violations recorded at multiple PV penetration levels (e.g., Feeder B at PV4-100%).

On the other hand, small improvements are demonstrated on Feeder S, which corresponds to the discussion in Section 5.3 where a number of potential voltage rise issues were missed. Since a voltage rise issue is captured when the aggregated inverter rating exceeds the transformer nameplate rating, undetected voltage rise issues may be caused by transformers and/or service lines with high impedance. Figure 5-22 displays the number of transformers for a given transformer loading (defined here as total PV inverter nameplate / transformer nameplate) for all transformers with potential voltage rise issues (same subset of transformers as in Figure 5-11). Figure 5-22 suggests that some undetected voltage rise issues may result in from high voltage rise over the service lines. Note that any transformers with values above 100% triggered a secondary VRS and thus an upgrade, based on the design criteria, and that some upgrades above 110-140% (depending on thermal rating) also had a thermal violation.

A key observation from Figure 5-22 is that some transformers with voltage rise issues are far from being overloaded suggesting that the voltage rise issue on these secondary circuits are coming from line impedances. However, these upgrades were not recommended since the design criteria (nameplate comparison) did not trigger a secondary VRS.

Figure 5-22
Count of Transformers With Voltage Rise Outside Design Guidelines Sorted by Transformer Loading (Defined Here as the Ratio of the Aggregated Inverter Nameplate Rating and the Transformer Nameplate Rating). Percentages Are Rounded Down to the Nearest Value.

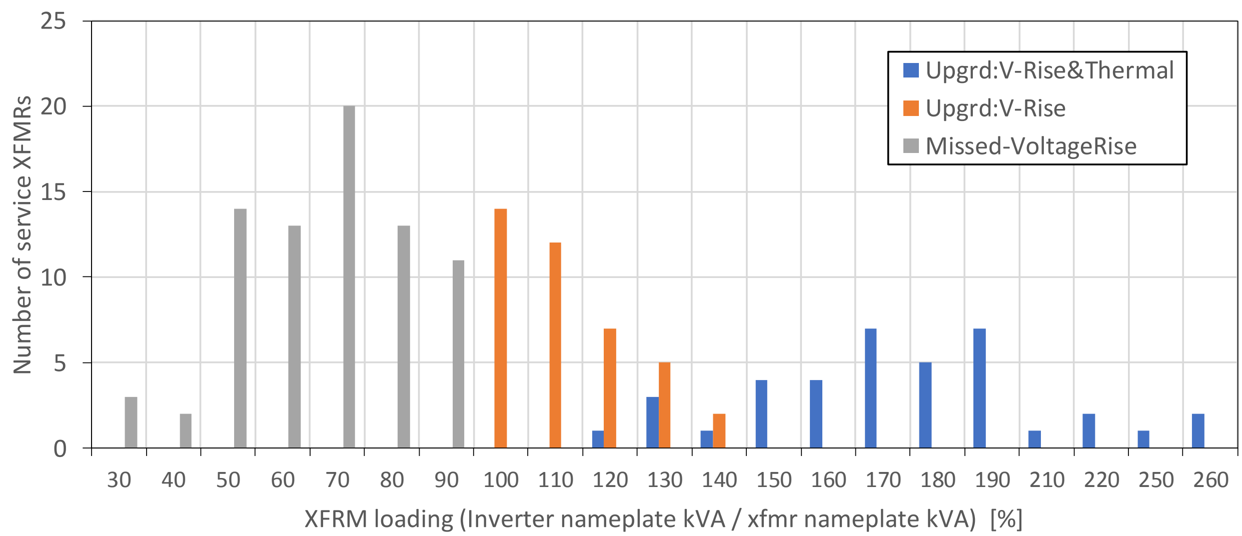

5.6 Conclusions

The objective of this chapter was to determine the conventional measures required to accommodate increased PV penetration levels. The upgrades were identified separately for the LV secondary circuits and the MV primary circuits. Since this modeling effort analyzed the impacts and benefits of residential smart PV inverters, almost all upgrades necessary were associated with the LV secondary circuit equipment.

A process for identifying the secondary circuit upgrades required was defined, reflecting PG&E's current design and engineering practices. This process was applied to determine is defined the equipment replacements required for each of the six feeders modeled, at each of the four PV penetration levels considered. The process identified secondary circuit upgrades to avoid potential thermal overloads and potential voltage rise issues.

Potential thermal overloads caused by reserve power due to PV were identified by comparing the total PV inverter rating of all PV systems served by a transformer to the transformer thermal rating. Once a potential overload was identified, the transformer was upgraded accordingly to avoid the potential overloads.

Similarly, potential voltage rise issues caused by reverse power flow due to PV were identified by comparing the total PV inverter rating of all PV systems served by a transformer to the transformer nameplate rating. Once potential voltage rise issues were detected, secondary voltage rise studies were conducted to determine whether secondary circuit upgrades were needed to avoid high voltage rise caused by PV. The concern with this approach was that the nameplate comparison may not always be a good indicator of potential voltage rise issues particularly when high voltage rise is due to the service lines (as opposed to the service transformer).

The effectiveness of the decision rules triggering thermal and secondary voltage rise upgrades at addressing potential adversarial PV impacts was also evaluated. QSTS simulation results suggest that the nameplate comparison approach currently used is very effective at capturing potential *thermal* overloads. Under PG&E's exiting practices, service transformers are sized for MAX load conditions. Screening them further for potential violations assuming MAX reverse power flow conditions (MAX PV/MIN load) appears to be a good complement: the combined criteria for MAX load conditions and MAX reverse power flow conditions bound the most extreme conditions.

Regarding *voltage rise* violations, QSTS simulation results suggest that the nameplate comparison approach currently used can properly flag transformer upgrades that resolve a majority of voltage rise issues. However, some issues remain since secondary voltage rise studies are *only* triggered when the aggregated PV inverter rating for all PV systems connected downstream of a given transformer exceeds the transformer nameplate. However, this decision rule may miss some voltage rise issues. In particular, the decision rule may miss voltage rise issues that are caused by high impedance transformers or service lines.

While the service transformer replacements triggered by PG&E's current decision rule for voltage violations were found to not suppress all the voltage rise issues, significant improvements were observed. To achieve realistic estimates of upgrade numbers, this modeling effort followed closely the current PG&E practices for identifying replacements.

Obtaining a realistic count of transformer replacements is critical for two reasons. First, these replacements, deferred when SI functions are activated, are considered as avoided costs in the economic analysis. Second, some of the "missed" violations not addressed by these replacements may be suppressed by SI functions, a potential benefit that must be recorded.

The following chapters provide a detailed discussion on the modeling of SI functions, and compare the QSTS simulation results obtained when convention upgrades are applied (this chapter), to the results obtained when SI functions are activated (Chapter 6).

6
ACCOMMODATING INCREASED PV PENETRATION LEVELS WITH AUTONOMOUS SMART INVERTER FUNCTIONS

This chapter describes the modeling approach used to simulate the operation and grid impacts of SIs, and presents a summary of the results obtained under different PV penetration scenarios. Three alternative combinations of autonomous inverter functions are assessed via QSTS simulations, evaluating their impact on overvoltage conditions, overload conditions, and power usage. Each combination of SI functions was simulated across multiple simulation cases representing a range of PV penetration levels, feeder load conditions, PV generation conditions, and ES penetration levels. In particular, this technical assessment was performed assuming penetration scenarios, constraints, and thresholds for voltage and loading conditions identical to the ones assumed in Chapter 4.

6.1 Modeling Approach

The operation of autonomous SI functions was modeled using the control strategy of "InvControl" objects in OpenDSS. The non-linearity of SI functions can make it challenging to achieve numerical convergence in scenarios with large number of autonomously controlled SIs. Therefore, the SI modeling approach and settings applied in this modeling effort were carefully considered. The OpenDSS "InvControl" object provides the necessary framework to independently calculate the output of each SI instance, without the need for any further interaction with any other external control algorithms. In addition to the PV system modeling approach described in Chapter 4, the SI controllers ("InvControl") were parametrized by means of the following properties:

1. Smart inverter function: Description of the function (mode property), and power-voltage characteristics (X-Y curves).
2. Reference of the power-voltage characteristic axes: Properties of reference for calculation of the inverter's output at specific voltage conditions.
3. Precedence of reactive power compensation: SIs were set to prioritize the reactive power production over the active power generation. This is also referred to as "reactive power priority" or "VAR priority".
4. Reactive power generation dependency to the inverter status: PV systems were set to cease the reactive power generation or absorption when the PV panel active power generation was insufficient for the inverter to operate. This is also referred to as no "VARs at night."
5. Maximum output power delta in each control iteration: Active and reactive power changes are limited to a maximum change in each control iteration. These parameters are fundamental in a simulation environment to avoid numerical instability due to the voltage fluctuations in high penetration scenarios.

Simulation models were required to represent SI deployment scenarios in which the Volt-VAR and Volt-Watt functions were enabled for simultaneous operation. These simulation scenarios, described in Section 6.1.1, were implemented with the combined mode algorithm included as the "CombiMode" option of the OpenDSS "InvControl". Currently, there are several SI operation modes included in the "InvControl" object; however, some changes to OpenDSS Delphi source code were implemented over the course of this modeling effort to achieve the Volt-Watt operation in compliance with the requirements of CA Rule 21 and HI Rule 14. These changes to the OpenDSS source code enabled to simultaneously consider Volt-VAR and Volt-Watt control modes to achieve the required power outputs based on the inverter capabilities, and the available PV panel active power at a given time. These changes to the OpenDSS source code will be incorporated into a future public release of OpenDSS.

Calculating the power output required by SI functions in simulation scenarios where a large number of PV systems coexist with feeder voltage regulating equipment can result in numerical instability. The method currently implemented in OpenDSS to determine the final state of each autonomous SI function assumes a specific power output from the smart inverter, and computes the power flow solution. The power flow solution returned is then used to determine whether the SI controller has the correct power output, and adjust its settings as needed before recomputing the power flow for that time-step. Multiple iterations may be required for each time-step (known as “control iterations”) due to the complex interactions between SIs and feeder voltage regulation equipment.

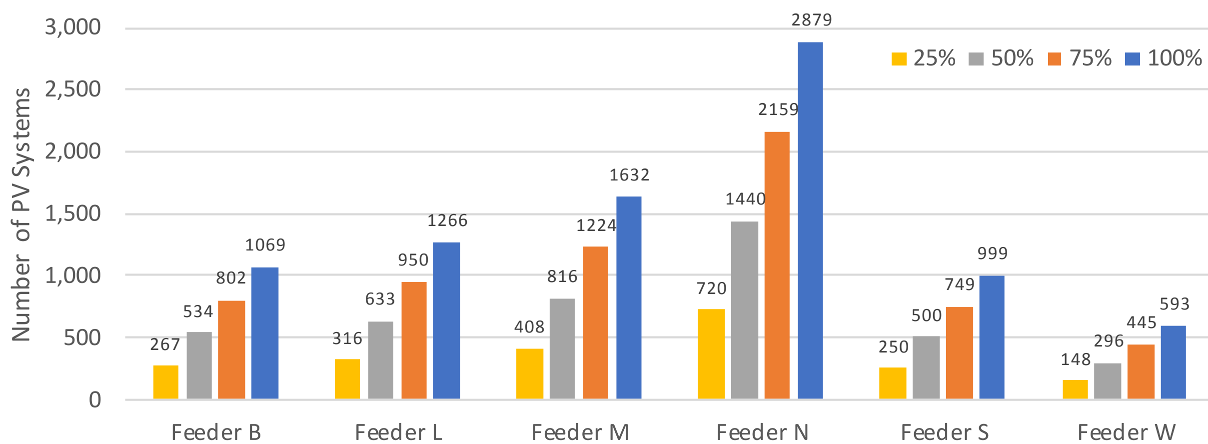

Figure 6-1 shows the maximum count of SIs devices that are simultaneously simulated for each of the six feeders, at each of the four PV penetration levels considered. As this modeling effort covers scenarios with as many as 13 independent voltage regulator controllers, 6 independent capacitor controllers, and 2,879 SIs, the convergence of certain simulation scenarios required as many as 200 control iterations for a single QSTS simulation time step. In this modeling effort, the risk of numerical instability was primarily addressed by reducing the maximum power delta that can be generated between control iterations (“deltaP_factor” and “deltaQ_factor” properties of the “InvControl”).

Figure 6-1
Maximum Count of Smart Inverters Per Feeder and PV Penetration Level

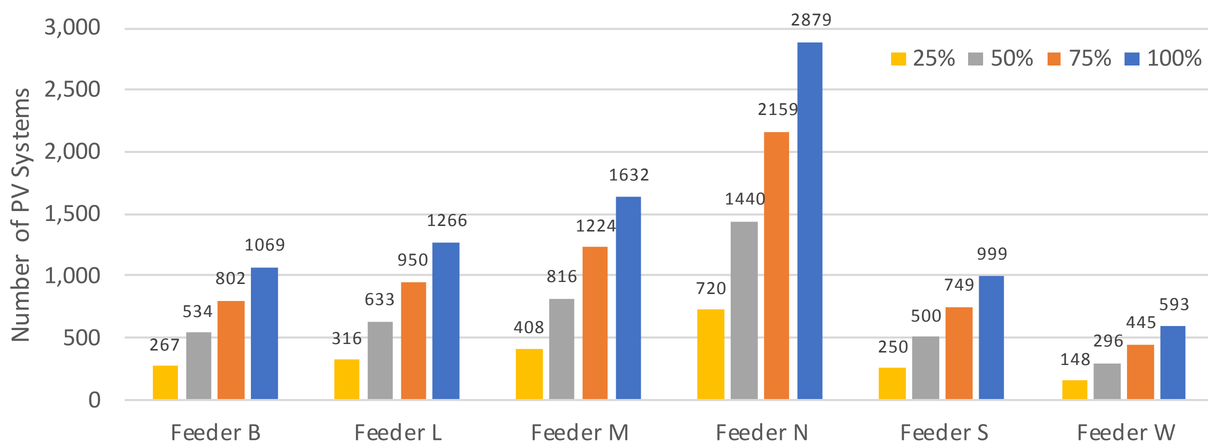

6.1.1 Smart Inverter Functions

CA Rule 21 defines the requirements applicable to most generating facility interconnections in PG&E service territory, including SI functions. These requirements include rules governing the production and consumption of reactive power in response to voltage conditions, reactive power priority over active power (Volt-VAR function), and rules governing the reduction of the active power production as a function of high voltage conditions (Volt-Watt function). The implementation of these requirements can result in conditions where the reactive power production of PV inverters is limited to prevent undesirable grid impacts.

In this modeling effort, three combinations of SI functions were evaluated:

1. *Volt-VAR* with the default settings defined in CA Rule 21 (referred to as “VV-R21”);
2. *Combined Volt-VAR & Volt-Watt* with the default settings defined in CA Rule 21 (referred to as “Combi-R21”); and
3. *Combined Volt-VAR & Volt-Watt* with the default settings defined in HI Rule 14 (referred as “Combi-R14”).

Figure 6-2 shows the Volt-VAR function with the default settings defined in CA Rule 21. In particular, the CA Rule 21 Volt-VAR function default settings have a maximum reactive power production of 30% of the apparent power nameplate when the voltage falls below 92% of the nominal voltage magnitude. Similarly, a maximum reactive power consumption of 30% is required at voltage magnitudes equal or greater than 107% of the nominal voltage. In this modeling effort, the Volt-VAR function settings shown in Figure 6-2 were assumed for VV-R21.

Figure 6-2
Voltage and Reactive Power Default Settings for the Volt-VAR Function Defined in CA Rule 21

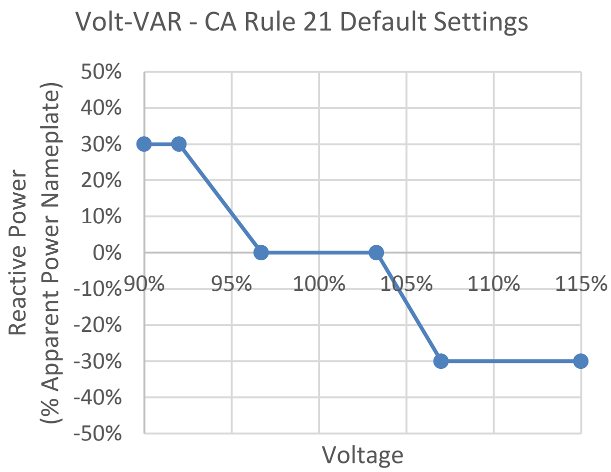

Voltage (%V nominal)	Reactive Power (% VA rating)
90.0%	30.0%
92.0%	30.0%
96.7%	0.0%
103.3%	0.0%
107.0%	-30.0%
115.0%	-30.0%

Figure 6-3 shows the Volt-Watt function with the default settings defined in both CA Rule 21 and HI Rule 14. Under both of the two rules, the Volt-Watt function default settings reduce the active power generation at a rate of 25% of the active power nameplate rating per one percent of nominal voltage above 106%, until zero power output is reached. In this modeling effort, the Volt-Watt function shown in Figure 6-3 was assumed for both Combi-R21 and Combi-R14.

Figure 6-3
Voltage and Active Power Settings for Volt-Watt Function as Defined in CA Rule 21 and HI Rule 14

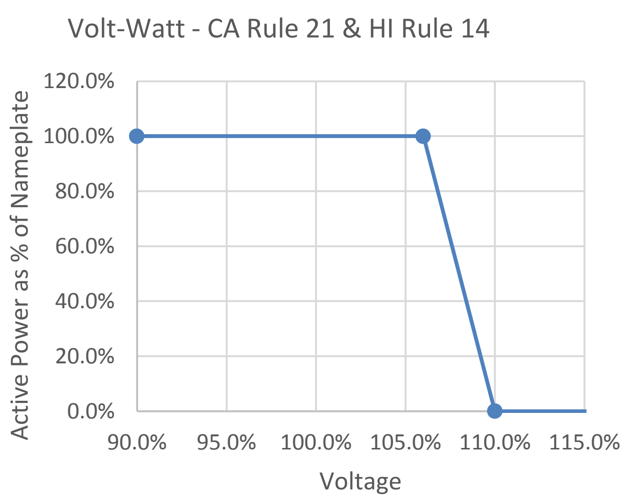

Voltage (%V nominal)	Active Power (% Nameplate)
90.0%	100.0%
106.0%	100.0%
110.0%	0.0%
120.0%	0.0%

Figure 6-4 represents the Volt-VAR function as defined in HI Rule 14. In particular, the HI Rule 14 Volt-VAR settings define a maximum reactive power production of 44% of the apparent power nameplate when the voltage conditions are 94% of the nominal voltage magnitude or below. Similarly, a maximum reactive power consumption of 44% is required for voltage magnitudes equal or greater than 106% of the nominal voltage. In this modeling effort, the Volt-VAR function settings shown in Figure 6-4 were assumed for Combi-R14 Volt-VAR.

Figure 6-4
Voltage and Reactive Power Settings for Volt-VAR Function From HI Rule 14

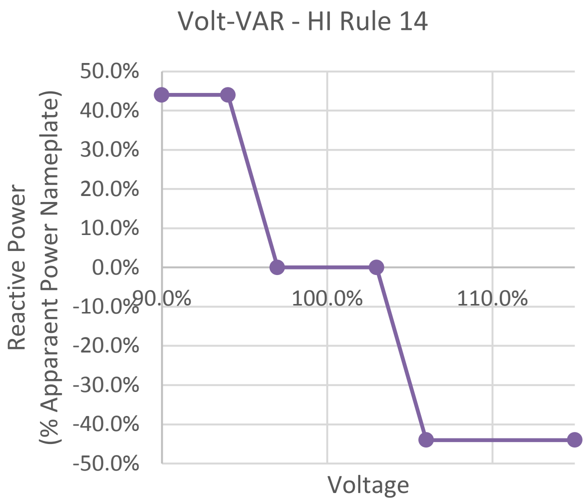

Voltage (%V nominal)	Reactive Power (% VA rating)
90.0%	44.0%
94.0%	44.0%
97.0%	0.0%
103.0%	0.0%
106.0%	-44.0%
115.0%	-44.0%

For each of the three combinations of SI functions considered, the voltage and thermal violations observed in the QSTS simulations were analyzed and compared. The detailed modeling of secondary circuits discussed in Chapter 3 enabled to assess in detail how effective each combination of SI functions was at mitigating voltage rise caused by PV through either reactive power compensation (Volt-VAR function) and/or active power reduction (Volt-Watt function), both operated based on the voltage measurement at the inverter terminals. Compared to conventional feeder voltage regulation equipment (located at the MV primary circuit level), SI functions of residential PV (located at the LV secondary circuit level), have a more restricted area of influence due to the relatively small size of each individual inverter. Therefore, to evaluate the effectiveness of SI functions of residential PV, it is fundamental to analyze high PV penetration levels across a range of different load and generation conditions on each feeder.

When SI functions with VAR priority are considered, certain voltage conditions may require reactive power support (consumption or generation) that can lead to a reduction in active power generation. Active power reduction depends on multiple factors, including the PV generation (dependent on irradiance, temperature, shading, etc.) and the voltage at the inverter terminals. Furthermore, the voltage at the PV inverter terminals depends on a myriad of further factors including feeder load conditions particularly in the secondary circuit where the PV is interconnected. Since many factors can potentially influence active power reduction, this modeling effort utilizes a set of local and global metrics (described in Chapter 4), applied in conjunction with the detailed modeling of secondary circuits and the assignation of load and PV generation profiles to realistically capture SI operation.

The combinations of SI functions considered in this modeling effort are directly relevant to PG&E service territory. The first function (not a combination), VV-R21, reflects the Volt-VAR function currently required under CA Rule 21. The second function combination, Combi-R21, reflects the new CA Rule 21 Phase III, which required the addition of Volt-Watt functions as a complementary measure to prevent extreme voltage rise conditions. The third function combination, Combi-R14, reflects the requirements specified by HI Rule 14, and is provided for comparison purposes to assess the impact of a more aggressive Volt-VAR curve. Figure 6-5 illustrates the three combinations of SI functions considered in this modeling effort.

Figure 6-5
Combinations of Smart Inverter Functions Considered

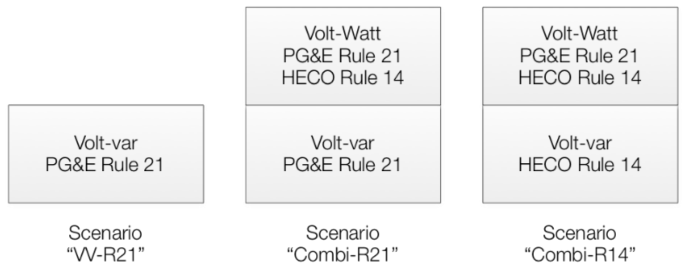

6.1.2 Smart Inverter Densities

Four different SI densities, 25%, 50%, 75%, and 100% of PV customers with SI functions, were evaluated in this modeling effort. Multiple SI densities were evaluated to assess the distribution impacts and benefits of SIs over the transitional period when conventional inverters (without SI capabilities) are being gradually retired.[83] The PV customers with SI function capable inverters were randomly selected as described in Chapter 4. This process was incremental from one SI density to the next. For example, all PV customers with SI functions enabled at the SI density of 50% were set the functions enabled also at the SI density of 75%, and these PV customers were supplemented with randomly chosen PV customers without SI functions enabled at 50% to reach a SI density of 75%. This incremental process was followed until a SI density of 100% was reached.

Three combinations of SI functions and four different SI densities were considered in addition to the other parameters previously introduced: six feeders, five PV penetration levels, three ES penetration levels, three load profiles, and five PV generation profiles. The combination of all these parameters resulted in a total of 12,960 QSTS simulation scenarios analyzed. These scenarios are sketched in Figure 6-6. Each scenario consisted of a daily 15-minute QSTS simulation. All scenarios cumulated represent an equivalent of 35 simulation years. Python scripts were therefore developed to achieve an efficient data processing of more than 65 gigabytes (GB) of results distributed across more than half a million of files.

[83] It should be noted that currently, there is no requirement to replace legacy inverters with SIs.

Figure 6-6
Summary of the Scenarios Simulated Including Smart Inverter Densities and Functions

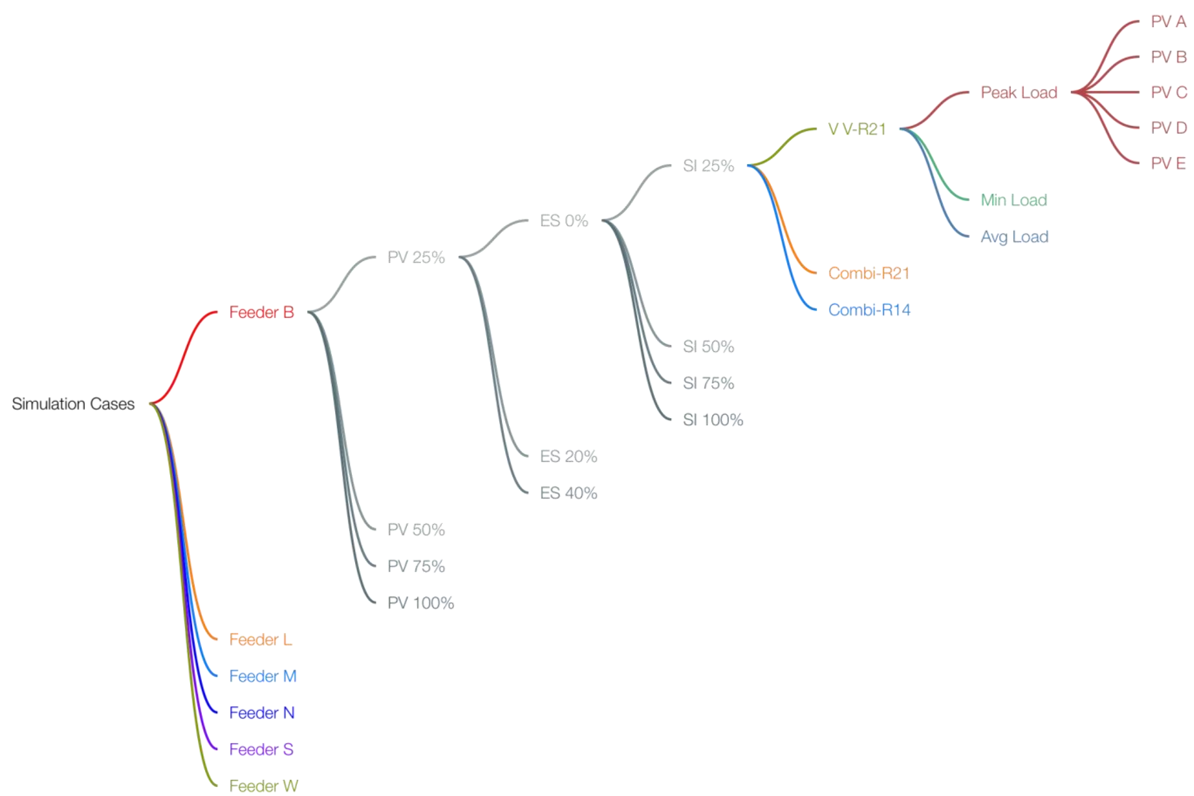

6.2 Examples of Smart Inverter Impact on PV Generation

6.2.1 Example #1: Typical Curtailment Conditions

The operation of the three combinations of SI functions considered are illustrated in Figure 6-7 for one example customer with a 5.75 kW (DC) – 4.792 kVA PV installation. Specifically, Figure 6-7 shows the results obtained at peak load conditions, assuming a sunny day in summer (PV profile A). This example was extracted from a simulation scenario assuming the maximum PV penetration level, with 0% ES penetration, and 100% SI density.

Figure 6-7A (resp. Figure 6-7B) represents the generated power (resp. voltage conditions) for this location. In each figure, the base case, where SI functions were *not* activated, is represented in black. Figure 6-7A shows some differences in reactive power compensation, with a consumption of up to 1.25 kVAR with Combi-R14 around noon-time. This reactive power compensation can be explained by the voltage conditions represented in Figure 6 7B: the voltage magnitude around noon-time exceeds the 1.033 Vpu threshold (1.030 Vpu for Combi-R14) that triggers reactive power compensation.

Figure 6-7A also shows minor differences in the maximum active power generated around noon-time as a result of the inverter prioritizing reactive power over active power. In particular, Combi-R14 results in slightly larger, albeit still minor, active power curtailment.

For each of the three combinations of smart functions considered, Figure 6-7C and Figure 6-7D represent the difference in power and voltage profiles between the case where the functions are activated, and the base case with no smart functions.

Based on Figure 6-7C, VV-R21 and Combi-R21 perform similarly[84] in terms of active power generation and reactive power consumption; indeed, the Volt-Watt function considered in Combi-R21 was not activated in this case, since the voltage level stayed below 1.06 p.u. In contrast, Combi-R14 shows a higher consumption of reactive power as the Volt-VAR function assumed in Combi-R14 has higher compensation requirements.

The voltage differences represented in Figure 6-7D show that the reactive compensation provided by each of the three combinations of functions considered effectively reduced the voltage magnitude. The maximum reduction was achieved by Combi-R14, which has the highest reactive power compensation of the three function combinations.

Note that for this particular customer, under these specific conditions, active power curtailment was small across all combinations of SI functions considered. However, there could be cases in which the voltage conditions require higher reactive power compensation, to a level that may lead to curtail active power generation.

Figure 6-7
Example of PV Generation for One Customer With Smart Inverter Functions Activated. A) PV Power Generation. B) Voltage Magnitude. C) PV Power Difference Based on Non-Smart Inverter Functions Results. D) Voltage Magnitude Differences

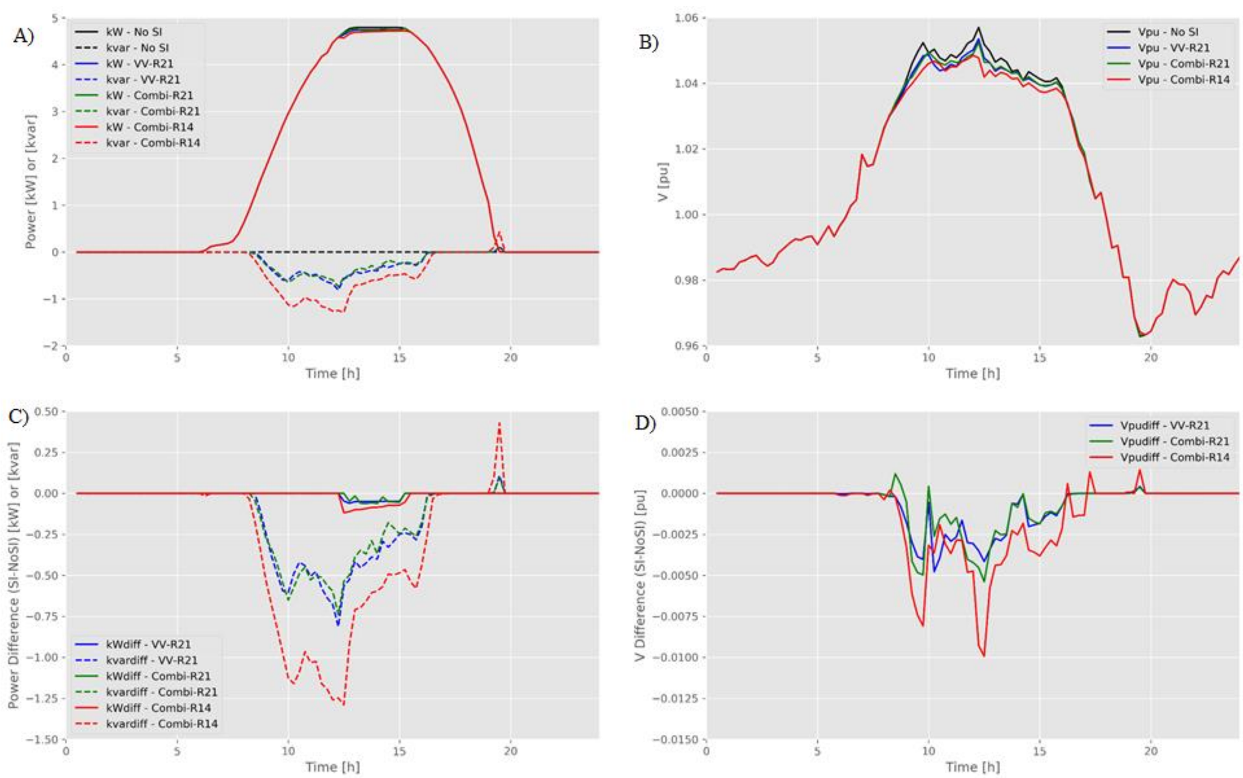

84 The minor differences between VV-R21 and Combi-R21 results are likely caused by differences in the operation of other smart inverters on the feeder. VV-R21 and Combi-R21 may also result in slightly different simulation convergence, which can cause negligible differences in simulation results.

6.2.2 *Example #2: High Curtailment Conditions*

This second example is an extreme case that corresponds to the maximum daily curtailment observed across all simulation results for the example customer previously considered, with 4.82% reduction in daily active power generation.[85] Simulation results suggest that such a high curtailment is rare across the six feeders and all other sensitivities analyzed. Still, the analysis of this extreme case illustrates the conditions that may lead to such notable active power curtailment.

Figure 6-8 shows the simulation results obtained for the same customer represented in Figure 6-7, but under different conditions. Figure 6-8 assumes the average load conditions, during a sunny day in summer (PV profile A). This example was extracted from a simulation scenario assuming the maximum PV penetration level, with 40% ES penetration, and 75% SI density. Under these new conditions, as shown in Figure 6-8A, reactive power compensation is much higher compared to values observed in Figure 6-7A for that same customer, but under different conditions.

The increased reactive power consumption observed in Figure 6-8A results from the high voltage magnitudes experienced at this location when no SI functions are activated, as seen in Figure 6-8B:

- VV-R21 reduces the maximum voltage to approximately 1.065 p.u., with a consequent reduction of the active power generation (solid blue curve in Figure 6 8C).
- Since PV voltages with VV-R21 exceed 1.065 p.u., Combi-R21 triggers the Volt-Watt mode, resulting in additional watt curtailment and an additional reduction in voltage (solid green curve in Figure 6-8C). In this particular example, the power curtailment resulting in from Combi-R21 is greater than the curtailment produced by Combi-R14.
- Similarly, Combi-R14 has also triggered its Volt-Watt mode (solid red curve in Figure 6-8C). However, under Combi-R14, no additional curtailment results from the Volt-Watt activation, contrary to Combi-R21. Indeed, by the time Combi-R14 activates its Volt-Watt mode, the Volt-VAR mode has already curtailed the active power output *more* than the Volt-Watt mode would. The reactive power support provided by Combi-R14 leads to the biggest voltage reduction (Figure 6-8D).

It is important to highlight that, from all the scenarios analyzed in this modeling effort, it has not been possible to identify a single instance where Combi-R14, combining HI Rule 14 Volt-VAR with HI Rule 14 Volt-Watt, would result in an active power curtailment *higher* than the curtailment observed with the activation of HI Rule 14 Volt-VAR alone. It should also be noted that different results may be obtained with different DC/AC ratios.

Additional analysis of these high curtailment conditions can be found in Section 6-4, where the daily simulation results are discussed to characterize the frequency of this phenomenon.

[85] This was the highest PV curtailment over a 24-hour period that was obtained for any customer on any feeder for any of the 12,000+ daily QSTS simulations.

Figure 6-8
Example for the Scenario Showing the Highest Reduction in Active Power Generation. A) PV Power Generation. B) Voltage Magnitude. C) PV Power Difference Based on Non-Smart Inverter Functions Results. D) Voltage Magnitude Differences

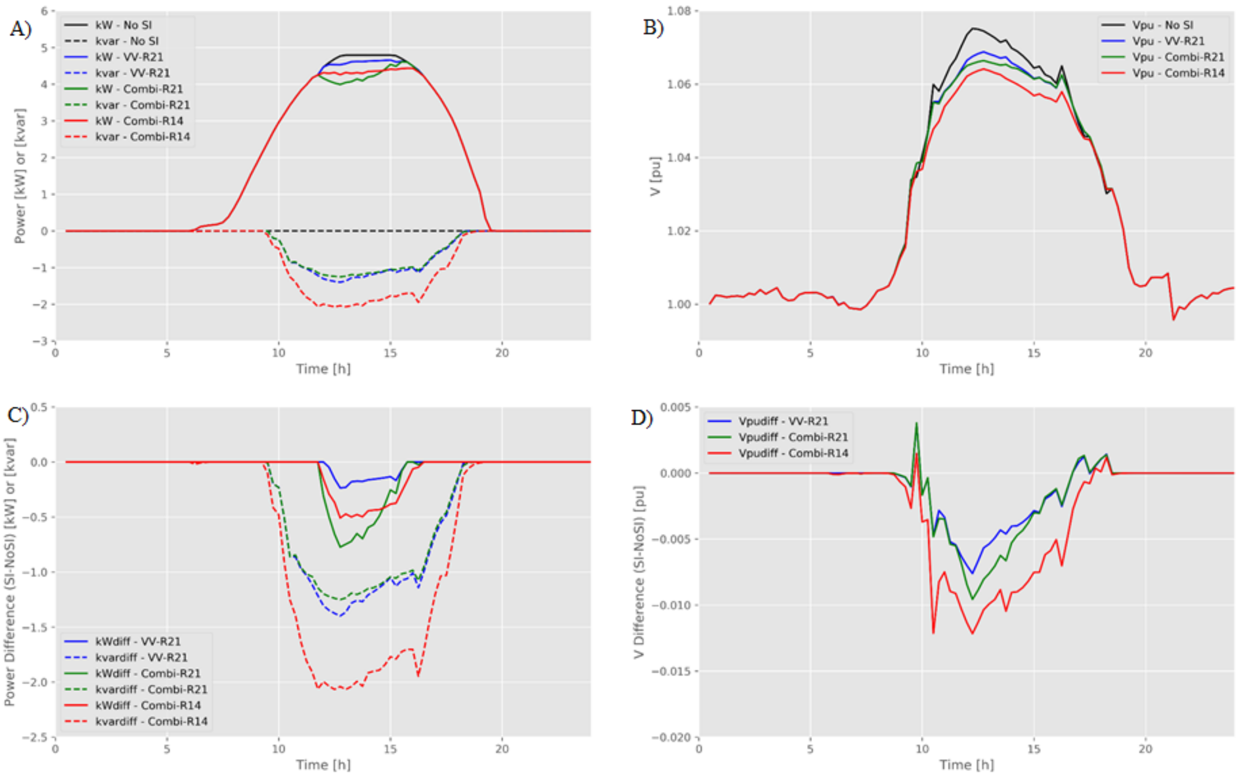

6.3 Smart Inverter Impacts on System Operation

Several metrics summarizing the voltage conditions, overload conditions, feeder head power consumption, and PV power generation were used to analyze the impacts of SI functions on grid operations. Each QSTS simulation completed in this modeling effort returned a set of results that were organized according to the *SI function*, *SI density*, *PV and ES penetration levels* selected. To facilitate the analysis, given the very large number of QSTS simulations completed, results obtained across the different daily *load profiles* and *PV profiles* were grouped and only maximum and minimum values were extracted for each group.

This section provides an introductory analysis to illustrate the impacts of SI functions over a range of scenarios. Chapter 7 provides a more detailed comparison of the results obtained when smart functions are activated, to the results obtained with conventional mitigation measurements, or under baseline PV conditions.

6.3.1 Effect of Smart Inverter Functions on Overvoltage Conditions

The diversity of load and PV generation profiles considered in this modeling effort required analysis of a wide range of system operation conditions to properly assess the impacts of activating SI functions. A first-order analysis focused on counting the number of QSTS simulations returning "significant" overvoltage conditions. Similar to Chapter 3, a significant overvoltage condition was defined as having a duration greater than 1 hour, or affecting more than 5% of the feeder buses.

The Volt-VAR function, present in each of the three combinations of functions considered (VV-R21, Combi-R21, and Combi-R14) is designed to directly address overvoltage conditions. Therefore, the impact of each combination on both the *frequency of occurrence*, and *severity* of overvoltage conditions was analyzed, across all simulation cases computed.

For each of the six feeders modeled, Figure 6-9 shows the *count* of QSTS simulations returning an overvoltage condition, across all PV penetration levels and SI functions considered. Detailed comparisons quantifying the *severity* of the overvoltage conditions recorded can be found on Chapter 7.

Note that for each feeder, each PV penetration level, and each combination of inverter functions, the results presented on Figure 6-9 cover 45 scenarios: three types of load days, five PV generation days, and three ES penetration levels. All results shown in Figure 6-9 assume 100% SI density. Therefore, the maximum QSTS simulation count per column in Figure 6-9 is 45.

Results in Figure 6-9 show that the activation of SI functions reduces the number of daily QSTS simulations displaying significant overvoltages:

- Feeder B, Feeder L, and the first PV penetration level for Feeder M display no significant overvoltage conditions after activation of the SI functions, across all three combinations considered: VV-R21, Combi-21 and Combi-14.
- Results for Feeder W show only two cases with significant overvoltage, at 75% PV penetration level with Combi-R21.
- Across all remaining cases of significant overvoltages, VV-R21 and Combi-R21 have a similar case count.
- Therefore, the inclusion of the Volt-Watt function in Combi-R21 did not significantly impact the results, when compared to VV-R21 which does not include the Volt-Watt function. In contrast, Combi-R14 tend to reduce the occurrence of significant overvoltages.

In additional to the analysis presented in this section focusing on the *frequency of occurrence*, the *severity* of overvoltage conditions was also analyzed by recording the MV magnitudes at MV and LV level, the percentage of affected buses, and the number of secondary circuits affected. Chapter 7 compares the severity metrics recorded for all scenarios leveraging SI functions, to the results obtained when assuming conventional mitigation upgrades.

Figure 6-9
Count of QSTS Simulations With Significant Overvoltage Per PV Penetration Level and SI Function (100% SI Density)

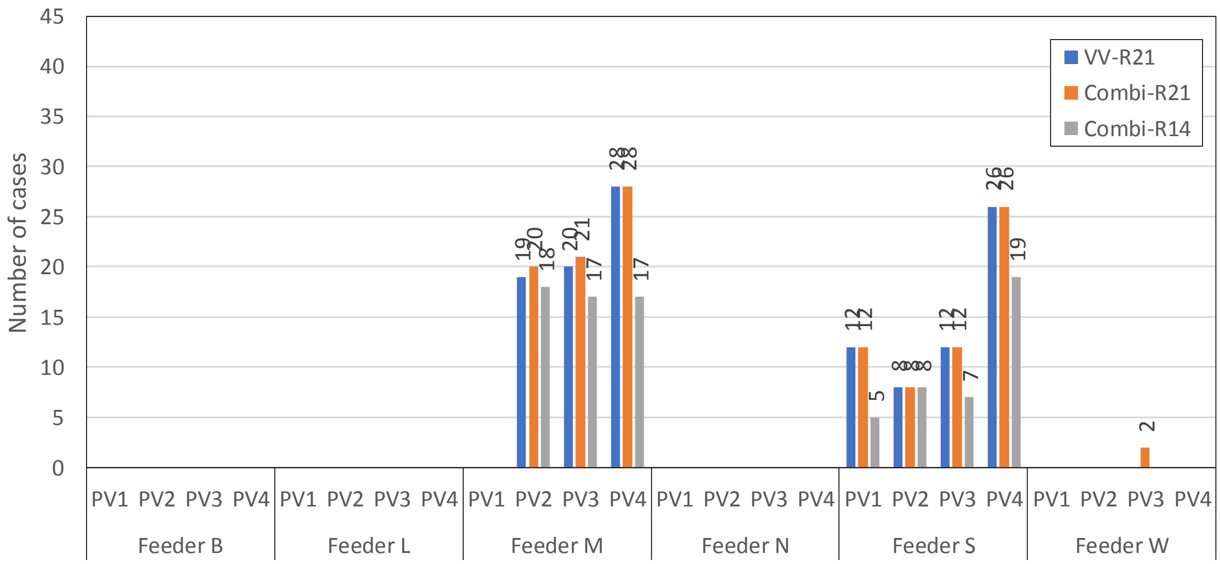

6.3.2 Effect of Smart Inverter Functions on Undervoltage Conditions

The first order analysis of undervoltage conditions was performed by tracking the number of daily QSTS simulations displaying significant undervoltages, similar to the approach followed for overvoltage conditions.

Figure 6-10 shows the number of daily QSTS simulations returning a significant undervoltage condition, organized by SI functions and PV penetration levels. All results shown in Figure 6-10 assume 100% SI density. Similar to Figure 6-9, the maximum count of QSTS simulations per column in Figure 6-10 is 45.

Feeder M had more cases with undervoltage issues at higher PV penetration levels, when compared to the other feeders studied. These results reflect challenging regulating conditions at the primary circuit level, since Feeder M has four cascaded voltage regulators. Most of the undervoltage conditions observed for Feeder M on Figure 6-10 correspond to scenarios with voltage violations at the medium voltage level, which are mainly caused by the operation of two cascaded open-delta voltage regulators at the feeder end. As shown in Chapter 7, results for Feeder M showed significant undervoltage conditions affecting the primary and secondary circuits, regardless of whether SI functions were activated. These voltage regulation challenges on Feeder M are discussed in further detail in Chapter 7.

Additionally, Feeder S and Feeder W also experienced undervoltage conditions. However, these conditions only affected on a small percentage of secondary buses and would have been classified as insignificant if their duration wasn't slightly above 1 hour. The simulation results of these feeders, which are shown in Chapter 7, indicated that these undervoltage conditions were not notably affected by the activation of SI functions.

Figure 6-10
Count of Cases With Significant Undervoltage Per PV Penetration Level and SI Function (100% SI Density)

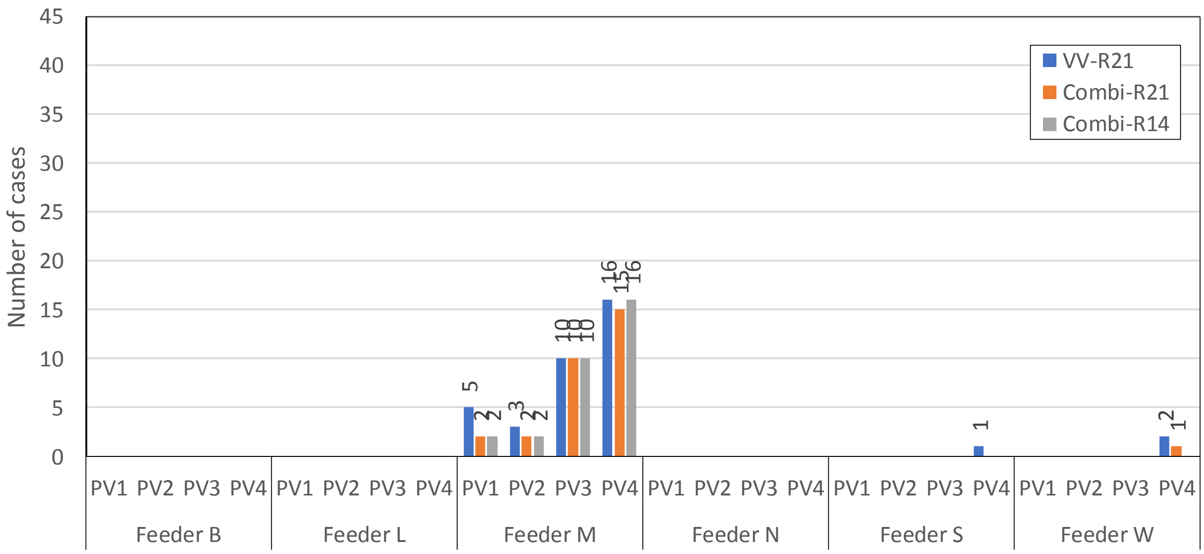

6.3.3 Effect of Smart Inverter Functions on Overload Conditions

For this analysis, all simulation scenarios were grouped per SI functions and SI densities (180 QSTS simulations in each group); the highest duration across all overload conditions recorded per group is reported on Figure 6-11. The summary metrics indicate that SI functions have *no impact* on the overload conditions, for any of the six feeders modeled.

Specifically, Feeder B and Feeder W did experience a few cases of *non-significant* overload conditions, with a MAX duration comprised between one- and three-time steps (0.25 to 0.75 hours). These conditions correspond to a total of three service transformers, with the transformer loading going up to 3.5% over the overload limit (additional results on this topic can be found in Chapter 7). However, since the duration and percentage of overload were found to be non-significant, and since the numbers presented in Figure 6-11 also represent worst-case conditions, one could conclude that SI functions have no significant impact on increasing the overload conditions in the feeders of interest.

It is important to highlight that these QSTS results are performed on feeder models that include service transformer replacements performed due to potential overloads as identified through the nameplate comparison (see Chapter 5). These upgrades were included in the analysis performed with SIs since the upgrades would be made regardless of whether or not SI functions were activated. Additionally, these results showed the effectiveness of the replacement criterion to avoid additional overload conditions when SI functions were activated.

Figure 6-11
Maximum Duration of Overload Conditions Per SI Function and SI Density

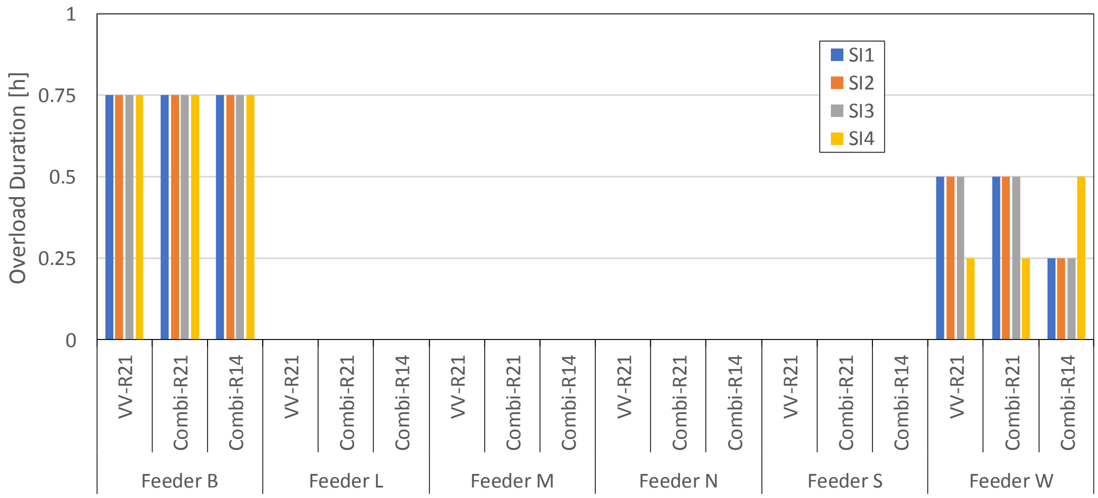

6.3.4 Effect of Smart Inverter Functions on Feeder Head Power

Little to no difference was observed in terms of the average active and reactive power at the feeder head when SI functions were activated compared to when the functions were not activated. To obtain this result, the average power was calculated by dividing the daily active and reactive energy results obtained from each QSTS simulation by the duration of the simulation, 24 hours. This calculation was first completed for every QSTS simulation. Then, the QSTS simulations were grouped according to the SI functions and SI densities assumed, and the average power across all simulations belonging to the same group was calculated (see Figures 6-12 and 6-13).

The results obtained also show that the feeder head power is not impacted by SI densities. Additional details regarding feeder head consumption are provided in Chapter 7.

Figure 6-12
Feeder average active power per SI function and SI density

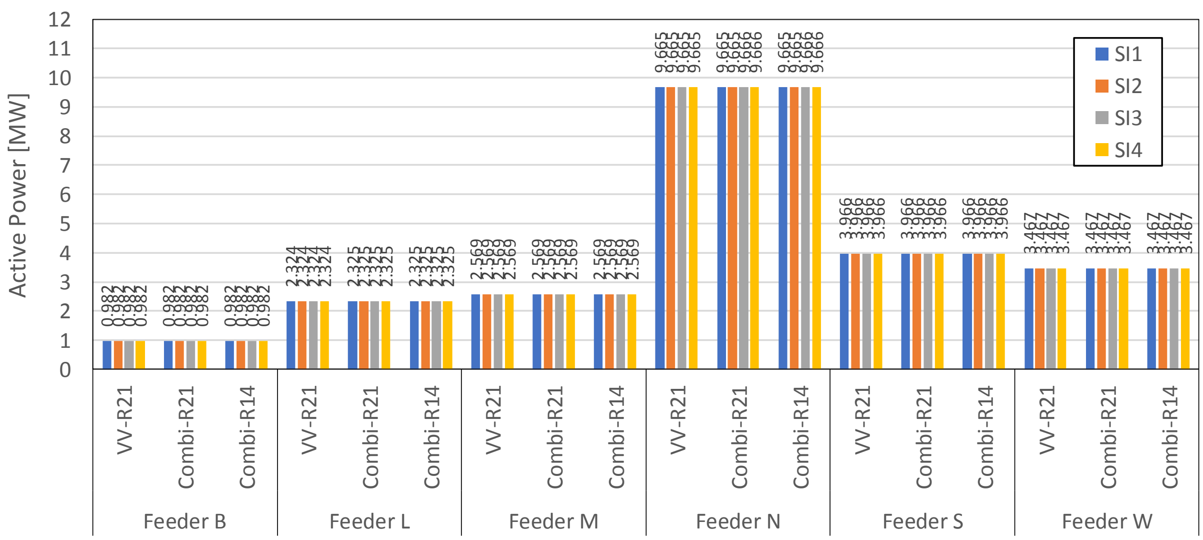

Figure 6-13
Feeder Average Reactive Power Per SI Function and SI Density

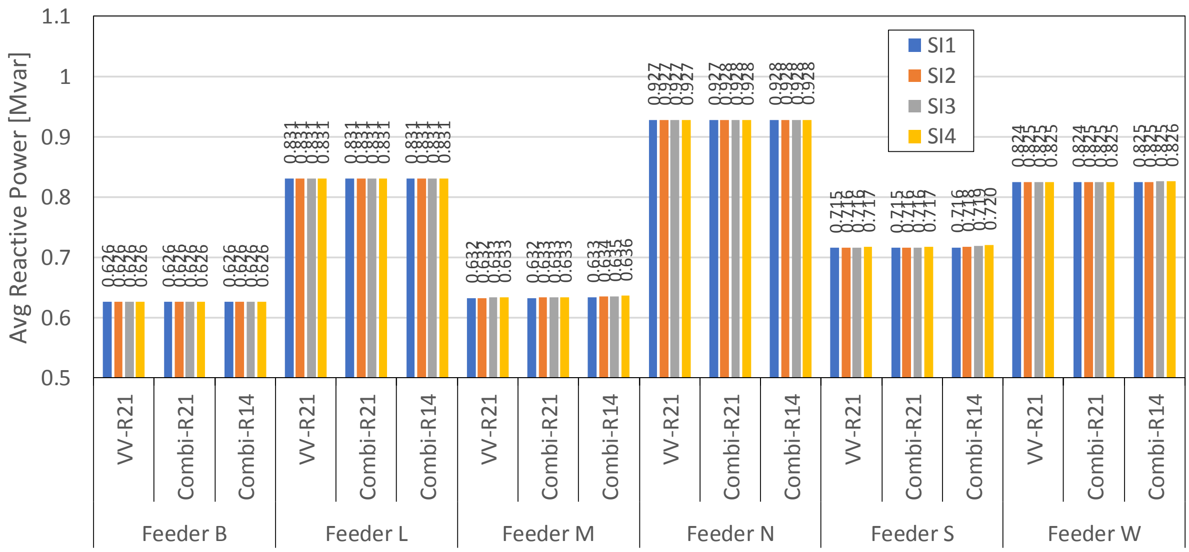

6.4 Smart Inverter Impacts on Active Power Generation

The activation of SI functions can result in reducing the active power output of PV systems. This in turn can potentially impact the electricity bills of PV customers. The impact of SI functions on active power generation was therefore carefully studied. Specifically, the PV generation recorded in QSTS simulations when conventional upgrades were implemented was compared to the PV generation recorded when smart functions were activated.

This comparison process was performed for each PV generation device as follows:

- First, for each daily QSTS simulation scenario, the total active energy generated over 24 hours by each PV inverter (in kWh) was calculated from power monitors configured in OpenDSS.
- Second, for each PV system, the total daily energy generated when smart functions were activated was subtracted from the total energy generated when conventional upgrades were implemented. This resulted in an energy difference (in kWh and %) for each PV customer with smart inverter in each QSTS simulation.
- Finally, the resulting set of differences was analyzed for each customer using descriptive statistics for each QSTS simulation. In particular, the *maximum* and a set of *percentile values* were calculated over the energy differences of all customers in each QSTS simulation. This resulted in a maximum and a set of percentile values of the energy differences (in kWh and %) for each of the 12,960 QSTS simulations.

To visualize the results from the process above, QSTS simulations were first grouped per feeder, SI function, and SI density. Then, the maximum values of the QSTS simulation maximum or percentile energy differences were obtained. Figure 6 14 shows the maximum (over all QSTS simulations in the group) of the 90th percentile values for QSTS simulations grouped per feeder, SI function, and SI density. Each column represents the maximum 90th percentile value for a group of 180 QSTS simulations.

Figure 6-14 shows the maximum value for the 90th percentile of energy difference (in %) categorized by SI functions and SI densities. Figure 6-14 shows that the daily energy difference (between smart inverter case and the conventional measure case) in always lower than 0.55%[86] when SI functions are activated, and can therefore be considered very small. The specific combination of SI functions selected, VV-R21, Combi-R21 or Combi-R14, appears to have little impact on the reduction of active energy generation; however, at higher smart energy densities assumed, the reduction of active energy generation appeared to be less severe.

Figure 6-14
Maximum Value for 90th Percentile of Active Energy Difference Per SI Functions and SI Density in 24-Hour Period

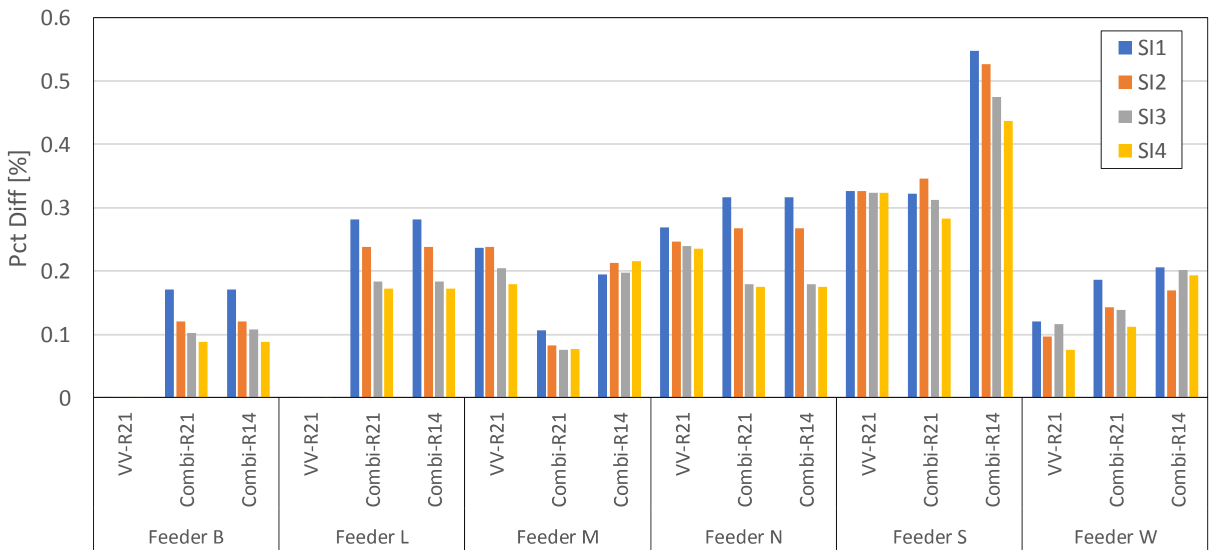

Figure 6-15 shows the maximum difference, *as well as* the maximum value for the 99th percentile, for the percentage of daily energy generation difference. The maximum of the 99th percentile differences was 1.85% meaning that 99% of the customers had differences ≤1.85% in all the QSTS simulations. On the other hand, the maximum difference was 4.83% indicating that there was at least one customer in one QSTS simulation with daily difference equal to 4.83%. The highest differences occurred on Feeder S and the differences were lower for the other feeders, as shown in Figure 6-15.

The maximum difference was obtained from simulation results for a customer at Feeder S with 100% PV penetration, 40% ES penetration, 75% SI density, average load profile, and PV profile A. While the most extreme 24-hour period PV curtailment resulted in a 4.83% reduction in kWh produced by the PV system, this same customer's annual PV curtailment resulted in only a 2.16% reduction in kWh produced.[87] The estimated annual PV generation for this customer is 9.45 megawatt-hour (MWh) when SI functions are activated, and 9.25 MWh when the conventional mitigation measures are deployed, leading to an annual PV curtailment of 204.3 kWh. However, for this customer, the estimated net

86 This reduction was obtained from simulation results over a 24-hour period.

87 The estimated annual generation was calculated based on the distribution of simulated days as described in Sections 8.3.1.and 4.2.1.

annual consumption increases only in 143.23 kWh, as the simulation results showed a slight reduction in power consumption when voltage magnitudes were reduced as a result of activating SI functions.[88]

Comparing Figure 6-14 and Figure 6-15, it appears that the maximum differences observed can be associated to a very small subset of PV customers, while the vast majority of PV customers only experienced a negligible power curtailment. Specifically, there are only 45 PV systems across all six feeders considered, connected to the distribution grid via 30 distinct service transformers, that experience a maximum daily curtailment over 1% across all PV and load profiles, PV and ES penetration levels, SI densities, and combinations of SI functions considered. These high curtailments are mainly caused by combi-R21 and Combi-R14. Only 10 customers experience a curtailment greater than 1% with VV-R21.

Figure 6-15
Maximum Value for 99th Percentile and Maximum Value of Active Energy Difference Per SI Functions and SI Density in 24-Hour Period

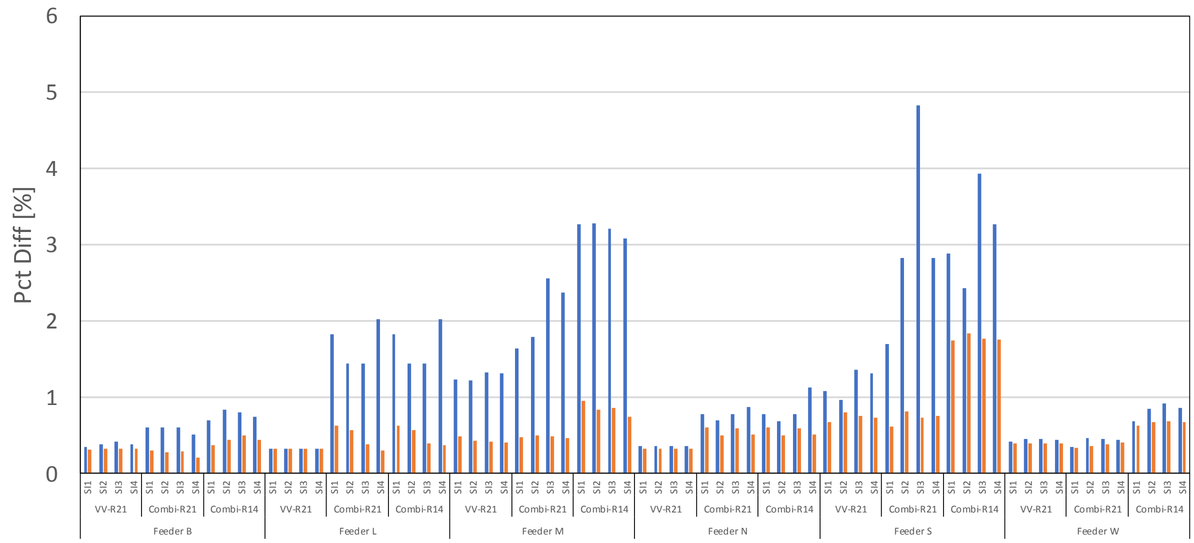

Additional detail on high curtailment examples and impacts has been included by the reconstruction of the annual PV generation based on the daily results described in this chapter. This analysis can be found in Chapter 8.

6.5 Smart Inverter Impacts on Inverter Utilization

The activation of SI functions may trigger the inverter to consume or generate reactive power. This can potentially increase the overall production of apparent energy, or “inverter utilization,” of a PV system. Increased inverter utilization could potentially reduce the inverter lifetime.[89] For this reason, this section analyzes PV inverter utilization with and without SI functions activated to assess the degree to which SI functions may increase inverter utilization.

---

88 In the OpenDSS models, the active power P depended linearly on the supply voltage, and the reactive power Q depended quadratically on the supply voltage. As a result, the net usage recorded for each customer directly depended on the supply voltage.

89 The impacts of increased inverter utilization to the inverter lifetime were out of the scope of this modeling effort.

Specifically, the daily apparent energy in kilo volt ampere hours (kVAh) was calculated across all PV installations when conventional upgrades are implemented (no smart functions), and when SI functions are activated. The difference between these two scenarios was calculated for each PV installation. This resulted in a difference (in kVAh and %) in inverter utilization between the case with SI functions and the case with conventional measures for each smart inverter (from hundreds to thousands) for each QSTS simulation. Then, the inverter utilization results were summarized analogously to the active power generation analysis shown in Section 6.4.

Figure 6-16 shows the maximum (over the group of QSTS simulations) of the 90th percentile values (daily inverter utilization differences in percentage) for QSTS simulations grouped per feeder, SI function and SI density. The activation of SI functions increased the daily inverter apparent energy by ≤0.3% for 90% of the customers across all QSTS simulations. This already small increase is even smaller at high SI densities. From Figure 6-16, the SI function combination, VV-R21, Combi-R21 or Combi-R14 does not appear to impact inverter utilization in any recognizable pattern that would apply for all the feeders.

Figure 6-16
Maximum Value for 90th Percentile of Apparent Energy Difference Per SI Functions and SI Density In 24-Hour Period

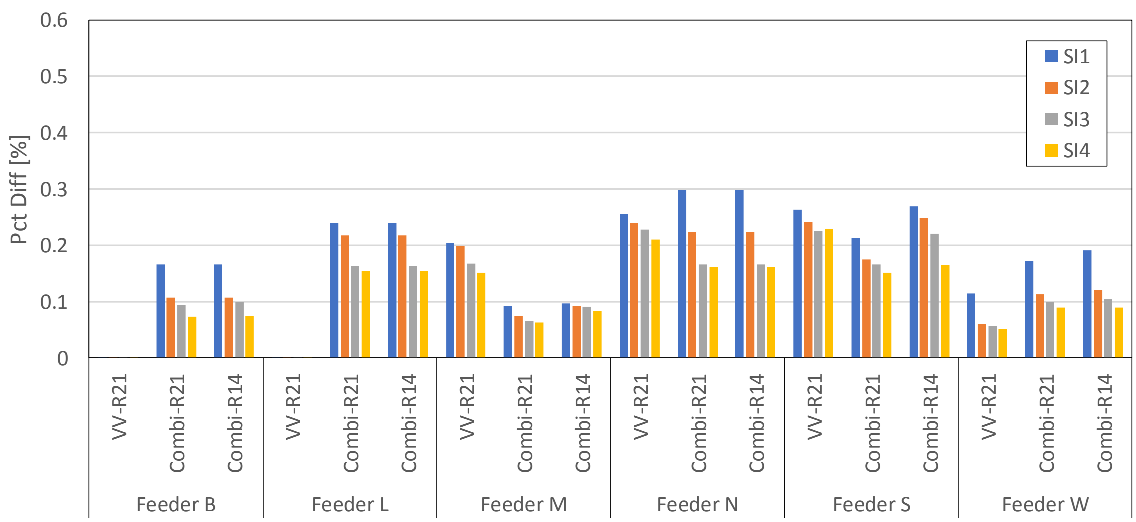

Figure 6-17 presents the *maximum* difference in smart inverter utilization, as well as the maximum values obtained for the 99th percentile. This metric shows that, when SI functions were activated, the increase in inverter utilization was ≤0.6% (of the inverter apparent energy without SI functions) for 99% of the customers in all the QSTS simulations. Results for the most extreme inverter utilization cases show that the maximum differences observed were always lower than 2.5% across all PV installations and QSTS simulations.

In conclusion, the simulation results obtained in this modeling effort suggest that the increase in inverter utilization can be considered negligible for the vast majority of PV inverters.

Figure 6-17
Maximum Value for Percentile 99th and Maximum Value of Apparent Energy Difference Per SI Functions and SI Density in 24-Hour Period

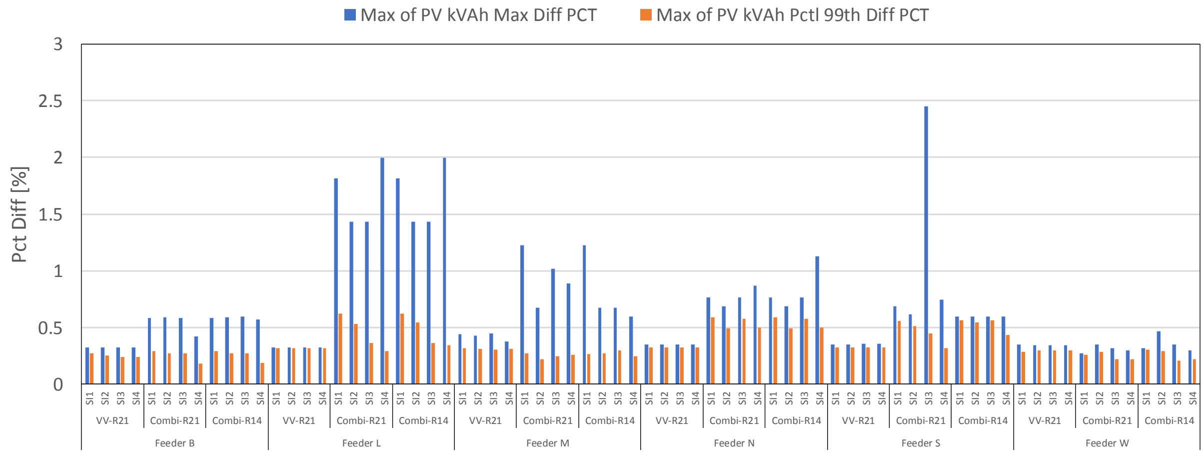

6.6 PV Wiring Sensitivity Analysis

Throughout this modeling effort, voltage conditions were always evaluated using system models that assume that the PV generation is interconnected *directly* at the customer service entrance. This assumption is consistent with the approach traditionally assumed when analyzing secondary circuits in the context of ANSI C84.1, where the service voltage limits are defined at the point where the electrical system of the user and the electrical system of the supplier are connected.

However, SI functions traditionally operate based on the voltage magnitude as measured *at the inverter terminal*, as opposed to the customer service entrance. Therefore, if the impedance between the PV inverter and the customer service entrance is large, there could be a notable voltage difference between the smart inverter terminal and the customer service entrance, resulting in potential differences between the way smart functions are expected to operate, and the way they actually operate.

This section investigates the impact of PV wiring (i.e., the wiring between the inverter terminal and the customer service entrance) on the operation of autonomous SI functions. This analysis was performed on Feeder M. This feeder was selected for displaying the most challenging conditions of voltage regulation at the MV level across the six feeders studied. This analysis was performed assuming the maximum PV penetration level (100% of residential customers), with no ES installations. The three load type days and five PV generation profiles described in Chapter 3 were considered.

6.6.1 Modeling Approach

Additional conductors were modeled to represent the PV wiring between the bus corresponding to the customer service entrance (to which the customer load model was otherwise directly connected), and the PV system terminal in OpenDSS (see Figure 5-18). The PV wiring characteristics were selected to represent an extreme scenario of voltage difference: for each individual PV installation, the impedance of the conductor added was selected to provide a 3% voltage rise at the PV inverter generation peak. All analysis performed in this section is based on the 3% voltage rise bookend assumption. In practice, field installations would likely include a wide range of design criteria, leading to a diversity of voltage rise magnitudes observed at peak generation. The goal of the 3% voltage rise assumption is to simply illustrate the impacts of PV wiring in a worst-case scenario.

Figure 6-18
Inclusion of Additional Conductors (PV Wires) in the Simulation Model

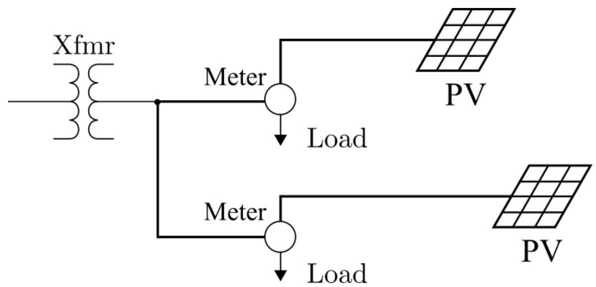

The PV wiring impedance was calculated considering a conservative constant R/X ratio equal to 5. Figure 6-19 shows the distribution of PV wire impedances (in Ohms) calculated for the 1,632 PV systems connected to Feeder M.

Figure 6-19
The Number of PV Systems With a Given Range of PV Wire Impedance

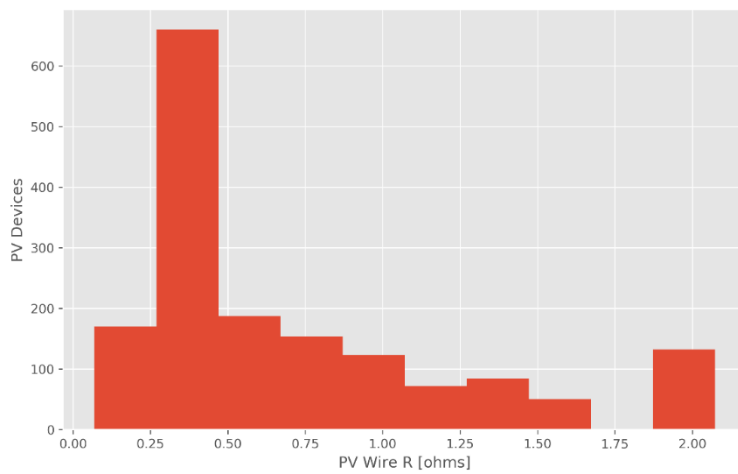

6.6.2 Simulation Results for the PV Baseline and Conventional Upgrades Scenarios

Simulation results show that PV wiring had no significant influence on the voltage violations recorded when SI functions were *not* activated. This conclusion was obtained by analyzing the change in occurrence and severity of voltage violations when properly modeling PV wiring, compared to scenarios where the PV terminal is modeled as directly connected to the point of connection. This analysis was conducted across the three load profiles and five PV generation profiles previously introduced.

Note that the voltages at the PV systems were not considered when determining voltage violations, since according to ANSI C84.1, the utility is responsible for maintaining the customer service voltages within the specified ranges. Although ANSI C84.1 specifies ranges for the utilization voltages, they are the facility (i.e., the customer) responsibility. For this reason, the utility is not responsible for maintaining the voltages at the PV systems behind the PV wires within a particular range.

Figure 6-20 shows, for an example PV system, the maximum and minimum voltages recorded for a given QSTS simulation. This specific simulation assumes the peak load profile, and PV generation profile A (sunny summer day). Figure 6-20 includes the extreme voltage magnitudes at the medium voltage level, and the extreme voltages at the meter location. For the reasons discussed above, PV voltages, which reflect the voltage rise over the PV wires, are not included in Figure 6-20. These results show that, as expected, the magnitudes obtained for the maximum and minimum voltages are similar whether PV wiring was considered in the models, or not.

Figure 6-20
Voltage Results at Peak Load Day With PV Generation Profile A Before (Left) and After (Right) Inclusion of PV Wiring

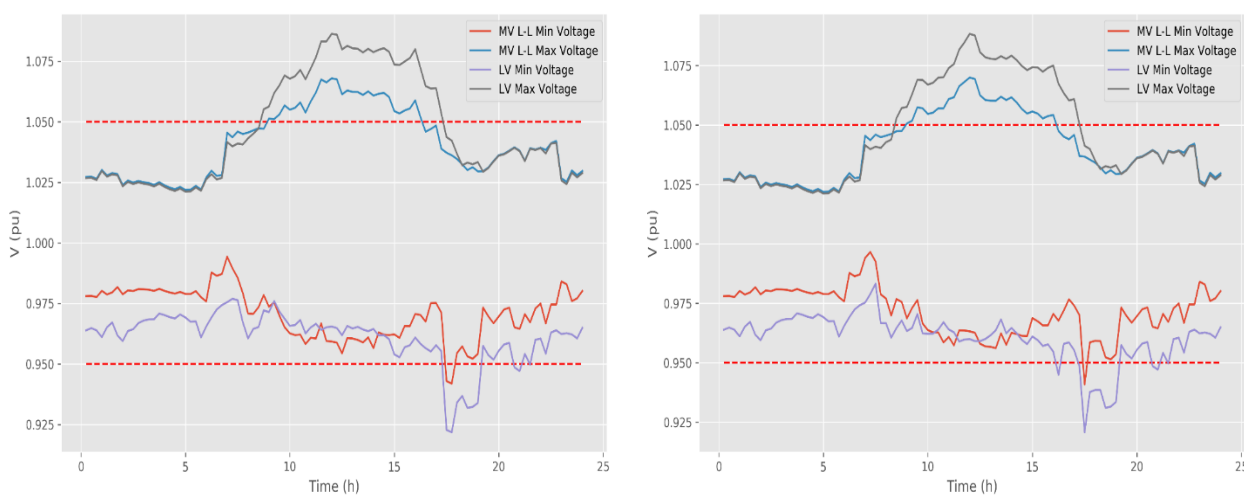

The following metrics were analyzed across 15 QSTS simulations (corresponding to all combinations across three load profiles and five PV generation profiles):

- Count of voltage violations
- Maximum and minimum voltages
- Maximum voltage violation durations
- Maximum percentage of buses affected
- Overloaded elements count

- Maximum overload duration
- Maximum percentage of overload magnitude

The differences in these metrics (with and without the inclusion of PV wires) were analyzed in detail. However, since there were only minor differences, PV wiring seemed to have no major influence on these results, either for the baseline PV assessment, or with the conventional upgrades.

For example, Figure 6-21 shows the comparison for the percentage of buses affected by voltage violations at MV and LV levels, before and after including PV wires. The figures are very similar. In other words, PV wiring has not had a major impact on the voltage violations in this particular case.

Figure 6-21
Percentage of Buses With Voltage Violation at Peak Load Day With PV Generation Profile A Before (Left) and After (Right) Inclusion of PV Wiring

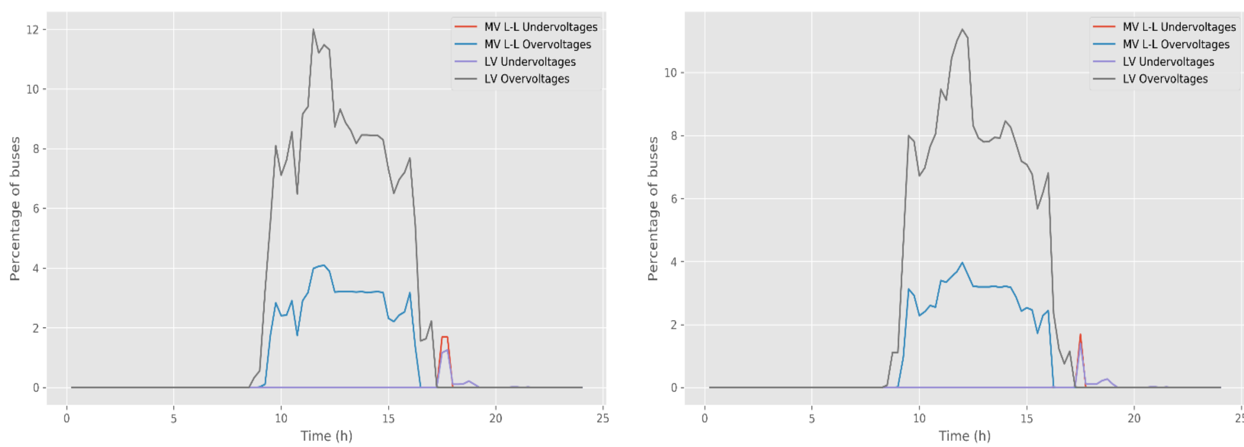

On the other hand, simulation results indicated a minor tendency of PV wires reducing the severity of overload conditions. A detailed analysis of this phenomenon has shown that the increment in losses related to the PV wiring (see left side of Figure 6-22) lead to a slight reduction in the current flow through the service transformers,[90] resulting in less severe overload conditions. Additionally, this reduction of exported power resulted in a slight difference in the tap selection from voltage regulators.

The right side in Figure 6-22 shows the difference in tap selection for the eleven voltage regulator controllers on the feeder of interest. As can be seen, there are two types of discrepancies in the tap selection (p.u.) from simulations with and without the PV wiring. First, the regulator controllers have shown some instances of delayed response to change the tap selection. This delay can be observed by the three spikes that imply a delayed operation of one-time step. Second, the tap selections in certain controllers have a steady-state difference of ±1 tap during the PV export time. Simulation results show that this minor difference in the voltage regulation at the MV level is the main factor of the slight change perceived by voltage violations metrics at the secondary circuits.

[90] Service transformers were the only elements that experienced overload conditions in both, PV baseline scenarios and conventional measurements scenarios.

Figure 6-22
Example of Differences From PV Wiring. Active Power Losses (Left) and Tap at Voltage Regulators (Right)

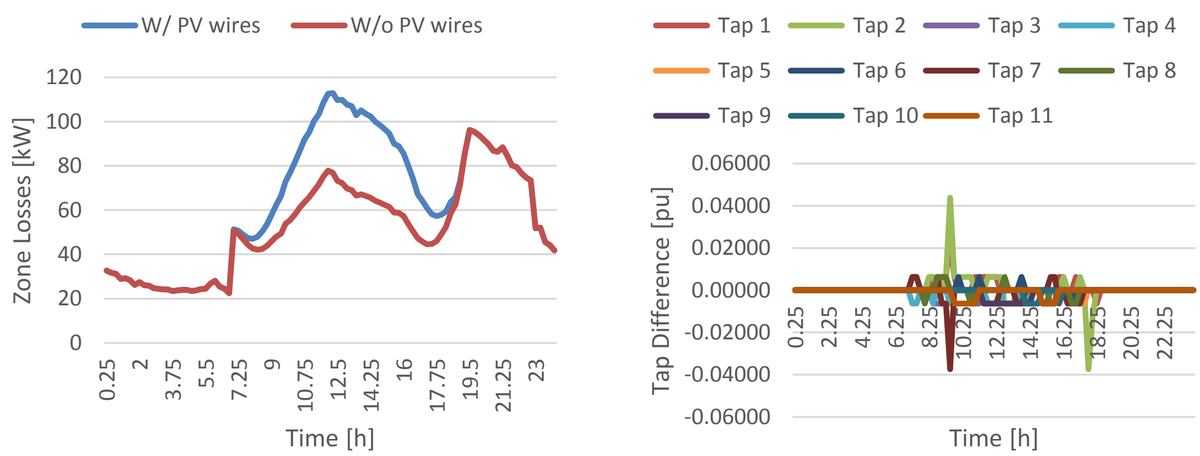

6.6.3 *Simulation Results With Smart Inverter Functions*

This section analyzes the impact of PV wiring on the voltage violations when smart functions are activated. A smart inverter density of 100% was assumed. Results are compared to scenarios relying on conventional upgrades (i.e., no smart functions activated).

The simulation results obtained from the 45 QSTS simulations[91] show that the additional voltage rise due to the PV wiring impedance tended to *increase* the smart inverter effectiveness at addressing overvoltage conditions. In contrast, results for undervoltage conditions were not significantly affected as expected.

Figure 6-23 shows the comparison of simulation count with at least one overvoltage condition (left) and at least one undervoltage condition (right) when PV wiring is included. The reduction in overvoltage case count, seen in Figure 6-23, is particularly noticeable for Combi-R14, where a larger reactive compensation was provided at higher voltage magnitudes. PV wiring was also observed to result in short overvoltage durations and fewer buses affected by overvoltages.

---

[91] These 45 QSTS simulations cover all the combinations with three load profiles, five PV generation profiles, and three combinations of smart inverter functions (VV-R21, Combi-R21 and Combi-R14).

Figure 6-23
Comparison of Case Count for Overvoltage (Left) and Undervoltage (Right) Conditions Per SI Function

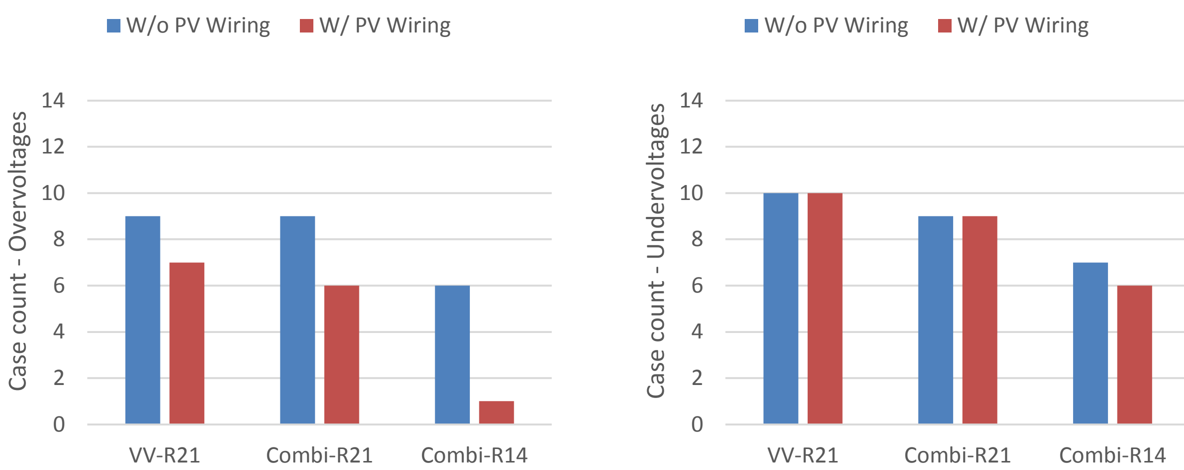

While simulation results show an increased effectiveness at addressing overvoltage conditions, results also show a tendency for increased curtailment of active power generation. Figure 6-24 shows the maximum percentage difference in active power generation classified by percentiles, to compare scenarios with and without PV wiring. Focusing on Combi-R14, the maximum active power curtailment observed in 90% of the cases recorded increased from 0.07% to 1% when PV wiring was included. These higher percentiles reflect increased curtailment. The same trend was observed for Combi-R21, where the maximum active power curtailment observed in the 24-hour period increased from 0.96% to 9.05% when PV wiring was included. Note that these values reflect the maximum curtailment that at most 10% of the customers exceed during the worst-case load day, PV day, and SI function. Annual PV curtailment would likely be significantly lower.

The maximum difference was obtained from simulation results for a customer with MIN load profile, and PV profile A. While the most extreme 24-hour period PV curtailment resulted in a 9.05% reduction in kWh produced by the PV system, this same customer's annual PV curtailment resulted in only a 1.41% reduction in kWh produced.[92] The estimated annual PV generation for this customer is 13.83 MWh when SI functions are activated, and 14.03 MWh when the conventional mitigation measures are deployed, leading to an annual PV curtailment of 198.49 kWh. For this customer, the estimated net annual consumption increases in 196.87 kWh, as the simulation results showed a minimal reduction in power consumption when voltage magnitudes were reduced as a result of activating SI functions.[93]

---

92 The estimated annual generation was calculated based on the distribution of simulated days as described in Sections 8.3.1.and 4.2.1.

93 In the OpenDSS models, the active power P depended linearly on the supply voltage, and the reactive power Q depended quadratically on the supply voltage. As a result, the net usage recorded for each customer directly depended on the supply voltage.

Figure 6-24
Difference in Active PV Power Generation (Curtailment) for Percentiles 90th, 99th, and 100th Due to the Inclusion of PV Wiring Models (24-Hour Period)

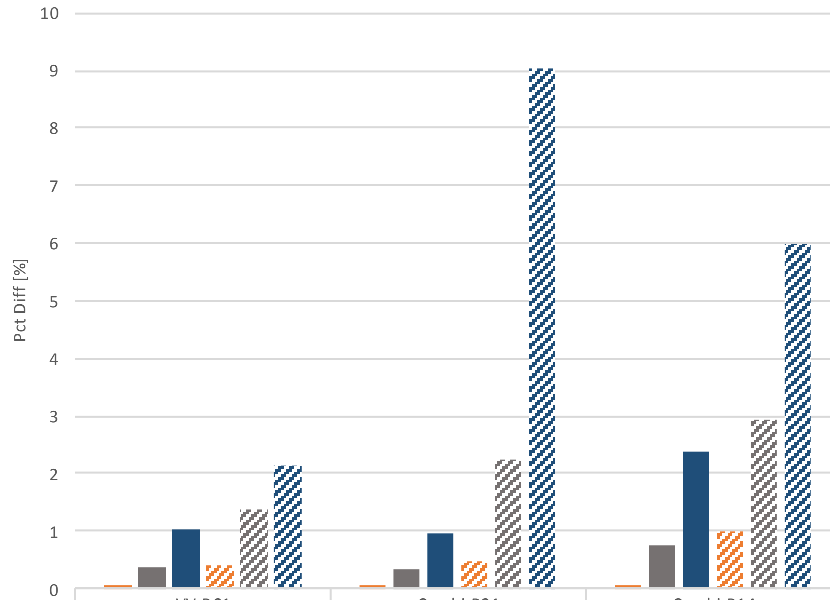

	VV-R21	Combi-R21	Combi-R14
W/o PV Wiring - Max of PV kWh Pctl 90th Diff PCT	0.04	0.05	0.07
W/o PV Wiring - Max of PV kWh Pctl 99th Diff PCT	0.36	0.33	0.75
W/o PV Wiring - Max of PV kWh Max Diff PCT	1.02	0.96	2.37
W/ PV Wiring - Max of PV kWh Pctl 90th Diff PCT	0.39	0.46	1.00
W/ PV Wiring - Max of PV kWh Pctl 99th Diff PCT	1.39	2.24	2.92
W/ PV Wiring - Max of PV kWh Max Diff PCT	2.13	9.05	5.97

The impact of PV wiring on inverter utilization was also analyzed, tracking potential differences in apparent energy generation across all the PV installations when PV wiring was added to the models. This analysis covered the three load profiles and five PV profiles considered.

Results show that PV wiring does not significantly impact smart inverter utilization (Figure 6-25). Specifically, for VV-R21, in all the QSTS simulations, 90% of the customers experienced an inverter utilization increase ≤0.25%. For Combi-R14, results actually show a *reduction* in inverter utilization. Combi-R21 saw the maximum difference in percentage observed, with a significant inverter utilization increase of 5.01%.

Figure 6-25
Difference in Apparent PV Power Generation (Utilization) for Percentiles 90th, 99th, and 100th Due to the Inclusion of PV Wiring Models (24-Hour Period)

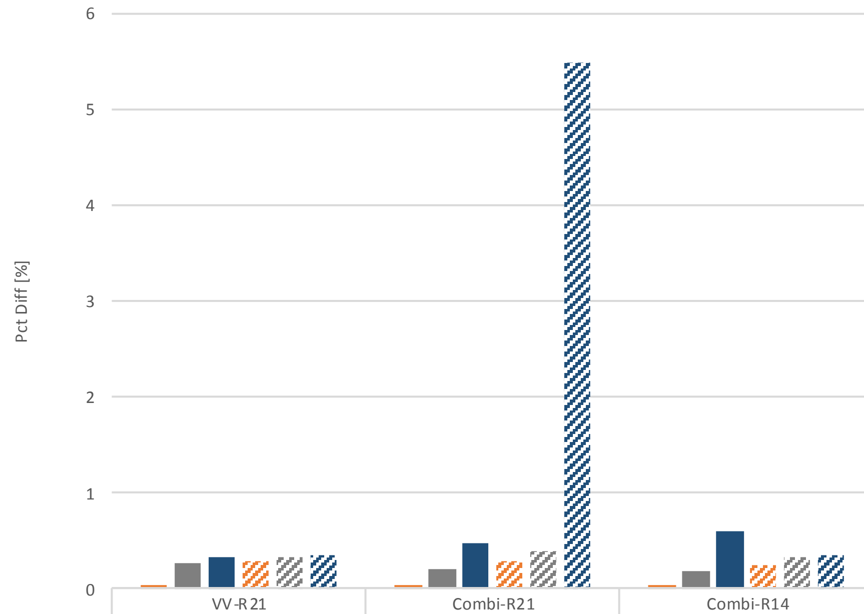

	VV-R21	Combi-R21	Combi-R14
W/o PV Wiring - Max of PV kVAh Pctl 90th Diff PCT	0.04	0.04	0.04
W/o PV Wiring - Max of PV kVAh Pctl 99th Diff PCT	0.27	0.19	0.18
W/o PV Wiring - Max of PV kVAh Max Diff PCT	0.32	0.48	0.60
W/ PV Wiring - Max of PV kVAh Pctl 90th Diff PCT	0.29	0.28	0.25
W/ PV Wiring - Max of PV kVAh Pctl 99th Diff PCT	0.32	0.39	0.32
W/ PV Wiring - Max of PV kVAh Max Diff PCT	0.35	5.49	0.35

6.7 Conclusions

The objective of this chapter was to determine the impacts of SI functions on the distribution system operations. The areas of focus included: v oltage conditions, equipment overloads, changes in the feeder head power consumption, and potential changes impacting the PV generation. QSTS simulations were conducted, covering all three combinations of functions, VV-R21, Combi-R21 and Combi-R-14, and all four SI densities considered. This set of scenarios was evaluated across all five PV generation conditions listed in Chapter 3, resulting in a total of 12,960 daily QSTS simulations over the six feeders, with up to 2,879 SI devices in a single feeder model. These simulations were performed in OpenDSS, where the OpenDSS built-in inverter control algorithm was customized to properly simulate the combined operation of Volt-VAR and Volt-Watt functions, as defined in CA Rule 21 and HI Rule 14.

The simulation results obtained show that SI functions are effective at reducing the occurrences of overvoltage conditions. This reduction reflects the effectiveness of the reactive power consumption required by Volt-VAR functions at high voltage magnitudes. Additional details on the *severity* of overvoltage conditions are provided in Chapter 7.

On the other hand, SI functions had little to no impacts on undervoltage conditions across the six feeders considered. This at least partly resulted in from assuming that the SI functions were only available during the PV generation times, whereas (some of) the undervoltages occurred outside of PV generation times.

As expected, SI functions were observed not to be effective in mitigating overload conditions. No pattern was observed between the combinations of smart functions or the SI densities on one hand, and the duration of the overloads on the other hand. Moreover, the simulation results demonstrated the effectiveness of the PG&E replacement criteria to prevent overload conditions in service transformers as described in Chapter 5.

Smart inverter functions were shown to have no significant impact on the average active or reactive power at the feeder head. Accordingly, the daily energy supplied by the bulk system to the distribution feeders was not significantly impacted when the smart functions were activated.

Simulation results showed that active power curtailment was negligible most of the time. Specifically, activating SI functions resulted in the daily active energy generation lower than 0.55% for 90% of the PV customers across all QSTS simulations. Further, active power curtailment was showed to be reduced at higher SI densities. Only 45 PV installations across all the combinations and feeders considered reported a daily curtailment greater than 1% (over any of the 15 combinations of load and PV profiles).

The increase in inverter utilization was very small for a vast majority of the cases. Across all QSTS simulations, the increase in inverter utilization was lower than 0.6% for ≥99% of the PV customers.

While this modeling effort evaluated SI functions assuming that the PV terminal was directly interconnected to the metering location, the potential influence of PV wiring was analyzed in detail in this chapter, as SI operations could potentially be affected by a large impedance between the inverter terminal and the metering location. The analysis of PV wiring was performed separately on Feeder M, which had the most challenging voltage conditions across all the six feeders. PV wires were designed and incorporated in the models to reflect an extreme voltage rise of 3% at PV peak generation. QSTS simulations showed that PV wiring had no major influence on the results when SI functions were not activated (i.e., in baseline PV assessment and with conventional measures). In contrast, the inclusion of PV wiring slightly reduced the severity of overload conditions due to an increase in the secondary circuit losses. For scenarios with SI functions, simulation results showed that the additional voltage rise from PV wiring tends to increase the smart inverter effectiveness at addressing overvoltage conditions, while undervoltage conditions are not significantly affected. While there was a noticeable improvement in voltage conditions, simulation results also showed that PV wiring with sufficiently high impedance could increase the PV curtailment.

7

SMART INVERTER FUNCTIONS VS. CONVENTIONAL MEASURES: A COMPARISON OF PERFORMANCE

This chapter analyzes the effectiveness of two different strategies to mitigate impacts caused by increased PV penetration levels. The first strategy relies on conventional distribution system upgrades; the second strategy leverages SI functions. In this chapter, the two strategies are compared to each other, and to the baseline PV impact assessment shown in Chapter 4, to assess their respective performance.

This chapter builds on the results from the previous chapters as follows:

- Chapter 4, which provided a baseline PV impact assessment (no mitigation strategies considered apart from manual changes to voltage regulation equipment settings);
- Chapter 5, which analyzed the first strategy relying on conventional distribution system upgrades; and
- Chapter 6, which analyzed the second strategy leveraging SI functions.

In particular, this chapter compares the results from the large number of daily 15-min QSTS simulations performed that evaluated the impacts of increased PV penetration levels across a wide range of feeder conditions and other sensitivities illustrated in Figure 7-1:

- For the baseline PV impact assessment, and the strategy leveraging conventional upgrades, three daily load profiles, five daily PV profiles, five PV penetration levels (including 0%) and three ES penetration levels (including 0%) introduced resulted in a total of 1,080 individual QSTS simulations across the six feeders considered;
- When considering SI functions, two additional sensitivities were considered: the three combinations of smart functions (VV-R21, Combi-R21 and Combi-R14), and five SI densities (including 0%). This resulted in a total of 12,960 QSTS simulations. For simplicity, most of the comparison performed in this chapter is shown for the SI density of 100%. Additionally, a separate analysis is shown for the impact of different SI densities.

Figure 7-1
QSTS Simulation Results Compared in This Chapter

Baseline PV Assessment	Conventional Measure Analysis	Smart Inverter Analysis
Circuits: Feeder B, Feeder L, Feeder M, Feeder N, Feeder S, Feeder W Day types: Peak, Min, Avg PV day types: Summer sunny, winter sunny, overcast, changeable, cloudy PV penetration levels: 0% (PV0), 25% (PV1), 50% (PV2), 75% (PV3), 100% (PV4) ES penetration levels: 0% (ES0), 20% (ES1), 40% (ES2)		
SI density: n/a SI functions: n/a	SI density: n/a SI functions: n/a	SI density: 25%, 50%, 75%, 100% SI functions: VV-R21, Combi-R21, Combi-R14
Upgrades Considered: Voltage regulation setting changes	**Upgrades Considered:** Voltage regulation setting changes Additional voltage regulator (Feeder M) Thermal upgrades Voltage Rise upgrades	**Upgrades Considered:** Voltage regulation setting changes Additional voltage regulator (Feeder M) Thermal upgrades
1080 QSTS simulations	1080 QSTS simulations	12,960 QSTS simulations

This chapter is structured as follows. The first five sections compare the performance of the two strategies to the baseline assessment (in the figures referred to as the "Reference"), focusing on five distribution impacts caused by PV: overvoltages, undervoltages, voltage-rise violations, overload conditions, and feeder power and losses. The last section analyzes the impact of SI densities on the results.

As discussed in Chapter 4, a number of summary metrics, including maximum voltage, number of service transformers with voltage rise issues, etc., are recorded for each QSTS simulation. The figures in this chapter show various "composite metrics" that provide summary results for groups of QSTS simulations, such as the maximum voltage experienced in any simulation in the group. Note that in the following five sections, each figure is sorted by the feeder and PV penetration level (PV1-25%, PV2-50%, PV3-75%, and PV4-100% of residential customers) and that there are 45 QSTS simulations per PV penetration level per circuit. In the last section, some of the figures are sorted by the feeder and the SI density (as opposed to PV penetration). The impact of ES penetration level was also analyzed as a part of this modeling effort but the results are omitted from this chapter since no major impact and no clear trends were observed for any of the metrics analyzed in this chapter.

7.1 Overvoltage Conditions

For each feeder and each PV penetration level, Figure 7-2 shows the number of QSTS simulations recording significant overvoltage conditions. As defined in Chapter 4, an overvoltage or undervoltage condition was considered "significant" if its duration was over an hour, or if it affected more than 5% of the feeder buses.

Feeder S was the only feeder where overvoltage conditions were recorded in QSTS simulations at a PV penetration level of 25%; all other feeders only recorded overvoltage conditions for PV penetration levels at or above 50% (Figure 7-2).

Figure 7-2
Number of QSTS Simulations Recorded With Significant Overvoltage Conditions for Each Feeder

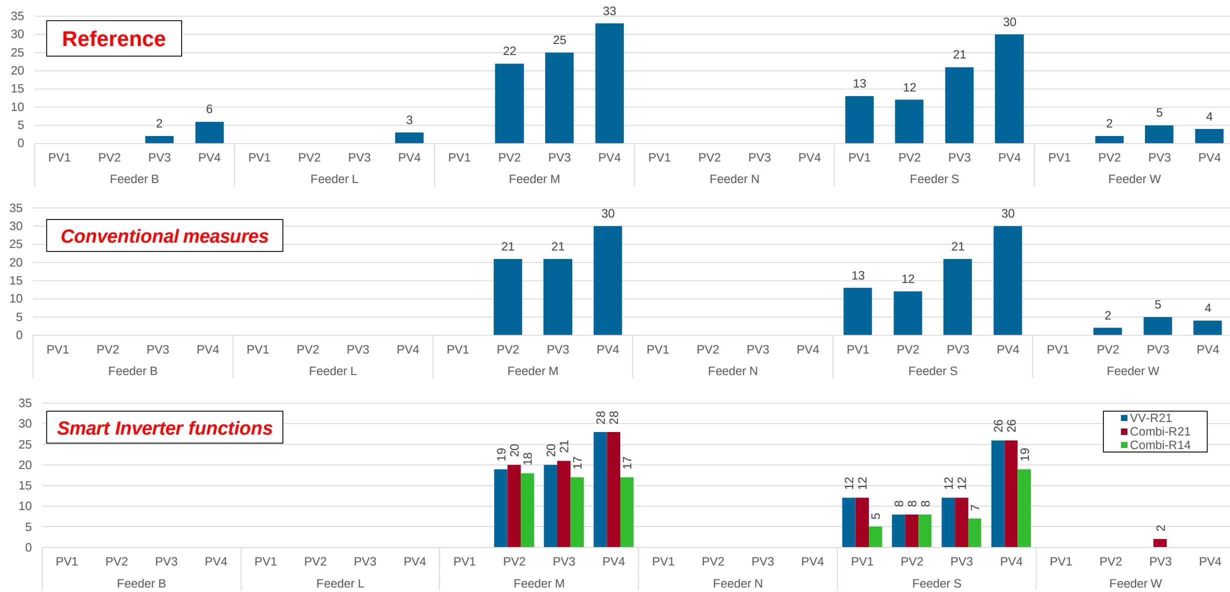

As discussed in Chapter 3, the baseline feeder models (without PV and ES systems) had no thermal or voltage violations. Therefore, all overvoltage conditions were caused by PV. As shown in Figure 7-3, no significant overvoltages were experienced at the MV level with the exception of Feeder M at PV2-PV4. The small increase in duration with SIs can be associated to the operation of voltage regulating equipment. In all other cases, all overvoltages occurred at the LV level, as illustrated in Figure 7-4.

Figure 7-3
Maximum Duration of Significant Overvoltages on the Medium Voltage System Reported in Hours

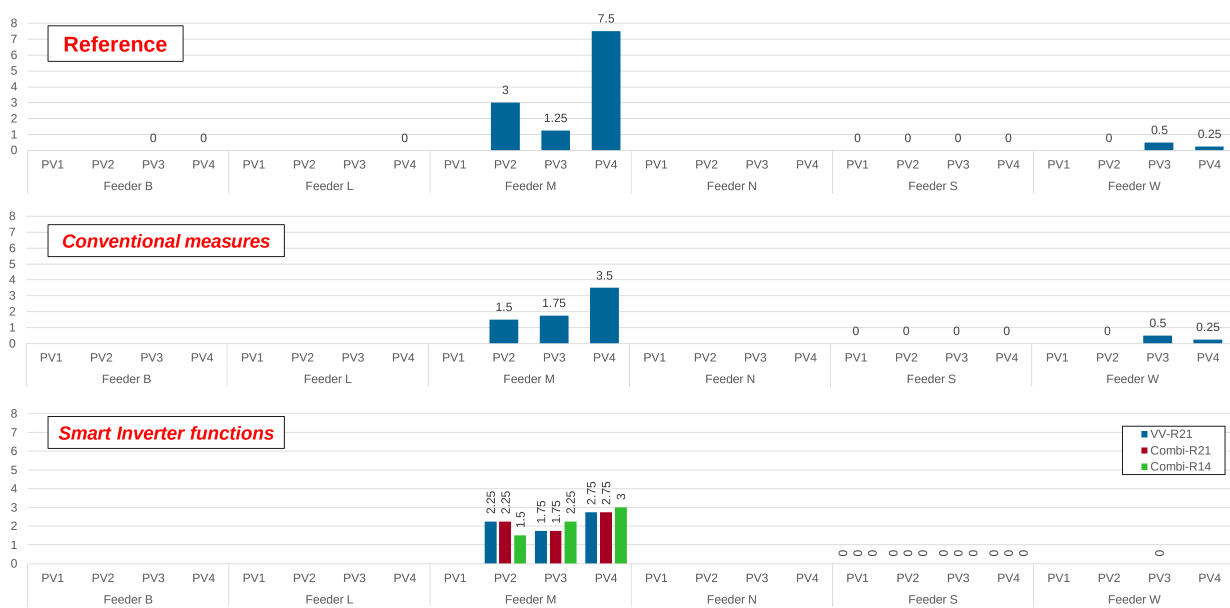

Figure 7-4
Maximum Duration of Significant Overvoltages on the Low Voltage System Reported in Hours

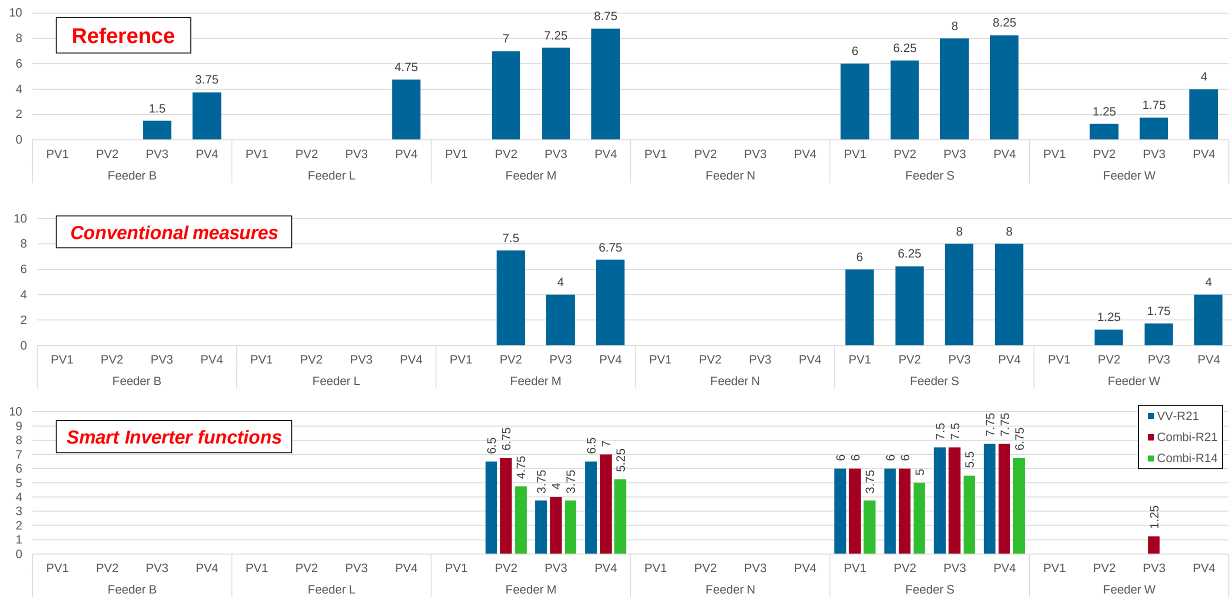

Based on the simulation results, SI functions were equally or more effective than conventional upgrades in reducing the overvoltage durations shown in Figure 7-4, the percentage of buses impacted by overvoltage conditions shown in Figure 7-5, and the number of transformers with downstream overvoltage conditions shown in Figure 7-6.

Only Feeder M, Feeder S, and Feeder W experienced overvoltages with conventional measures and/or SI functions. However, both PV impact mitigation strategies reduced the overvoltage magnitudes shown in Figure 7-7 and the number of buses affected by overvoltages as shown in Figure 7-5. On Feeder W, SI functions were more effective than conventional measures at addressing overvoltages, as seen in the reduced number of cases with significant violations shown in Figure 7-2, and the reduced duration of overvoltages shown in Figure 7-4. Feeders B and L did not experience overvoltage conditions with both SI functions and conventional measures.

Combi-R14 appeared to be marginally more effective at addressing overvoltage conditions, when compared to VV-R21 and Combi-R21. Indeed, the activation of Combi-R14 resulted in slightly reduced overvoltage magnitudes as shown in Figure 7-7, and lower maximum voltages, even at buses not experiencing overvoltage conditions. These trends are particularly visible on Feeder L and Feeder N.

Figure 7-5.
Maximum Percentage of Buses Affected by Significant Overvoltage Conditions

Figure 7-6.
Maximum Transformer Count With Secondary Overvoltages

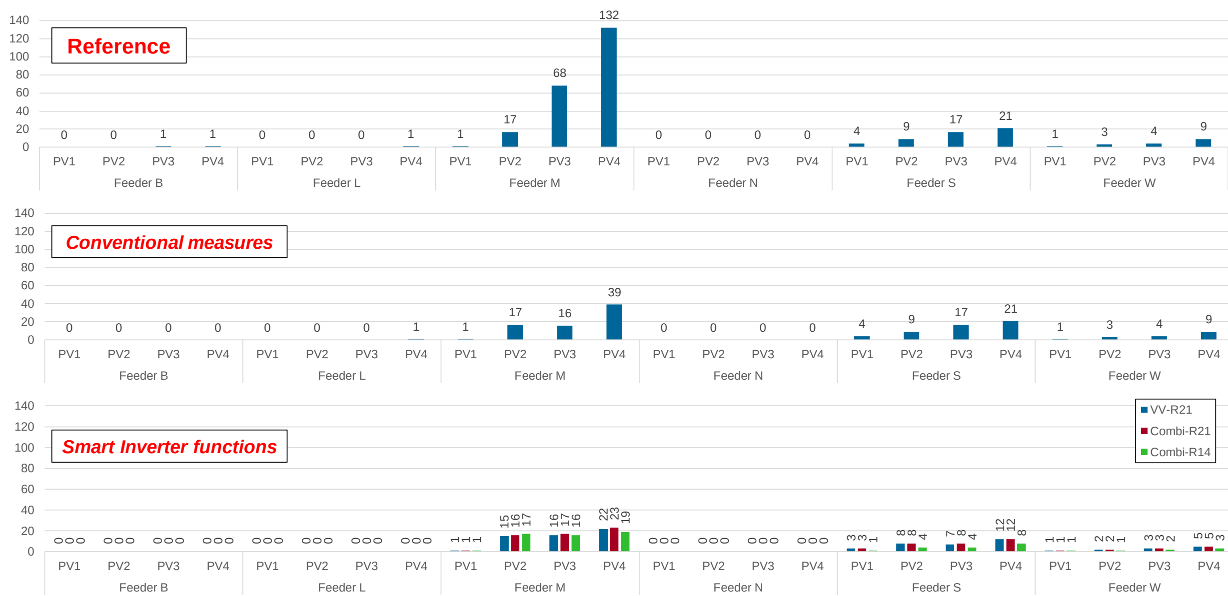

Figure 7-7.
Maximum Overvoltages on the Low Voltage System

7.2 Undervoltage Conditions

Figure 7-8 shows the number of QSTS simulations (out of 45 simulations) with significant undervoltage conditions (>1hr or >5% of buses). For a given PV penetration level, little to no improvements were observed when smart functions were activated. This result suggests that undervoltage conditions may occur outside PV generation hours, when PV was able to provide voltage support through consuming/ generating reactive power (PV inverters were assumed not to provide “VARs at night”). Somewhat more sever undervoltage conditions are observed at higher PV penetration levels as a result of the interplay between PV generation and feeder voltage regulation, and manual changes to the voltage regulation equipment settings.

Figure 7-8.
Number of QSTS Simulations With Significant Undervoltages

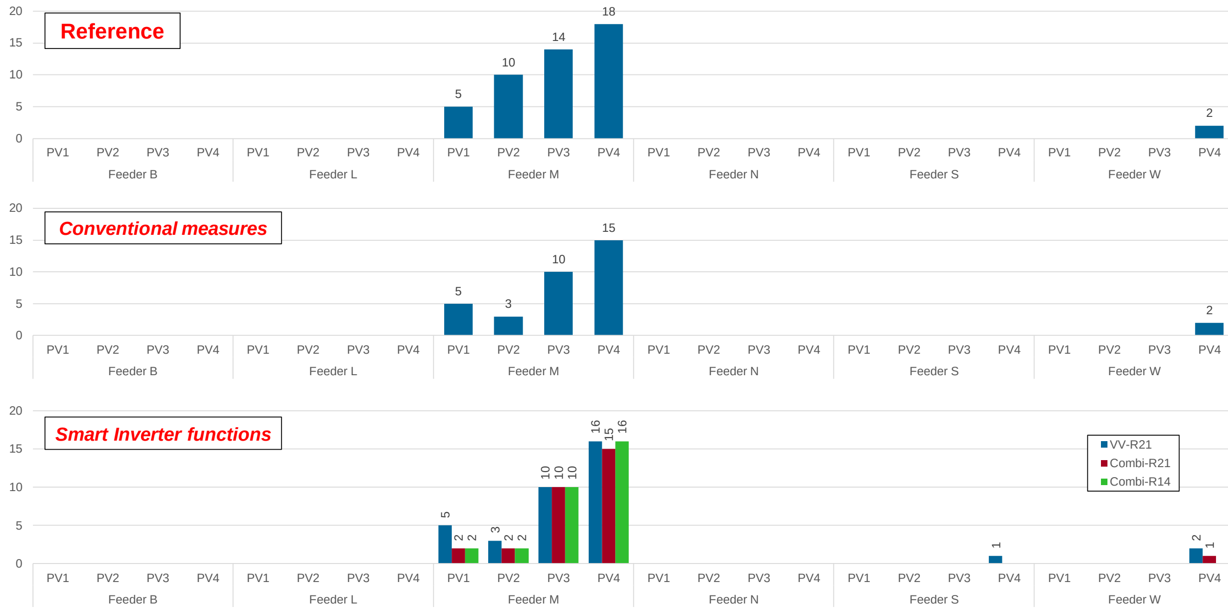

Compared to the baseline PV assessment, SI functions resulted in somewhat reduced undervoltage durations as shown in Figure 7-9. However, this improvement was also observed with the conventional measures. The reduction in overvoltages is likely associated with new voltage regulator introduced on Feeder M in PV penetration levels PV2-PV4, as opposed to the activation of SI functions. Moreover, as shown in Figure 7-10, the undervoltage durations at the secondary circuit level were similar between the SI functions and conventional measures indicating that SI functions did not mitigate undervoltages.

Figure 7-9.
Maximum Duration of Significant Undervoltages on Medium Voltage System Reported in Hours

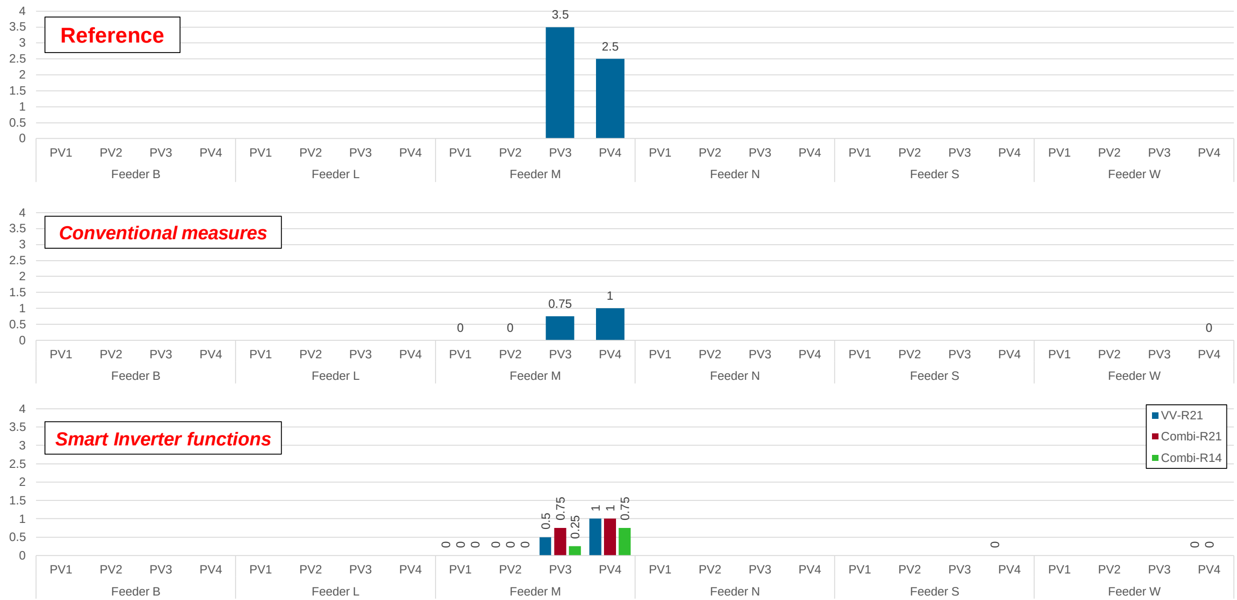

Figure 7-10.
Maximum Duration of Significant Undervoltages on Low Voltage System Reported in Hours

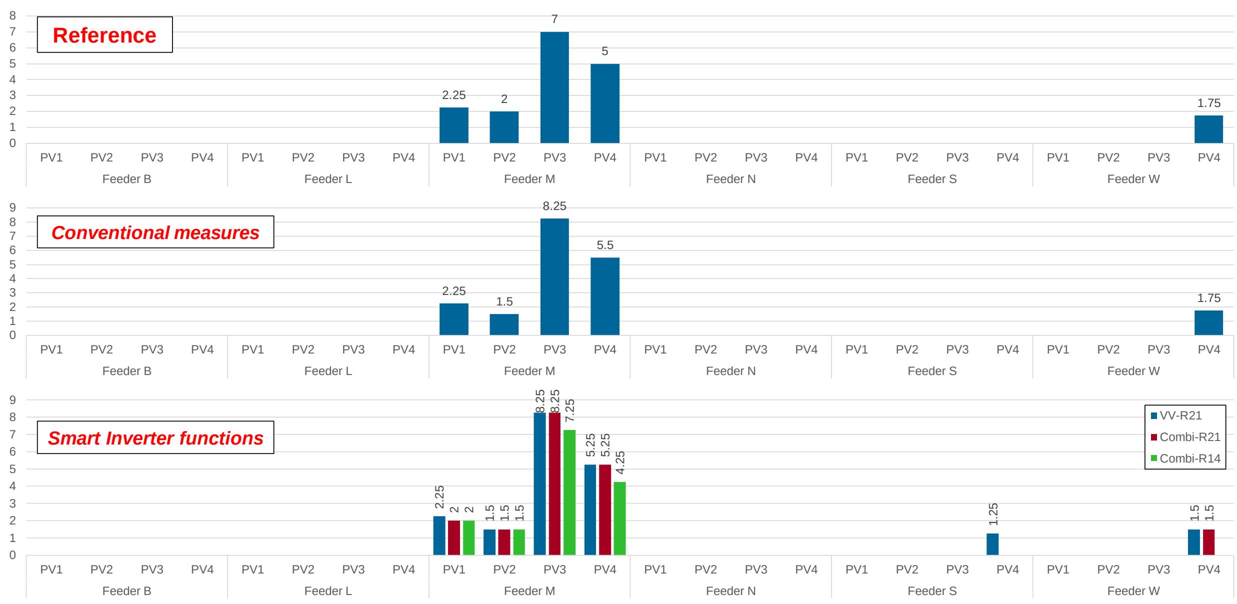

Aside from the maximum undervoltage durations, SI functions did not mitigate the undervoltage conditions as seen in the number of buses affected by undervoltages shown in Figure 7-11 or the lowest voltage magnitudes shown in Figure 7-12. Note also that there were no significant differences between the SI functions.

Figure 7-11.
Maximum Percentage of Buses Affected by Significant Undervoltages Conditions

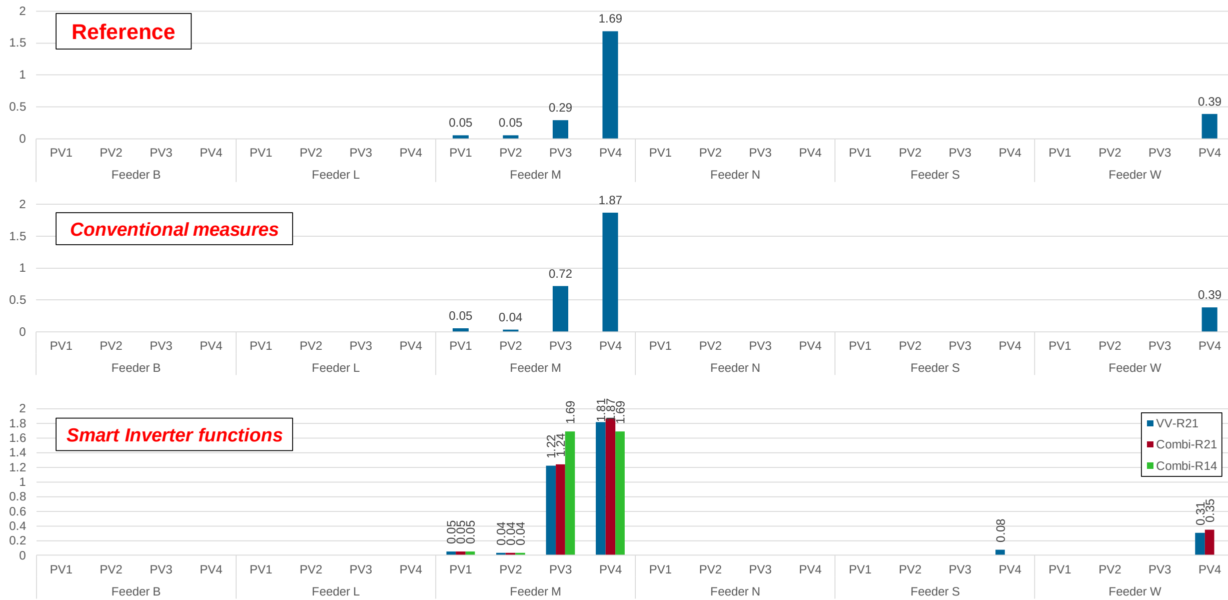

Figure 7-12.
Minimum Voltage at the Low-Voltage Level

7.3 Secondary Voltage Rise Violations

In this modeling effort, a key concern associated with the residential PV systems were overvoltages due to voltage rise particularly over the LV secondary circuits. At the time of this modeling effort, PG&E identified PV interconnections and secondary circuits subject to high voltage rise through a process that involved performing a secondary VRS if the total nameplate of PV on a transformer exceeded the transformer nameplate. This process is discussed in detail in Chapter 5.

Conventionally, any potential violations flagged during the secondary VRS would trigger replacing the associated service transformer and/or service lines. However, as discussed in Chapter 5, the process would not identify potentially high voltage rise when the aggregated PV inverter nameplate rating is lower than the service transformer nameplate rating, a condition required to trigger the secondary VRS. On the other hand, SI functions, although not their primary objective, could reduce the secondary voltage rise avoiding the need for equipment replacements. The QSTS simulation results discussed in this section analyzes how effective the conventional upgrades and the SI functions were in mitigating secondary voltage rise issues.

Based on the simulation results, neither conventional measures nor SI functions were able to address all voltage rise violations. As shown in Figure 7-13, some QSTS simulations with one or more voltage rise violations still occurred with both approaches at different PV penetration levels. Results from enabling SI functions appeared to provide small improvements across all PV penetration levels but were not able to address extreme voltage rise conditions.

Figure 7-13.
Number of QSTS Simulations With Secondary Voltage Rise Issues

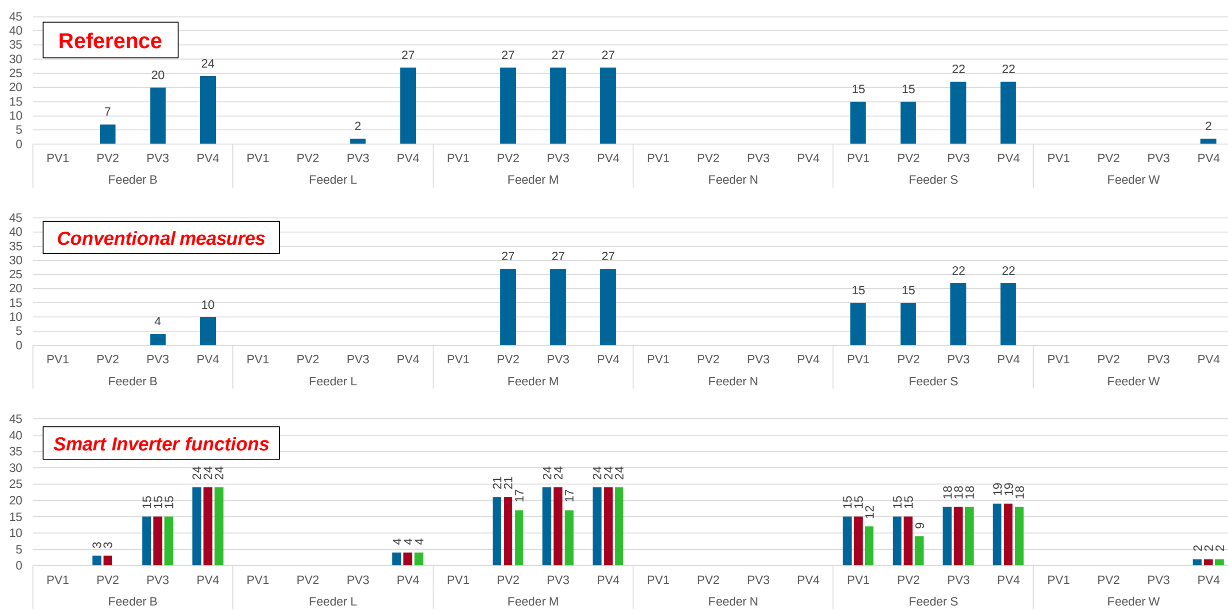

SIs functions reduced the maximum voltage rise magnitudes, but did not typically outperform the conventional measures as shown in Figure 7-15. There were, however, cases where SIs performed better (e.g., Feeder S in Figure 7-15). Note also that while SI functions directly reduce voltage, they only indirectly reduce secondary voltage rise. Compared to VV-R21 and Combi-R21, Combi-R14 function resulted in marginally lower voltage rise (see Chapter 5 for additional discussion).

Figure 7-14.
Maximum Count of Transformers With Voltage Rise Violations (Above PG&E Guidelines)

Figure 7-15.
Maximum secondary voltage rise violations (above PG&E guidelines)

7.4 Overload Violations

As discussed in Chapter 6, the SI functions considered in this modeling effort are not effective in addressing thermal violations created by PV systems. Thus, conventional upgrades due to thermal violations were considered both with and without SI functions. As a result, the QSTS simulation results for thermal violations were very similar between conventional measures and SI functions as shown in Figure 7-16. For both approaches, the thermal violations were minimal both in terms of magnitude (<4%) and duration (<1hr) as shown in Figures 7-17 and 7-18. Moreover, these violations were isolated cases as shown by the number of elements with thermal violations (Figure 7-19). Consequently, there were no distinctions between specific SI functions.

Figure 7-16.
Number of QSTS Simulations With Overload Conditions

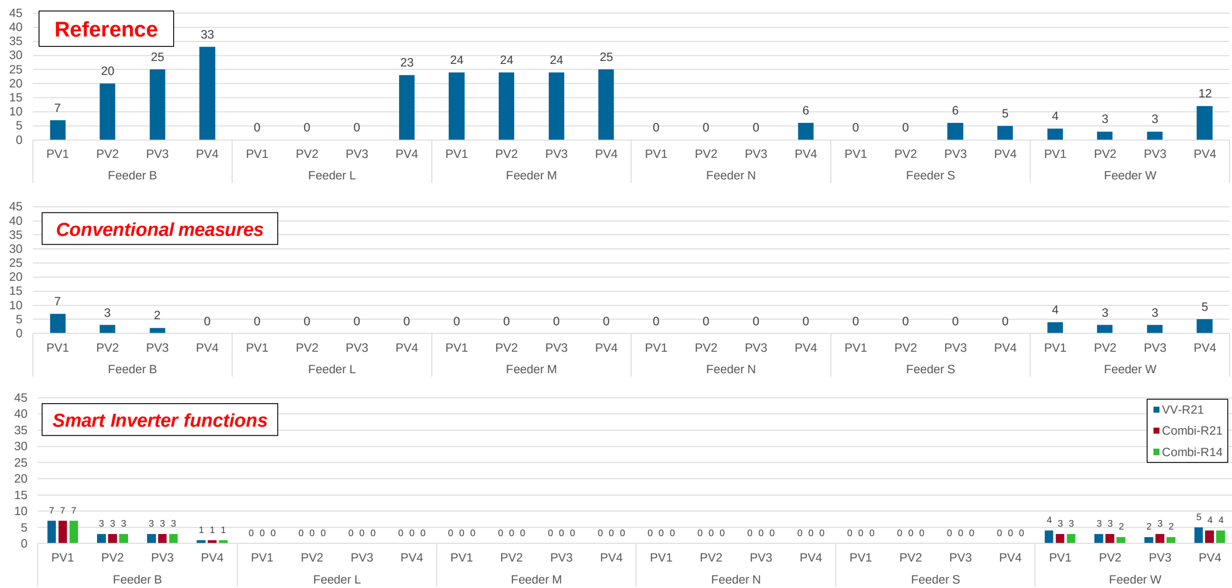

Figure 7-17.
Maximum Duration of Overloads Reported in Hours

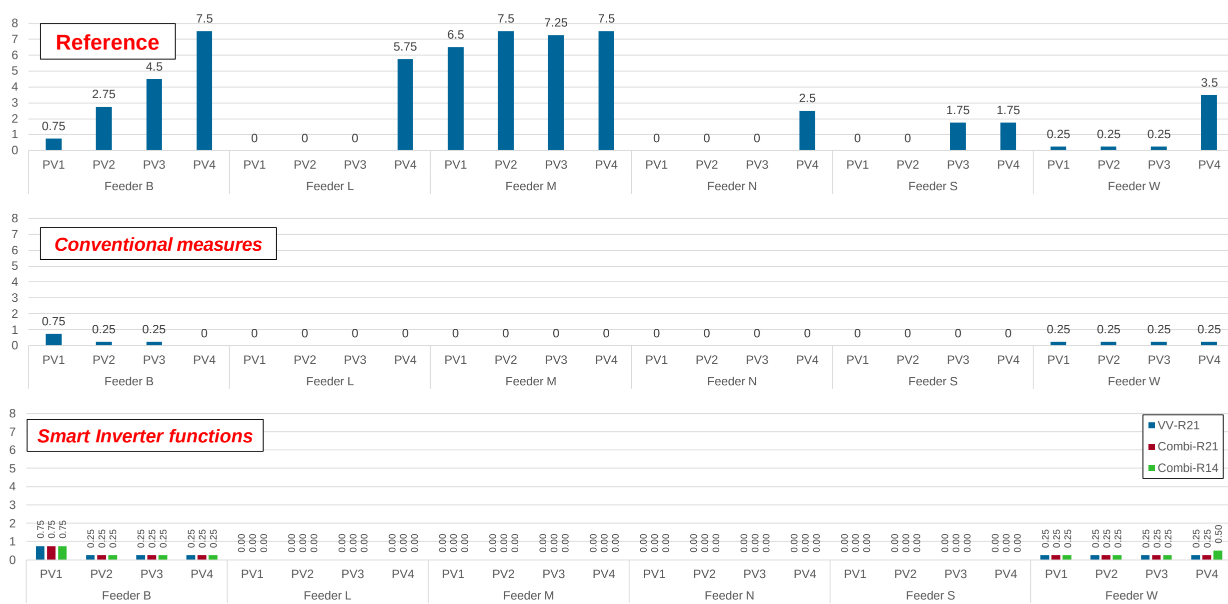

Figure 7-18.
Maximum Magnitude of Overloads Reported in Percentage

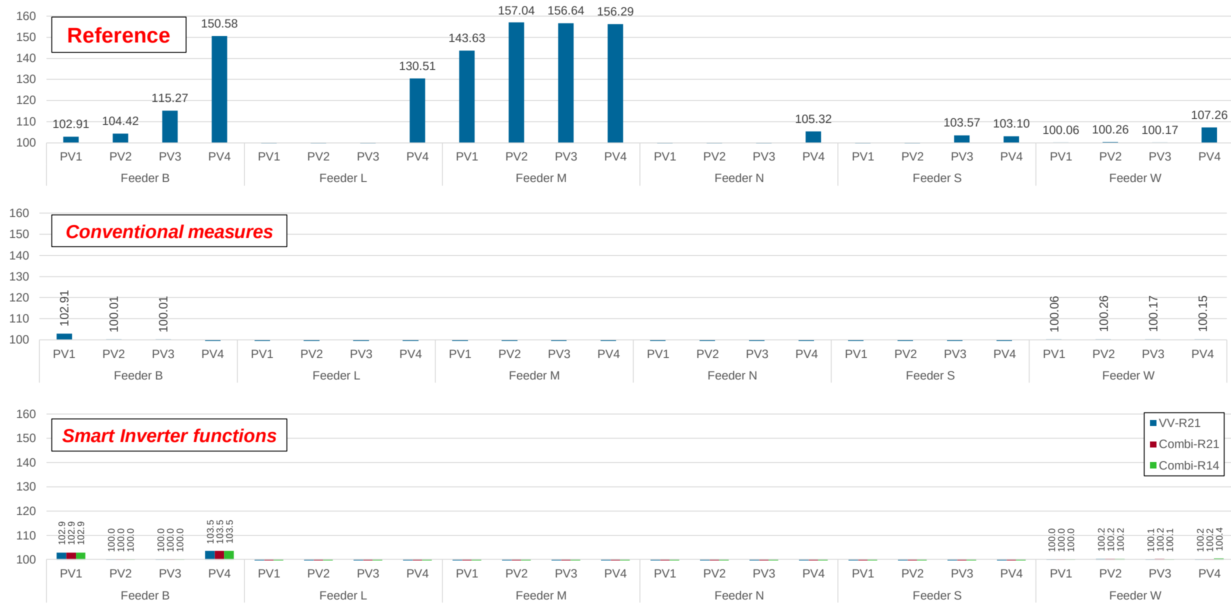

Figure 7-19.
Maximum Number of Overloaded Elements

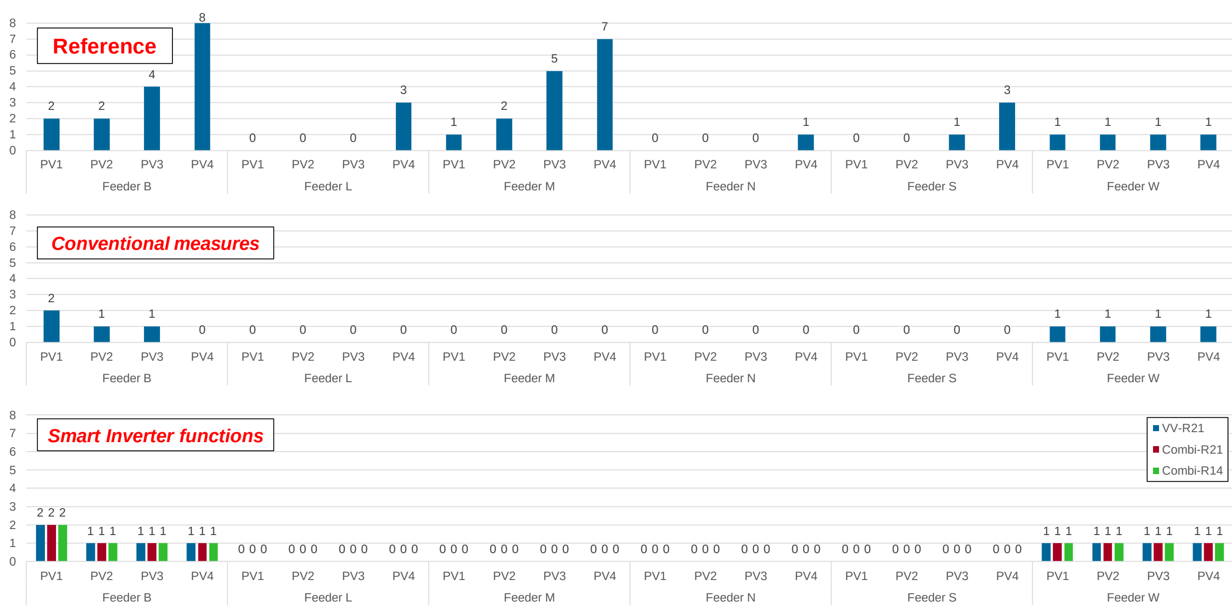

7.5 Feeder Power and Losses

Little to no changes were observed in terms of the average feeder power consumption and losses as a percentage of its total value as shown in Figures 7-20, 7-21 and 7-22. This is because the service transformer replacements did not result in noticeable loss reduction at the feeder level and because SI functions did not cause sufficiently large reactive power injection or curtailment in PV output to significantly affect the feeder level powers or losses. Note that, as opposed to quantifying PV impacts at each penetration level, this chapter focuses on comparing the impacts of conventional measures versus SI functions. Hence, the "Reference" case results already include PV system impacts (without conventional measure or SIs).

Figure 7-20.
Feeder Average Active Power in MW

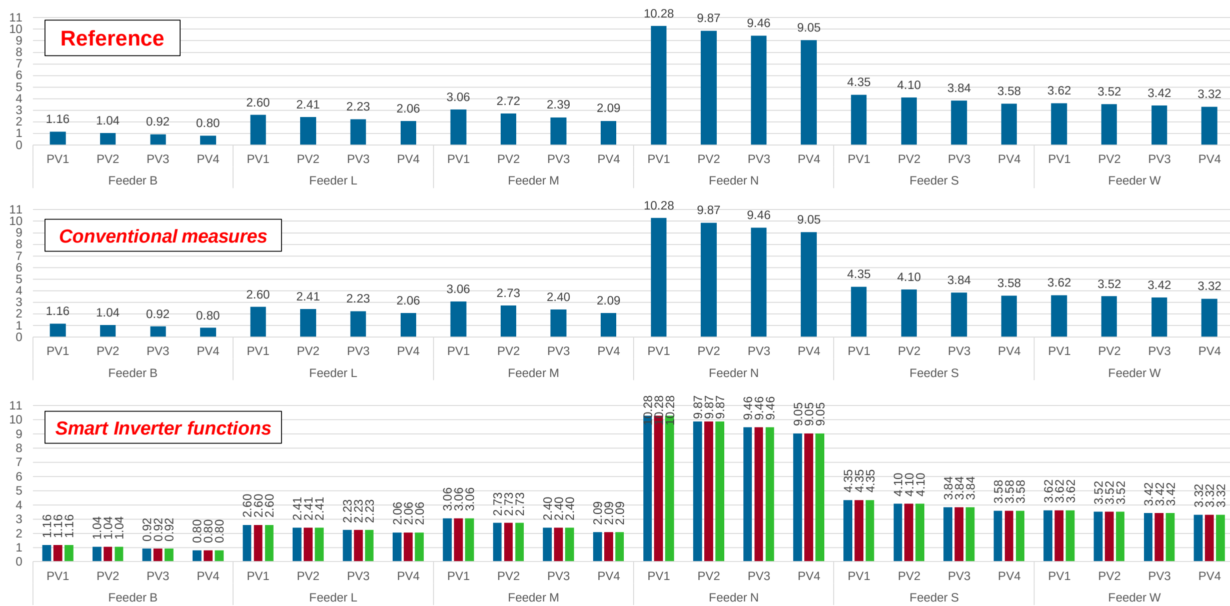

Figure 7-21.
Feeder Average Reactive Power in Mvar

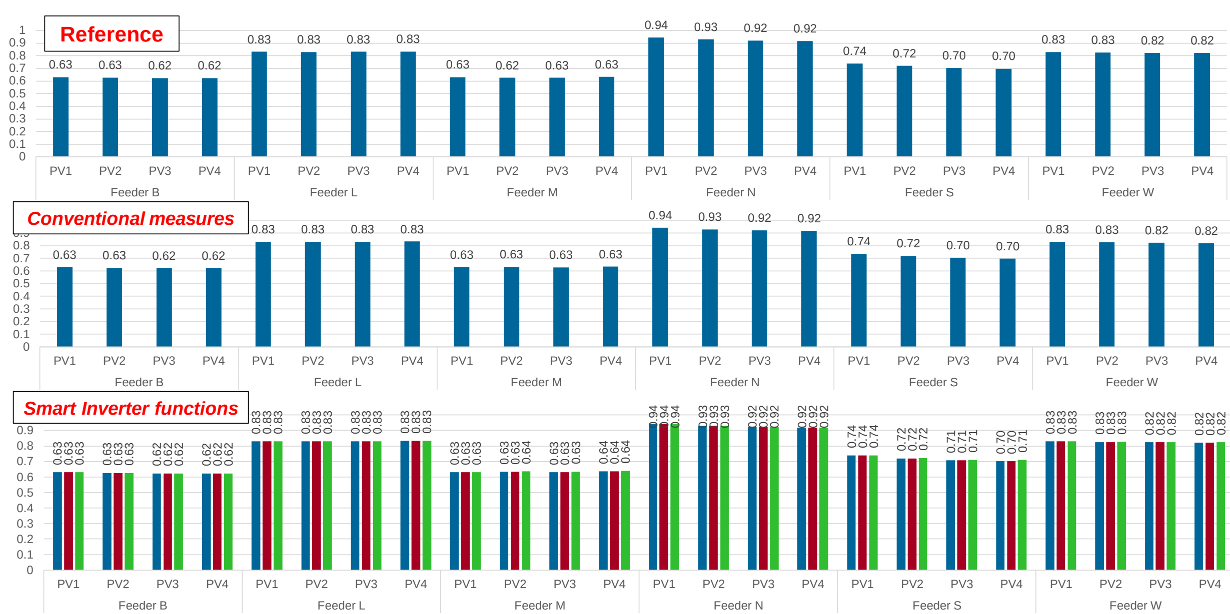

Figure 7-22.
Feeder Average Active Power Losses in kW

7.6 Smart Inverter Impact With Incremental Smart Inverter Densities

In the first five sections of this chapter, all QSTS simulation results with SI functions were obtained assuming that a 100% SI density (i.e., every PV inverter is a smart inverter). This last section evaluates the impact of lower SI densities of 25%, 50% 75% and 100%. Results for the same impacts are compared, at the exception of overload violations since the SI functions considered in this modeling effort are not effective in addressing thermal violations caused by PV systems, as previously discussed.

7.6.1 Overvoltage Conditions

Figure 7-23 shows the case count with significant overvoltage conditions per PV level and SI density. Higher SI densities generally returned a lower count of cases with significant overvoltages. For example, Feeder B had no significant voltage violations for SI densities over 50%. In some cases, this pattern was only observed at the higher PV penetration levels. For example, Feeder M only experienced a reduction in the number of overvoltage cases as the SI density was increasing for a PV penetration level of 100%. Feeder S and Feeder W exhibited the same trends, but for PV penetrations of 75% and 100%, respectively.

The decreased count of cases with overvoltage condition suggests that high densities of SI functions were more effective in reducing overvoltages caused by PV. However, the case counts observed across all feeders modeled did not reveal any clear SI density threshold that would result in significant beneficial effects on overvoltage conditions.

Figure 7-23
Count of Cases With Significant Overvoltage Per PV Level and SI Density

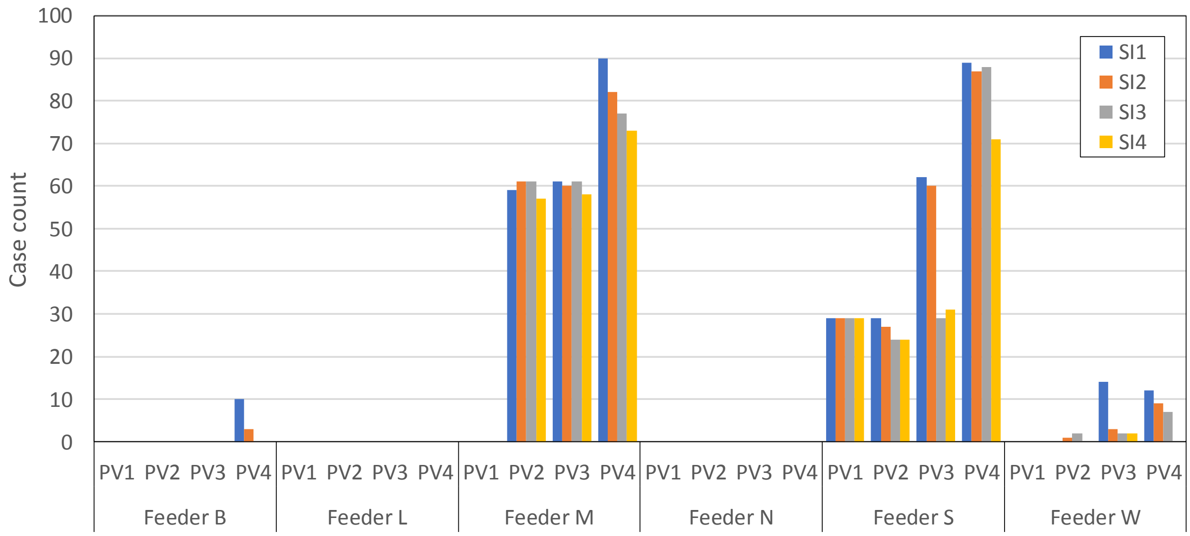

Figure 7-24 shows the maximum MV voltage magnitude obtained from combinations of SI functions and SI density. The Max MV voltages were largely unaffected by SI functions. There were some slight differences in Feeder M. However, these differences were associated to minor changes in the tap selection of voltage regulators for a short period of time. To summarize, based on these results, SI density has no notably impact on MV voltage violations.

Figure 7-24
Max MV Voltage Per SI Function and SI Level

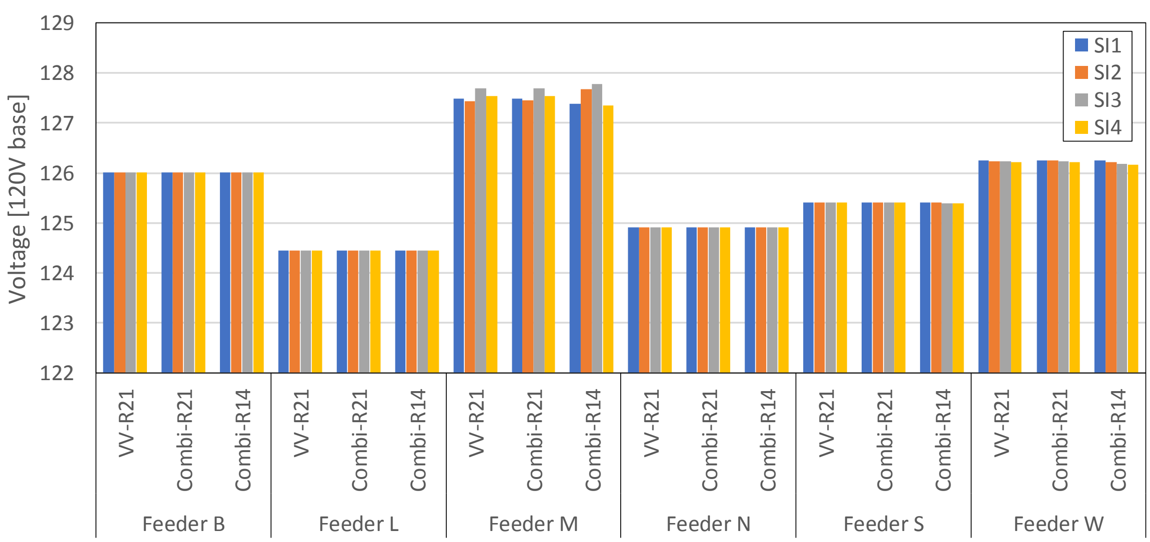

Simulation results indicate that higher SI densities tended to reduce the maximum LV voltages observed. Figure 7-25 shows the maximum LV voltage magnitudes grouped by SI functions and SI densities. In Feeder B, the overvoltages were avoided for SI densities equal and greater than 75%, while results from Feeder L and Feeder N show that the overvoltages were avoided for SI densities at 25% and above.

Results from Feeder M and Feeder W showed a lower impact of the SI density, with a difference between the maximum voltages recorded at 25% and 100% less than 0.005 V p.u. On the other hand, results from Feeder S indicate that there was at least 0.01 V p.u. difference between the maximum voltages recorded at SI densities 25% and 100%, with differences more noticeable when reaching 75% of PV customers with SI capabilities.

Figure 7-25
Max LV Voltage Per SI Function and SI Level

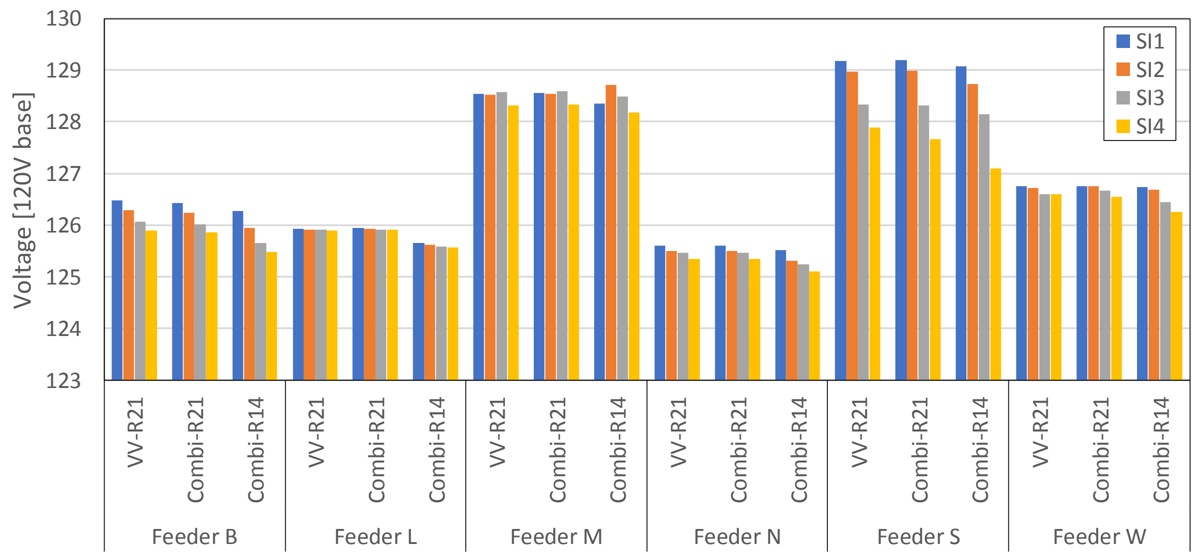

7.6.2 *Undervoltage Conditions*

Figure 7-26 shows the count of cases with significant undervoltages per SI function and SI density. The comparison of values obtained from all the scenarios in each combination shows that the SI density did not influence the count of significant undervoltages.

Figure 7-26
Count of Cases With Significant Undervoltages Per SI Function and SI Level

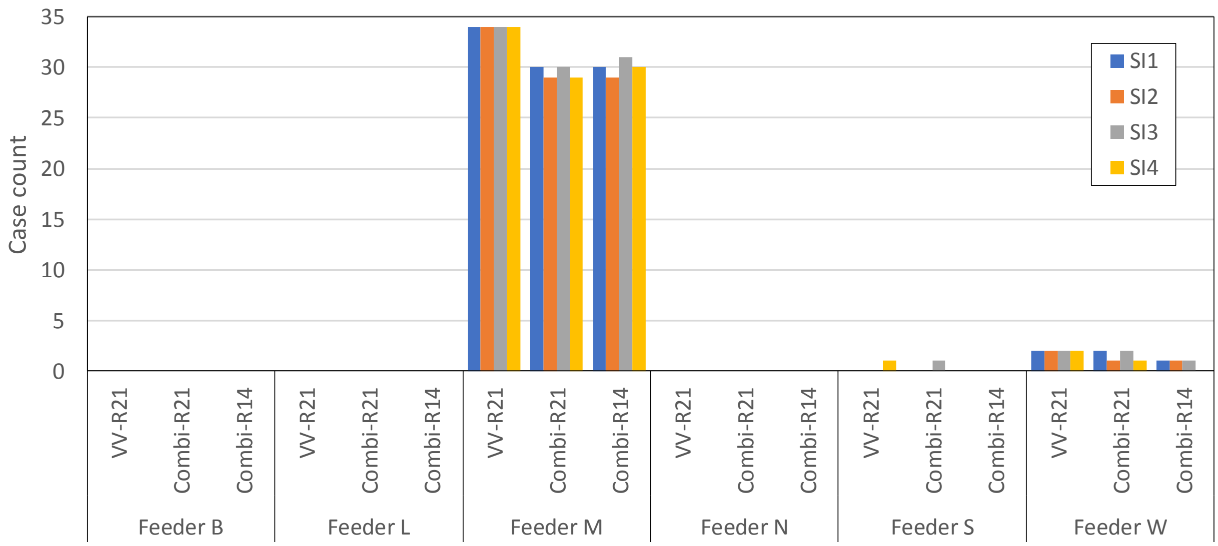

7.6.3 Secondary Voltage-Rise Violations

Figure 7-27 shows the maximum secondary voltage rise per SI function and SI density. SI penetration level notably influences the max secondary voltage rise in Feeder S, where the differences between results from 25% and 100% densities were about 0.01 V p.u. However, the remaining feeders showed little influence of the SI density for this metric.

Figure 7-27
Max Secondary Voltage Rise Per SI Function and SI Level

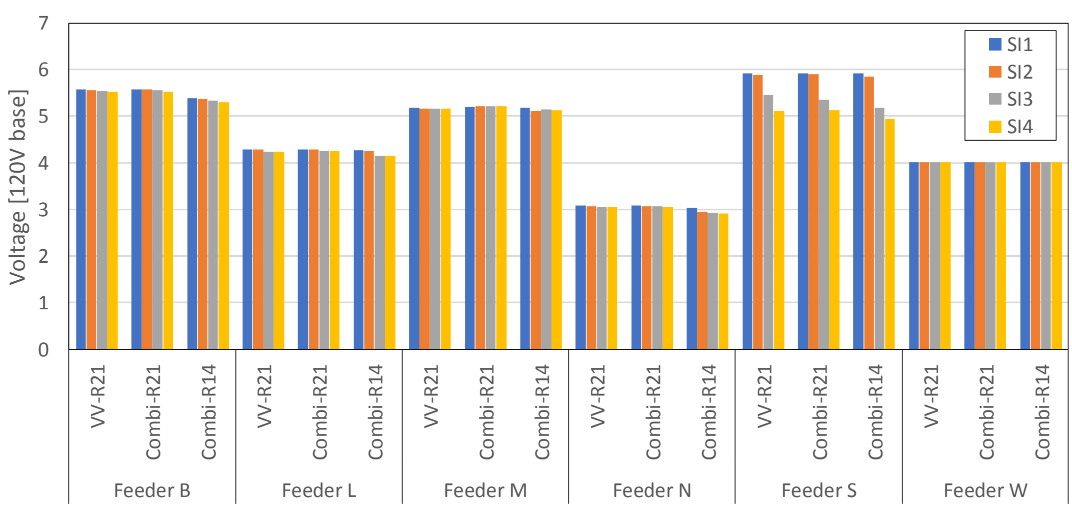

The maximum count of transformers with voltage rise exceeding PG&E design criteria per SI function and SI density is shown in Figure 7-28. Simulation results show that SI density had a small influence on this metric. For instance, Feeder B, Feeder M and Feeder S showed a reduction of up to two secondary circuits for scenarios with SI density higher than 25%. However, this difference is small and a clear deduction cannot be made.

Figure 7-28
Max Count of Transformers With Voltage Rise Exceeding PG&E Design Criteria Per SI Function and SI Level

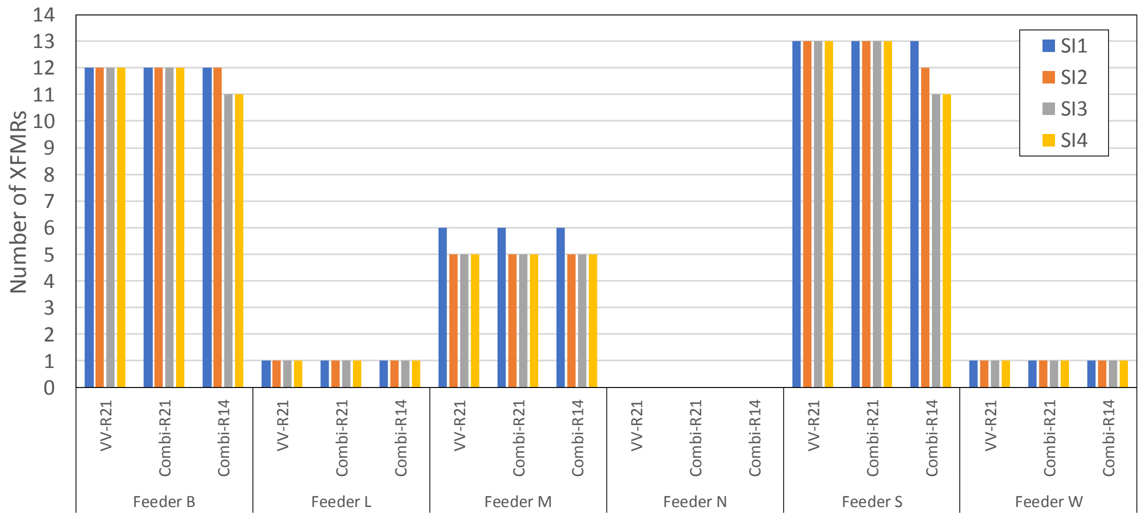

Figure 7-29 shows the maximum transformer counts experiencing secondary overvoltages per SI function and SI density. Results for this metric reflect a relatively small improvement when the SI density was higher than 25%. For Feeder M, a notable improvement was observed between SI density 25% and 50%, but much smaller improvement at SI density was further increased. For Feeder S and Feeder W, there was a rather constant improvement between all incremental SI density increases.

Figure 7-29
Max Transformer Count With Secondary Overvoltages Per SI Function and SI Density

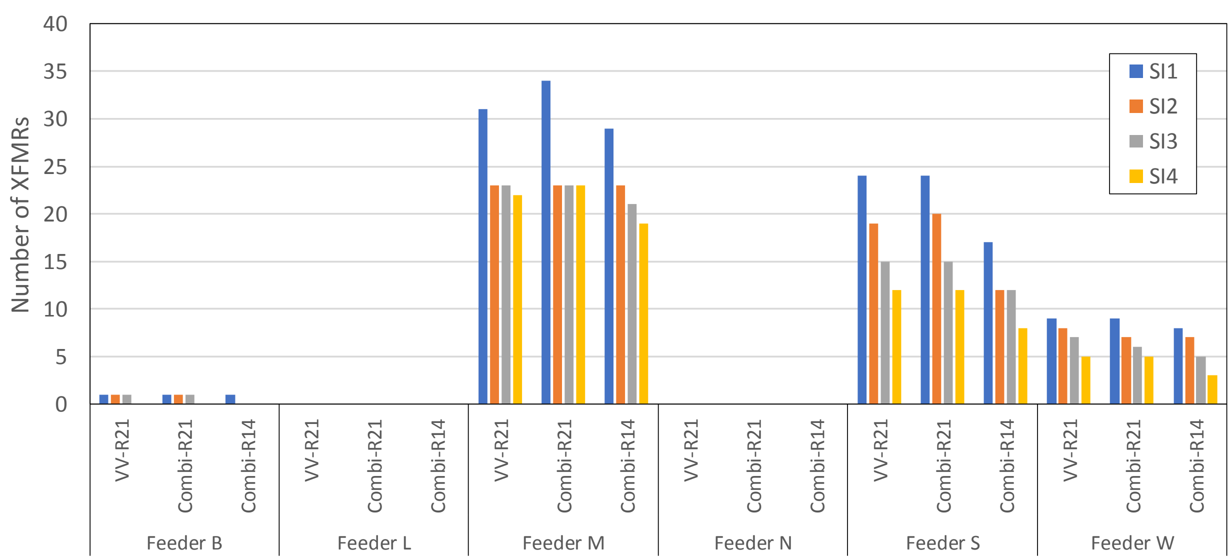

7.6.4 Feeder Power and Losses

Figure 7-30 and Figure 7-31 show the average active and reactive power respectively. These results are distributed by SI functions and SI densities to highlight the average result across all the combinations in each case. The comparison of values for each combination suggests that SI densities have negligible impact on feeder average MW and Megavolt Ampere Reactive.

Figure 7-30
Active Power Per SI Function and SI Level

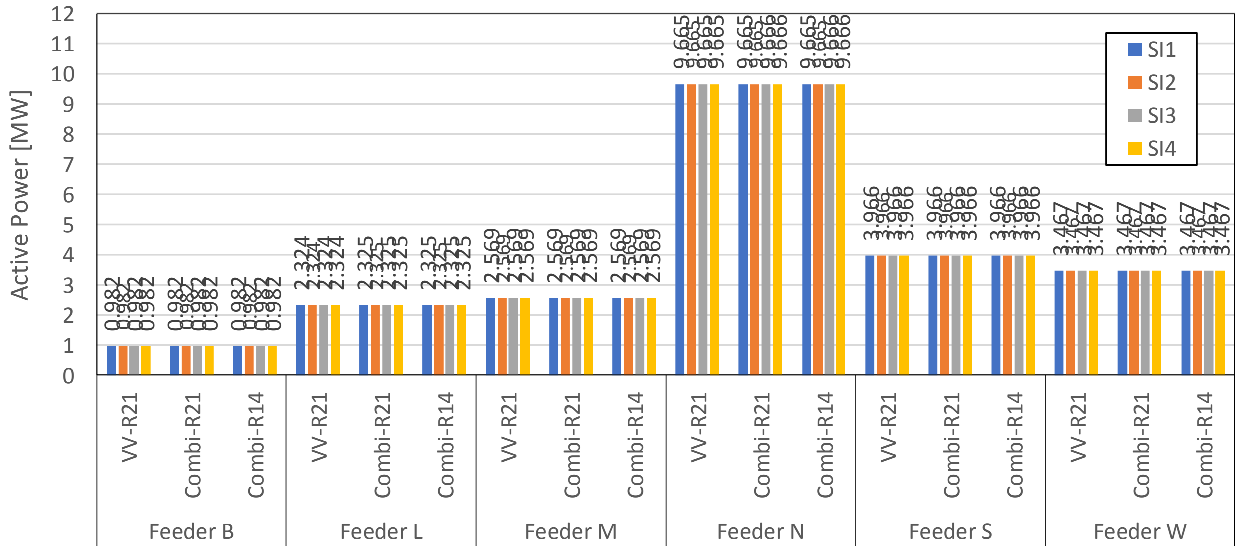

Figure 7-31
Reactive Power Per SI Function and SI Level

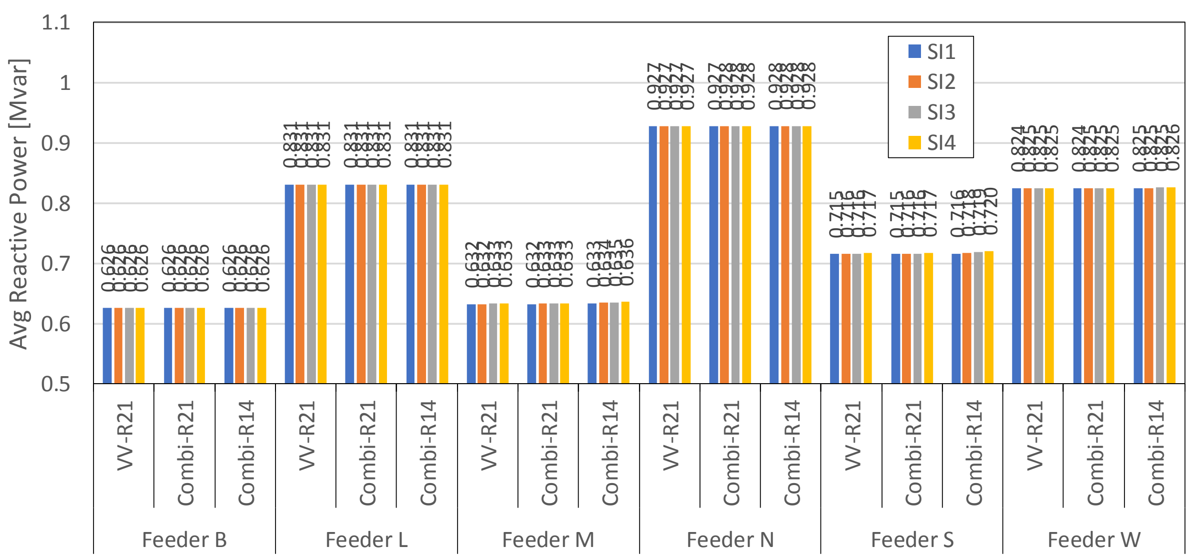

Figure 7-32 shows the distribution of active power losses in percent of the active power magnitude across SI functions and densities. These values indicate that SI densities had negligible impact on feeder active power losses as the SI density increases.

Figure 7-32
Active Power Losses in Percent Per Feeder and SI Function

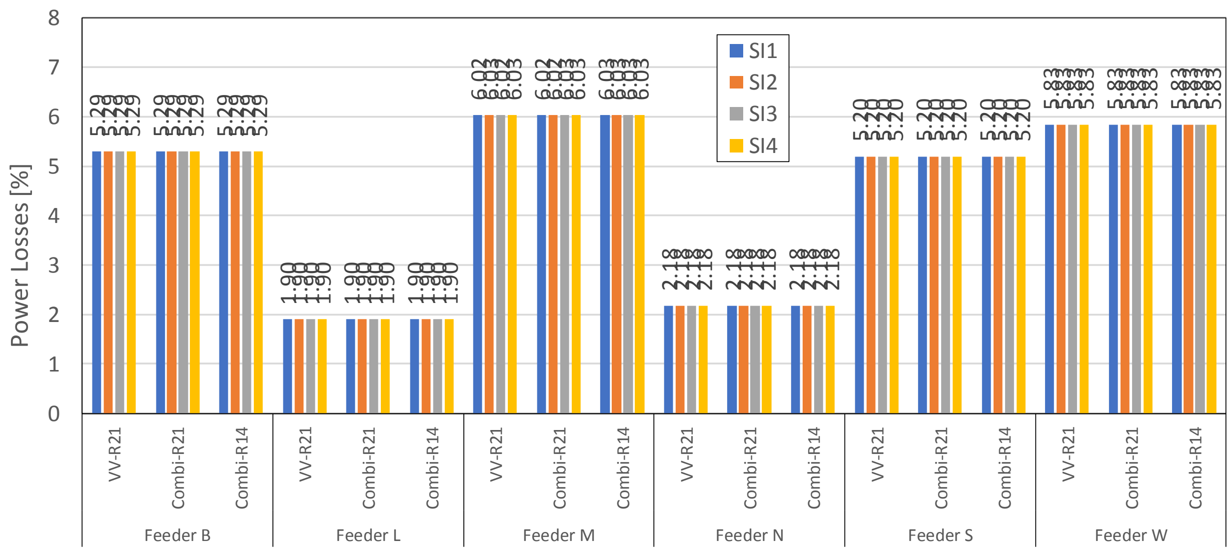

7.7 Conclusions

In this chapter, a technical performance comparison between SI functions and conventional distribution upgrade measures was presented in terms of the voltage conditions (overvoltage, undervoltage, and voltage rise), overload conditions, and feeder power and losses. The objective was to compare and contrast the effectiveness of autonomous SI functions to support increased PV penetration levels with conventional upgrade measures. These two approaches were compared to a reference simulation of baseline PV impacts without conventional upgrade measures or SI functions.

In terms of overvoltage conditions, SI functions provided similar if not marginally better improvements than conventional measures. Because overvoltage conditions were caused by the increased PV penetration levels, SI functions were able to address some but not all of these issues through reactive power management and active power curtailment. Combi-R14 demonstrated to be marginally more effective at addressing overvoltage conditions, when compared to VV-R21 and Combi-R21.

In terms of undervoltage conditions, SI functions did not provide any significant improvements compared to the reference—similar performance as conventional measures. This behavior was not due to the lack of reactive power management in SI functions at lower voltage conditions, but instead due to the assumption that PV inverters were not able to consume or generate reactive power outside daylight hours when these conditions occur.

Smart inverter functions provided some reduction in voltage rise issues but were not as effective as conventional measures in addressing extreme issues but neither SI functions nor conventional measures fully addressed all violations. Although not intended to address voltage rise issues, SI functions provided some voltage rise reduction whether or not a secondary VRS was conducted. Again, Combi-R14 showed marginally better results compared to the other two functions.

As expected, SI functions did not provide any noticeable improvements in the number of overloaded elements since the SI functions analyzed are designed for voltage regulation support. Smart inverter functions were also observed not to result in any noticeable changes in feeder power consumption or losses.

Finally, the influence of SI density (i.e., the share of PV inverters with smart inverter capabilities) was studied. The simulation results confirmed that higher percentages of activated devices were more effective in mitigating overvoltages. However, simulation results did not suggest any specific SI density at which significant benefits would be achieved.

8
ECONOMIC IMPACT ANALYSIS

This chapter analyzes the economic implications of activating SI functions, building on the technical findings presented in the previous chapters.

8.1 Objectives and Approach

The previous chapters explored several areas where SI functions can potentially have beneficial or detrimental *technical impacts*, focusing on six of PG&E's distribution feeders. These areas included: system upgrades required to maintain the grid in normal operating conditions under increased PV penetration levels; number of voltage-rise studies triggered; impacts on inverter active power output; and more generally, impacts on inverter utilization when SI functions are activated.

This chapter analyzes the *economic implications* of these technical impacts. The economic impacts of activating SI functions on the six feeders previously studied are estimated across four cost categories, through the lens of four canonical cost tests that serve as a general standard of cost-effectiveness analysis in California. In addition, a more detailed analysis for a subset of customers particularly impacted by the activation of SI functions is provided.

8.2 Economic Analysis Metrics

8.2.1 Cost Categories

Seven cost categories were considered for inclusion in the economic analysis (Table 8-1). In this chapter, the term "cost" is used indifferently to refer to a *net cost* incurred by the activation of SI functions, or a *net avoided cost* (i.e., a *net benefit*).

Four cost categories were retained for detailed analysis:

- The *increased electricity cost* category reflects the expected increase in energy transferred from the bulk system to the distribution feeders to which SIs are connected, to make up for any PV generation curtailed when smart functions are activated. For each feeder, the associated change in electricity cost is assessed at the feeder head.
- The *bill increases to participants* category reflect the expected increase in electricity bills as seen by PV customers activating SI functions. These bill increases reflect the need for customers to import more energy from the grid to make up for any PV generation curtailed when smart functions are activated. This change in electricity bills is assessed at the customer level, using the retail electricity tariff applicable to each customer.
- The *avoided voltage-rise upgrades (VRU) cost* category reflects that, as shown in the technical analysis, service transformer upgrades can be deferred when SI functions are activated.
- Similarly, the *avoided voltage-rise studies (VRS) cost* category reflects that voltage-rise studies may be avoided when SI functions are activated, as shown in the technical analysis.

In addition, three cost categories were considered, but not included in the economic analysis:

- The *avoided thermal upgrades on secondary circuits* were considered but not included, because the SI functions considered in this modeling effort are not suitable to efficiently address thermal constraints. As a result, any upgrades triggered by thermal constraints remain required even when the SI functions considered in this modeling effort are activated.

- The *avoided primary upgrades* were considered but not included. Indeed, in the case of the six feeders studied in this project, only one primary upgrade (voltage regulator) was identified, for one of the six feeders analyzed. This specific upgrade could not be deferred using SI functions.
- The *increase in inverter utilization* was considered but not included, based on the simulations results showing minimal impact on inverter utilization when smart functions are activated.

8.2.2 Cost Tests

The four cost tests considered in this modeling effort were taken from the most recent version (2001) of the *California Standard Practice Manual.*[94] The California cost tests were historically developed to assess the cost-effectiveness of energy efficiency and demand-side management programs from four major perspectives: participants, ratepayers, program administrator, and society.

In the context of this modeling effort, these cost tests were adapted to measure the economic impacts of activating SI functions. Table 8-1 identifies how each of the four canonical cost tests relates to the four cost categories considered.

The *Total Resource Cost (TRC)* measures the total costs of activating SI functions, including both the participants' and PG&E's cost. The TRC is composed of the increased electricity cost, the avoided VRU cost, and the avoided VRS cost. A variation of the TRC, sometimes referred to as the Societal Test, includes externalities associated with a measure, process or program. The analysis of potential externalities associated with the activation of SI functions was out of scope for this modeling effort.

The *Program Administrator Cost (PAC)* measures the net costs of activating SI functions based on the costs incurred by PG&E and excluding any net costs incurred by the participants. The PAC is composed of the increased electricity cost, and the portion of the avoided VRU cost corresponding to transformer replacements serving multiple customers, which are rate based. For transformer replacements serving a single customer, the replacement cost is charged directly to that customer.

[94] CPUC, *"California Standard Practice Manual,"* October 2001.

Table 8-1
Cost Categories and Cost Tests Considered

Category	Consideration in Analysis Performed	Total Resource Cost (TRC)	Program Administrator Cost (PAC)	Ratepayer Impact Measure (RIM)	Participant[6] Cost Test (PCT)
Increased Electricity Cost	Included	🔴[1]	🔴[1]	🔴[1]	
Bill Increases to Participants[6]	Included	*	*	🟢[2]	🔴[2]
Avoided Voltage-Rise Upgrades (VRU) Cost	Included	🟢[3,4]	🟢[3]	🟢[3]	🟢[4]
Avoided Voltage-Rise Studies (VRS) Cost	Included	🟢			🟢
Avoided Secondary Thermal Upgrades	Considered but not included	🟢[3,4]	🟢[3]	🟢[3]	🟢[4]
Avoided Primary Upgrades	Considered but not included[5]	🟢	🟢	🟢	
Increase in Inverter Utilization	Considered but not included	🔴			🔴

🟢 *Benefit of smart inverter functions*
🔴 *Cost of smart inverter functions*
* *Transfer payment from participants to non-participants*
[1]*Evaluated using proxy for energy cost at feeder head.*
[2]*Evaluated using applicable retail tariffs.*
[3]*Replacements serving multiple customers (rate-based)*
[4]*Replacements serving a single customer (charged to customer)*
[5]*In the case of the six feeders studied, a single primary upgrade was identified for one of the six circuits. This specific upgrade could not be deferred using smart inverter functions.*
[6]*In the context of this modeling effort, "participants" refers to PV customers.*

The *Ratepayer Impact Measure (RIM)* evaluates the net impact on all customer bills due to changes in PG&E revenues and operating costs caused by the activation of SI functions. The RIM is composed of the increased electricity cost, the bill increases to participants (treated as a benefit), and the portion of the avoided VRU cost that can be rate based (transformers serving multiple customers).

The *Participant Cost Test (PCT)* is a measure of the costs to the PV customers due to the activation of SI functions. The PCT is composed of the bill increases to participants, the portion of the VRU cost charged directly to customers (transformers serving a single customer), and the avoided VRS cost.

8.2.3 Cost-Effectiveness Indicators

Four cost-effectiveness indicators were defined to express the cost test results. Each cost test can be expressed using multiple indicators (Table 8-2).

The *Net Present Value (NPV)* is the primary way of expressing cost test results, as per the *California Standard Practice Manual*. Secondary indicators of cost-effectiveness considered include the *Net Present Value Per Customer (NPV/customer)*, the *Net Present Value Per Participant (NPV/participant)*, and the *Net Present Value Per kW of PV installed (NPV/kW$_{PV}$)*, as defined in Table 8-2.

In this modeling effort, a "participant" is defined as a residential customer with PV, for which SI functions are activated. However, for simplicity, when the NPV/participant for a given PV penetration level is calculated, the NPV is normalized by the total number of PV customers for that PV penetration level, irrespective of the SI densities considered. This simplifying assumption is justified for two reasons. First, the estimated VRU and VRS counts developed as part of the technical analysis are independent of the SI densities. Second, the *increased electricity cost* and *bill increases to participants* categories will be shown to be very small.

Table 8-2
Cost-Effectiveness Indicators Considered

Cost-Effectiveness Indicator	Definition	TRC	PAC	RIM	PCT
Net Present Value (NPV)	Calculated by subtracting the present values of all costs from the present values of all benefits identified on the previous slide.	●	●	●	●
Net Present Value Per Customer (NPV/customer[1])	Calculated by scaling the net present worth by the number of customers.	●	●	●	
Net Present Value Per Participant (NPV/participant[2])	Calculated by scaling the net present worth by the number of participants.				●
Net Present Value Per kW of PV Installed[3] (NPV/kW$_{PV}$)	Calculated by scaling the net present worth by the total DC capacity (kW) of PV installed.	●	●	●	●

[1] "Customers" and "Ratepayers" are used interchangeably to refer to the number of customer accounts.
[2] "Participants" refers to the PV customers for each PV penetration level L*i considered.*
[3] This indicator was computed for the six circuits selected for detailed modeling effort, for which the PV capacity installed was known.

8.3 Key Assumptions

8.3.1 Construction of Time-Differentiated Energy Usage Profiles

PV customers under NEM 2.0 must take service on TOU rates. Therefore, estimating the bill increases to PV customers requires to first estimate the net change in their annual, time-differentiated electricity usage when smart functions are activated.

For each of the six feeders modeled, five typical PV days and three typical load days were considered. This corresponds to a total of 15 daily profiles studied. Using these profiles, a full year was reconstructed for each feeder, assuming that each of the 15 profiles studied repeats multiple times over 365 days.

The annual distribution of PV profiles was based on climate data available for each feeder (Table 8-3). The distribution of load profiles was based on load data at the feeder head (Table 8-4). The dataset used for modeling and simulation was used to derive this distribution, with the exception of feeder S. The dataset for feeder S was initially based on data from December through mid-July. To calculate the distribution of load profiles, the dataset was updated through September. The three types of load days, "peak," "average," and "minimum," remained the same. Since the revised dataset included only 306 days, the peak and MIN load days were scaled for the remainder of the year, assuming no peak days would occur in October and November.

Table 8-3
Distribution of PV profiles by Climate Zone and Feeder

		Summer Sunny	**Winter Sunny**	**Cloudy**	**Changeable**	**Overcast**
Climate Zone	**Feeder(s) in Zone**	PV Profile A (PVA)	PV Profile B (PVB)	PV Profile C (PVC)	PV Profile D (PVD)	PV Profile E (PVE)
2	M	35.1%	29.0%	16.7%	5.5%	13.7%
3	B, N	31.5%	30.7%	17.3%	7.7%	12.9%
4	L	37.5%	32.3%	15.3%	4.7%	10.1%
12	W	40.3%	26.6%	13.7%	3.3%	16.2%
13	S	36.7%	27.7%	14.2%	6.8%	14.5%

Table 8-4
Distribution of Load Profiles by Feeder

Feeder	Peak	Average	Minimum
B	11%	73%	16%
L	4%	69%	27%
M	24%	47%	29%
N	4%	69%	27%
S	10%	57%	33%
W	11%	63%	26%

Calculating the annual electricity bills for each customer requires to further distribute the occurrence of each of the 15 daily profiles seasonally (summer vs. winter), and intra-seasonally (weekday vs. off-peak day) because the retail electricity rates applicable are functions of these parameters.

As per PG&E's tariffs, the summer period is defined to start on June 1 and end on September 30 (122 days); the winter period starts on October 1 and ends on May 31 (243 days). Weekdays and off-peak days are also defined consistently with PG&E's tariffs. Weekdays are days where the time-differentiated rates are applicable. Off-peak days are weekend days and other holidays where a flat rate is applicable. For the purpose of this project, all holidays are assumed to take place on non-weekend days.

For each feeder studied, using the PV distribution data shown in Table 8-3, the number of summer sunny days (PV profile A) was first calculated. Based on this information, the occurrence of the 15-day types across the various seasonal and intra-seasonal categories was calculated as follows:

1. If the number of summer sunny (PVA) days was *larger than or equal to* the 122 summer days:
    a. All summer days were considered to be PVA type, and distributed according to the (PK, AVG, MIN) distribution for the feeder considered, as shown in Table 8-4.
    b. The remaining PVA days were considered to be winter days, and distributed according to the (PK, AVG, MIN) distribution.
    c. All PVB days were considered to be winter days, and distributed according to the (PK, AVG, MIN) distribution.
    d. The remaining winter days were distributed across PVC, PVD, PVE, keeping the relative ratios between these days the same as the one defined in the (PVA, PVB, PVC, PVD, PVE) distribution for that feeder, as shown in Table 8-3.
    e. PVC, PBD and PVE days were distributed according to the (PK, AVG, MIN) distribution.
2. If the number of summer sunny (PVA) days was *smaller than* the 122 summer days:
    a. All PVA days were considered to be summer days, distributed according to the (PK, AVG, MIN) distribution for the feeder considered, as shown in Table 8-4.
    b. The remaining summer days were distributed across PVC, PVD, and PVE keeping the relative ratios between these days the same as in the (PVA, PVB, PVC, PVD, PVE) distribution for that feeder, as shown in Table 8-3. The PVC, PVD and PVE days in summer were further distributed according to the (PK, AVG, MIN) distribution, as shown in Table 8-4.
    c. All PVB days were considered to be winter days, distributed according to the (PK, AVG, MIN) distribution, as shown in Table 8-4.
    d. The remaining winter days were distributed across PVC, PVD, and PVE keeping the relative ratios between these days the same as in the (PVA, PVB, PVC, PVD, PVE) distribution for that feeder, as shown in Table 8-3. The PVC, PVD and PVE days in winter were further distributed according to the (PK, AVG, MIN) distribution, as shown in Table 8-4.

Following the process above, the occurrence of each of the 15-day types was calculated across the various seasonal and intra-seasonal categories considered, for all six circuits studied. Table 8-5 provides the results for feeder B as an example.

Table 8-5
Example of Day Type Distribution for Feeder B

Profile	Total (annual)	Summer	Summer-Week	Summer-Off-Peak	Winter	Winter-Week	Winter-Off-Peak
PVA-PK	13	13	9	4	0	0	0
PVA-AVG	84	84	58	26	0	0	0
PVA-MIN	18	18	12	6	0	0	0
PVB-PK	12	0	0	0	12	8	4
PVB-AVG	82	0	0	0	82	57	25
PVB-MIN	18	0	0	0	18	12	6
PVC-PK	7	0	0	0	7	5	2
PVC-AVG	46	2	1	1	44	31	13
PVC-MIN	10	1	1	0	9	6	3
PVD-PK	3	0	0	0	3	2	1
PVD-AVG	21	2	1	1	19	13	6
PVD-MIN	4	0	0	0	4	3	1
PVE-PK	5	0	0	0	5	3	2
PVE-AVG	35	2	1	1	33	23	10
PVE-MIN	7	0	0	0	7	5	2

The reconstructed annual profiles were subsequently used to evaluate the *Increased Electricity Cost* and *Bill Increases to Participants* cost categories.

8.3.2 Tariff Assignation to Customers

Each PV customer modeled was assigned a retail electricity tariff to evaluate the changes impacting their electricity bills when SI functions are activated.

This tariff assignation process was conducted assuming a PV penetration level of 100%, which contains the maximum number of PV customers considered in this modeling effort. This ensured that all PV customers were assigned a tariff. In addition, the tariff assignation was conducted assuming that no storage was deployed, and no smart functions activated. The assumption is that customers have already made their tariff selection prior to installing a smart inverter, and/or a storage system; this modeling effort evaluates possible bill increases resulting from those upgrades.

The tariffs assigned under the assumptions stated above were then used in all other technology penetration scenarios considered.

For each PV customer, three PG&E TOU tariffs were screened:

- *E-TOU-A* and *E-TOU-B* (using the tariff information filled on July 27, 2018 and effective since September 1, 2018 as reference); and
- *E-TOU-C3* (using the tariff information filled on March 12, 2018 and effective since April 1, 2018 as reference).

The following considerations were incorporated into the bill calculations:

- *Non-Bypassable Charges (NBCs)* Under NEM 2.0: Customers did not receive credits for solar power exports against the four NBCs. This includes the Public Purpose Program, Nuclear Decommissioning, DWR Bond Charge, Competition Transition Charge. Accordingly, when valuing power exports, the rate components for the four NBCs as defined in the tariffs were subtracted from the time-differentiated bundled rates.
- *Unused Credits*: At the end of the 12-month period, unused credits were voided.
- *Net Surplus Compensation (NSC)* was considered, assuming for all PV customers an NSC rate of $0.02837/kWh, corresponding to the NSC rate defined by PG&E for October 2018. The NSC rate is based on a 12-month average of the market rate for energy. Customers who generate more electricity than they use over their 12-month billing cycle are eligible to NSC.

For each customer, the tariff leading to the lowest annual bill *before voiding any unused credits and adding any NSC if eligible* was selected. The determination was made before voiding any unused credits to address all cases where two or three of the tariffs considered would lead to a negative annual bill, creating scenarios where all three tariffs would return the same annual bill. The tariff leading to the largest unused credit was selected, maximizing the possibility for the customer to potentially increase their annual consumption at no extra cost.

Tariffs E-TOU-A and E-TOU-C3 are different from E-TOU-A in that customers taking service on these tariffs receive a Baseline Credit calculated on a monthly basis, using a Baseline Allowance (in kWh). The Baseline Allowance itself is calculated for each customer based on (1) the geographical location of the customer ("Baseline Territory"); and (2) whether the customer has permanently-installed electric heating as the primary heat source ("Code H") or not ("Code B").

The Baseline Territory information was provided by PG&E for each of the six feeders studied (Table 8-6). All customers connected to a given feeder were assumed to belong to the same Baseline Territory.

The probability distribution between Code B and Code H customers was estimated from the Energy Information Agency's 2015 Residential Energy Consumptions Survey (RECS) Survey Data,[95] which provides space heating statistics by "Building America" climate zone, and data from PNNL[96] mapping each U.S. county to a "Building America" climate zone. Table 8-6 shows the Code B-Code H distributions for each feeder studied. Customers were randomly assigned a code B or H according to the Code B-Code H probability distribution defined for the feeder they were connected to.

---

95 EIA, *"RECS Survey Data"*, 2015, available at https://www.eia.gov/consumption/residential/data/2015/.

96 PNNL, *"Guide to Determining Climate Regions by County"*, August 2015, https://www.energy.gov/sites/prod/files/2015/10/f27/ba_climate_region_guide_7.3.pdf.

Table 8-6
Baseline Territory and Code B/H Information for Each Feeder

Feeder	BA Climate Zone	Code B Probability	Code H Probability	Baseline Territory
B	Marine	0.60	0.40	X
L	Marine	0.60	0.40	X
M	Mixed-Dry	0.71	0.29	P
N	Marine	0.60	0.40	X
S	Hot-Dry	0.71	0.29	W
W	Hot-Dry	0.71	0.29	S

Using the information from Table 8-6, the Baseline Allowance was calculated for E-TOU-A and E-TOU-C3 as follows:

- For each customer, the Baseline Quantity (kWh per day) was assigned based on their Baseline Territory and Code B/H, using the Baseline Quantity values specified in the tariffs; and
- While the Baseline Allowance is normally calculated monthly (30-day billing cycle), for simplification, this modeling effort calculated the Baseline Allowance seasonally (122 days in winter, and 243 days in summer) since the occurrence of each day type was calculated seasonally (as shown in Table 8-5 for feeder B).

The results of the tariff assignation process for the 8,438 PV customers considered are as follows: E-TOU-A was assigned to 8,414 customers; E-TOU-B was assigned to 24 customers; E-TOU-C3 was never assigned. Figure 8-1 compares the annual electricity bills for the three tariffs considered.

E-TOU-B was designed for higher energy customers, with a price of electricity lower than E-TOU-A once the monthly electricity usage exceeds the Baseline Allowance. E-TOU-B was assigned to a few large customers, but the vast predominance of E-TOU-A reflects that the customers considered were not large enough to benefit from E-TOU-B, compared to E-TOU-A.

Rate components in E-TOU-C3 are always lower than E-TOU-A, except for winter during peak pricing. The fact that E-TOU-C3 never got selected for the PV customers modeled is likely due to the higher credits received for exports under E-TOU-A, i.e., higher rate components in all periods except winter-peak (4-9 p.m., an interval during which PV exports are limited).

For each feeder and each PV penetration level, the aggregated bill changes across all customers resulting from activating SI functions were summarized using two metrics: the *average* aggregated bill change across all combinations of SI functions and SI densities considered; and the *maximum* aggregated bill change across all combinations of SI functions and SI densities considered.

Figure 8-1. Annual Customer Bills for the Three Tariffs Screened Across All Feeders Studied

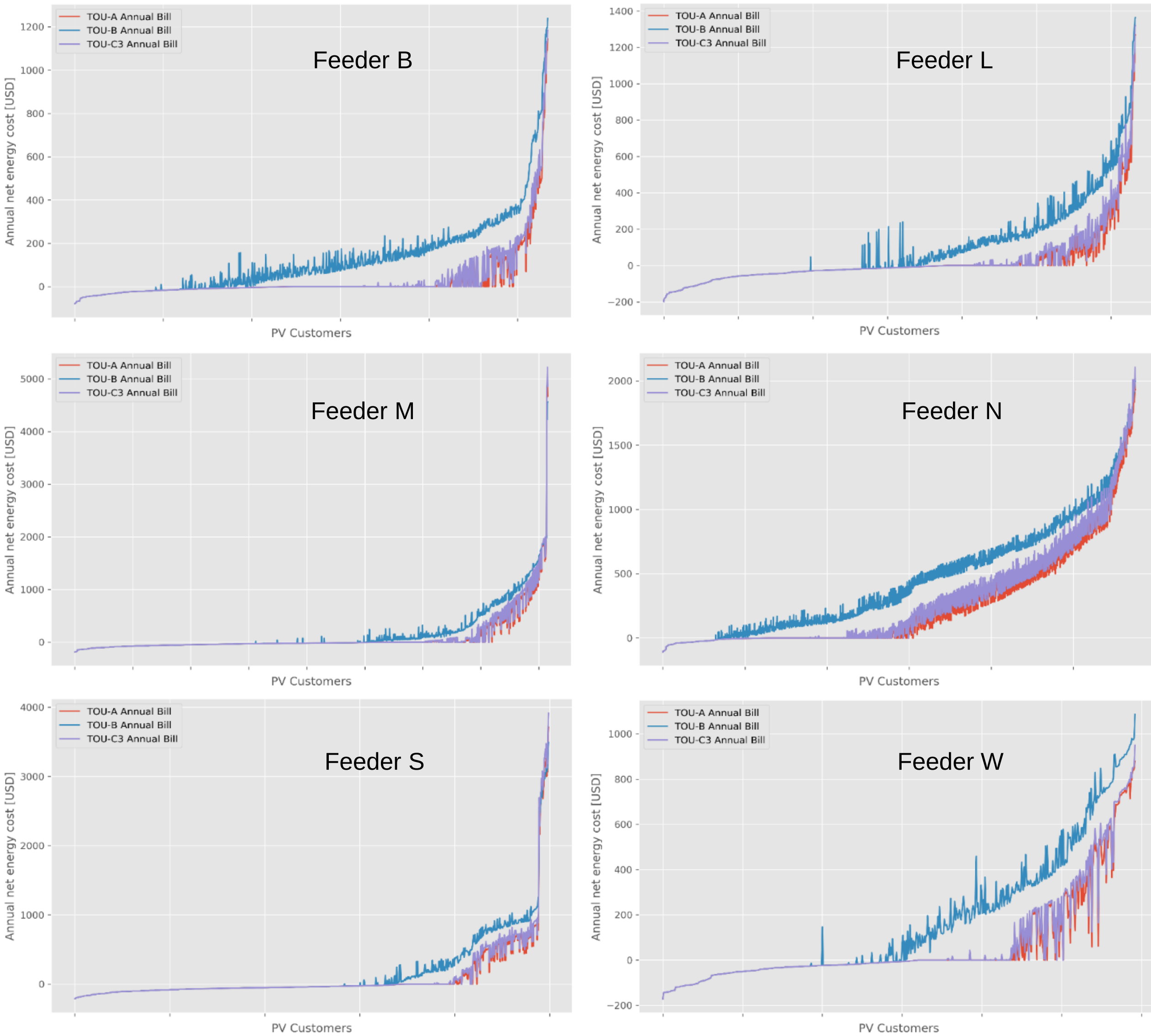

8.3.3 *Energy Cost at Feeder Heads*

Using the reconstructed annual profiles, the change in energy transferred from the bulk system to the distribution circuits when SI functions are activated was computed. The NSC rate of $0.02837/kWh (12-month average of the market rate for energy in PG&E's territory as of October 2018) was assumed to value the change.

For each circuit and each PV penetration level, the increased electricity cost at the feeder head resulting from activating SI functions was summarized using two metrics: the *average* change in cost across all combinations of smart functions and SI densities considered; and the *maximum* change in cost across all combinations of smart functions and SI densities considered.

8.3.4 *Temporal Staging of PV Installs and Associated VRU and VRS Costs*

8.3.4.1 Staging Profiles Considered

The technical analysis was conducted for four distinct PV penetration levels, PV1 to PV4, assuming respectively that 25%, 50%, 75%, and 100%[97] of residential customers have PV. The economic analysis requires to make assumptions on "how fast" these PV penetration levels are reached over time to properly allocate capital investments and other expenses.

Two distinct staging profiles were assumed, reflecting two ways to stage PV installations over the 10-year horizon considered. The associated capex and expenses were assumed to follow the same temporal profiles:

- The *All-in-Y0* staging profile assumes that, for each PV penetration level L*i*, 100% of the VRU and VRS required as per the technical analysis are executed in year 0, with no subsequent upgrades or studies; and
- The *LINEAR* staging profile assumes that PV installations, and the associated VRU costs and VRS expenses, are linearly staged over 10 years, until 100% of the VRU and VRS required for L*i* as per the technical analysis are fully executed by year 10.

The two staging profiles are shown in Figure 8-2.

Figure 8-2
Cumulative Percentage of VRU and VRS Executed Under All-in-Y0 and LINEAR

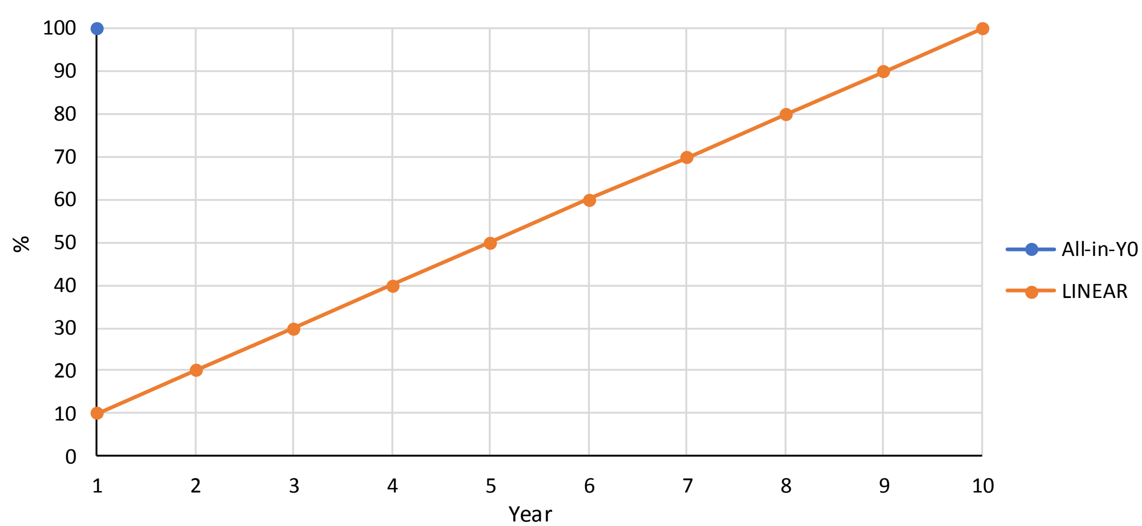

8.3.4.2 Distribution Between Single- and Multi-Customer VRU

In addition to temporal staging, the distribution between single-customer and multi-customer VRU was considered, as it impacts how the VRU capex are distributed between (1) the PAC and RIM costs tests; which collect all multi-customer replacements (rate-based); and (2) the PCT cost test, which collects all single-customer replacements (charged to customers directly).

97 A residual number of customers were too small to have PV at penetration level L4. For simplicity, this level is still referred to as 100% PV penetration.

Two bookend cases were examined for the distribution between single- and multi-customer VRU. The first bookend case assumes that all VRU are multi-customer. This first bookend reflects that the maximum proportion of single-customer VRU observed across all scenarios studied for the six feeders considered was 2.7% (PV4). The second bookend case assumes that VRU follow the distribution of single/multi-customer transformer across PG&E's territory (Figure 8-3), with 70% of VRU being multi-customer replacements.

Figure 8-3
Distribution of Single- vs. Multi-Customer Transformers (Domestic and Mixed)

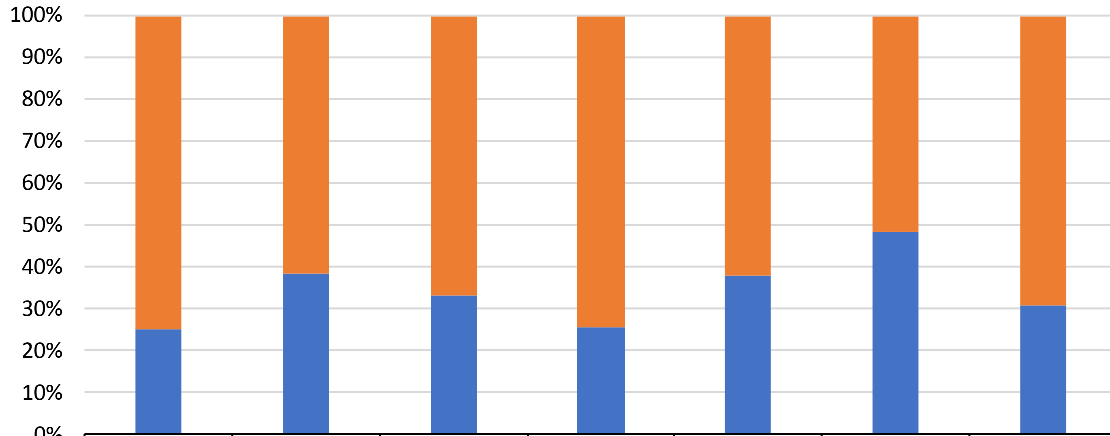

	Feeder M	Feeder W	Feeder L	Feeder N	Feeder B	Feeder S	PG&E-wide
% of Multi	75.07%	61.40%	66.82%	74.66%	62.12%	51.57%	69.47%
% of Single	24.93%	38.60%	33.18%	25.34%	37.88%	48.43%	30.53%

8.3.4.3 Upper and Lower VRS Estimates

As part of the technical analysis, two estimates of the VRU counts, upper and lower, were developed. These counts are used to estimate the VRS costs.

8.3.5 Summarized Measure of Sensitivities Explored When Calculating the Cost Tests

For each of the four cost categories, two bookend scenarios were considered:

- For the *Increased Electricity Cost*, the *average* and *maximum* cost increase across all combinations of SI functions and SI densities;
- For the *Bill Increases to Participants*, the *average* and *maximum* aggregated bill increase across all SI functions and SI densities;
- For the *Avoided VRU Cost*, a scenario assuming *100% of VRU* serving multiple customers, and another reducing that proportion to *70% of VRU*; and
- For *Avoided VRS Cost*, *lower* and *upper* cost estimates, based on lower and upper estimates of the VRS count.

Accordingly, for each of the six circuits analyzed, for each PV level considered, the four cost tests were calculated four (for PAC) to eight times (for TRC, RIM, PCT) to account for the various combinations of bookend scenarios summarized above and in Table 8-7.

For simplicity, the results for each cost test presented in this report were limited to the combination of bookend scenarios resulting in the minimum (MIN) and maximum (MAX) values of the associated cost-effectiveness indicators.

Table 8-7
Summary of Bookend Scenarios for Each Cost Category

Category	Bookend Scenarios for Cost-Effectiveness Indicators	TRC	PAC	RIM	PCT
Increased Electricity Cost	AVG, MAX	●	●	●	
Bill Increases to Participants	AVG, MAX			●	●
Avoided Voltage-Rise Upgrades (VRU) Cost	MULTI-100%, MULTI-70%	●	●	●	●
Avoided Voltage-Rise Studies (VRS) Cost	UPPER, LOWER	●			●
	Scenarios Explored Per Circuit Per PV Level to Calculate MIN and MAX	***8***	***4***	***8***	***8***

8.3.6 Financial and Costing Assumptions

Table 8-8 summarizes the financial parameters assumed. A time horizon of 10 years was assumed for this analysis. This horizon is aligned with the typical lifetime of a PV inverter. The discount and inflation rates assumed were provided by PG&E.

The Annual Charge Rates (ACR) assumed for the VRU (Figure 8-4) come from PG&E's charge model. The Economic Carrying Cost (ECC) calculated reflects the economic value of differing the service transformer upgrades by activating SI functions. The ECC is used to annualize the VRU costs over 10 years, in combination with the two staging profiles, *All-in-Y0* and *LINEAR*, which determine how many VRU are executed each year.

The VRS costs are treated as expenses allocated annually based on the two possible VRS schedules, *All-in-Y0* and *LINEAR*.

The VRU and VRS costs were provided by PG&E. The VRU and VRS costs are assumed to escalate with inflation.

Based on the evolution of the NSC rate over the past few months (Figure 8-5), a 0% escalation rate was assumed for the electricity cost at the feeder heads, and for the retail electricity rates.

Table 8-8
Financial Parameters

	Parameter	Variable	Value
General Assumptions	Time Horizon	-	10 years
	Discount rate	d	7%
	Inflation rate	e	2.5%
	Energy escalation rate	-	0%
Assumptions specific to service transformers	Annual Charge Rates	ACR_i	From PG&E charge model (Figure 8-4)
	Service Transformer Lifetime	LT	30 years
	K-Factor (Accumulated PW)	$Kf = \sum_{i=1}^{LT} \frac{ACR_i}{(1+d)^i}$	1.27
	Time Factor	$Tf = \frac{1+e}{1+d}$	0.96
	Replacement Factor	$Rf = \frac{1}{1-Tf}$	1.38
	Economic Carrying Cost	$ECC\% = Kf \cdot Rf \cdot (d-e)$	7.88%

Figure 8-4
Annual Charge Rates Assumed for the Service Transformer Upgrades

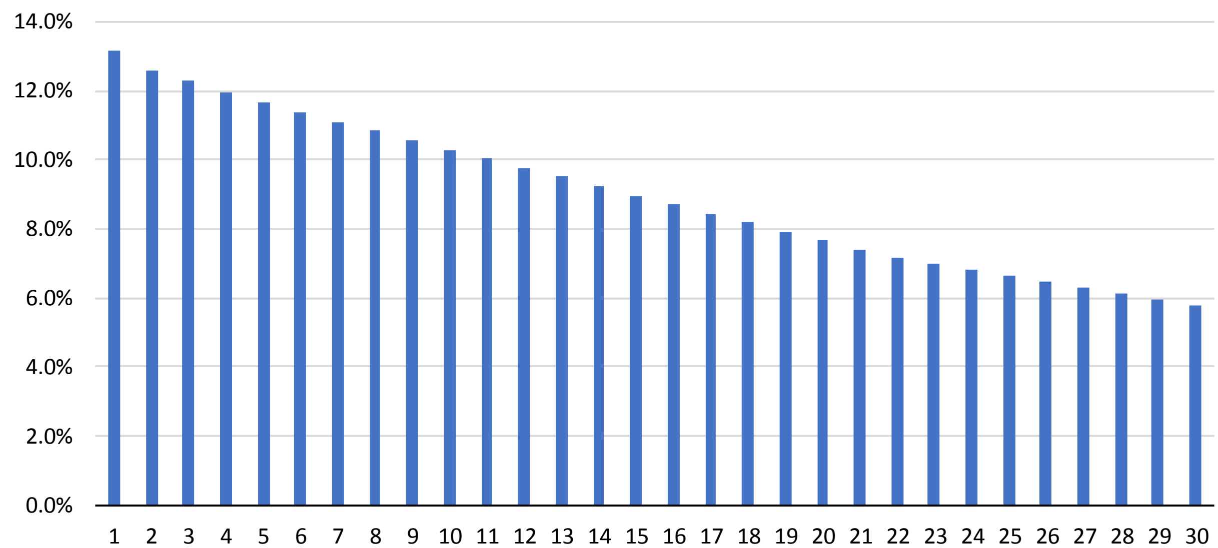

Figure 8-5
Historical NSC Rate ($/kWh)

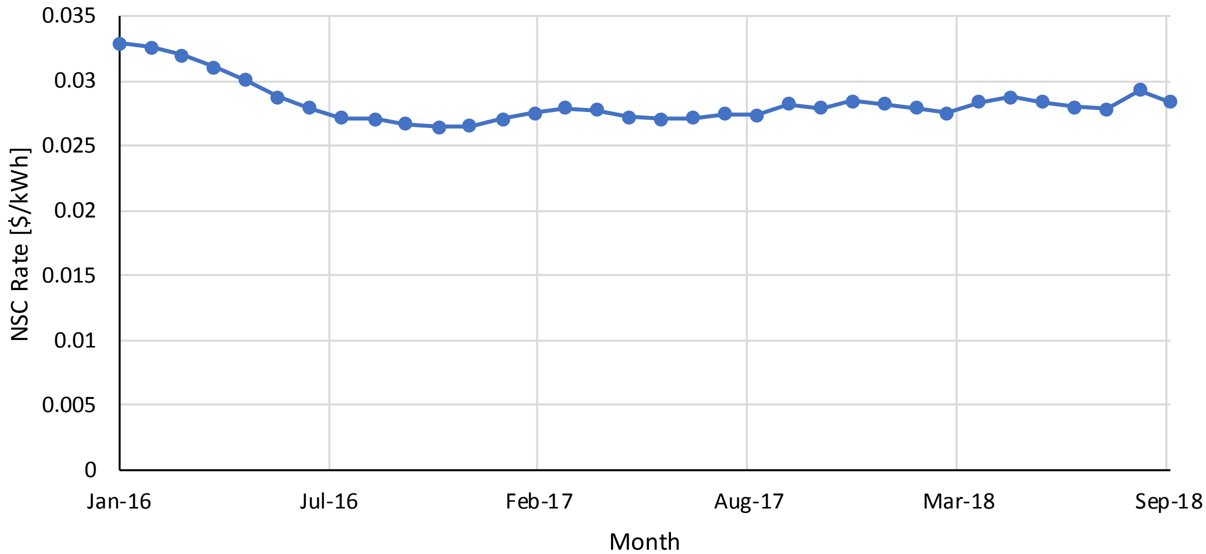

8.4 Feeder-Specific Economic Analysis

8.4.1 Increased Electricity Cost

The annual energy transferred from the bulk system to the six circuits studied increases by up to 0.1% across all scenarios analyzed, as a result of SI functions curtailing PV generation (Figure 8-6). This increased energy transfer translates into an annual cost of electricity at the feeder heads that increases by up to $262 annually (Figure 8-7). This worst case corresponds to a net increase of $1,595 over 10 years in $2018 (7% discount rate, 0% escalation rate for NSC). The maximum *average* increase in electricity cost across all scenarios analyzed is $167 annually (Figure 8-8). Table 8-9 summarizes the average and maximum annual increases in energy cost for each feeder and each PV penetration levels, across all smart function combinations and all SI densities studied. Table 8-10 summarizes the NPV of the average and maximum cost increases over 10 years.

Table 8-9
Average and Maximum Annual Increase in Electricity Costs at Feeder Heads ($2018)

	Average Annual Increase ($)				Maximum Annual Increase ($)			
Feeder	PV1	PV2	PV3	PV4	PV1	PV2	PV3	PV4
B	2.89	4.49	65.77	162.72	5.97	11.42	79.58	181.29
L	8.08	12.36	37.17	44.26	17.27	26.80	59.87	75.46
M	10.01	26.14	24.95	62.37	20.16	79.34	93.15	101.59
N	20.50	32.03	42.04	54.26	42.55	67.88	86.44	101.33
S	23.52	50.69	8.24	133.40	75.96	122.74	49.85	262.09
W	5.28	8.47	14.77	23.58	10.93	21.39	34.57	53.22

Table 8-10
NPV of Average and Maximum Increases in Electricity Costs at Feeder Heads Over 10 Years ($2018)

	NPV of Average Increase ($2018)				NPV of Maximum Increase ($2018)			
Feeder	PV1	PV2	PV3	PV4	PV1	PV2	PV3	PV4
B	20.3	31.5	461.9	1142.9	41.9	80.2	558.9	1273.3
L	56.8	86.8	261.1	310.9	121.3	188.2	420.5	530.0
M	70.3	183.6	175.2	438.1	141.6	557.3	654.2	713.5
N	144.0	225.0	295.3	381.1	298.9	476.8	607.1	711.7
S	165.2	356.0	57.9	936.9	533.5	862.1	350.1	1840.8
W	37.1	59.5	103.7	165.6	76.8	150.2	242.8	373.8

Figure 8-6
Maximum Annual Increase in Energy Supplied to Circuits by Bulk System

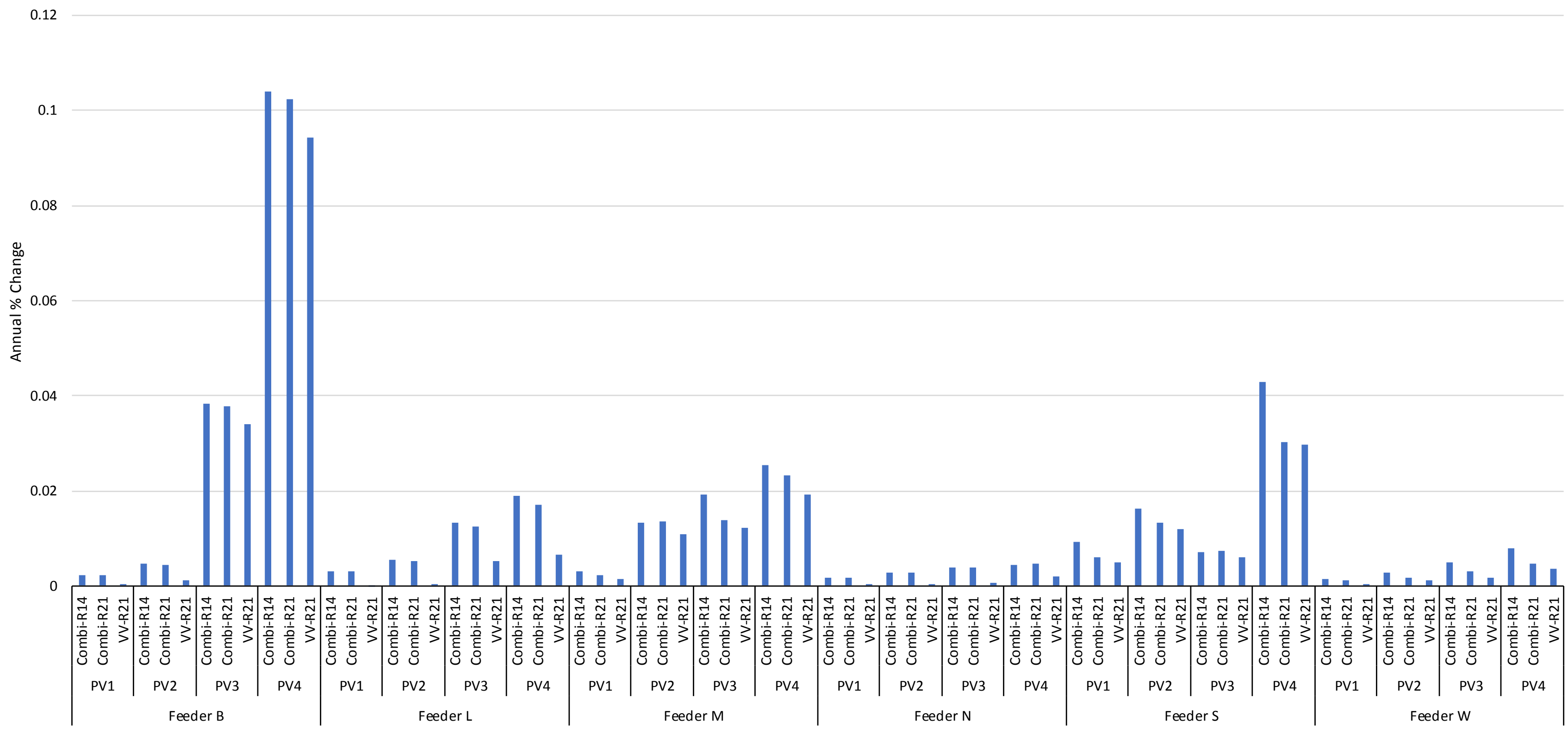

Figure 8-7
Maximum Annual Increase in Electricity Cost at Feeder Heads

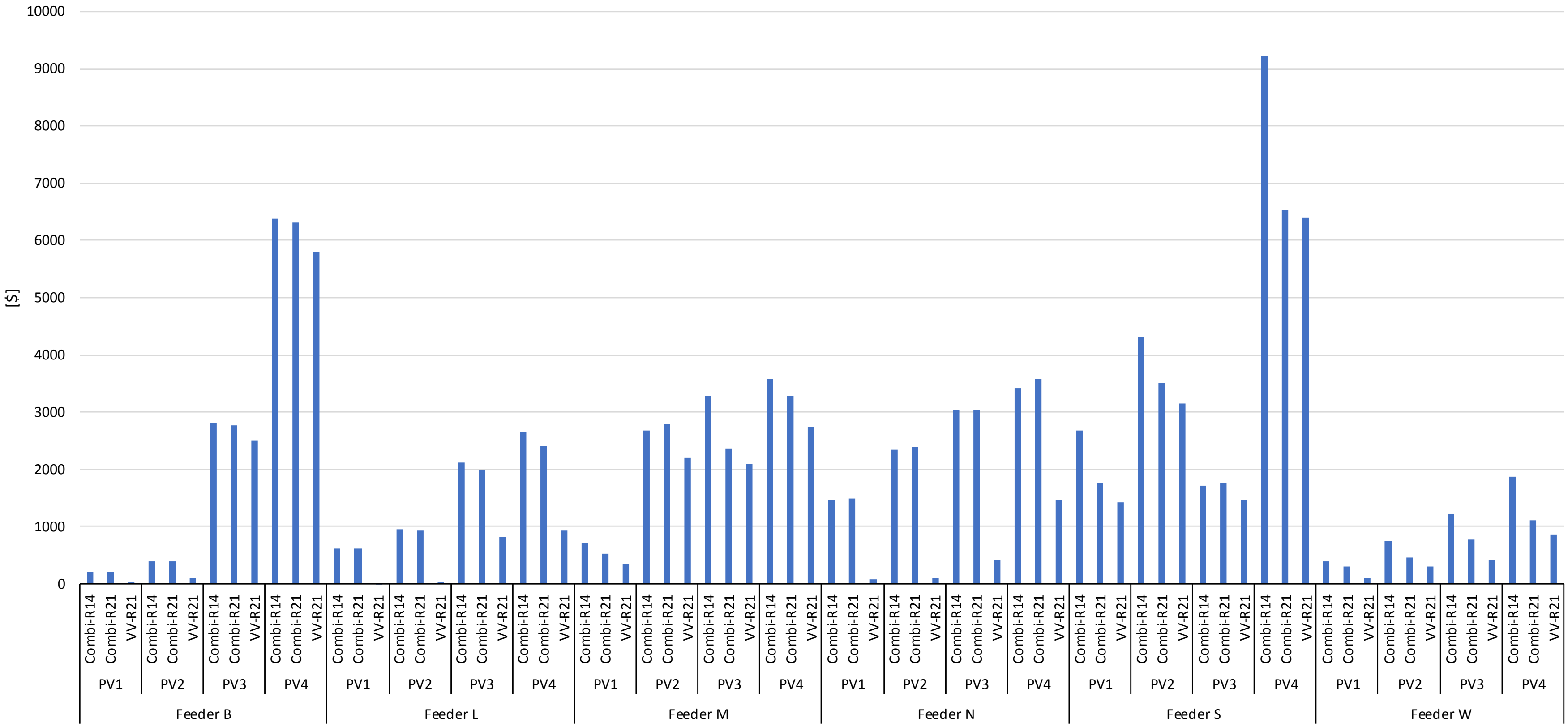

Figure 8-8
Average Annual Increase in Electricity Cost at Feeder Heads

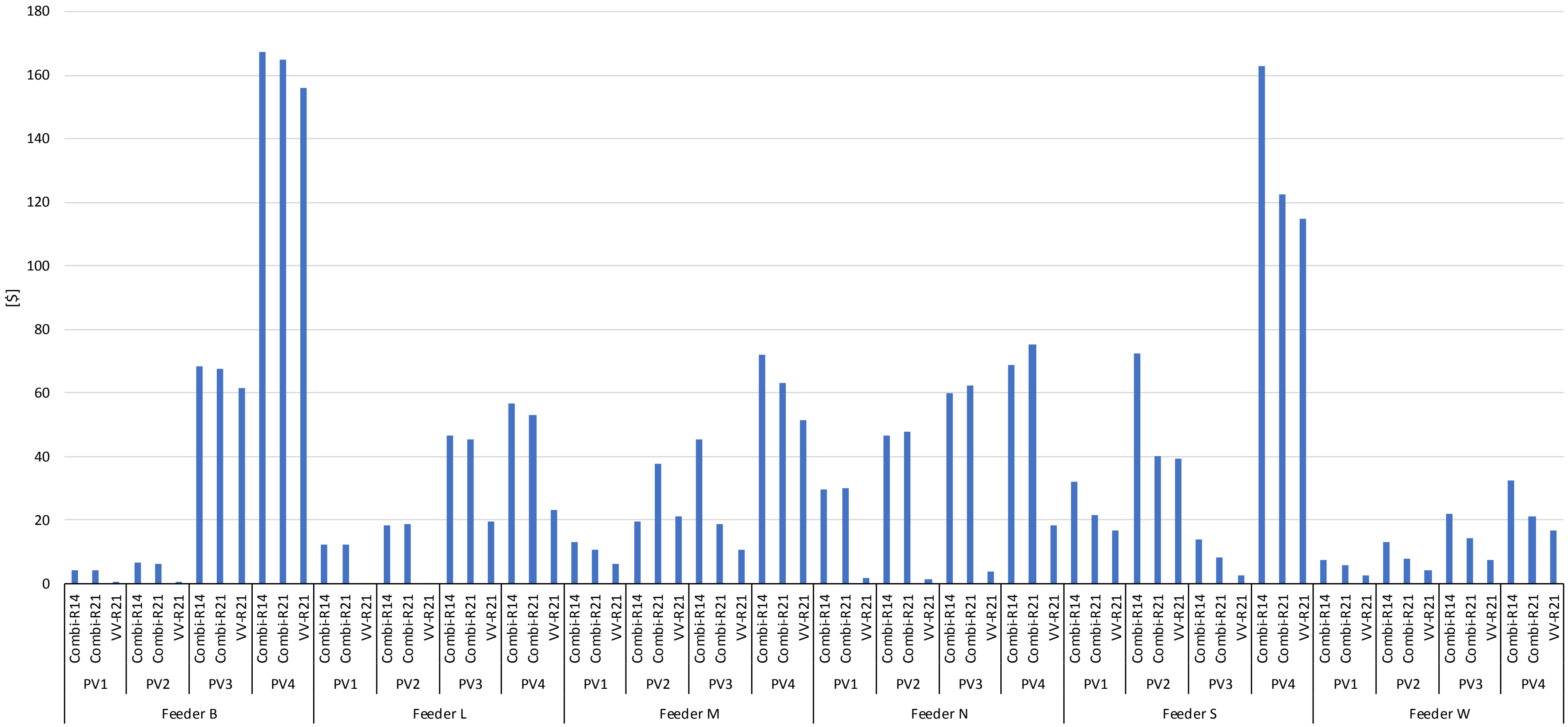

8.4.2 Bill Increases to Participants

The average individual energy usage increases by up to 5.7 kWh annually due to smart functions curtailing PV generation across all scenarios analyzed (Figure 8-9).[98] This increased usage translates into an increase in the average individual bill by up to $0.6 annually (Figure 8-10). These results suggest that the annual bill increase impacting the average participant due to the activation of smart functions remains very limited.

Figure 8-9
Average Increase in Annual Individual Energy Usage to Participants

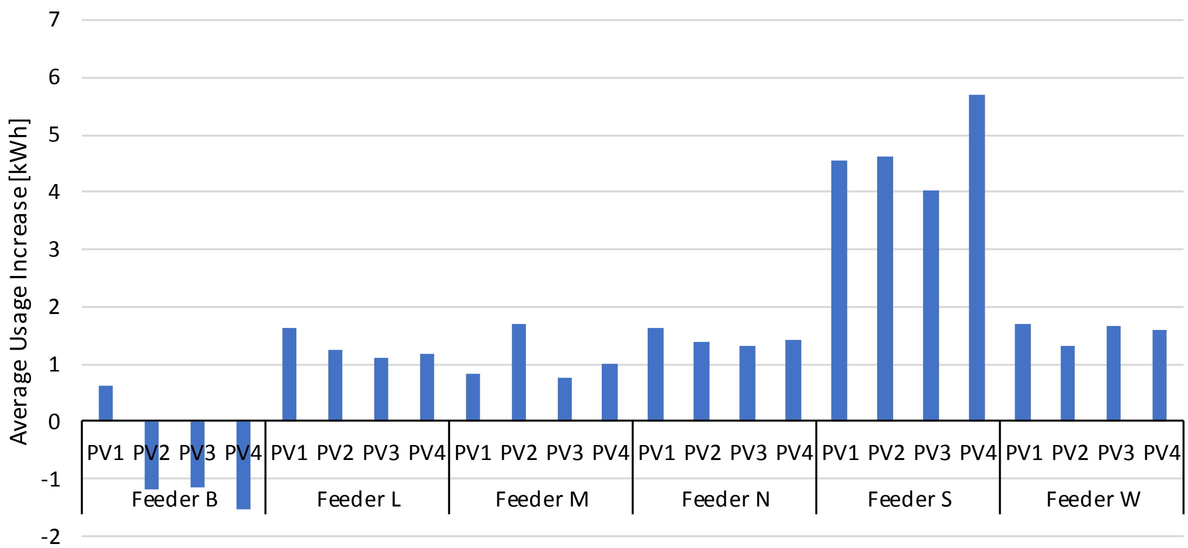

98 In the OpenDSS models, the active power P depended linearly on the supply voltage, and the reactive power Q depended quadratically on the supply voltage. As a result, the net usage recorded for each customer directly depended on the supply voltage. This modeling approach led to a slight reduction in power consumption when voltage magnitudes were reduced as a result of activating smart inverter functions. For Feeder B, this reduction in power consumption was sufficient to *decrease* the average annual usage and average annual bill, as reflected by the negative values shown on Figures 8-10 and 8-11 for Feeder B.

Figure 8-10
Average Individual Bill Increases to Participants

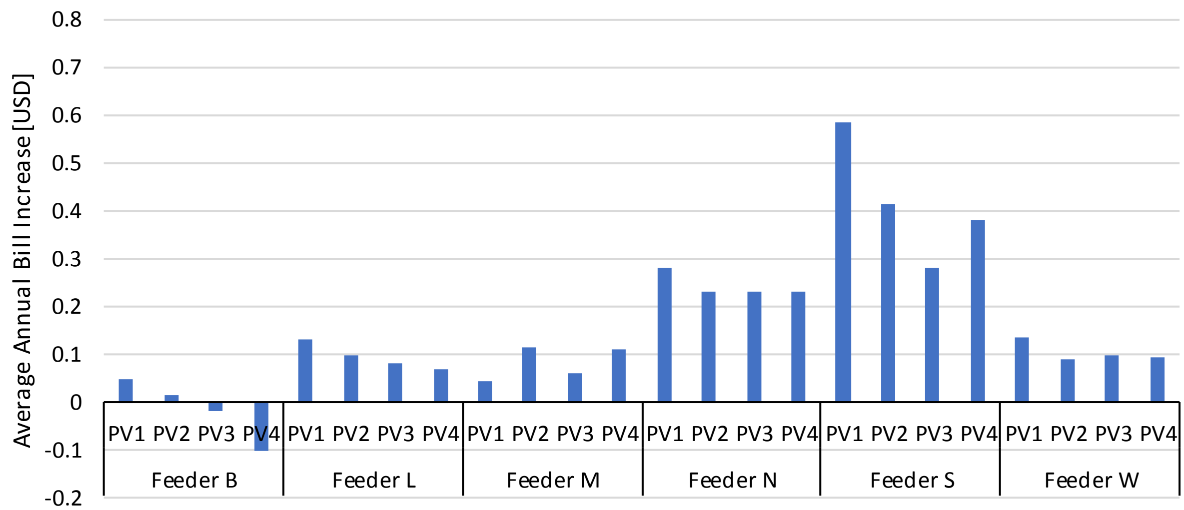

An analysis of the most extreme increases, affecting the net usage and/or the electricity bill, revealed a small set of customer outliers: 10 customers (out of 8,438 for PV4 across the six feeders studied) experienced an annual increase of their individual net usage above 150 kWh (Figure 8-11), and four customers experienced an annual increase of their individual bill over $40 (Figure 8-12). A more detailed analysis of these customer outliers is provided in the next section.

Figure 8-11
Maximum Increase in Individual Annual Energy Usage to Participants

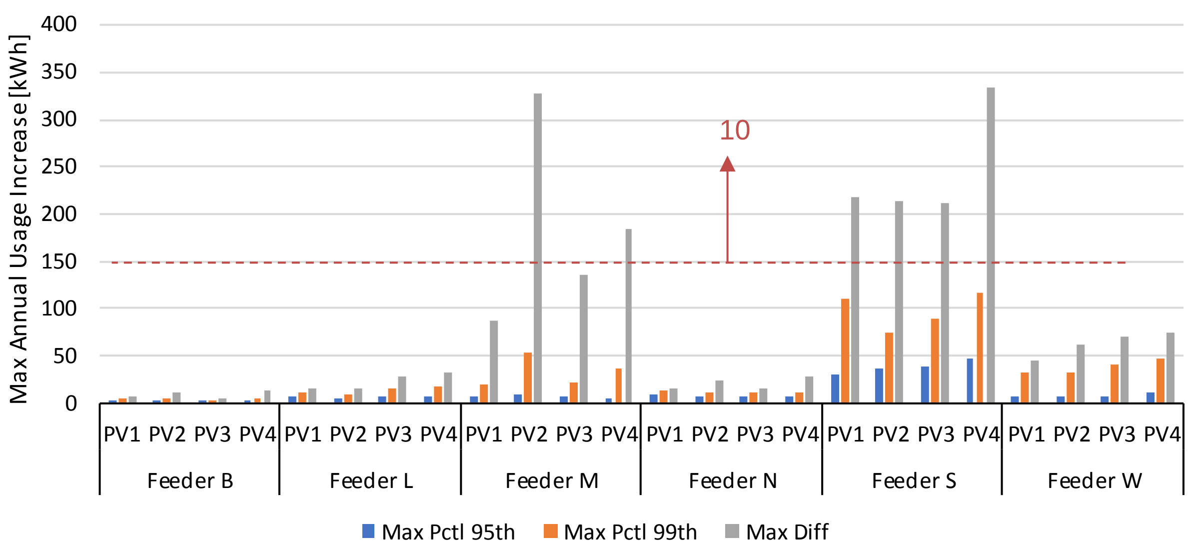

Figure 8-12
Maximum Individual Bill Increases to Participants

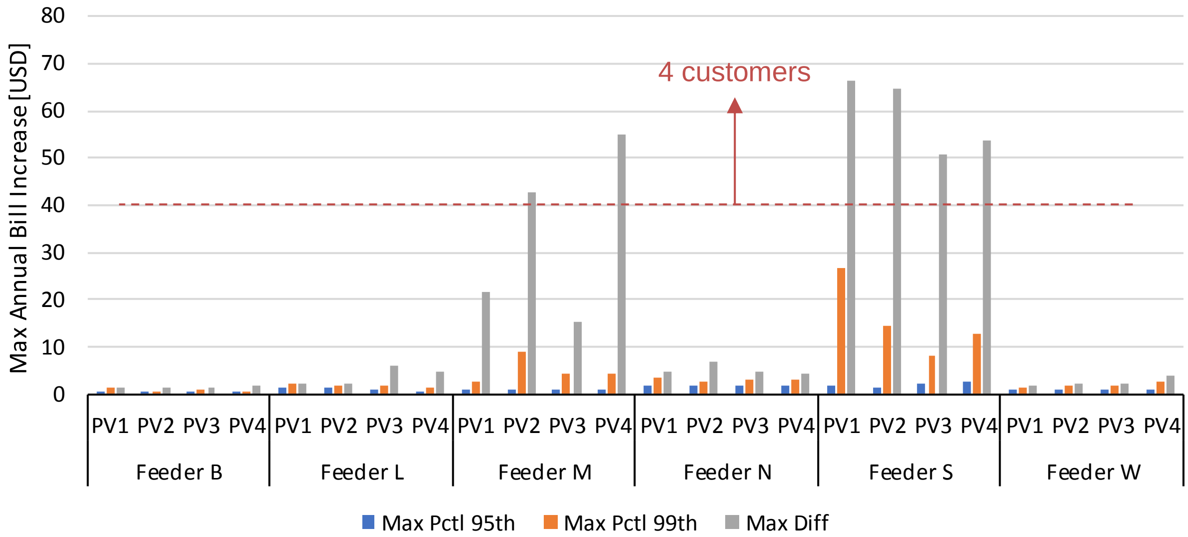

Table 8-11
Average and Maximum Annual Bill Increases Aggregated Across All Participants ($2018)

	Average Annual Increase ($)				Maximum Annual Increase ($)			
Feeder	PV1	PV2	PV3	PV4	PV1	PV2	PV3	PV4
B	7.13	3.17	-13.34	-65.17	14.50	13.40	4.05	-28.68
L	23.00	34.17	41.43	54.30	45.98	71.54	84.11	132.87
M	12.79	40.28	43.56	91.22	39.94	121.87	151.06	253.78
N	115.75	195.68	279.63	373.71	245.93	423.60	564.18	676.07
S	77.91	111.86	112.71	227.79	141.53	215.11	214.19	482.78
W	11.23	15.70	25.11	33.24	22.00	53.50	58.66	110.90

Table 8-12
NPV of Average and Maximum Annual Bill Increases Aggregated Across All Participants ($2018)

	NPV of Average Increase ($)				NPV of Maximum Increase ($)			
Feeder	PV1	PV2	PV3	PV4	PV1	PV2	PV3	PV4
B	50.1	22.3	-93.7	-457.7	101.8	94.1	28.4	-201.4
L	161.5	240.0	291.0	381.4	322.9	502.5	590.8	933.2
M	89.8	282.9	305.9	640.7	280.5	856.0	1061.0	1782.4
N	813.0	1374.4	1964.0	2624.8	1727.3	2975.2	3962.6	4748.4
S	547.2	785.7	791.6	1599.9	994.0	1510.8	1504.4	3390.8
W	78.9	110.3	176.4	233.5	154.5	375.8	412.0	778.9

8.4.3 Avoided VRU and VRS Costs

Using the VRU and VRS unit costs, and the VRU and VRS count estimates developed as part of the technical analysis, the total VRU capex and the upper and lower bounds of the VRS expenses can be calculated. These VRU and VRS costs are staged over 10 years according to the All-in-Y0 and LINEAR profiles. For each of the six feeders, Figure 8-13 represents the combined VRU and VRS costs, assuming the upper VRS count estimate and the All-in-Y0 staging profile.

Figure 8-13
VRU Capex and VRS Expenses (Upper Estimate) Combined, Assuming All-in-Y0 Staging Profile ($2018)

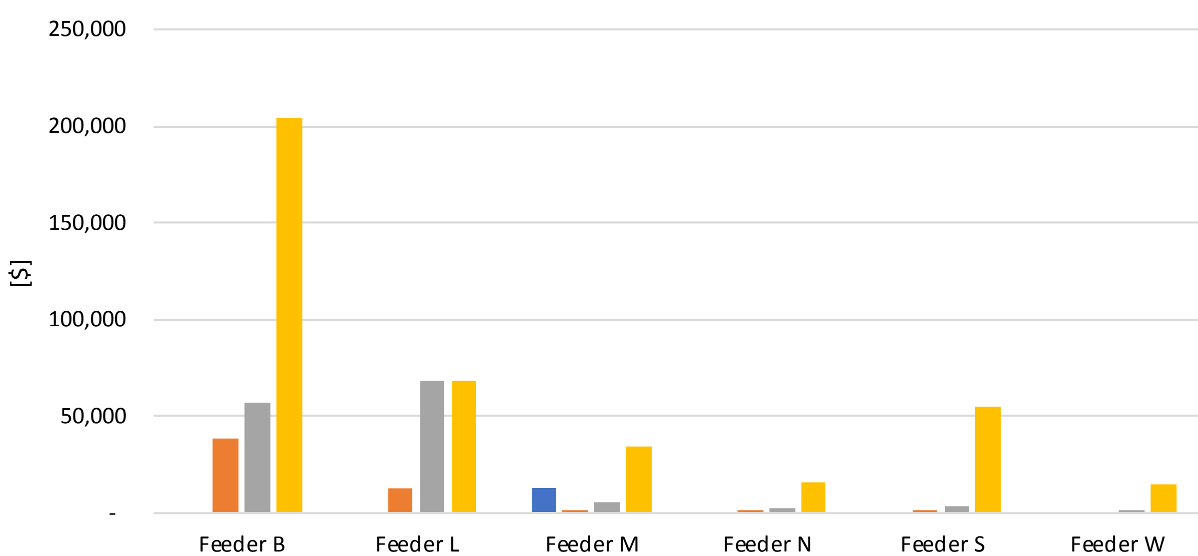

8.4.4 *Cost Test Results*

For each of the six feeders studied, the following sections present the TRC and PCT results in graphical form (Figure 8-14 to Figure 8-19), focusing on two cost-effectiveness indicators: NPV/customer for TRC, and NPV/participant for PCT. A graphical comparison of the TRC and PCT results across all six feeders is also provided (Figure 8-20 to Figure 8-27). In all figures, a *positive* cost test indicates a *net benefit* over 10 years, and a *negative* cost test indicates a *net cost*.

Numerical results for all cost tests and all cost-effectiveness indicators shown in Table 8-2 can be found in Appendix. All cost-effectiveness indicators are calculated over 10 years, assuming the financial parameters shown in Table 8-8, and expressed in $2018.

The key findings from the feeder-specific economic analysis can be summarized as follows:

- For the six feeders analyzed in this modeling effort, the activation of SI functions yields very limited economic impacts over 10 years, positive or negative, when compared to the traditional approach relying on VRU and VRS. Focusing on TRC with the LINEAR staging profile as an example, TRC values range from a total NPV of -$4/customer (net cost) to $57/customer[99] (net benefit) over 10 years ($2018).
- The benefits of activating SI functions generally increase with the PV penetration level. This reflects that a larger number of VRU capex and VRS expenses are avoided at higher PV penetration levels, leading to larger avoided costs, which translate into larger benefits. The savings resulting from these avoided costs are expected to benefit electric ratepayers, interconnecting customers, and PV developers.
- The *Increased Electricity Cost* and *Bill Increases to Participant* cost categories are always small in absolute value when expressed as NPV/customer or NPV/participant. For the highest PV penetration levels returning the most significant cost test values, these two cost categories are also small in relative terms when compared to the *Avoided VRU* and *Avoided VRS* cost categories. A discussion of the customer outliers seeing bill increases larger than the average customer is provided in the next section.
- The differences in economic impacts seen across the six feeders studied can be largely explained by different VRU and VRS requirements, as informed by the technical analysis, and ultimately different feeder characteristics.

[99] The maximum NPV of $57 over 10 years was obtained on one modeled feeder with an atypical voltage class relative to other PG&E feeders. The next largest maximum NPV seen on a more typical feeder assuming a linear PV penetration increase over time was closer to $15 over 10 years.

8.4.4.1 Feeder B

In the figures below, MIN and MAX refer to the minimum and maximum values of the cost-effectiveness indicators across all bookend scenarios presented in Table 8-7.

Figure 8-14
TRC and PCT for Feeder B, 10-Year Horizon, $2018

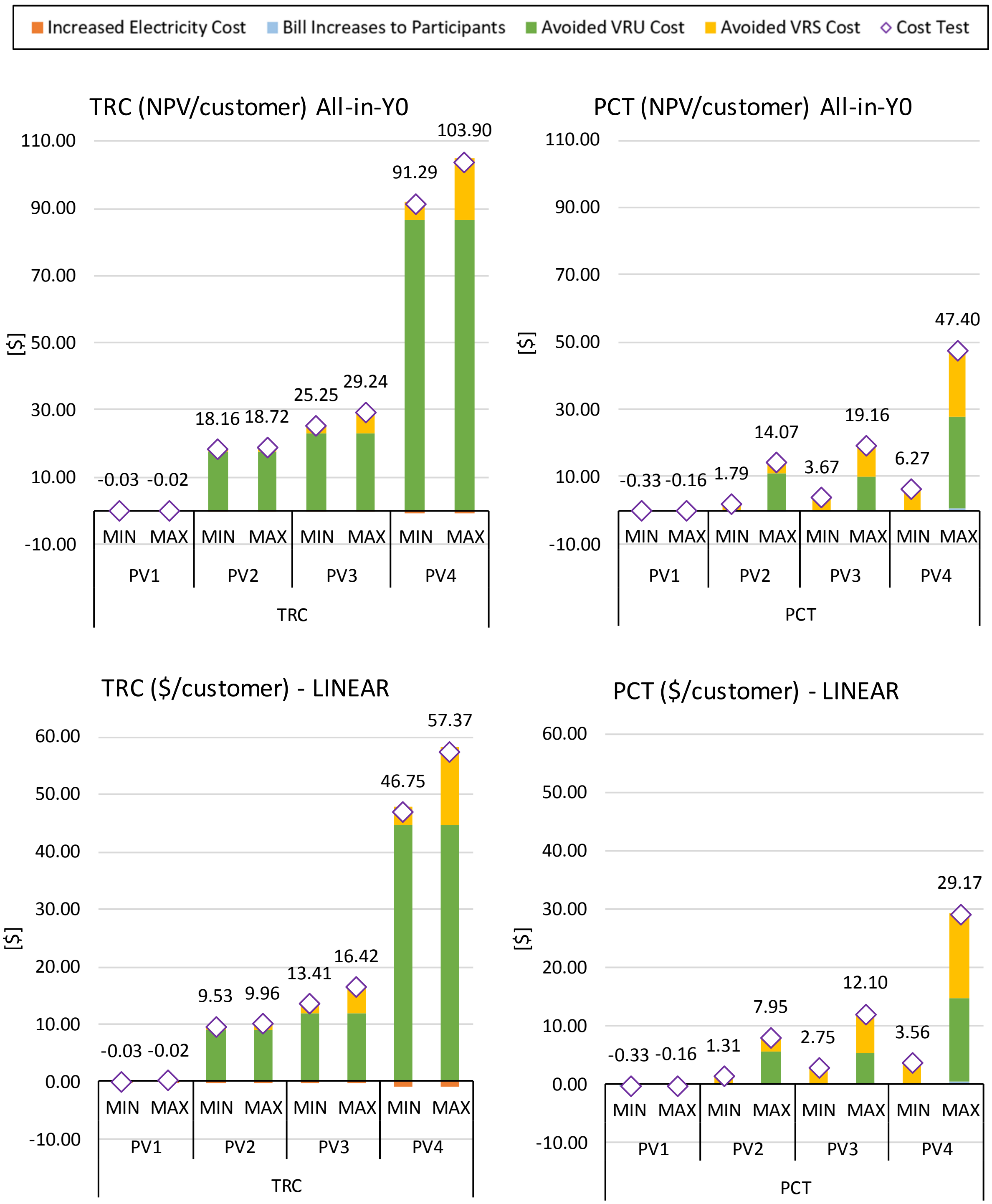

8.4.4.2 Feeder L

Figure 8-15
TRC and PCT for Feeder L, 10-Year Horizon, $2018

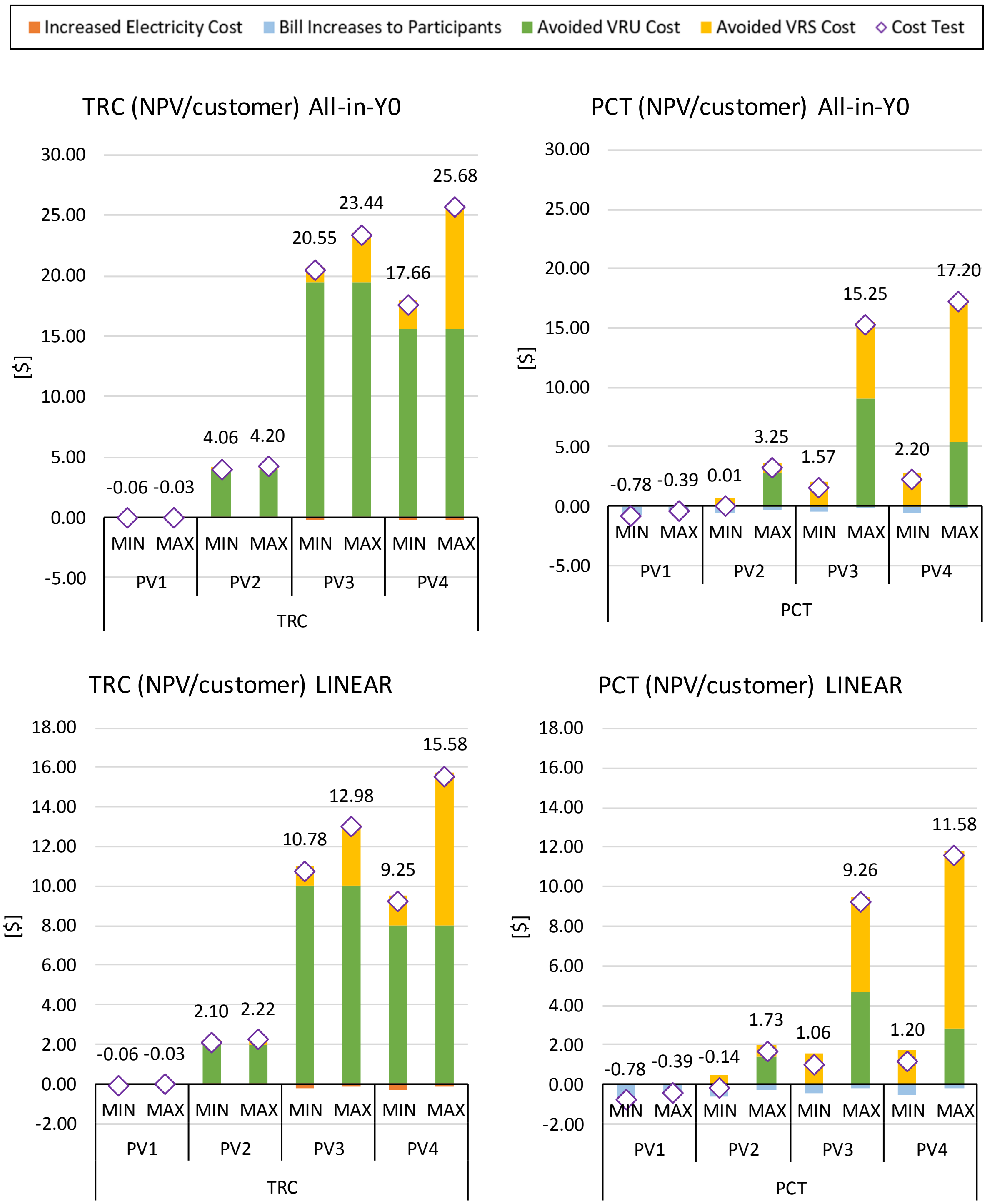

8.4.4.3 Feeder M

Figure 8-16
TRC and PCT for Feeder M, 10-Year Horizon, $2018

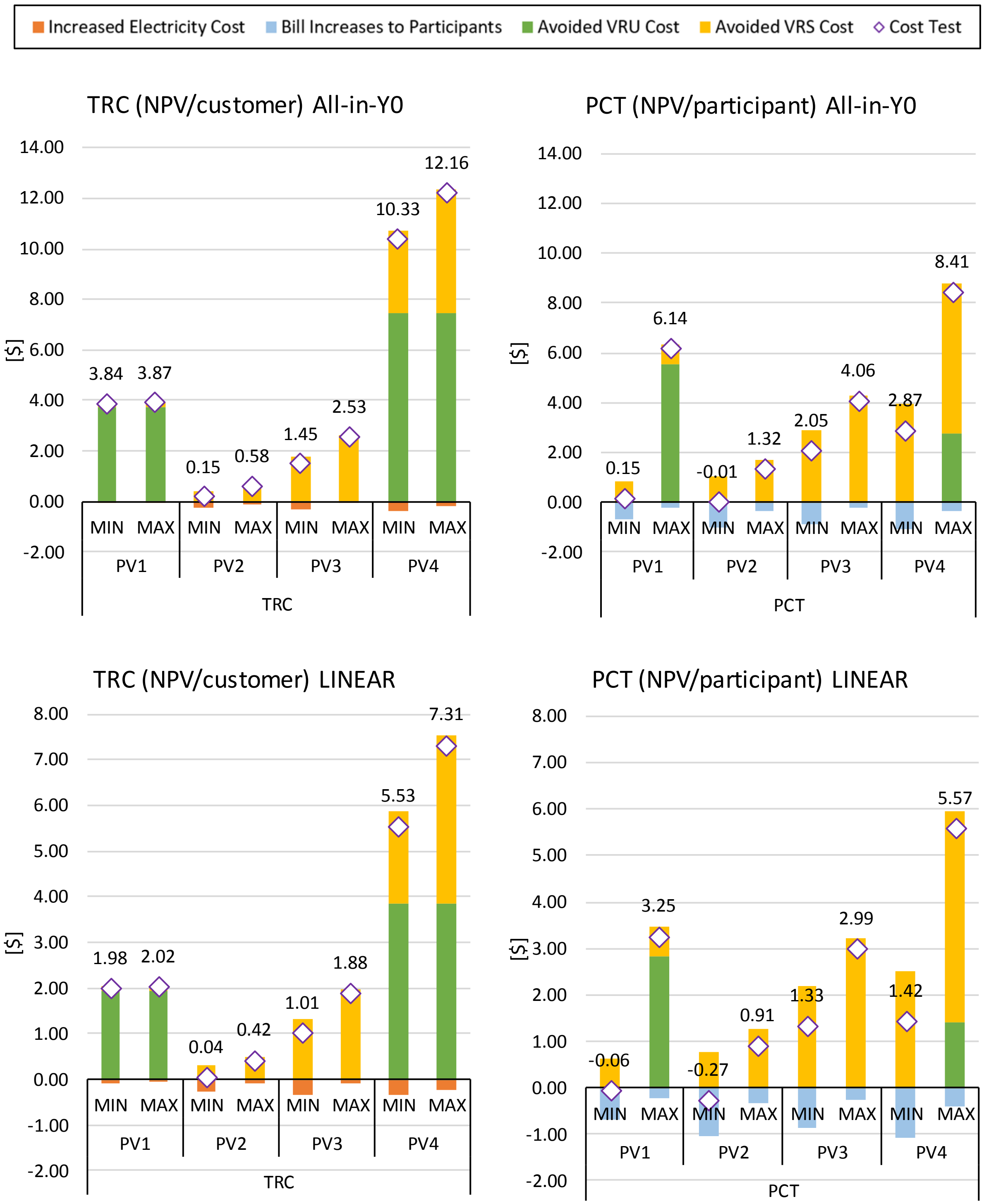

8.4.4.4 Feeder N

Figure 8-17
TRC and PCT for Feeder N, 10-Year Horizon, $2018

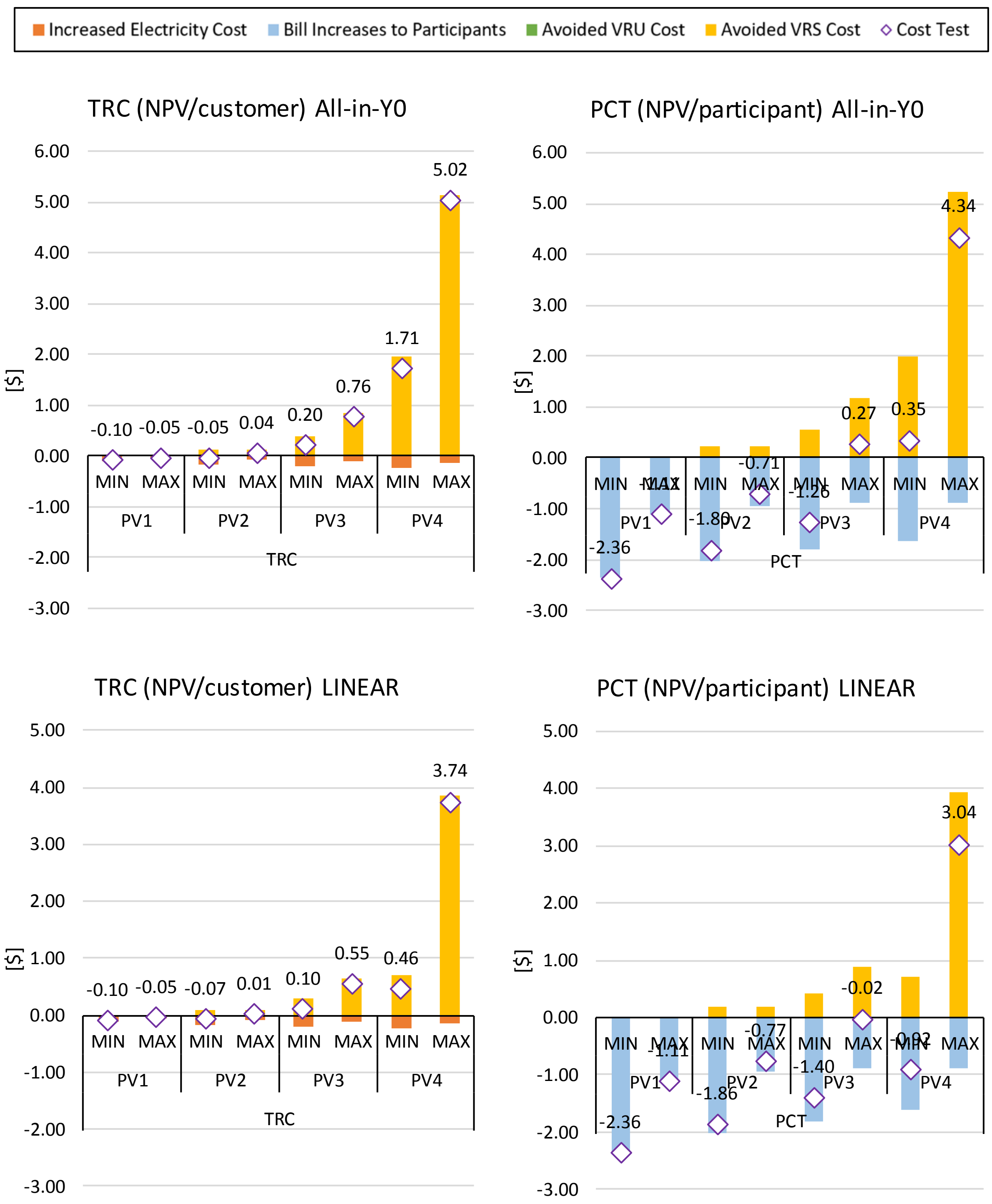

8.4.4.5 Feeder S

Figure 8-18
TRC and PCT for Feeder S, 10-Year Horizon, $2018

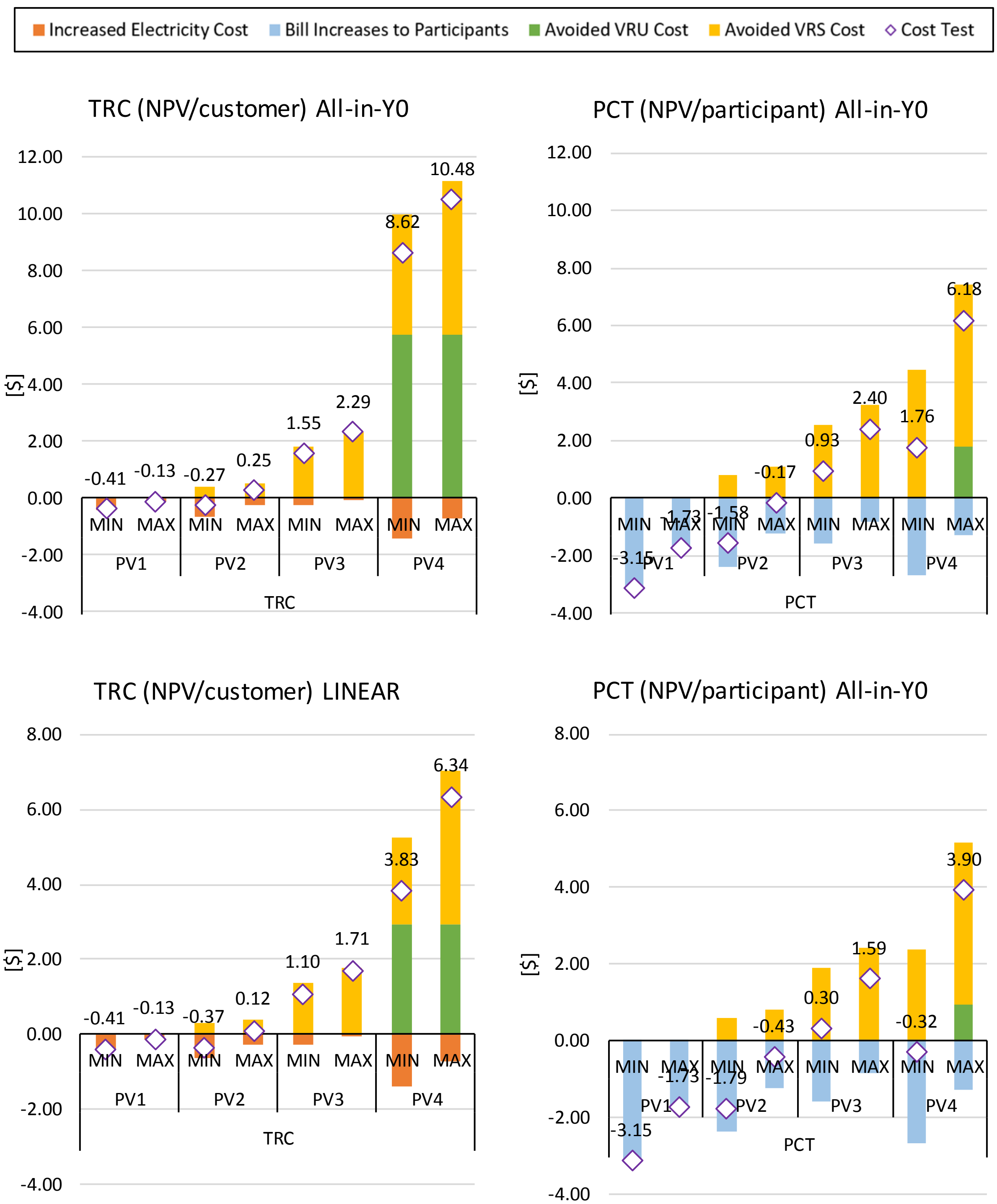

8.4.4.6 Feeder W

Figure 8-19
TRC and PCT for Feeder W, 10-Year Horizon, $2018

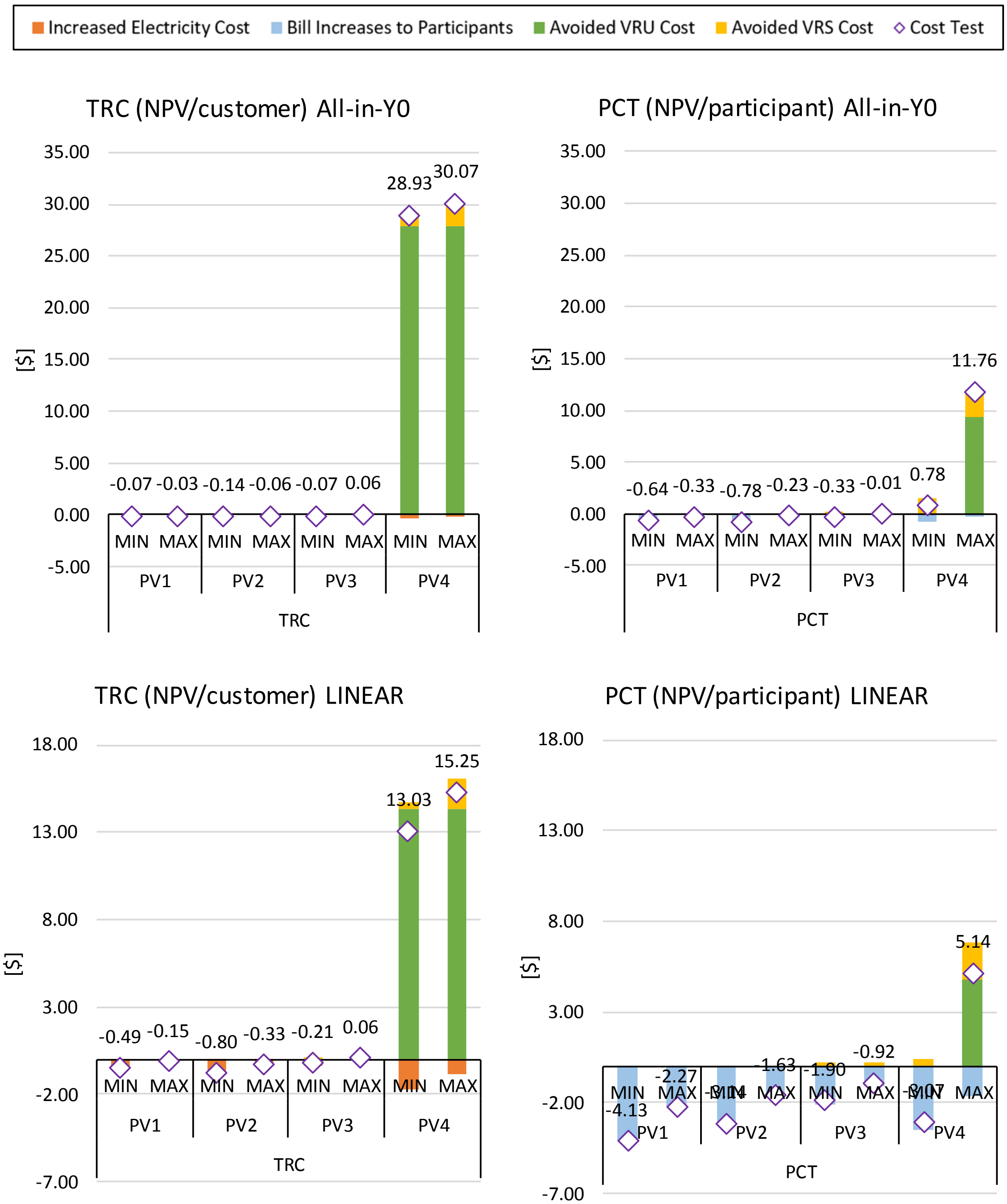

8.4.4.7 Comparison Across Feeders

Figure 8-20
MIN TRC, All-in-Y0, 10-Year Horizon, $2018

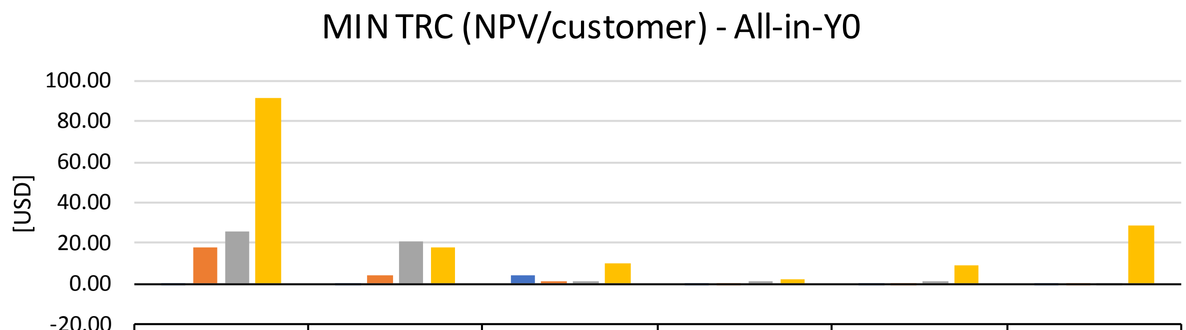

	Feeder B (C8)	Feeder L (C5)	Feeder M (C2)	Feeder N (C6)	Feeder S (C9)	Feeder W (C3)
PV1	-0.03	-0.06	3.84	-0.10	-0.41	-0.07
PV2	18.16	4.06	0.15	-0.05	-0.27	-0.14
PV3	25.25	20.55	1.45	0.20	1.55	-0.07
PV4	91.29	17.66	10.33	1.71	8.62	28.93

Figure 8-21
MAX TRC, All-in-Y0, 10-Year Horizon, $2018

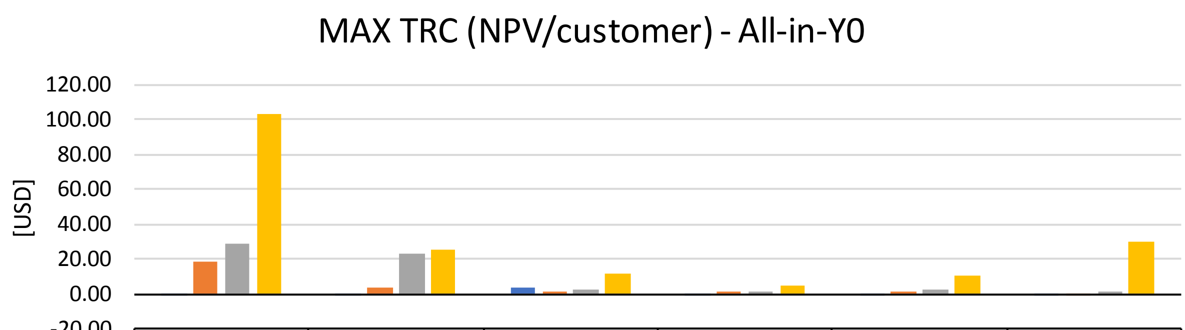

	Feeder B (C8)	Feeder L (C5)	Feeder M (C2)	Feeder N (C6)	Feeder S (C9)	Feeder W (C3)
PV1	-0.02	-0.03	3.87	-0.05	-0.13	-0.03
PV2	18.72	4.20	0.58	0.04	0.25	-0.06
PV3	29.24	23.44	2.53	0.76	2.29	0.06
PV4	103.90	25.68	12.16	5.02	10.48	30.07

Figure 8-22
MIN TRC, LINEAR, 10-Year Horizon, $2018

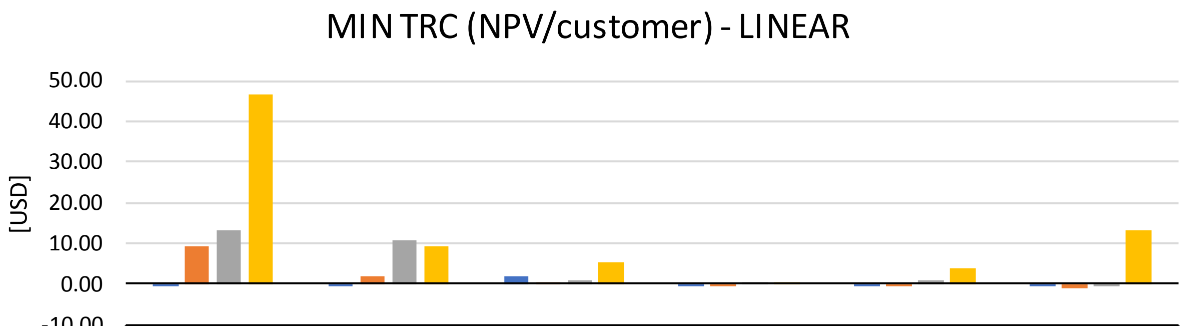

	Feeder B (C8)	Feeder L (C5)	Feeder M (C2)	Feeder N (C6)	Feeder S (C9)	Feeder W (C3)
PV1	-0.03	-0.06	1.98	-0.10	-0.41	-0.49
PV2	9.53	2.10	0.04	-0.07	-0.37	-0.80
PV3	13.41	10.78	1.01	0.10	1.10	-0.21
PV4	46.75	9.25	5.53	0.46	3.83	13.03

Figure 8-23
MAX TRC, LINEAR, 10-Year Horizon, $2018

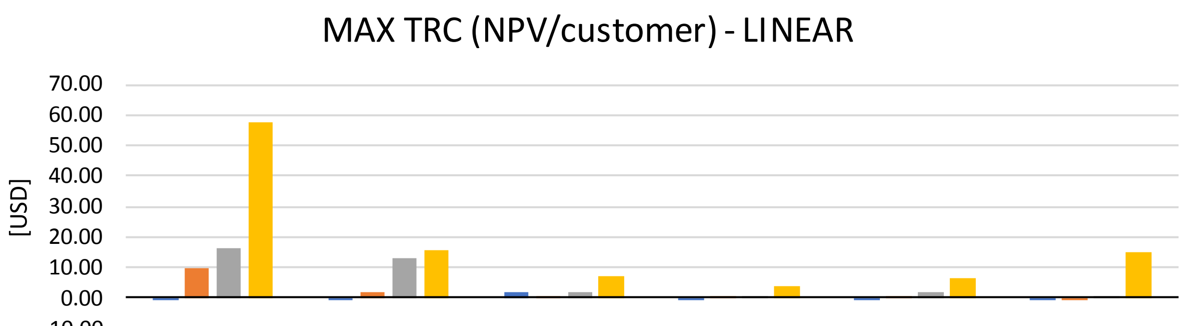

	Feeder B (C8)	Feeder L (C5)	Feeder M (C2)	Feeder N (C6)	Feeder S (C9)	Feeder W (C3)
PV1	-0.02	-0.03	2.02	-0.05	-0.13	-0.15
PV2	9.96	2.22	0.42	0.01	0.12	-0.33
PV3	16.42	12.98	1.88	0.55	1.71	0.06
PV4	57.37	15.58	7.31	3.74	6.34	15.25

Figure 8-24
MIN PCT, All-in-Y0, 10-Year Horizon, $2018

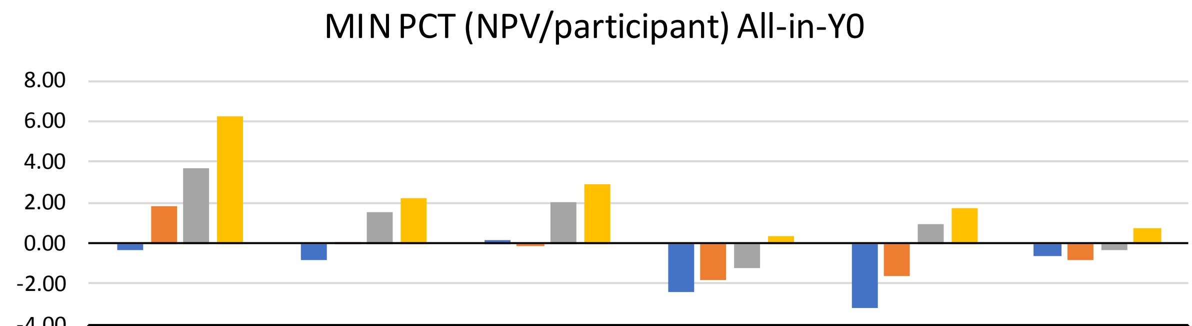

	Feeder B (C8)	Feeder L (C5)	Feeder M (C2)	Feeder N (C6)	Feeder S (C9)	Feeder W (C3)
PV1	-0.33	-0.78	0.15	-2.36	-3.15	-0.64
PV2	1.79	0.01	-0.01	-1.80	-1.58	-0.78
PV3	3.67	1.57	2.05	-1.26	0.93	-0.33
PV4	6.27	2.20	2.87	0.35	1.76	0.78

Figure 8-25
MAX PCT, All-in-Y0, 10-Year Horizon, $2018

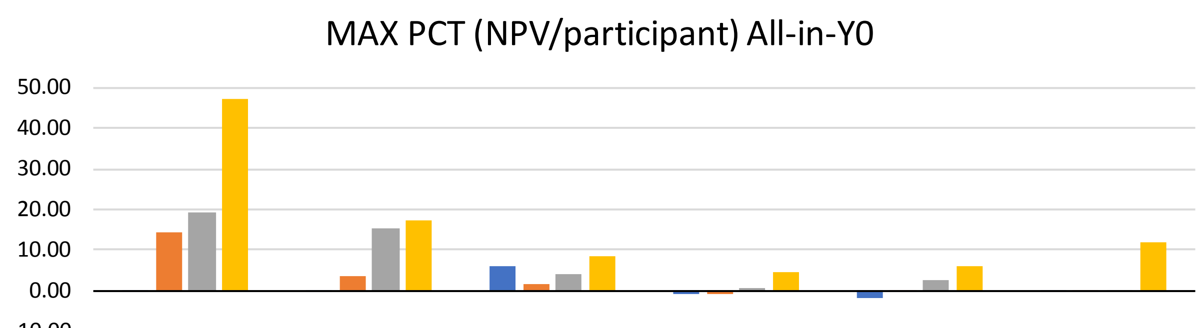

	Feeder B (C8)	Feeder L (C5)	Feeder M (C2)	Feeder N (C6)	Feeder S (C9)	Feeder W (C3)
PV1	-0.16	-0.39	6.14	-1.11	-1.73	-0.33
PV2	14.07	3.25	1.32	-0.71	-0.17	-0.23
PV3	19.16	15.25	4.06	0.27	2.40	-0.01
PV4	47.40	17.20	8.41	4.34	6.18	11.76

Figure 8-26
MIN PCT, LINEAR, 10-Year Horizon, $2018

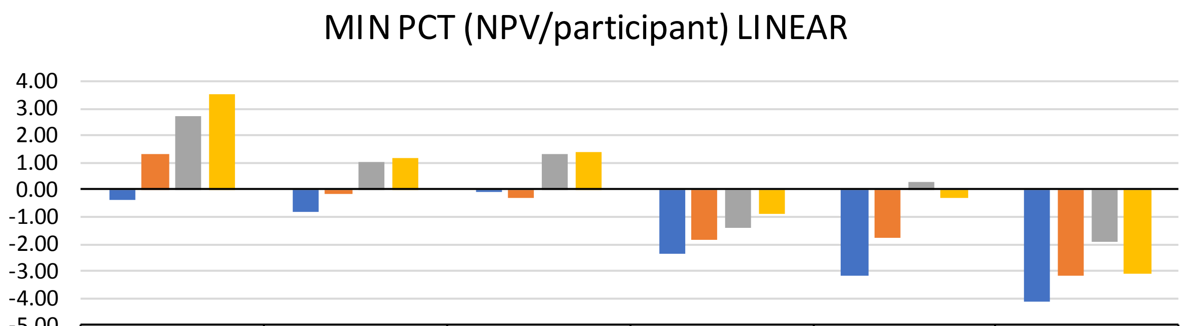

	Feeder B (C8)	Feeder L (C5)	Feeder M (C2)	Feeder N (C6)	Feeder S (C9)	Feeder W (C3)
PV1	-0.33	-0.78	-0.06	-2.36	-3.15	-4.13
PV2	1.31	-0.14	-0.27	-1.86	-1.79	-3.14
PV3	2.75	1.06	1.33	-1.40	0.30	-1.90
PV4	3.56	1.20	1.42	-0.92	-0.32	-3.07

Figure 8-27
MAX PCT, LINEAR, 10-Year Horizon, $2018

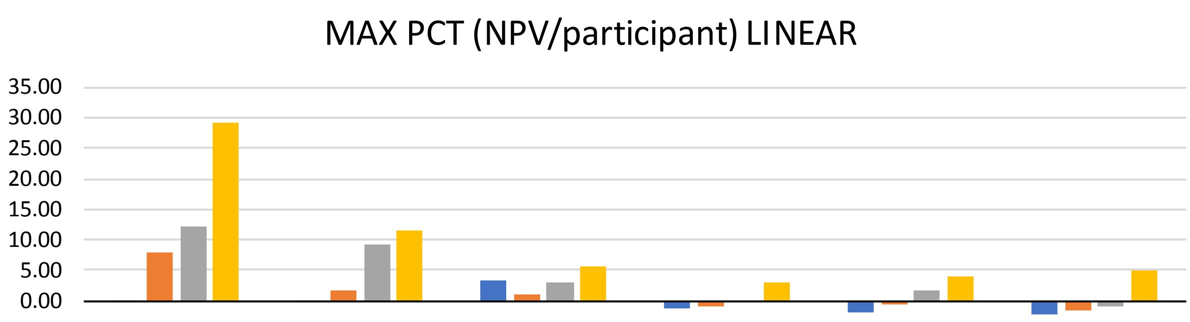

	Feeder B (C8)	Feeder L (C5)	Feeder M (C2)	Feeder N (C6)	Feeder S (C9)	Feeder W (C3)
PV1	-0.16	-0.39	3.25	-1.11	-1.73	-2.27
PV2	7.95	1.73	0.91	-0.77	-0.43	-1.63
PV3	12.10	9.26	2.99	-0.02	1.59	-0.92
PV4	29.17	11.58	5.57	3.04	3.90	5.14

8.5 Analysis of Customers Most Impacted by Smart Inverter Functions

Results of the economic analysis for the six feeders studied show that the activation of SI functions has a very limited impact on electricity bills for the *average* PV customer, with a maximum *average* bill increase of $4 over 10 years ($2018, seen on Feeder W for PV1, MIN). Yet, a small subset of PV customers, referred to as "customer outliers", can experience bill increases much higher than the *average* PV customer. This section takes a closer look at these customer outliers.

8.5.1 Occurrence of "Customer Outliers"

This modeling effort analyzed changes in annual electricity bills across 474,633 individual customer cases, each time comparing the electricity bill *without* smart functions activated (where VRU and VRS may be required) to the bill *with* SI functions (where VRU capex and VRS cost may be avoided). These 474,633 customer cases cover all possible combinations of sensitivity variables previously described: feeder, PV penetration level, SI density, smart functions considered, etc. Each customer is therefore associated to *multiple* cases, each case analyzing the bill difference for that unique customer under different conditions. For each of these 474,633 customer cases, the difference in electricity bill was calculated using the tariffs previously assigned.

From the 474,633 customer cases analyzed, 354,096 cases showing an annual bill change higher than $3 were selected for further analysis. The remaining 120,537 cases were removed to avoid flagging customers experiencing high percentage changes that correspond to very small changes in dollar terms. Figure 8-28 shows the distribution of annual electricity bill differences (expressed in percentage) across the 354,096 customer cases selected for detailed analysis. A positive difference corresponds to a bill increase. For 94% of the customer cases analyzed, the customer annual electricity bill either decreased[100] when activating SI functions, or increased by less than 0.375% when compared to the scenario without smart functions. On the other end of the spectrum, 0.748% of the cases analyzed returned an annual bill increase higher than 3%.

[100] In the OpenDSS models, the active power P depended linearly on the supply voltage, and the reactive power Q depended quadratically on the supply voltage. As a result, the net usage recorded for each customer directly depended on the supply voltage. This modeling approach led to a slight reduction in power consumption when voltage magnitudes were reduced as a result of activating smart inverter functions. Depending on the customer, this reduction in power consumption was sometimes sufficient to *decrease* the average annual bill.

Figure 8-28
Annual Bill Difference in Percentage for Customers and Scenarios of Interest

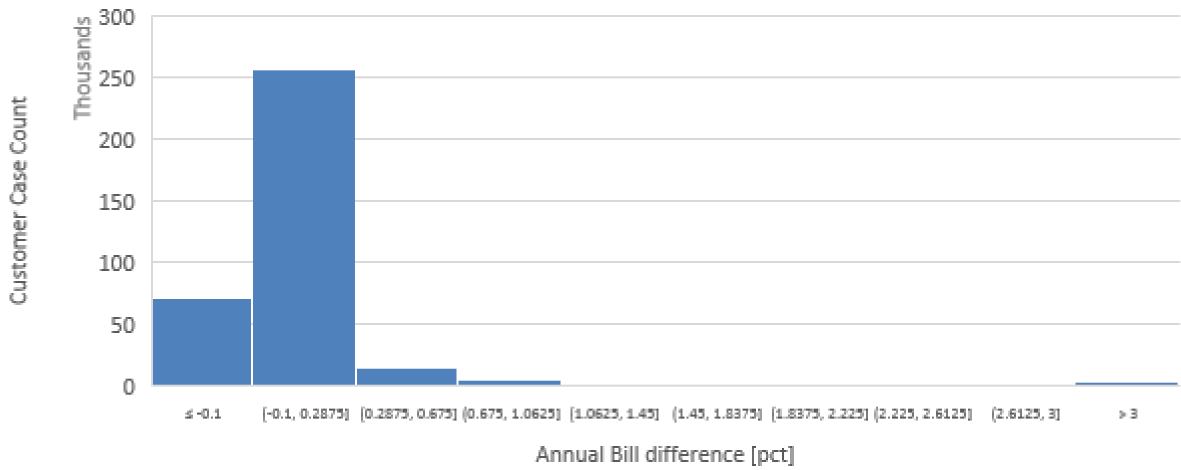

Further analysis was conducted among the customer cases assuming a PV penetration level of 100%, focusing on the subset of customer cases with a bill increase higher than $10 annually. This subset contains a total of 233 customer cases[101] associated to 15 unique customers across all the ES penetration levels, SI densities, and SI functions.[102]

For each of these 233 cases, Figure 8-29 represents the change in annual bill expressed in percentage as a function of that same change expressed in dollar terms. A positive difference reflects a bill increase when smart functions are activated. The smart function considered in each customer case is also identified (Combi-R14, Combi-R21, or VV-R21).

For the subset of 233 cases considered, Figure 8-29 shows that the largest bill increases were recorded for customer cases where the Combi-R14 function was activated. While the Combi-R14 is associated to this very small subset of customer outliers, it is important to recognize that this function has also shown higher effectiveness at avoiding grid overvoltage conditions, when compared to Combi-R21 and VV-R21 in Chapters 5 and 6.

Four specific customer cases, numbered 1 to 4 on Figure 8-29, can illustrate the diversity of customer cases in this subset of 233 cases:

- Case #1: An annual increase of $49, corresponding to a bill increase of 54%.
- Case #2: An annual increase of $55, corresponding to a bill increase of 20%.
- Case #3: An annual increase of $54, corresponding to a bill increase of 2%.
- Case #4: The annual bill increases from $0 in the scenario with no smart functions, to $12 when smart functions are activated. Recall that an annual bill of $0 corresponds to a NEM customer that ends the year with a net credit, which is voided at the end of the 12-month billing cycle, and does not receive any NSC (i.e., a net energy importer over the 12-month cycle).

---

101 These 233 customer cases represent 0.049% of the 474,633 cases analyzed in this modeling effort.

102 These 15 customers represent 0.178% of the 8,438 customers with smart inverter functions activated analyzed in this modeling effort.

Figure 8-29 shows that the largest bill increases in dollar terms, ranging from $20 to $60 annually, represent an increase of less than 10% of the annual bill in most customer cases. This reflects that the largest differences in dollar terms are impacting customers with a relatively large bill. In addition, there were three customer cases, all associated to the same customer, with annual bill increases over $20, or 40% of the annual bill.

Only three out of the 15 customers included in the subset considered experienced an annual bill increase larger than 4% *and* larger than $10. The customer cases associated to these three customers (labeled A, B and C in the following) are shown on Figure 8-30, and discussed in further details in the next section.[103]

Figure 8-29
Bill Increase in Percentage vs. Bill Increase in Dollar for a Subset of 233 Customer Cases at 100% PV Penetration, Showing an Annual Bill Increase Larger Than $10

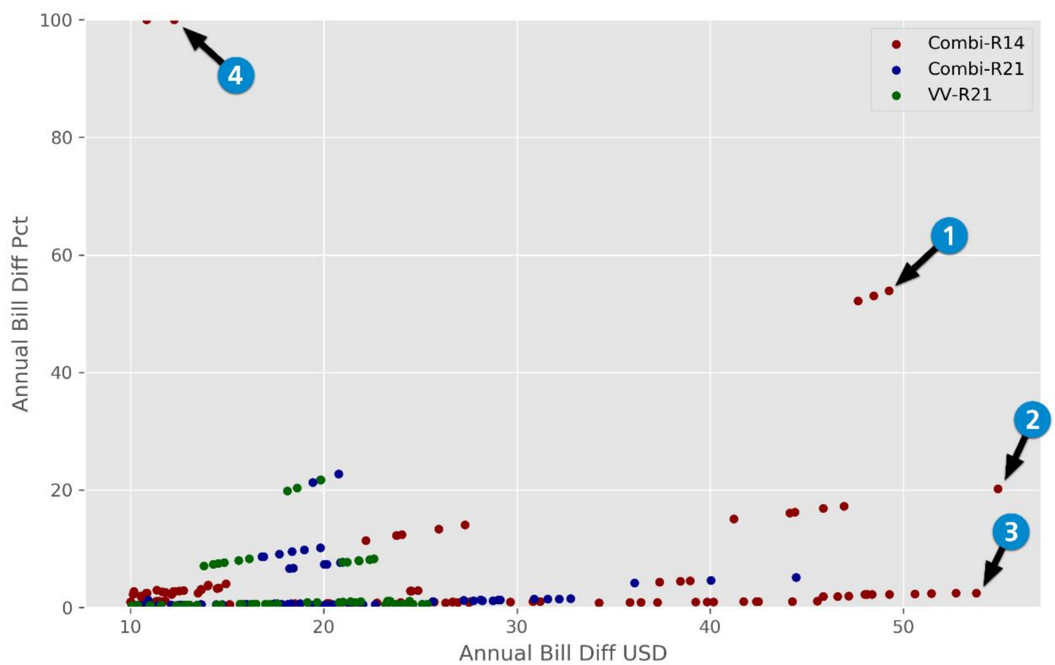

[103] Cases shown in Figure 8-30 are also contained in Figure 8-29.

Figure 8-30
Bill Increase in Percentage vs. Bill Increase in Dollars for the Three "Extreme" Customer Outliers: Customer A (Red), Customer B (Blue), and Customer C (Green)

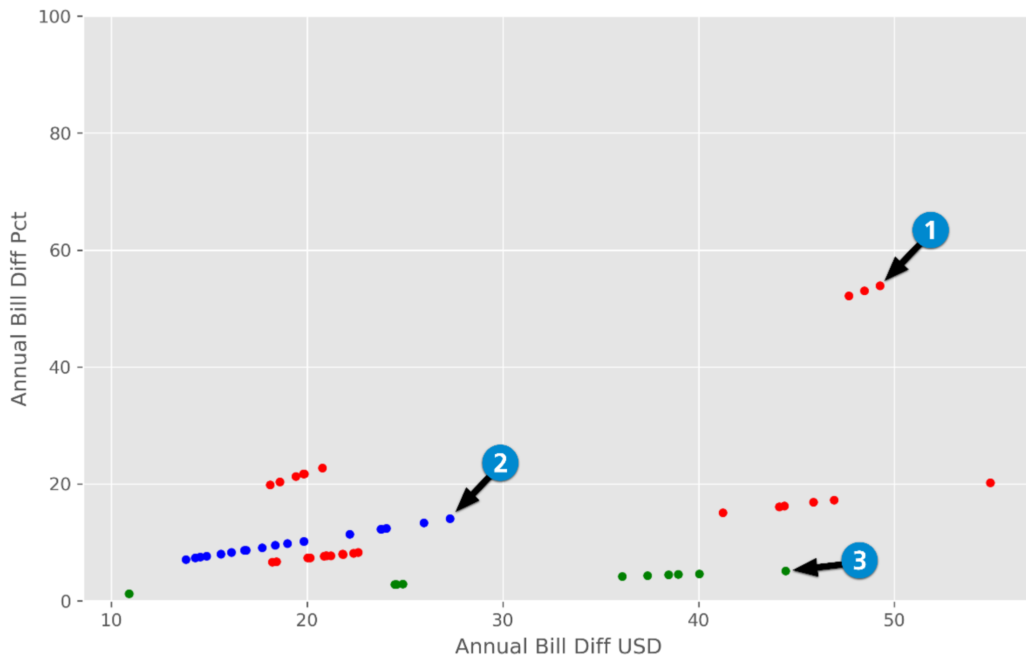

8.5.2 Three Examples of "Extreme" Customer Outliers

8.5.2.1 Customer A

The customer cases associated with Customer A display the highest bill increases out of the three customer outliers investigated in this section, both percentage- and dollar-wise. All cases associated with Customer A are depicted in red on Figure 8-30. Among these cases, the case showing the highest bill increase percentage-wise, associated with label "1" on the graph, will be discussed in the following.

Customer A is located on Feeder M, with a PV capacity of 11.75 kW (DC), and an inverter capacity of 9.79 kVA (AC). The transformer associated to this PV installation has a nominal capacity of 15 kVA dedicated to this single customer. The secondary circuit for this customer was modeled as a 300 feet triplex line (gauge No. 2 AWG). The customer case highlighted with the label "1" on Figure 8-30 assumes: 100% of residential customers with PV installation, no ES, maximum density of SI functions (100% of PV customers).

The customer case labeled "1" had an annual net usage of 1777.6 kWh before activating SI functions, corresponding to an annual bill of $91.31. After activating SI functions, the annual bill increased to $140.56. This $49.25 difference corresponds to an annual increase of 53.93%. The secondary circuit associated with Customer A was not flagged for either voltage-rise studies, or any other conventional upgrades related to overload conditions. However, simulation results for Customer A, assuming the average load day and PV profile A (Figure 8-31), show that the active power generation is significantly curtailed as a result of reactive compensation needs, reflecting high voltage magnitudes experienced at the specific location to which Customer A is connected (see Chapter 5 for further discussion of these technical results).

Therefore, while no "direct" benefits to Customer A in the form of avoided VRU capex or avoided VRS expenses could be traced, the activation of SI functions did provide reactive power support to the grid, resulting in the bill increase observed.

Figure 8-31
Example Day for Customer A, With Smart Inverter Functions Activated. Quadrant A: PV Generation. Quadrant B: Voltage Magnitude. Quadrant C: Differences in PV Output With and Without Smart Inverter Functions. Quadrant D: Differences in Voltage Magnitude.

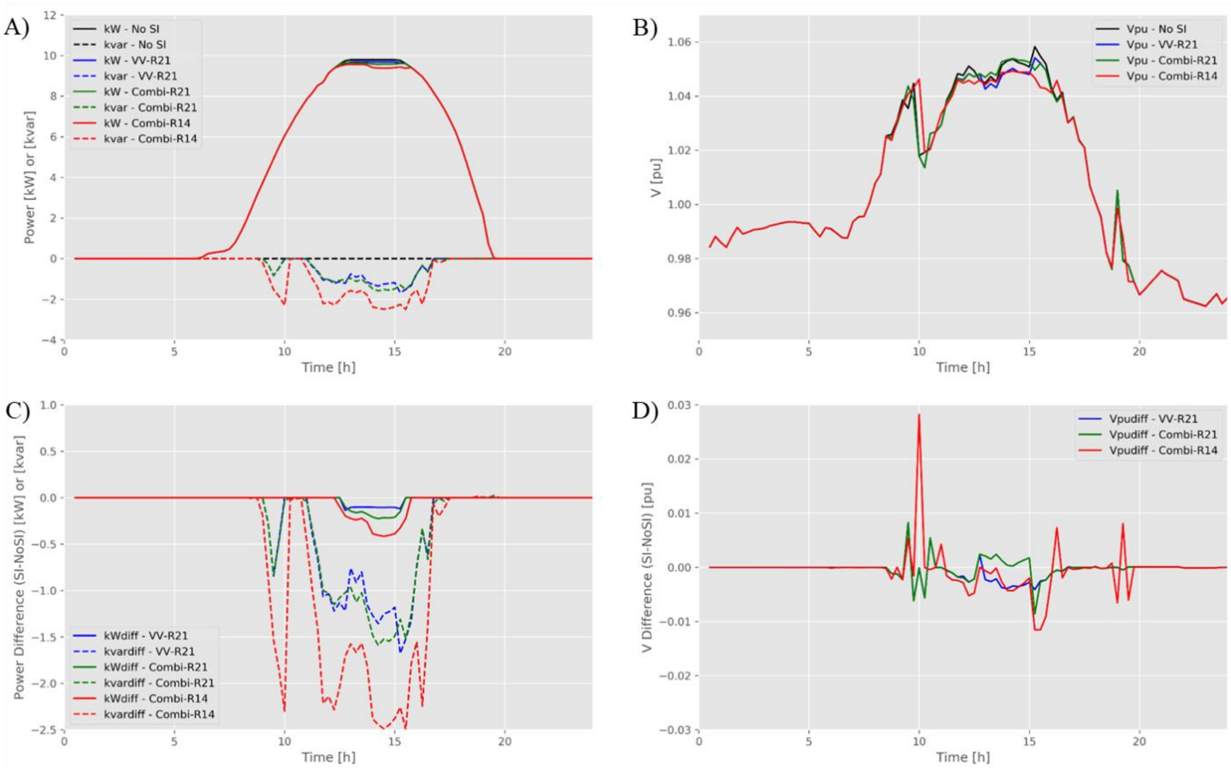

8.5.2.2 Customer B

The customer cases associated with Customer B represent the second higher annual bill increases percentage-wise, out of the three customer outliers investigated in this section. Cases associated with Customer B are depicted in blue on Figure 8-30, and the customer case associated with the largest bill increase percentage-wise is labeled "2."

Customer B is located on Feeder S, with a PV capacity of 13.5 kW (DC), and a 11.25 kVA inverter (AC capacity). The secondary circuit for this location was modeled with a 100-kVA transformer that serves eight customers, with an aggregated inverter capacity at PV level 4 (100% penetration) of 66.25 kVA. Therefore, no voltage-rise studies or overload upgrades were flagged for this location. The customer case highlighted with the label "2" on Figure 8-30 assumes: 100% of residential customers with PV installation, ES penetration of 40%, SI density of 75%.

The customer case labeled "2" had an annual net usage of 2182.9 kWh before activating SI functions, corresponding to an annual bill of $194.1. After activating SI functions, the annual bill increased to $221.38. This difference corresponds to an annual increase of 14.07%.

Simulations for Customer B (Figure 8-32) show that the observed bill increase results primarily from active power curtailment experienced during the average load day, with PV generation profile A. More precisely, reactive power compensation, triggered by Combi-R14 due to high voltage magnitudes experienced at this location during the solar power export period, leads to a curtailment of the active power generation.

Therefore, and similar to Customer A, while no “direct” benefits to Customer B could be traced in the form of avoided VRU capex or avoided VRS expenses, the activation of SI functions did provide reactive power support to the grid, resulting in the bill increase observed.

Figure 8-32
Example Day for Customer B, With Smart Inverter Functions Activated. Quadrant A: PV Generation. Quadrant B: Voltage Magnitude. Quadrant C: Differences in PV Output With and Without Smart Inverter Functions. Quadrant D: Differences in Voltage Magnitude.

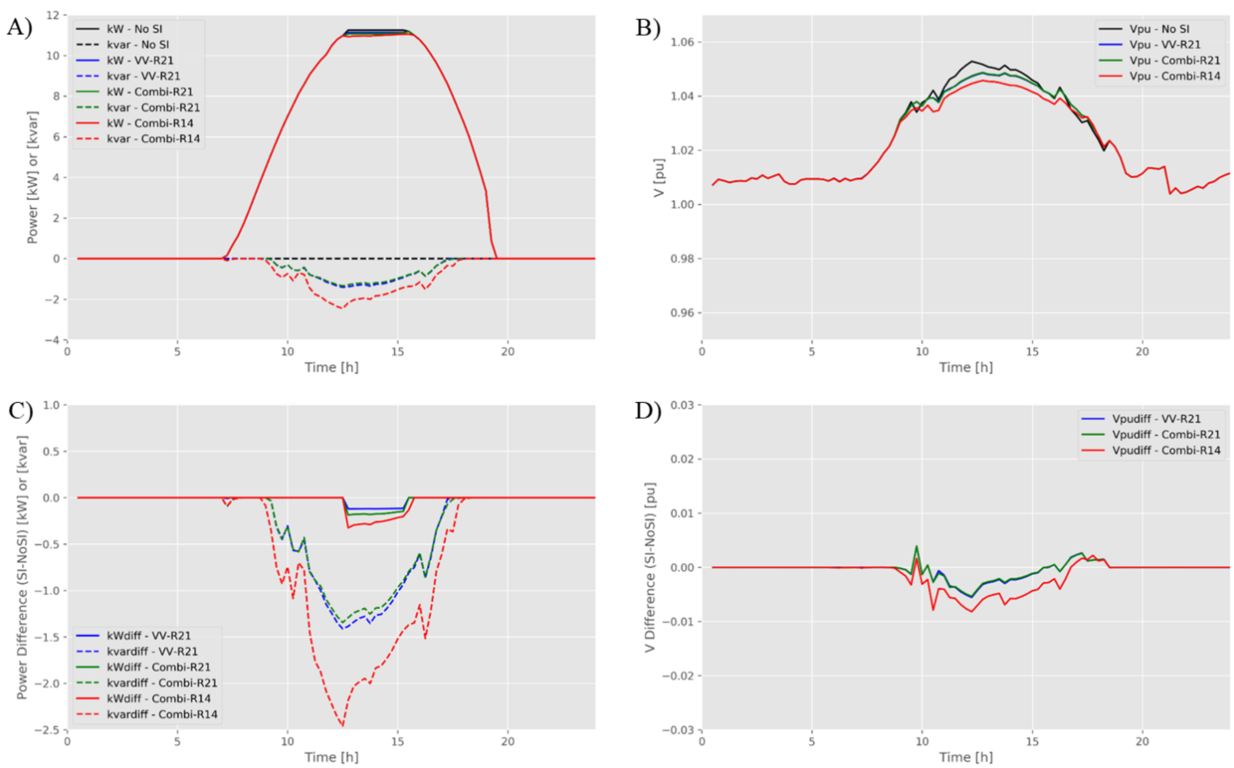

8.5.2.3 Customer C

The customer cases associated with Customer C represent the second higher annual bill increases dollar-wise, out of the three customer outliers investigated in this section. Cases associated with Customer C are depicted in green on Figure 8-30, and the customer case associated with the largest bill increase dollar-wise is labeled “3.”

Customer C is located on Feeder S, with a 5.75 kW PV installation and a peak of 4.79 kVA generation on the AC side of the inverter. The transformer modeled at this location had a nominal capacity of 50 kVA, serving 10 customers with an aggregated PV inverter capacity of 54.17 kVA at PV level 4. The customer case highlighted with the label “3” on Figure 8-30 assumes: PV penetration level of 100%, ES penetration level corresponding to 40% of the PV customers, and SI density of 75%.

The customer case labeled "3" had an annual net usage of 4353 kWh before activating smart functions, corresponding to an annual bill of $859.7. After activating smart functions, the annual bill increased to $904.2. This difference corresponds to an annual increase of 5.17%.

The aggregated PV capacity across all customers connected to the service transformer at this location triggered one voltage-rise modeling effort, which resulted in one transformer upgrade due to the voltage-rise criteria (see Chapter 4 for a detailed discussion on upgrades). Therefore, the activation of smart functions at this location resulted in benefits in the form of avoided VRU capex (rate based in this case, since the transformer replaced was servicing multiple customers), and VRS expenses.

Simulations for Customer C (Figure 8-32) show that, for the average load day with the PV profile A, high voltage magnitudes at this location triggered the activation of SI functions. Specifically, voltage magnitudes over 1.06 V p.u. created a significant need for reactive power compensation, and the smart inverter consequently curtailed the active power generation. Note that, for this specific location, the transformer replacement implemented in the base scenario (no SI functions) resulted in lower voltage magnitudes, as recorded from the QSTS simulations performed, when compared to the scenario involving SI functions.

Therefore, the activation of Customer C's SI functions avoided one VRU and one VRS, and provided reactive power support to the grid. This activation resulted in the bill increase observed. The results obtained when the VRU is performed suggest that the active power curtailment could be decreased if a transformer upgrade was performed at this location. This would likely reduce the bill increase experienced by this customer. However, the cost of this upgrade, intended to reduce the bill increase, may possibly be higher than the bill increase itself.

Figure 8-33
Example Day for Customer C, With Smart Inverter Functions Activated. Quadrant A: PV Generation. Quadrant B: Voltage Magnitude. Quadrant C: Differences in PV Output With and Without Smart Inverter Functions. Quadrant D: Differences in Voltage Magnitude.

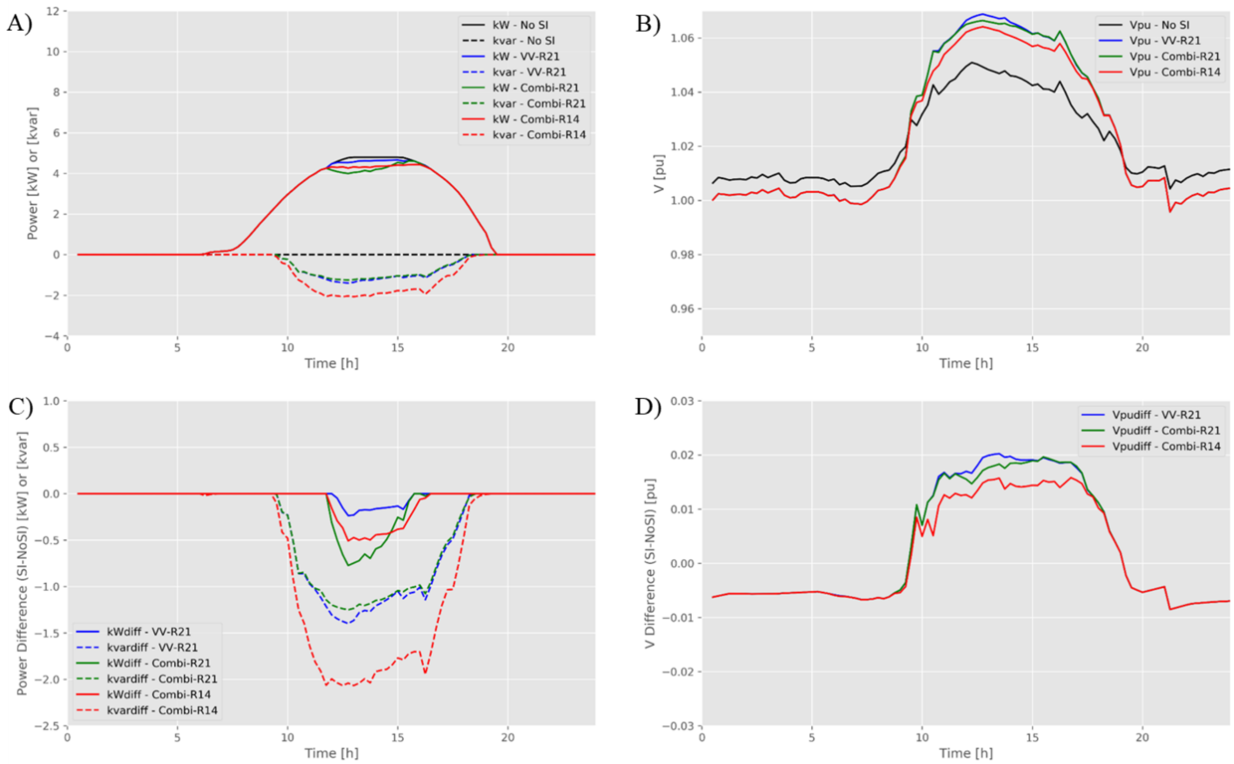

8.5.3 Summary of Findings

The analysis of the customer outliers, i.e., customers experiencing bill increases higher than the average PV customer activating SI functions, resulted in the following findings:

- Customer outliers represent a very small subset of the total number of PV customers. Among the customer cases involving an annual bill increase higher than $3, only 0.748% of the customer cases returned an annual bill increase higher than 3%.
- It is important to recognize that, while SI functions may result in a net cost for a very small subset of customer outliers, they generally result in a net, yet small benefit across all ratepayers, as discussed in Section 8.4.4.
- A detailed analysis of three customers showing, at PV level 4, the highest bill increases, revealed that in all three cases, the bill increase could be explained by SI functions triggering active power curtailment to respond to high voltage conditions.
- For the three customers analyzed, customers A and B were not flagged for VRS or VRU while customer C was flagged for VRS and VRU. In other words, the existing PG&E processes would proactively identify only one of these three problematic customers. For the two other customers, reactive replacements would likely be required to address overvoltages caused by the PV systems after the interconnection. AMI voltage measurements could potentially be leveraged to identify such problematic conditions.

- For two of the three customers analyzed, no VRU capex or VRS expenses were directly avoided. However, there would be similar if not higher costs associated with reactively identifying such cases and replacing the transformers. Some of these costs could potentially be avoided with SI functions. For the third customer, the activation of SI functions did avoid one VRU serving multiple customers (i.e., rate-based) and one VRS.
- However, all three customers provided value to the grid in the form of reactive power support to address high voltage conditions experienced at the specific locations to which they were connected.

9
CONCLUSION

The sustained deployment of grid-connected distributed solar PV systems across PG&E's service territory, driven in part by customer preferences and a favorable policy environment, has the potential to directly support the California objectives of increased grid reliability, resiliency, security, flexibility, and adaptability to climate change. Yet, operational challenges arise at high PV penetration levels, requiring the development of new solutions to mitigate any adverse PV impacts to the electricity grid.

Several technical requirements and standards for PV inverters, including California Electric Rule 21 ("CA Rule 21"), have been developed over the past few years. The objective is to enable distributed PV resources to support grid operations more effectively. In particular, all new interconnected PV systems are now required to have SIs compliant with CA Rule 21, Phase I autonomous functions, including Volt-VAR. Furthermore, at the time of writing this report, CA Rule 21 requires that all new PV systems interconnected after February 22, 2019 comply with CA Rule 21 Phase II communications, and CA Rule 21 Phase III advanced functions including Volt-Watt mode.

This modeling effort explored the technical impacts and economic value of multiple SIs functions, at a level of detail that represents a significant advancement compared to previous studies conducted on this topic. The modeling effort objectives were twofold: (1) inform PG&E of the opportunities for successful utilization and configuration of SIs functions on PG&E distribution circuits; and (2) provide an understanding of the economic impact of SI functions from perspectives: PV customers activating SI functions, ratepayers, the utility, and society. The focus was placed on residential PV systems.

Six PG&E distribution feeders were selected for detailed analysis, based on an array of representative feeder characteristics including: nominal voltage level, feeder length, voltage regulation schemes, load mix and shape, existing PV penetration levels, utility operational practices and system protection devices. The feeder models were refined to include: (a) detailed LV secondary feeder models; (b) real residential AMI load profiles, specific to each feeder, with a large variety of profile types between—and within—feeders; and (c) accurate non-residential load models that capture the actual load profiles seen on these specific circuits at a higher level of accuracy. Extended model validation ensured a realistic representation of the actual distribution circuits.

For each of the six feeders, four variations of the feeder models were created, reflecting four different PV penetration levels (25%, 50%, 75%, and 100% of residential customer). Further sub-versions of the models were developed to reflect three different ES penetration levels (0%, 20%, and 40% of residential PV customers). To capture the PV generation variability in the simulations, five different irradiance profiles were generated using actual California PV data to represent typical weather conditions: summer clear sky (high irradiance, no variation), autumn clear sky (low irradiance, no variation), cloudy (morning variation), extremely variable clouds (large irradiance swings), and overcast (small irradiance). In addition, for each feeder, three typical load profiles were considered: peak day, minimum day, and average day.

For each variation of the feeder models, covering all possible combinations of PV and ES penetration levels, and PV and load profiles, a quasi-static time-series (QSTS) simulation was conducted for a 24-hour period at 15-minute resolution. Thus, a total of 1,080 QSTS simulations across the six feeders were conducted to capture the grid impacts of distributed PV systems under a range of scenarios. This initial analysis was conducted without activating SI functions.

Two strategies aiming to mitigate any PV-driven impacts and expenditures were then evaluated and compared: one strategy relying on conventional distribution upgrades, the other on smart PV inverters, including several combinations of the Volt-VAR and Volt-Watt functions.

Under the first strategy, for each of the six feeders analyzed, the conventional upgrades required to maintain normal operating conditions were determined for all combinations of PV and ES penetration levels considered. These equipment replacements were based on threshold criteria reflecting potential *thermal* overloads and potential *voltage rise* issues, closely following PG&E's design and engineering practices.

An important byproduct of this modeling effort—developed while analyzing the conventional mitigation strategy—consisted of the critical evaluation of PG&E's decision rules triggering equipment upgrades. Simulation results suggested that the current threshold criteria for thermal overloads are adequate to successfully avoid potential thermal violations. However, voltage rise issues were still detected in the QSTS simulations, even after applying PG&E's existing threshold criteria triggering replacements to avoid voltage rise issues. These undetected issues reflected situations where, while the total PV inverter nameplate was well below the transformer rating—the threshold criteria used by PG&E for secondary voltage rise upgrades—voltage violations would still occur, as recorded in the QSTS simulations.

A second strategy, leveraging autonomous SI functions, was analyzed and compared to the traditional approach relying on distribution system upgrades. Three combinations of advanced functions were considered: (1) CA Rule 21 Volt-VAR; (2) combined CA Rule 21 Volt-VAR and Volt-Watt; and (3) combined HI Rule 14 Volt-VAR and Volt-Watt. The proposition was that, while none of the three combinations evaluated was designed to reliability reduce the occurrence or duration of *thermal* overload conditions, all of them could help address overvoltage violations, at varying levels of performance. Each combination of functions was therefore enabled into separate models for all six feeders to evaluate their merit in mitigating PV-driven impacts and expenditures.

The main technical findings, specific to the six feeders analyzed in this modeling effort, were as follows:

1. When SI functions were activated, occurrences of secondary overvoltage conditions were reduced, but not entirely suppressed. Still, the reduction observed suggested that the combinations of functions evaluated in this modeling effort were able to address secondary high voltage issues via reactive power compensation (absorbing VARs from the utility).
2. Smart inverter functions generally provided similar, and in some cases superior performance when addressing secondary overvoltage issues, with the exception of a discrete set of worst-case conditions where inverter functions were not as effective as conventional measures to address secondary overvoltage conditions.
3. Smart inverter functions were not as effective in keeping secondary voltage rise issues below the design threshold for a discrete set of worst-case conditions.
4. Both mitigation strategies, relying on either SI functions or conventional upgrades, showed little to no influence on secondary undervoltage conditions. While limited improvements were sometimes observed, they were due to indirect consequences impacting voltage-regulating devices, and not the mitigation strategies themselves.
5. Three penetration levels of residential ES systems, which were assumed to be solely used for TOU tariff reduction, were analyzed in this modeling effort. The storage penetration level was

observed to have a limited impact without any clear trends on the metrics analyzed in this report. Different storage operating schemes could have had a more notable impact on these metrics. Conversely, the analyzed storage operating scheme may have had a more notable impact on other metrics not analyzed in this modeling effort.

6. Active power curtailment, resulting from the activation of SI functions, appeared extremely limited: 90% of the cases considered showed a reduction in daily active PV generation lower than 0.55%. This reduction was shown to be even smaller at higher SI densities. Across all combinations of feeders, functions, inverter densities, etc. considered in this modeling effort, only 45 of the 8,414 PV installations modeled experienced active power curtailment greater than 1% over a 24-hour period.
7. Simulation results suggested that the increase in inverter utilization when smart functions were activated was significantly small in a large number of scenarios: inverter utilization increased by less than 0.6% for 99% of the scenarios evaluated.

Building on the technical findings, for each of the six feeders modeled, the economic impacts resulting from activating residential SI functions were estimated across four categories: (1) the *increased electricity cost* at feeder heads; (2) the *bill increases to participants*, both resulting from possible PV generation curtailment when smart functions are activated; the (3) *avoided secondary voltage rise upgrades*; and (4) *avoided secondary voltage rise studies* achieved when transitioning from the conventional distribution upgrade strategy to a strategy leveraging SI functions. These cost categories were mapped to four cost tests that serve as the general standard of cost-effectiveness analysis, reflecting various stakeholder perspectives: PV customers activating SI functions, ratepayers, the utility, and society.

A key step of the economic analysis consisted of constructing a time-differentiated annual energy usage profile for each individual residential PV customer modeled, decomposing a full year into the five typical PV days and three typical load days previously studied for each feeder. This, along with an algorithm emulating PG&E's billing system for three relevant retail electricity tariffs, provided detailed estimates of the individual bill increases potentially impacting residential PV customers activating SI functions. Other sensitivities analyzed as part of the economic analysis included: two staging profiles reflecting different assumptions on "how fast" PV penetration levels were reached over time; two bookend cases reflecting different ratios between transformer replacements serving multiple customers (rate based), and single customers (charged directly to customers); two bookend cases reflecting an upper and lower estimate of the number of secondary voltage rise studies.

The main findings of the economic analysis, specific to the six feeders analyzed in this modeling effort, were as follows:

1. The activation of SI functions yielded very limited economic impacts over 10 years, positive or negative, when compared to traditional upgrades: the TRC assuming a linear residential PV penetration increase showed values ranging from a total NPV of -$4 per customer (net cost) to $57[104] per customer (net benefit) over 10 years (in $2018).
2. The benefits of activating SI functions generally increased at higher PV penetration levels, reflecting a larger number of upgrades avoided leading to larger avoided costs.

104 The maximum NPV of $57 over 10 years was obtained on one modeled feeder with an atypical voltage class relative to other PG&E feeders. The next largest maximum NPV seen on a more typical feeder assuming a linear PV penetration increase over time was closer to $15 over 10 years.

3. The *Increased Electricity Cost* and *Bill Increases to Participant* cost categories were always small in absolute value and also small in relative terms at the highest PV penetration levels, when compared to the avoided upgrade costs.
4. The differences in economic impacts across the six feeders studied seemed to be largely explained by different conventional upgrade requirements, resulting from different feeder characteristics.

A detailed analysis of the "customer outliers", i.e., residential customers experiencing bill increases much higher than the *average* residential PV customer, revealed that customer outliers represented a very small subset of the total number of PV customers activating SI functions. Among the customer cases involving an annual bill increase higher than $3, only 0.748% of the customer cases returned an annual bill increase higher than 3%. A possible two-step approach was identified to drastically limit the (already very small) number of customer outliers in practice: first, detect circuit locations prone to overvoltage conditions early via AMI or other data analysis; second, proactively apply upgrades at problematic locations, to ensure that nearby PV customers do not experience excessive active power curtailment, when compared to the average PV customer.

In summary, from the technical results obtained, the two strategies evaluated–conventional distribution upgrades and autonomous SI functions—are expected to perform similarly at addressing PV-driven secondary impacts and expenditures. This result is specific to the six distribution feeders analyzed in this modeling effort. However, results from the economic analysis suggest that positive economic impacts, yet very small, are expected when conventional measures, in particular secondary VRUs and secondary voltage rise studies (VRS), are deferred by activating SI functions.

Following completion of this modeling effort, EPRI recommends to further validate the results obtained following two complementary directions. First, this modeling effort could be supplemented by additional analysis to further explore the impact of SIs on additional feeders with larger datasets of real data. Second, findings from this modeling effort, and in particularly the opportunity to defer conventional measures by activating SI functions, should be tested and validated as part of a field demonstration pilot.

10
APPENDIX – SPECIAL VOLTAGE RISE REMEDIATION

As discussed in Chapter 5, a small number of secondary circuits experienced voltage rise issues in which the nameplate rating of the new transformer that would address the issue was unrealistic. Thus, distribution lines with a large voltage rise were investigated on a case by case basis to remediate this issue whenever a secondary VRS was triggered. This appendix details the process.

In the process of determining equipment replacements, secondaries with voltage rise above PG&E voltage rise design threshold first triggered a transformer upgrade with the next available transformer nameplate to remediate any issues. If the transformer upgrade did not address the voltage rise issue, a closer analysis was performed to determine if another transformer size upgrade would address the voltage rise issue or if service line upgrades would be needed. While the majority of voltage rise issues were addressed with a single transformer upgrade, a small number of secondaries (6 on Feeder B, 2 on Feeder L, 2 on Feeder M, and 3 on Feeder S) required a closer analysis to address voltage rise concerns. On most of these secondaries, the voltage rise issue was addressed by second transformer size upgrades (3/6 on Feeder B, 2/2 on Feeder L, 1/2 on Feeder M, and 0/3 on Feeder S). The remaining secondaries required service line upgrades. The list of each occurrence is presented in Table 10-1.

Table 10-1
Summary of Secondaries Requiring Additional Upgrades on a Case-by-Case Basis

Feeder	XFMR Case	Upgrades
Feeder B	1	Few secondary line upgrades
	2	Few secondary line upgrades
	3	XFMR upgrade (2 sizes up)
	4	Few secondary line upgrades
	5	XFMR upgrade (2 sizes up)
	6	XFMR upgrade (2 sizes up)
Feeder L	1	XFMR upgrade (2 sizes up)
	2	XFMR upgrade (2 sizes up)
Feeder M	1	XFMR upgrade (2 sizes up)
	2	Few secondary line upgrades
Feeder S	1	Few secondary line upgrades
	2	Few secondary line upgrades
	3	Few secondary line upgrades

For each secondary, the final recommended transformer size was considered in all the results discussing in this report, including the economic analysis. On the other hand, the costs of distribution line upgrades were not considered in the economic analysis because of the negligible number of cases with respect to the total distance of secondary lines on each feeder.

Export Control Restrictions

Access to and use of EPRI Intellectual Property is granted with the specific understanding and requirement that responsibility for ensuring full compliance with all applicable U.S. and foreign export laws and regulations is being undertaken by you and your company. This includes an obligation to ensure that any individual receiving access hereunder who is not a U.S. citizen or permanent U.S. resident is permitted access under applicable U.S. and foreign export laws and regulations. In the event you are uncertain whether you or your company may lawfully obtain access to this EPRI Intellectual Property, you acknowledge that it is your obligation to consult with your company's legal counsel to determine whether this access is lawful. Although EPRI may make available on a case-by-case basis an informal assessment of the applicable U.S. export classification for specific EPRI Intellectual Property, you and your company acknowledge that this assessment is solely for informational purposes and not for reliance purposes. You and your company acknowledge that it is still the obligation of you and your company to make your own assessment of the applicable U.S. export classification and ensure compliance accordingly. You and your company understand and acknowledge your obligations to make a prompt report to EPRI and the appropriate authorities regarding any access to or use of EPRI Intellectual Property hereunder that may be in violation of applicable U.S. or foreign export laws or regulations.

The Electric Power Research Institute, Inc. (EPRI, www.epri.com) conducts research and development relating to the generation, delivery and use of electricity for the benefit of the public. An independent, nonprofit organization, EPRI brings together its scientists and engineers as well as experts from academia and industry to help address challenges in electricity, including reliability, efficiency, affordability, health, safety and the environment. EPRI members represent 90% of the electric utility revenue in the United States with international participation in 35 countries. EPRI's principal offices and laboratories are located in Palo Alto, Calif.; Charlotte, N.C.; Knoxville, Tenn.; and Lenox, Mass.

Together…Shaping the Future of Electricity

© 2018 Electric Power Research Institute (EPRI), Inc. All rights reserved. Electric Power Research Institute, EPRI, and TOGETHER…SHAPING THE FUTURE OF ELECTRICITY are registered service marks of the Electric Power Research Institute, Inc.

10xxxxx

Electric Power Research Institute
3420 Hillview Avenue, Palo Alto, California 94304-1338 • PO Box 10412, Palo Alto, California 94303-0813 • USA
800.313.3774 • 650.855.2121 • askepri@epri.com • www.epri.com